



UvA-DARE (Digital Academic Repository)

Unravelling early pathogenesis of pandemic and epidemic viruses

Infection and viral dissemination at barrier tissues

Eder, J.

Publication date

2023

Document Version

Final published version

[Link to publication](#)

Citation for published version (APA):

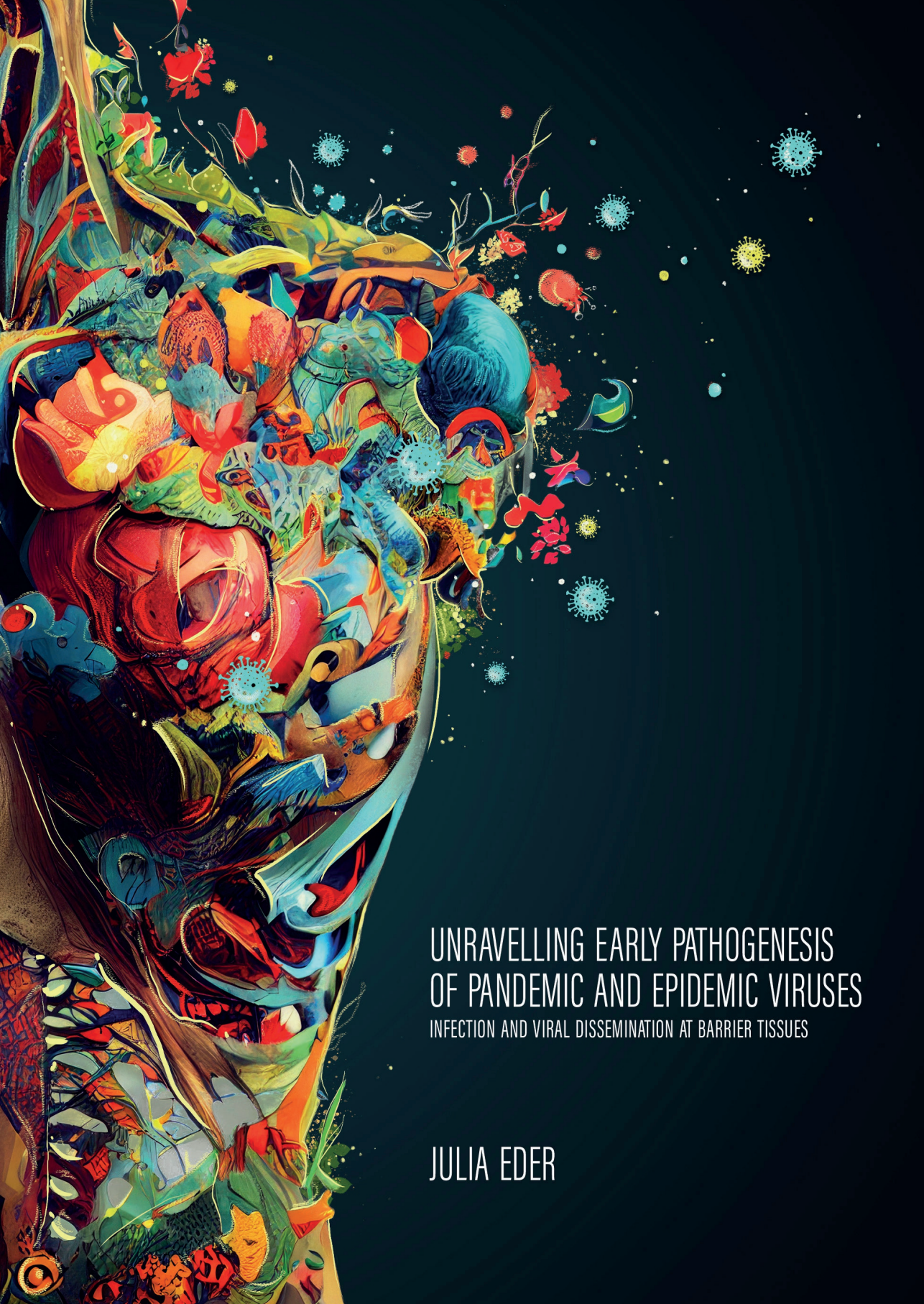
Eder, J. (2023). *Unravelling early pathogenesis of pandemic and epidemic viruses: Infection and viral dissemination at barrier tissues*. [Thesis, fully internal, Universiteit van Amsterdam].

General rights

It is not permitted to download or to forward/distribute the text or part of it without the consent of the author(s) and/or copyright holder(s), other than for strictly personal, individual use, unless the work is under an open content license (like Creative Commons).

Disclaimer/Complaints regulations

If you believe that digital publication of certain material infringes any of your rights or (privacy) interests, please let the Library know, stating your reasons. In case of a legitimate complaint, the Library will make the material inaccessible and/or remove it from the website. Please Ask the Library: <https://uba.uva.nl/en/contact>, or a letter to: Library of the University of Amsterdam, Secretariat, Singel 425, 1012 WP Amsterdam, The Netherlands. You will be contacted as soon as possible.



UNRAVELLING EARLY PATHOGENESIS OF PANDEMIC AND EPIDEMIC VIRUSES

INFECTION AND VIRAL DISSEMINATION AT BARRIER TISSUES

JULIA EDER

Unravelling early pathogenesis of pandemic and epidemic viruses

Infection and viral dissemination at barrier tissues

Julia Eder

Unravelling early pathogenesis of pandemic and epidemic viruses:
Infection and viral dissemination at barrier tissues

Thesis, University of Amsterdam, the Netherlands.
ISBN: 978-94-6469-444-4

Cover design & Interior: Sophia Strydom
Figure design and layout: Julia Eder
Printing: Proefschriftmaken, www.proefschriftmaken.nl
Copyright © 2023 Julia Eder | All rights reserved.

This research was performed at the department of Experimental Immunology (EXIM) at the Amsterdam UMC, location Academic medical center (AMC).

The copyright of the articles that have been accepted for publication or published has been transferred to the respective journals. No part of this thesis may be reproduced, stored or transmitted in any form or by any means without the permission of the author or publishers of the included scientific papers.

The printing of this thesis was financially supported by the Academic Medical Center, Academic Medical Research (AMR) and Stichting Proefdiervrij.

Unravelling early pathogenesis of pandemic and epidemic viruses

Infection and viral dissemination at barrier tissues

ACADEMISCH PROEFSCHRIFT

ter verkrijging van de graad van doctor
aan de Universiteit van Amsterdam
op gezag van de Rector Magnificus
prof. dr. ir. P.P.C.C. Verbeek

ten overstaan van een door het College voor Promoties ingestelde
commissie,

in het openbaar te verdedigen in de Agnietenkapel
op vrijdag 6 oktober 2023, te 16.00 uur

door

Julia Eder
geboren te Schwarzach im Pongau

Promotiecommissie

| | | |
|-----------------------|------------------------------|---------------------------------------|
| Promotor: | prof. dr. T.B.H. Geijtenbeek | AMC-UvA |
| Copromotor: | dr. N.A. Kootstra | AMC-UvA |
| Overige leden: | prof. dr. M. van Egmond | Vrije Universiteit Amsterdam |
| | dr. K. Strijbis | Universiteit Utrecht |
| | prof. dr. D. Pajkrt | AMC-UvA |
| | prof. dr. M.D. Hazenberg | AMC-UvA |
| | dr. J. den Dunnen | AMC-UvA |
| | prof. dr. D. Wilflingseder | Medizinische Universität Innsbruck |

Faculteit der Geneeskunde

“A certain type of perfection can only be realized through a limitless accumulation of the imperfect.”

— Haruki Murakami, *Kafka on the Shore*

Table of contents

| | | |
|------------------|---|-----|
| CHAPTER 1 | General Introduction | 9 |
| CHAPTER 2 | Transmission of Zika virus by dendritic cell subsets in skin and vaginal mucosa <i>Frontiers in Immunology, 2023</i> | 39 |
| CHAPTER 3 | Immune activation of vaginal human Langerhans cells increases susceptibility to HIV-1 infection <i>Scientific Reports, 2023</i> | 73 |
| CHAPTER 4 | SARS-CoV-2 infection activates dendritic cells via cytosolic receptors rather than extracellular TLRs <i>European Journal of Immunology, 2022</i> | 97 |
| CHAPTER 5 | Syndecan 4 upregulation on activated Langerhans cells counteracts langerin restriction to facilitate Hepatitis C virus transmission <i>Frontiers in Immunology, 2020</i> | 119 |
| CHAPTER 6 | Infection and transmission of SARS-CoV-2 depend on heparan sulfate proteoglycans <i>EMBO Journal, 2021</i> | 147 |
| CHAPTER 7 | Inhalation of Low Molecular Weight Heparins as prophylaxis against SARS-CoV-2 <i>mBio, 2022</i> | 183 |
| CHAPTER 8 | General Discussion | 215 |
| ADDENDUM | | 239 |
| | Summary | 240 |
| | Samenvatting | 243 |
| | PhD Portfolio | 246 |
| | List of publications | 249 |
| | Curriculum Vitae | 250 |
| | Acknowledgements | 251 |



CHAPTER

General Introduction

1

Global pandemics start small. It only takes a person, a virulent pathogen and the right conditions for transmission to others. Our globalized world does not only make human transport convenient but also supports rapid, worldwide spread of viruses. As an example, during the COVID19 pandemic, caused by SARS-CoV-2, it took only little over three months to move from the first local COVID19 cases in Wuhan, China in November of 2019 to the declaration of a global pandemic. SARS-CoV-2 is transmitted from person-to-person primarily through aerosols and droplets and causes mild symptoms in the majority of the population. These factors have contributed to widespread and rapid transmission of SARS-CoV-2. However, in the past, viral pandemics have also been caused by viruses that transmit through completely different mechanisms. What these mechanisms are, what host defenses we got to protect ourselves from these viruses and what therapeutic strategies can be employed to assist our defenses, are part of this thesis and are discussed in the following chapters.

The barrier against (pandemic) viruses

Humans have many defenses to protect against infection with viral pathogens. These defenses can be mechanical, chemical and immunological and are all found at barrier tissues. Barrier tissues are the external surfaces of mammalian hosts and form an important interface with the environment ¹. The main barriers include the skin as well as mucosal surfaces that line all internal surfaces like the intestines, respiratory and genital tract ² (**Figure 1**). All barrier tissues are composed of an outer epithelial layer of highly specialized cells organized either into a monolayer (intestines) ³, pseudo-stratified (airways) ⁴ (**Figure 1A**) or stratified (skin and vagina) ^{5, 6} (**Figure 1B and C**) epithelium. Mucosal surfaces can further be divided into those covered by simple type I epithelia that only constitute one cell layer (intestines and lung) and multilayered squamous type II epithelia (oral cavity and vagina) that share close similarities with skin ⁷. These epithelial layers constitute a physical barrier to the environment. The skin is further inhabited by millions of beneficial microorganisms ⁸, whereas mucosal surfaces are covered by a protective layer of microorganism-harboring mucus ^{9, 10} with both providing chemical as well as immunological protection. This community of microorganisms in various internal environments and the skin is called microbiota and contributes to host immunity during healthy conditions ¹¹ while dysbiosis can lead to higher susceptibility to invading pathogens and disease exacerbation ^{12, 13}. Underlying the epithelial layer, dermis and lamina propria harbor a wide variety of resident and migratory immune cells. These include dendritic cells (DCs), T cells, B cells and macrophages that work in assent to mount immune responses and promote homeostasis (**Figure 1A-C**) ^{14, 15}. Even though barrier tissues have many overlapping characteristics and functions, they contain tissue-specific cells and respond to defined challenges in a specialized manner ^{14, 16}.

Thus, barrier tissues protect human hosts from invasion of harmful pathogens like viruses. However, viruses have evolved different strategies to overcome host defenses provided at barrier tissues in order to establish disease in humans nonetheless¹⁷.

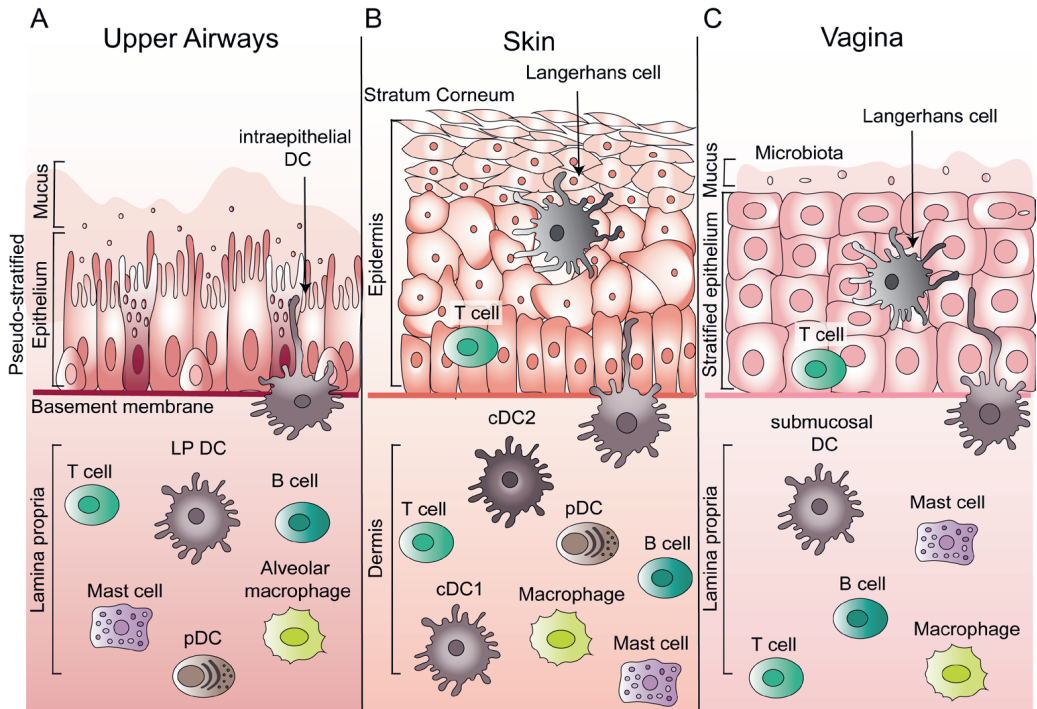


Figure 1 | Barrier tissues between hosts and viruses. (A) The upper airway epithelium constitutes a pseudo-stratified monolayer of cells covered by mucus. The lamina propria below the airway epithelial is home to lamina propria DCs, B cells, T cells, Mast cells, alveolar macrophages and pDCs. (B) The skin is composed of two layers: the epidermis and dermis. Epidermis is made up of multiple layers of stratified epithelial cells with the stratum corneum as a layer of dead cells on top. In the epidermis, immune cells are rare except for Langerhans cells and T cells. On the contrary, the dermis harbors an array of different immune cells including cDC1 and cDC2. (C) The vaginal mucosa as part of the genital tract constitutes multiple layers of stratified squamous type II epithelia covered by mucus. The epithelial layer is similar to epidermis and harbors LCs and T cells but few other immune cells. The mucus is colonized by different species of microbes that together make up the microbiota. Below the epithelial layer, lamina propria host immune cells. LP DC: Lamina Propria Dendritic cell; pDC: plasmacytoid DC; cDC: classical DC

Viral mechanisms of breaching barrier tissues

In order to infect susceptible target cells, viruses need to pass barrier tissues like skin, respiratory tract, gastrointestinal tract or genital tract^{7, 18}. Respiratory viruses target mucosal airway surfaces^{19, 20} whereas epitheliotropic viruses cross the skin barrier either with the help of a vector or after rupture to the epidermis²¹. Sexually transmitted viruses

enter through anogenital mucosa^{22,23}.

This thesis contains research on four viruses: SARS-CoV-2, Zika virus, HIV-1 and HCV that have acquired mechanisms to cross one or more of these barrier tissues to establish infections in human hosts. SARS-CoV-2, HIV-1 and HCV have caused global pandemics within the past decades and the Zika virus epidemic was declared a Public Health Emergency of International Concern by the WHO in 2016. Each of these four viruses is a threat to global public health with high morbidity and/or mortality. The mode of transmission employed by different viruses determines which barrier tissues are encountered. Viruses can be transmitted through direct contact between individuals including droplet expulsion and sexual intercourse, while indirect transmission occurs between an individual and contaminated agents (blood) or objects (fomites). Moreover, viruses can indirectly be spread through aerosols suspended in the air or through engagement of arthropod vectors²⁴. Importantly, many viruses are not restricted to only one mode of transmission and hence are also able to cross multiple host barrier tissues.

SARS-CoV-2 infects mucosal tissues of the respiratory tract

The respiratory tract is a common entry portal for viruses and can be reached through direct as well as indirect contact²⁵. Airborne viruses and those transmitted via fomites or aerosolized droplets encounter mucosal tissues of the upper and lower respiratory tract that include the nose, pharynx and lungs (**Figure 2A**)²⁶. Severe acute respiratory syndrome coronavirus 2 (SARS-CoV-2) is a recently emerged respiratory virus that causes coronavirus disease 2019 (COVID19)²⁷. Initially isolated from pneumonia patients in China at the end of 2019²⁸, SARS-CoV-2 rapidly spread around the world and led to a global pandemic characterized by large infection numbers and significant morbidity. Since 2019, almost 800 million people have tested positive for SARS-CoV-2 infection and nearly seven million people have died from consequences relating to COVID19²⁹. Even though the widespread distribution of vaccines against SARS-CoV-2 has heavily curbed the pandemic impact^{30,31}, the emergence of new variants of concern (VoC) that are more contagious and less susceptible to current vaccines or neutralizing antibodies^{32,33,34}, underscore the continuous threat SARS-CoV-2 poses for global health. One of the main reasons for the remarkably successful spread of SARS-CoV-2 is its mode of transmission and viral uptake into susceptible hosts. The main route for SARS-CoV-2 transmission is respiratory where people infected with SARS-CoV-2 expel droplets and small aerosols filled with viral particles through coughing, sneezing or singing^{35,36,37}. Subsequently, SARS-CoV-2 is taken up through mucosal surfaces of the upper respiratory tract through inhalation or contact with droplets or contaminated surfaces³⁸. Once the mucosal barrier is reached, SARS-CoV-2 preferentially infects respiratory epithelial cells, including ciliated cells in the nose and type II alveolar cells in the lung^{39,40,41}. The obligate infection receptor for SARS-CoV-2 is angiotensin-converting enzyme-2 (ACE-2), which is engaged by the SARS-CoV-2 Spike (S) protein receptor-binding

domain (RBD) for entry into human cells⁴². Following ACE-2 engagement, SARS-CoV-2 S protein is primed and cleaved by transmembrane protease, serine 2 (TMPRSS2) at the cell surface⁴³ or cathepsin L in lysosomes⁴⁴. ACE-2 is expressed on a wide range of cells and medium expression levels are detected in the lungs, colon and liver while small intestine, testis and kidneys expressing the highest ACE-2 levels⁴⁵. SARS-CoV-2 infection and pathogenicity have primarily been observed in respiratory tissues, close to viral entry sites. However, SARS-CoV-2 has also been detected in other tissues like intestine, kidneys and heart, indicating multi-organ invasion⁴⁶. In order to reach tissues not belonging to the respiratory tract, SARS-CoV-2 therefore needs to be spread throughout the body.

Zika virus utilizes arthropods for transmission

Many viruses do not rely on direct or indirect contact transmission and instead employ arthropod vectors⁴⁷. Zika virus is an enveloped, single stranded RNA virus that belongs to the family of Flaviviridae. The main transmission route of Zika virus is transfer through the epidermis via mosquito vectors taking a blood meal⁴⁸ (**Figure 2B**). However, Zika virus also uses alternate transmission routes like *in utero* from mother to child through crossing of the maternal fetal barrier⁴⁹. Zika virus has been found in amniotic fluid of infected pregnant women as well as fetal brain tissue^{50, 51}, indicating successful viral transfer to the unborn fetus. While the exact mechanisms for transfer through the maternal-fetal barrier are still unclear, Zika virus infects primary placental cells like trophoblasts and Hofbauer cells and induces damage in placentae of women infected with Zika virus^{52, 53, 54}. Infection during pregnancy is associated with severe neurological malformations in the developing fetus and increased risk of miscarriage^{55, 56}, which makes this virus in particular dangerous for unborn fetuses and pregnant women. In addition to vector-borne and vertical transmission from mother-to-child, Zika virus is also spread from person-to-person during sexual contact⁴⁹. Infectious virus and Zika virus RNA can persist in semen for several weeks^{57, 58} posing a risk for transmission to a sexual partner long after initial exposure. To a lesser extent, Zika virus also presents in cervicovaginal fluid^{58, 59, 60}. Sexual transmission of Zika virus has been reported for male-to-male, male-to-female and female-to-male contact⁶¹ with Zika virus transmission from male to female being more likely than vice versa⁶¹. Sexual transmission of Zika virus might therefore contribute to higher disease incidence observed in women compared to men⁶². In adults, Zika virus primarily induces asymptomatic or mild disease⁶³ but has also been associated with triggering Guillain Barré Syndrome⁶⁴. Once the skin or mucosal barrier is crossed, Zika virus exhibits a broad cell tropism⁶⁵. Cell entry of Zika virus is linked to Clathrin-mediated cytosin and attachment to negatively charged Glycosaminoglycans (GAGs). It is likely that Zika virus utilizes a combination of receptors and host proteins to gain cell entry⁶⁶. One of the putative entry receptors for Zika virus is AXL, a receptor tyrosine kinase that is highly expressed on glial cells⁶⁷. However, the role of AXL is not entirely clear as AXL knockouts do not abrogate Zika virus infection in mice⁶⁸, and AXL

instead might aid infection through attenuation of type I interferon responses⁶⁹. Another proposed candidate for Zika virus entry is Neural Cell Adhesion Molecule (NCAM1)⁷⁰. Yet further research is needed to clearly ascertain Zika virus infection receptors on different target cells. Zika virus infection has been observed for various brain cells expressing high levels of AXL and NCAM1 like neuronal progenitor cells, radial glia cells and astrocytes⁷¹. However, since these cells are not located at Zika virus entry sites, the virus first needs to be disseminated to these target tissues. The ability to employ multiple modes of transmission and subsequently cross different barrier tissues suggest that different cells are targeted for dissemination. Hence it is important to understand which cells are involved in the different tissues encountered by Zika virus and what common features they share.

HIV-1 and HCV are sexually transmitted via vaginal and anorectal tissues

During sexual transmission, viruses are present in bodily fluids like semen, vaginal fluids or blood and are taken up through mucosal surfaces in the vagina, rectum or foreskin^{23, 72, 73} (**Figure 2C**). Human immunodeficiency virus 1 (HIV-1) is, when left untreated, the virus with the highest morbidity and mortality amongst sexually transmitted infections (STIs)^{74, 75, 76}. HIV-1 is a blood-borne, sexually transmitted RNA virus and the causative agent for Acquired Immunodeficiency Syndrome (AIDS)^{77, 78}. HIV-1 is mostly transmitted through sexual contact^{23, 79, 80}, while other transmission routes include direct blood-blood contact through blood transfusions or sharing of contaminated intravenous drug injection equipment^{81, 82} and from mother to child *in utero* during birth or while breastfeeding^{83, 84}. HIV-1 remains a global health problem, especially in young women in sub-Saharan Africa who are at a disproportionally higher risk of acquiring HIV-1 than their male peers⁸⁵. This increased risk for women to acquire HIV-1 is partially attributed to their comparably larger genital mucosal surface area, difficulties in diagnosing STIs and increased likelihood of tissue damage during sexual intercourse⁸⁶. Microbiome diversity, co-infection and genital inflammation strongly increase the risk of vaginal HIV-1 acquisition and make the tissue an important target for HIV-1 prevention^{12, 87, 88, 89, 90}. The HIV-1 envelope glycoproteins gp120 and gp41 mediate attachment and membrane fusion to target cells^{91, 92}. The main receptor for HIV-1 is CD4 and, depending on the genetic makeup of the viral envelope, CCR5 (R5) or CXR4 (X4) are major co-receptors for successful viral internalization^{93, 94, 95, 96}. HIV-1 mainly infects CD4+ T cells, which eventually leads to severe depletion of these cells^{97, 98}. However, CD4 and HIV-1 co-receptors CCR5 and CXR4 are also expressed on other immune cells including DCs⁹⁹, making them important HIV-1 target cells. Upon sexual transmission, HIV-1 infection is not a very efficient process since mucosal tissues do not harbor a plethora of target cells and restrictive mechanisms in immune cells can prevent infection. However, changes in the environment and co-infections strongly enhance the risk of HIV-1 infection, which indicates an important opportunity for prevention.

Another blood-borne virus is Hepatitis C virus (HCV). HCV is a Flavivirus and contains a positive-sense RNA genome covered by an envelope¹⁰⁰. Infection with HCV causes both acute and chronic liver infection and even though about 30% of people with acute HCV infection clear the virus, approximately 58 million people are living with chronic hepatitis¹⁰¹. HCV transmission occurs primarily through contact with infected blood during drug injection, tattooing or piercing, intranasal cocaine use and vertically from mother to child^{102, 103, 104, 105, 106, 107, 108}. Importantly, over the past 20 years, HCV has emerged as a sexually transmitted virus, particularly amongst HIV-1 positive men who have sex with men (MSM)^{109, 110, 111}. However, while HIV-1 status in MSM was thought to be an important to HCV susceptibility, these claims were later weakened as HIV-1 negative MSM are at similar risk of HCV infection through sexual contact^{112, 113}. Instead, high-risk unprotected sexual

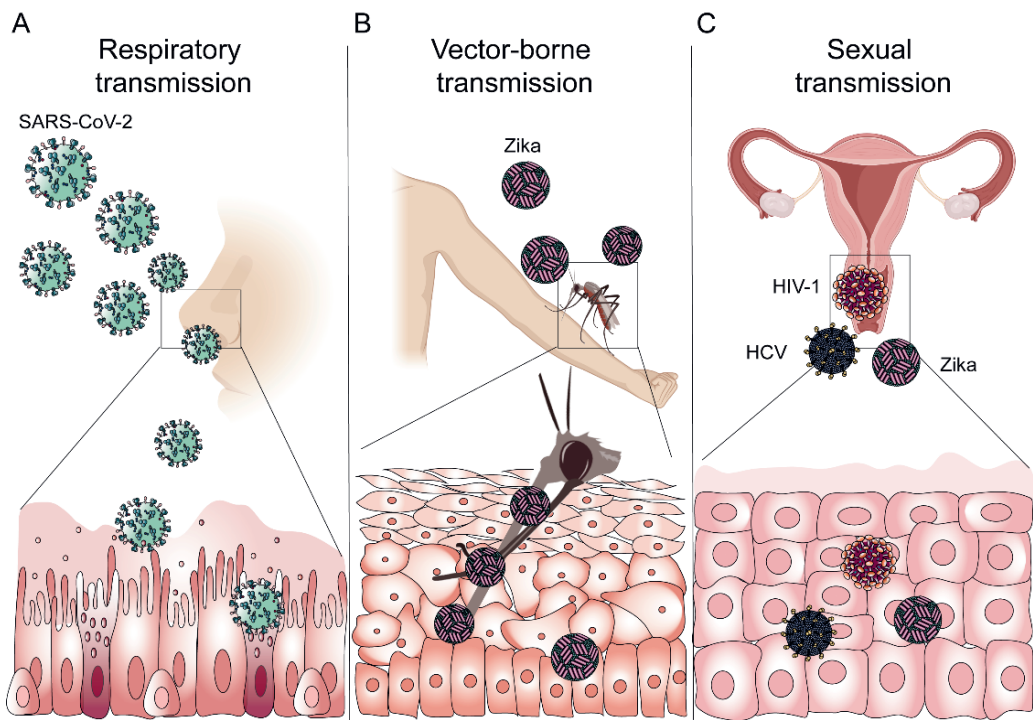


Figure 2 | Viral pathogens reach and breach barrier tissues. (A) Respiratory viruses like SARS-CoV-2 are primarily transmitted via aerosolized droplets and aerosols expelled by infected people or through fomites. Upon contact with contaminated air or objects, SARS-CoV-2 is taken up by mucosal tissues of the upper and lower respiratory tract. These tissues include the nose, mouth, pharynx and lungs. (B) Vector-borne viruses utilize animals to initiate barrier breach of human tissues. Zika virus is injected into the epidermis and dermis during the blood meal of an infected mosquito. (C) During sexual contact, viruses like HIV-1, HCV and Zika virus are transmitted with the aid of bodily fluids like semen, blood and vaginal secretions. These bodily fluids transport the viruses to the mucosal surfaces of vagina and rectum where they breach the barrier and come into contact with susceptible target cells. SARS-CoV-2: Severe Acute Respiratory Virus; HIV: Human Immunodeficiency virus; HCV: Hepatitis C virus Created with Biorender.com

practices and traumatic injury to tissues in the rectum and anogenital mucosa are likely contributing to sexual transmission of HCV^{72, 109, 112}. The HCV entry process requires multiple steps and utilizes numerous host proteins and receptors^{114, 115, 116}. The HCV envelope glycoproteins E1 and E2 interact with CD81 and scavenger receptor class B type I, for cell entry^{117, 118}. Additionally, the tight junction proteins claudin-1, -6 and -9 as well as occludin are important HCV entry co-receptors^{119, 120}. The liver is the main target organ for HCV with hepatocytes being the main target cells for HCV¹²¹. However, besides hepatocytes, circulating DCs have been described as HCV targets and potential viral reservoirs¹²², postulating a role for DCs to facilitate viral transfer from mucosal entry sites to the liver. In conclusion, viruses need to cross barrier tissues they encounter in order to enter and infect the human host with many viruses being able to cross multiple different host barrier tissues. However, immune cells present in barrier tissues at the site of virus entry can protect the host from infection.

Dendritic cell subsets patrol barriers against invading viruses

Due to their constant exposure to external stimuli, stress signals and pathogens, barrier tissues are some of the most immunologically active sites of the body and need continuous monitoring by the immune system¹²³. In case of a barrier invasion, epithelial and immune cells cooperate in order to prevent infection and promote tissue healing¹⁴. Within barrier tissues, numerous cells of the immune system stand guard to protect from external and internal threats alike. One of the most important cells found in barrier tissues are dendritic cells (DCs).

DCs are characterized as phagocytic cells with dendritic or stellate protrusions¹²⁴ and encompass a heterogeneous group of antigen presenting cells (APCs) that link innate and adaptive immune responses^{125, 126}. Depending on the tissue, different DC subsets with specialized functions are present, either as resident cells or following migration^{127, 128, 129}. Location and tissue residency further influence the phenotype and function of different DC subsets¹³⁰. DCs are primarily categorized into conventional or “classical” DCs (cDCs), plasmacytoid DCs (pDCs), monocyte-derived DCs (moDCs) and Langerhans cells (LCs)^{127, 131, 132}. Each DC subset is equipped with unique features that allow for an efficient response toward immune challenges¹²⁷.

Classical DC (cDC) and plasmacytoid DC (pDC)

cDCs are present in lymphoid and non-lymphoid tissues alike that efficiently present exogenous antigens and excel at cross-presentation^{133, 134}. They can be further sub-divided into type 1 cDCs (cDC1) and type 2 (cDC2)^{132, 135}. cDC1 express CD141, and XCR1 and are

superior at cross-presentation of antigens^{133, 136} whereas the CD1c, BDCA1 expressing cDC2 are imperative for Th17 differentiation¹³⁷. Both cDC1 and cDC2 are resident cells in the dermis of skin (**Figure 1B**)¹³⁸. Unlike cDCs, pDCs make up a distinct, bone marrow derived class of DCs that are primarily located in blood and lymphoid organs¹³⁹. pDCs are recognized for producing large amounts of type I interferons in response to viral infections^{140, 141} even though they only make up around 0.2%-0.8% of peripheral blood mononuclear cells^{142, 143}. Moreover, pDCs activate Natural Killer (NK) cells and induce differentiation of antibody-producing plasma cells^{144, 145}. While cDCs are continuously found in dermis and lamina propria of mucosal tissues, pDCs are recruited during inflammation, injury or infection^{146, 147, 148}. However, both cell types are important in viral defense and antigen presentation in barrier tissues.

Monocyte-derived DC (moDC)

moDCs are closely related to cDCs, with whom they share the ability to capture and present antigens and subsequently stimulate T cells^{149, 150, 151}. Moreover, moDCs express MHC class I and class II molecules, allowing them to present and cross present antigens to both CD4+ and CD8+ T cells and promoting T cell differentiation into effector cells^{152, 153}. Monocytes can differentiate into DCs *in vivo*¹⁵⁴ and are important during infection^{151, 155} and inflammation^{156, 157}. Importantly, moDCs can also be generated *in vitro* through stimulation with granulocyte colony-stimulating factor (GM-CSF) and interleukin 4 (IL-4), as first described in 1994¹⁵⁰ and which has since become common research practice. Differentiating moDCs from blood monocytes allows for large quantities of cells^{158, 159} that express an immature phenotype^{150, 160}. Importantly, their convenient use in *in vitro* settings and closely related phenotype to the less abundant cDCs make them invaluable tools to study host defense mechanisms.

Langerhans cell (LC)

LCs are tissue-resident DCs that form a dense network in the epidermis of skin and stratified epithelia of mucosal tissues (**Figure 1B-C**)^{7, 161, 162}. Unlike other DC subsets that develop from bone marrow progenitors^{163, 164}, LCs are seeded into skin and mucosa from fetal liver and yolk sac precursors during embryonic development and repopulate locally^{165, 166}. In the skin, LCs have an immature phenotype but the cells mature upon migration to lymph nodes^{167, 168}. LCs are characterized by their expression of the CLR langerin and Birbeck granules^{169, 170}. Birbeck granules are specialized rod shaped organelles that act as endosomal recycling compartments and are linked to langerin accumulation¹⁷¹. LCs are ideally positioned for defense against invading pathogens. However, the role of LCs upon viral infection is two-fold and can lead either to viral degradation or infection and viral dissemination^{172, 173}. Hence LCs are the most controversial DC subset due to their differences to other DC subsets

both in morphology as well as functionality. Thus, barrier tissues harbor a plethora of different DC subsets that play an important role host defense and viral protection.

DCs protect against viruses at the barrier

In skin and mucosal tissues, DCs act as tissue sentinels and are the first line of defense against invading pathogens^{174, 175, 176}. The main function of DCs is to sense, capture and transport invading pathogens to lymph nodes before presenting their antigens to naïve T lymphocytes^{177, 178}. Beyond priming of naïve T and B cells, DCs lead to the activation of a number of innate and adaptive immune responses by secretion of cytokines and inflammatory mediators¹⁷⁷.

To this end, DCs are ideally equipped to continuously sample foreign molecules in barrier tissues by engaging their pathogen recognition receptors (PRRs). PRRs include C-type lectin receptors (CLRs), Toll-like receptors (TLRs) and RIG-I-like receptors (RLRs). By means of these receptors, DCs sense pathogen-associated molecule patterns (PAMPs)¹⁷⁹. CLRs are cell surface PRRs that recognize carbohydrate structures with high affinity in a calcium-dependent manner upon which various innate signaling pathways are activated¹⁸⁰. Signaling through CLR pathways induces specific cellular immune responses either independently or through crosstalk with other PRRs¹⁸¹. Different DC subsets express distinct CLR subsets¹⁸² that likely influence pathogen recognition and subsequent immune responses. Contrary to CLRs, TLRs not only localize on the cell surface but also intracellularly on endosomes. While cell surface TLRs recognize microbial proteins, lipoproteins and lipids from both bacteria and viruses, intracellular TLR sense nucleic acids^{183, 184, 185}. The specific TLRs activated by pathogenic products therefore influence cell signaling, corresponding immune activation and cytokine production^{186, 187}. RLRs are only found in the cytosol and compose a group of cytosolic RNA helicase proteins sensing nucleic acids. RLRs sense viral RNA upon which they induce strong anti-viral immune responses^{188, 189}. Thus, interaction of PRRs with (viral) pathogens on DCs releases inflammatory molecules and mediators that shape the innate and adaptive immune response. These include interferons (IFNs), a potent class of inflammatory cytokines that interfere with viral replication^{190, 191}. There are three types of IFNs, of which type I IFNs are paramount in viral defense and primarily induced by DCs. Type I IFNs encompass IFN-alpha (IFN α) and IFN-beta (IFN β) that are secreted by various DC subsets^{192, 193, 194}. Secreted IFN α /b proteins in turn trigger the induction of a plethora of interferon stimulated genes (ISGs)¹⁹⁵ by binding cell surface heterodimeric transmembrane IFN receptors (IFNARs)¹⁹⁶. ISGs are restriction factors that exhibit direct antiviral properties and attack specific phases of the viral life cycle^{197, 198}. Type I IFN secretion further indirectly advances antiviral immune responses through activation of proximate DCs^{199, 200} and polarization of T cells²⁰¹. In summary, DCs at barrier tissues are well equipped to induce strong antiviral responses upon infection and are crucial in curbing

virus replication and spread. However, viruses have developed a myriad of strategies to alter, counteract or control DC activation and type I IFN responses for their own benefit.

DCs promote viral dissemination from the barrier

Depending on the virus, DC subset and receptors involved, virus-host interactions can result in vastly different outcomes. While their prime location and ability to sense and capture viruses make DCs ideal host sentinels with a crucial role in immune activation and viral degradation, it also makes them a target for viral exploitation through infection and dissemination. In order to present antigens to T lymphocytes, DCs have to migrate from barrier tissues towards draining lymph nodes²⁰², a feature that can be exploited for viral transfer.

As mentioned above, CRLs are expressed on DCs and in order to mount an effective immune response they capture and internalize invading viruses¹⁸⁰. Binding of viruses to CLR^s primarily results in degradation in lysosomes²⁰³ or autophagosomes¹⁷². However, many viruses have established mechanisms to subvert these degradation pathways and instead exploit CLR internalization for immune evasion and trafficking to susceptible target cells.

Langerin, a CLR highly expressed on LCs¹⁶⁹, exerts an important role in protecting against viruses like HIV-1, through capture and subsequent Trim5 α -induced autophagosomal degradation in Birbeck granules¹⁷². LCs are one of the initial target cells for HIV-1 as well as HCV after sexual exposure and act as a protective barrier against infection due to their largely refractory nature^{22, 204}. However, co-infection, inflammation and activation renders LCs susceptible to HIV-1 infection and transmission^{168, 205, 206}. Similarly, co-infection with HIV-1 allows LCs to transmit HCV to hepatocytes²². These data highlight a controversial role for LCs in viral acquisition and dissemination. While there is ample research on LC/Langerin interaction with HIV-1, there is little known about their role in the dissemination of other viruses like HCV, Zika virus and SARS-CoV-2, a gap that is discussed further in this thesis.

moDCs express high levels of Dendritic-cell-specific ICAM-3 grabbing nonintegrin (DC-SIGN)²⁰⁷. This CLR is expressed on various DC subset *in vivo*¹⁵⁵ and *in vitro*^{208, 209}. Besides DCs, DC-SIGN is also expressed on tissue specific macrophages but not LCs^{207, 210, 211, 212}. DC-SIGN is well-known to facilitate virus binding^{213, 214, 215}. To date, HIV-1 is one of the best studied viruses known to circumvent DC-SIGN mediated degradation. DCs harbor intact HIV-1 particles intracellularly while migrating to draining lymph nodes and transfer intracellular stored or newly produced HIV-1 to T cells^{213, 216, 217}. Upon DC-SIGN internalization into a non-lysosomal compartment, HIV-1 particles remain infectious^{207, 218}. Similar mechanisms have been described for HCV internalization into DCs with subsequent protection in endosomal compartments^{122, 219}. Zika virus has been shown to bind DC-SIGN *in vitro* which mediated infection^{220, 221}, yet it remains unclear what happens to Zika virus upon internalization. SARS-CoV-2 also binds DC-SIGN, thereby enhancing ACE-2 mediated internalization²²². While, little is known about subsequent internalization or degradation of

SARS-CoV-2, evidence suggests that SARS-CoV-2 is unable to use DC-SIGN for infection ²²³. The ability of DCs to migrate to lymph nodes, in combination with the attraction of cells and formation of "infectious synapses" ^{224, 225} make them a particularly efficient tool for spread of virus to target cells not located at initial viral entry sites. DCs can transfer viruses via two different pathways: *cis* and *trans* ^{226, 227} (**Figure 3**) whereas LCs primarily transfer viruses in *cis* ^{73, 228}. *Cis*-transmission refers to the transfer of progeny virus and requires DCs to become productively infected before *de novo* produced virions infect target cells ²²⁴ (**Figure 3A**). During *trans*-infection, viruses are transferred to target cells independently of viral replication ²²⁶. *Trans*-infection involves the capture of viruses, internalization into "safe" endosomal compartments within the cell and subsequent transfer of the intact viral particle to preferred target cells without becoming infected themselves (**Figure 3B**) ^{213, 219, 229} which is particularly interesting for viruses that cannot infect DCs. For example, SARS-CoV-2 is able to use DCs for *trans*-infection of other, more susceptible, target cells ²²³. Besides DC-SIGN however, this process might be facilitated by Heparan sulfate proteoglycans (HSPGs). HSPGs are transmembrane proteoglycans that are characterized by the attachment of negatively charged heparan sulfate (HS) chains, a type of GAG. HSPGs are primarily signaling and adhesion receptors that interact with a diverse set of extracellular ligands. These ligands can further be transmitted to the intracellular cytoskeleton ²³⁰. This binding is mainly facilitated through binding to their HS chains. Alternatively, HSPGs can also bind ligands with their core proteins, independent of HS ²³¹. One family of type I transmembrane HSPGs are Syndecans. There are four Syndecan members (Syndecan 1 - 4) that differ in cell expression, structure and function. Syndecans are ubiquitously expressed with one or more Syndecan members found on most cells ²³². Syndecan 1 is often enriched on epithelial tissues ²³³ whereas Syndecan 2 is mainly found on mesenchymal and fibroblast cells ²³⁴. Syndecan 3 is highly expressed on neuronal tissues as well as DC subsets ^{235, 236} and Syndecan 4 is the most ubiquitously expressed HSPG and found on most cells co-expressed with other Syndecans, albeit at lower amounts ^{237, 238}. However, Syndecan 4 expression is upregulated in response to inflammatory or infectious stimuli ^{239, 240, 241}. Syndecans primarily function as receptors and co-receptors for growth factors, cytokines and chemokines ^{232, 242}. However, Syndecans can also mediate viral uptake and contribute to cell infections with different Syndecans serving as attachment receptors for viruses ^{235, 243, 244, 245}. These data signify an important role for Syndecans in initiation and establishment of viral infection.

Taken together, different receptors on DCs and LCs mediate infection, dissemination or protection once barrier tissues are invaded by viral pathogens. How these receptors interact with the viruses described in this thesis and what can be done to prevent disease establishment and exacerbation is something we further elucidate in the following chapters.

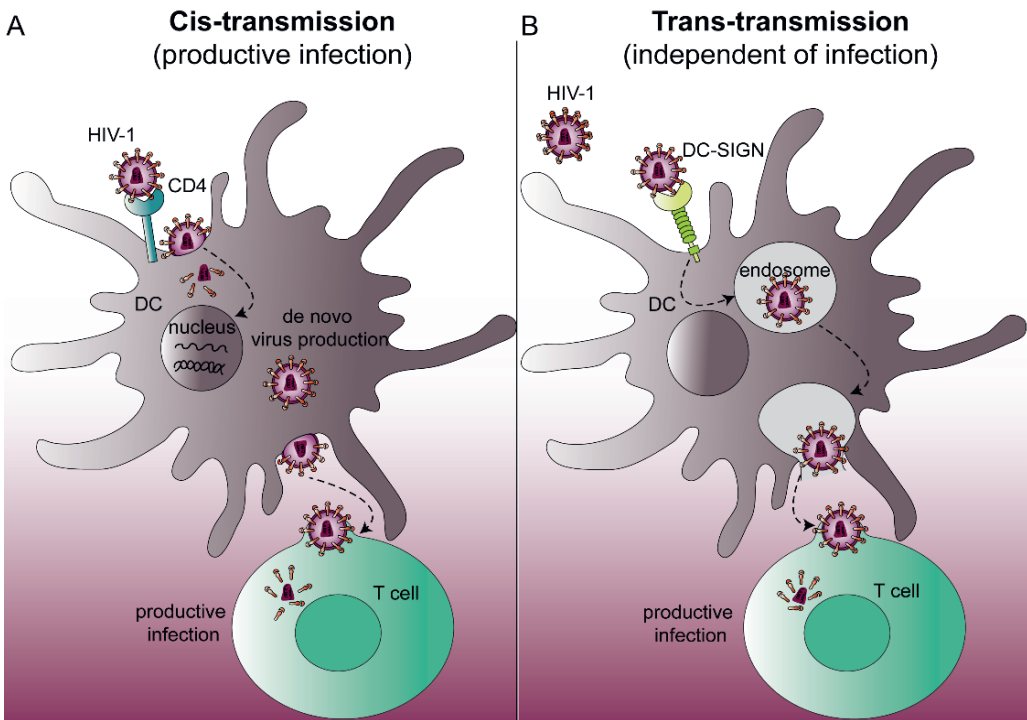


Figure 3 | Dendritic cells enable viral dissemination from barrier site in *cis* and *trans*. (A) Viruses like HIV-1 are transmitted by DCs in *cis* after infection of DCs via CD4. After binding CD4, HIV-1 fuses with the cell membrane and viral RNA integrates into the nucleus where it is transcribed into DNA and integrates into the host genome. This leads to the formation of newly produced replicative virions. These newly formed virions are released from the infected DCs through membrane budding, ready to infect nearby CD4+ T cells. (B) *Trans*-transmission of HIV-1 involves binding to attachment receptors like DC-SIGN and Heparan sulfate proteoglycans. DC-SIGN routes HIV-1 to "safe" endosomal compartments that keep HIV-1 virions intact and infectious. During contact with CD4+ T cells, HIV-1 is released from the endosomal compartment and in turn infects T cells. the infection of DCs via CD4. DC: Dendritic cell, HIV: Human Immunodeficiency virus

Scope of this thesis

This thesis describes research on different viruses and their interaction with a host of human cells located in various barrier tissues. We aimed to better understand what happens during the earliest stages of viral infection and to identify new strategies to prevent infection.

During the Zika virus epidemic in 2016, knowledge about transmission routes were unclear. In **chapter 2** we show how DC subsets in the skin and vaginal mucosa contribute to Zika virus infection and transmission. While monocyte derived DCs (moDC) were readily infected by Zika virus, Langerhans cells (LCs) in the skin and vaginal mucosa did not become infected. However, we observed that both moDCs and LCs transmit Zika virus to target cells, indicating an important role for DC subsets in viral dissemination from barrier tissues to other susceptible organs.

In **chapter 3** we describe the isolation, phenotype and functionality of vaginal LCs with regard to HIV-1 infection. Immature vaginal LCs were poorly susceptible to HIV-1 whereas they became readily infected once activated through tissue migration or TLR stimulation. Unlike skin LCs, vaginal LC expressed TLR4 and were activated by bacterial TLR4 agonists. TLR4 activation of immature vaginal LCs strongly enhanced HIV-1 infection and transmission, suggesting a role for bacterial co-infections in HIV-1 susceptibility.

At the start of the SARS-CoV-2 pandemic, it was suggested that SARS-CoV-2 binds TLR4. However, in **chapter 4** we observe that TLR4 is not involved in sensing SARS-CoV-2. SARS-CoV-2 did neither infect nor activate DCs. Moreover, SARS-CoV-2 did not trigger extracellular TLRs including TLR4. Our data suggest that SARS-CoV-2 escapes immune sensing and thereby might prevent effective immune control of infection.

In **chapter 5** we show that Syndecan 4 is an important receptor for HCV on activated LCs involved in viral capture and transfer to target cells. Importantly, immature LCs did not transmit HCV but activation led to upregulation of Syndecan 4 and subsequent transmission. Early during the SARS-CoV-2 pandemic ACE-2 was identified as the putative infection receptor. In **chapter 6** we identified Syndecan 1 and 4 as crucial attachment receptors for SARS-CoV-2 that aid ACE-2-mediated infection. We identified Heparin and low molecular weight heparins (LMWH) as potent inhibitors of SARS-CoV-2 binding to epithelial cells, supporting a use of LMWH as prophylaxis to prevent SARS-CoV-2 infection.

Therefore, in **chapter 7** we set up a non-randomized controlled trial to study the prophylactic effects of LMWHs in humans. We applied either LMWHs or a placebo into the nose of healthy volunteers and after retrieving nasal epithelial cells with a brush, we incubated them with SARS-CoV-2 and measured virus binding *ex vivo*. We observed lower SARS-CoV-2 binding to LMWH treated cells compared to those receiving placebo but did not observe phenotypic changes in the tissue. This let us to conclude that LMWHs might be easy and safe preventative therapeutic against SARS-CoV-2 infection.

Our findings are discussed in **chapter 8** with regard to transmission by the four viruses, the use of different cell models and primary cells and importance of human volunteer studies over animal studies.

References

1. Moens, E. & Veldhoen, M. Epithelial barrier biology: good fences make good neighbours. *Immunology* **135**, 1-8 (2012).
2. Nel, I., Bertrand, L., Toubal, A. & Lehen, A. MAIT cells, guardians of skin and mucosa? *Mucosal Immunol* **14**, 803-814 (2021).
3. Kong, S., Zhang, Y.H. & Zhang, W. Regulation of Intestinal Epithelial Cells Properties and Functions by Amino Acids. *Biomed Res Int* **2018**, 2819154 (2018).
4. Crystal, R.G., Randell, S.H., Engelhardt, J.F., Voynow, J. & Sunday, M.E. Airway epithelial cells: current concepts and challenges. *Proc Am Thorac Soc* **5**, 772-777 (2008).
5. Anderson, D.J., Marathe, J. & Pudney, J. The structure of the human vaginal stratum corneum and its role in immune defense. *Am J Reprod Immunol* **71**, 618-623 (2014).
6. Roberts, N. & Horsley, V. Developing stratified epithelia: lessons from the epidermis and thymus. *Wiley Interdiscip Rev Dev Biol* **3**, 389-402 (2014).
7. Iwasaki, A. Mucosal Dendritic Cells. *Annual Review of Immunology* **25**, 381-418 (2007).
8. Byrd, A.L., Belkaid, Y. & Segre, J.A. The human skin microbiome. *Nature Reviews Microbiology* **16**, 143-155 (2018).
9. McGuckin, M.A., Lindén, S.K., Sutton, P. & Florin, T.H. Mucin dynamics and enteric pathogens. *Nature Reviews Microbiology* **9**, 265-278 (2011).
10. Vagios, S. & Mitchell, C.M. Mutual Preservation: A Review of Interactions Between Cervicovaginal Mucus and Microbiota. *Front Cell Infect Microbiol* **11**, 676114 (2021).
11. Belkaid, Y. & Hand, T.W. Role of the microbiota in immunity and inflammation. *Cell* **157**, 121-141 (2014).
12. van Teijlingen, N.H. *et al.* Vaginal bacterium *Prevotella timonensis* turns protective Langerhans cells into HIV-1 reservoirs for virus dissemination. *Embo j* **41**, e110629 (2022).
13. Ren, L. *et al.* Dynamics of the Upper Respiratory Tract Microbiota and Its Association with Mortality in COVID-19. *Am J Respir Crit Care Med* **204**, 1379-1390 (2021).
14. Niec, R.E., Rudensky, A.Y. & Fuchs, E. Inflammatory adaptation in barrier tissues. *Cell* **184**, 3361-3375 (2021).
15. Nguyen, A.V. & Soulika, A.M. The Dynamics of the Skin's Immune System. *Int J Mol Sci* **20** (2019).
16. Belkaid, Y. & Naik, S. Compartmentalized and systemic control of tissue immunity by commensals. *Nat Immunol* **14**, 646-653 (2013).
17. Rouse, B.T. & Mueller, S.N. Host Defenses to Viruses.
18. Belkaid, Y. & Artis, D. Immunity at the barriers. *Eur J Immunol* **43**, 3096-3097 (2013).
19. Morrison, C.B. *et al.* SARS-CoV-2 infection of airway cells causes intense viral and cell shedding, two spreading mechanisms affected by IL-13. *Proc Natl Acad Sci U S A* **119**, e2119680119 (2022).
20. Blaas, D. & Fuchs, R. Mechanism of

- human rhinovirus infections. *Mol Cell Pediatr* **3**, 21 (2016).
21. Lei, V., Petty, A.J., Atwater, A.R., Wolfe, S.A. & MacLeod, A.S. Skin Viral Infections: Host Antiviral Innate Immunity and Viral Immune Evasion. *Front Immunol* **11**, 593901 (2020).
 22. Nijmeijer, B.M. *et al.* HIV-1 exposure and immune activation enhance sexual transmission of Hepatitis C virus by primary Langerhans cells. *J Int AIDS Soc* **22**, e25268 (2019).
 23. Tebit, D.M., Ndembi, N., Weinberg, A. & Quiñones-Mateu, M.E. Mucosal transmission of human immunodeficiency virus. *Curr HIV Res* **10**, 3-8 (2012).
 24. Louten, J. Virus Transmission and Epidemiology. *Essential Human Virology*, 71-92 (2016).
 25. Leung, N.H.L. Transmissibility and transmission of respiratory viruses. *Nature Reviews Microbiology* **19**, 528-545 (2021).
 26. Wang, C.C. *et al.* Airborne transmission of respiratory viruses. *Science* **373**, eabd9149 (2021).
 27. Hu, B., Guo, H., Zhou, P. & Shi, Z.-L. Characteristics of SARS-CoV-2 and COVID-19. *Nature Reviews Microbiology* **19**, 141-154 (2021).
 28. Lu, H., Stratton, C.W. & Tang, Y.W. Outbreak of pneumonia of unknown etiology in Wuhan, China: The mystery and the miracle. *J Med Virol* **92**, 401-402 (2020).
 29. WHO. WHO Coronavirus (COVID-19) Dashboard. [Web page] 2023 06.02.2023 [cited 2023 07.02.2023] Available from: <https://covid19.who.int/>
 30. Watson, O.J. *et al.* Global impact of the first year of COVID-19 vaccination: a mathematical modelling study. *Lancet Infect Dis* **22**, 1293-1302 (2022).
 31. Chi, W.-Y. *et al.* COVID-19 vaccine update: vaccine effectiveness, SARS-CoV-2 variants, boosters, adverse effects, and immune correlates of protection. *Journal of Biomedical Science* **29**, 82 (2022).
 32. Lopez Bernal, J. *et al.* Effectiveness of Covid-19 Vaccines against the B.1.617.2 (Delta) Variant. *N Engl J Med* **385**, 585-594 (2021).
 33. Andrews, N. *et al.* Covid-19 Vaccine Effectiveness against the Omicron (B.1.1.529) Variant. *New England Journal of Medicine* **386**, 1532-1546 (2022).
 34. Planas, D. *et al.* Considerable escape of SARS-CoV-2 Omicron to antibody neutralization. *Nature* **602**, 671-675 (2022).
 35. Santarpia, J.L. *et al.* The size and culturability of patient-generated SARS-CoV-2 aerosol. *Journal of Exposure Science & Environmental Epidemiology* **32**, 706-711 (2022).
 36. Duval, D. *et al.* Long distance airborne transmission of SARS-CoV-2: rapid systematic review. *BMJ* **377**, e068743 (2022).
 37. Johnson, T.J. *et al.* Viral load of SARS-CoV-2 in droplets and bioaerosols directly captured during breathing, speaking and coughing. *Scientific Reports* **12**, 3484 (2022).
 38. CDC. Scientific Brief: SARS-CoV-2 Transmission. 2021 May 7, 2021 [cited] Available from: <https://www.cdc.gov/coronavirus/2019>

- ncov/science/science-briefs/sars-cov-2-transmission.html#previous
39. Hou, Y.J. *et al.* SARS-CoV-2 Reverse Genetics Reveals a Variable Infection Gradient in the Respiratory Tract. *Cell* **182**, 429-446.e414 (2020).
 40. Ahn, J.H. *et al.* Nasal ciliated cells are primary targets for SARS-CoV-2 replication in the early stage of COVID-19. *J Clin Invest* **131** (2021).
 41. Mulay, A. *et al.* SARS-CoV-2 infection of primary human lung epithelium for COVID-19 modeling and drug discovery. *Cell Rep* **35**, 109055 (2021).
 42. Shang, J. *et al.* Structural basis of receptor recognition by SARS-CoV-2. *Nature* **581**, 221-224 (2020).
 43. Hoffmann, M. *et al.* SARS-CoV-2 Cell Entry Depends on ACE2 and TMPRSS2 and Is Blocked by a Clinically Proven Protease Inhibitor. *Cell* **181**, 271-280.e278 (2020).
 44. Ou, X. *et al.* Characterization of spike glycoprotein of SARS-CoV-2 on virus entry and its immune cross-reactivity with SARS-CoV. *Nature Communications* **11**, 1620 (2020).
 45. Li, M.-Y., Li, L., Zhang, Y. & Wang, X.-S. Expression of the SARS-CoV-2 cell receptor gene ACE2 in a wide variety of human tissues. *Infectious Diseases of Poverty* **9**, 45 (2020).
 46. Liu, J. *et al.* SARS-CoV-2 cell tropism and multiorgan infection. *Cell Discovery* **7**, 17 (2021).
 47. Rosenberg, R. & Beard, C.B. Vector-borne infections. *Emerg Infect Dis* **17**, 769-770 (2011).
 48. Malone, R.W. *et al.* Zika Virus: Medical Countermeasure Development Challenges. *PLoS Negl Trop Dis* **10**, e0004530 (2016).
 49. Gregory, C.J. *et al.* Modes of Transmission of Zika Virus. *J Infect Dis* **216**, S875-s883 (2017).
 50. Mlakar, J. *et al.* Zika Virus Associated with Microcephaly. *New England Journal of Medicine* **374**, 951-958 (2016).
 51. Mercado, M. *et al.* Zika virus detection in amniotic fluid and Zika-associated birth defects. *Am J Obstet Gynecol* **222**, 610.e611-610.e613 (2020).
 52. Rabelo, K. *et al.* Zika Induces Human Placental Damage and Inflammation. *Front Immunol* **11**, 2146 (2020).
 53. Tabata, T. *et al.* Zika Virus Targets Different Primary Human Placental Cells, Suggesting Two Routes for Vertical Transmission. *Cell Host Microbe* **20**, 155-166 (2016).
 54. Sheridan, M.A. *et al.* Vulnerability of primitive human placental trophoblast to Zika virus. *Proc Natl Acad Sci U S A* **114**, E1587-e1596 (2017).
 55. Brasil, P. *et al.* Zika Virus Infection in Pregnant Women in Rio de Janeiro. *N Engl J Med* **375**, 2321-2334 (2016).
 56. Schaub, B. *et al.* Late miscarriage: another Zika concern? *Eur J Obstet Gynecol Reprod Biol* **207**, 240-241 (2016).
 57. Atkinson, B. *et al.* Presence and Persistence of Zika Virus RNA in Semen, United Kingdom, 2016. *Emerg Infect Dis* **23**, 611-615 (2017).
 58. Reyes, Y. *et al.* Prolonged Shedding of Zika Virus RNA in Vaginal Secretions, Nicaragua. *Emerg Infect Dis* **25**, 808-810 (2019).
 59. Nicastrì, E., Castillettì, C., Balestra, P.,

- Galgani, S. & Ippolito, G. Zika Virus Infection in the Central Nervous System and Female Genital Tract. *Emerg Infect Dis* **22**, 2228-2230 (2016).
60. Murray, K.O. *et al.* Prolonged Detection of Zika Virus in Vaginal Secretions and Whole Blood. *Emerg Infect Dis* **23**, 99-101 (2017).
61. Major, C.G. *et al.* Risk Estimation of Sexual Transmission of Zika Virus—United States, 2016–2017. *The Journal of Infectious Diseases* **224**, 1756-1764 (2021).
62. Coelho, F.C. *et al.* Higher incidence of Zika in adult women than adult men in Rio de Janeiro suggests a significant contribution of sexual transmission from men to women. *Int J Infect Dis* **51**, 128-132 (2016).
63. Haby, M.M., Pinart, M., Elias, V. & Reveiz, L. Prevalence of asymptomatic Zika virus infection: a systematic review. *Bull World Health Organ* **96**, 402-413d (2018).
64. Cao-Lormeau, V.M. *et al.* Guillain-Barré Syndrome outbreak associated with Zika virus infection in French Polynesia: a case-control study. *Lancet* **387**, 1531-1539 (2016).
65. Ngonu, A.E. & Shresta, S. Immune Response to Dengue and Zika. *Annu Rev Immunol* **36**, 279-308 (2018).
66. Agrelli, A., de Moura, R.R., Crovella, S. & Brandão, L.A.C. ZIKA virus entry mechanisms in human cells. *Infect Genet Evol* **69**, 22-29 (2019).
67. Meertens, L. *et al.* Axl Mediates ZIKA Virus Entry in Human Glial Cells and Modulates Innate Immune Responses. *Cell Rep* **18**, 324-333 (2017).
68. Wang, Z.Y. *et al.* Axl is not an indispensable factor for Zika virus infection in mice. *J Gen Virol* **98**, 2061-2068 (2017).
69. Chen, J. *et al.* AXL promotes Zika virus infection in astrocytes by antagonizing type I interferon signalling. *Nat Microbiol* **3**, 302-309 (2018).
70. Srivastava, M. *et al.* Chemical proteomics tracks virus entry and uncovers NCAM1 as Zika virus receptor. *Nature Communications* **11**, 3896 (2020).
71. Komarasamy, T.V., Adnan, N.A.A., James, W. & Balasubramaniam, V. Zika Virus Neuropathogenesis: The Different Brain Cells, Host Factors and Mechanisms Involved. *Front Immunol* **13**, 773191 (2022).
72. Schmidt, A.J. *et al.* Trouble with bleeding: risk factors for acute hepatitis C among HIV-positive gay men from Germany--a case-control study. *PLoS One* **6**, e17781 (2011).
73. Nijmeijer, B.M. *et al.* HIV-1 subverts the complement system in semen to enhance viral transmission. *Mucosal Immunol* **14**, 743-750 (2021).
74. Zhao, Y. *et al.* Immediate Antiretroviral Therapy Decreases Mortality Among Patients With High CD4 Counts in China: A Nationwide, Retrospective Cohort Study. *Clin Infect Dis* **66**, 727-734 (2018).
75. Mocroft, A. *et al.* Changing patterns of mortality across Europe in patients infected with HIV-1. EuroSIDA Study Group. *Lancet* **352**, 1725-1730 (1998).
76. Roth, G.A. *et al.* Global, regional, and national age-sex-specific mortality for 282 causes of death in 195 countries and

- territories, 1980–2017: a systematic analysis for the Global Burden of Disease Study 2017. *The Lancet* **392**, 1736-1788 (2018).
77. Gallo, R.C. *et al.* Frequent detection and isolation of cytopathic retroviruses (HTLV-III) from patients with AIDS and at risk for AIDS. *Science* **224**, 500-503 (1984).
78. Barré-Sinoussi, F. *et al.* Isolation of a T-lymphotropic retrovirus from a patient at risk for acquired immune deficiency syndrome (AIDS). *Science* **220**, 868-871 (1983).
79. Deeks, S.G., Overbaugh, J., Phillips, A. & Buchbinder, S. HIV infection. *Nature Reviews Disease Primers* **1**, 15035 (2015).
80. Royce, R.A., Seña, A., Cates, W., Jr. & Cohen, M.S. Sexual transmission of HIV. *N Engl J Med* **336**, 1072-1078 (1997).
81. Baggaley, R.F., Boily, M.C., White, R.G. & Alary, M. Risk of HIV-1 transmission for parenteral exposure and blood transfusion: a systematic review and meta-analysis. *Aids* **20**, 805-812 (2006).
82. CDC. HIV and People Who Inject Drugs. 2022 June 28, 2022 [cited 2023 26-05-2023] Available from: <https://www.cdc.gov/hiv/group/hiv-idu.html>
83. Teasdale, C.A., Marais, B.J. & Abrams, E.J. HIV: prevention of mother-to-child transmission. *BMJ Clin Evid* **2011** (2011).
84. Taha, T.E. Mother-to-child transmission of HIV-1 in sub-Saharan Africa: past, present and future challenges. *Life Sci* **88**, 917-921 (2011).
85. de Oliveira, T. *et al.* Transmission networks and risk of HIV infection in KwaZulu-Natal, South Africa: a community-wide phylogenetic study. *Lancet HIV* **4**, e41-e50 (2017).
86. Ackermann, L. & de, K. Social factors that make South African women vulnerable to HIV infection. *Health Care Women Int* **23**, 163-172 (2002).
87. Alisoltani, A. *et al.* Microbial function and genital inflammation in young South African women at high risk of HIV infection. *Microbiome* **8**, 165 (2020).
88. Masson, L. *et al.* Genital inflammation and the risk of HIV acquisition in women. *Clin Infect Dis* **61**, 260-269 (2015).
89. McClelland, R.S. *et al.* Evaluation of the association between the concentrations of key vaginal bacteria and the increased risk of HIV acquisition in African women from five cohorts: a nested case-control study. *Lancet Infect Dis* **18**, 554-564 (2018).
90. Liebenberg, L.J.P. *et al.* HPV infection and the genital cytokine milieu in women at high risk of HIV acquisition. *Nature communications*; 2019. p. 5227.
91. Chan, D.C., Fass, D., Berger, J.M. & Kim, P.S. Core structure of gp41 from the HIV envelope glycoprotein. *Cell* **89**, 263-273 (1997).
92. Kwong, P.D. *et al.* Structure of an HIV gp120 envelope glycoprotein in complex with the CD4 receptor and a neutralizing human antibody. *Nature* **393**, 648-659 (1998).
93. Berkowitz, R.D. *et al.* CCR5- and CXCR4-utilizing strains of human immunodeficiency virus type 1 exhibit differential tropism and pathogenesis in vivo. *J Virol* **72**, 10108-10117 (1998).
94. Dragic, T. *et al.* HIV-1 entry into CD4+

- cells is mediated by the chemokine receptor CC-CKR-5. *Nature* **381**, 667-673 (1996).
95. Choe, H. *et al.* The beta-chemokine receptors CCR3 and CCR5 facilitate infection by primary HIV-1 isolates. *Cell* **85**, 1135-1148 (1996).
 96. Feng, Y., Broder, C.C., Kennedy, P.E. & Berger, E.A. HIV-1 entry cofactor: functional cDNA cloning of a seven-transmembrane, G protein-coupled receptor. *Science* **272**, 872-877 (1996).
 97. Cooper, A. *et al.* HIV-1 causes CD4 cell death through DNA-dependent protein kinase during viral integration. *Nature* **498**, 376-379 (2013).
 98. Brenchley, J.M. *et al.* CD4+ T cell depletion during all stages of HIV disease occurs predominantly in the gastrointestinal tract. *J Exp Med* **200**, 749-759 (2004).
 99. Lee, B., Sharron, M., Montaner, L.J., Weissman, D. & Doms, R.W. Quantification of CD4, CCR5, and CXCR4 levels on lymphocyte subsets, dendritic cells, and differentially conditioned monocyte-derived macrophages. *Proc Natl Acad Sci U S A* **96**, 5215-5220 (1999).
 100. Moradpour, D., Penin, F. & Rice, C.M. Replication of hepatitis C virus. *Nat Rev Microbiol* **5**, 453-463 (2007).
 101. WHO. Hepatitis C Key Facts. 2022 24 June 2022 [cited 2023 03.04.2023] Available from: <https://www.who.int/news-room/fact-sheets/detail/hepatitis-c>
 102. Mast, E.E. *et al.* Risk factors for perinatal transmission of hepatitis C virus (HCV) and the natural history of HCV infection acquired in infancy. *J Infect Dis* **192**, 1880-1889 (2005).
 103. Benova, L., Mohamoud, Y.A., Calvert, C. & Abu-Raddad, L.J. Vertical transmission of hepatitis C virus: systematic review and meta-analysis. *Clin Infect Dis* **59**, 765-773 (2014).
 104. Hagan, H. *et al.* Attribution of hepatitis C virus seroconversion risk in young injection drug users in 5 US cities. *J Infect Dis* **201**, 378-385 (2010).
 105. Page, K. *et al.* Acute hepatitis C virus infection in young adult injection drug users: a prospective study of incident infection, resolution, and reinfection. *J Infect Dis* **200**, 1216-1226 (2009).
 106. Tohme, R.A. & Holmberg, S.D. Transmission of hepatitis C virus infection through tattooing and piercing: a critical review. *Clin Infect Dis* **54**, 1167-1178 (2012).
 107. Teles, S.A. *et al.* Emergent predictors of hepatitis C infection among non-injection drug users. *Journal of Infection and Public Health* **11**, 526-529 (2018).
 108. Scheinmann, R. *et al.* Non-injection drug use and Hepatitis C Virus: a systematic review. *Drug Alcohol Depend* **89**, 1-12 (2007).
 109. Danta, M. *et al.* Recent epidemic of acute hepatitis C virus in HIV-positive men who have sex with men linked to high-risk sexual behaviours. *Aids* **21**, 983-991 (2007).
 110. Hagan, H., Jordan, A.E., Neurer, J. & Cleland, C.M. Incidence of sexually transmitted hepatitis C virus infection in HIV-positive men who have sex with men. *Aids* **29**, 2335-2345 (2015).
 111. Lambers, F.A. *et al.* Alarming incidence of hepatitis C virus re-infection after

- treatment of sexually acquired acute hepatitis C virus infection in HIV-infected MSM. *Aids* **25**, F21-27 (2011).
112. Hoornenborg, E. *et al.* High incidence of HCV in HIV-negative men who have sex with men using pre-exposure prophylaxis. *J Hepatol* **72**, 855-864 (2020).
113. McFaul, K. *et al.* Acute hepatitis C infection in HIV-negative men who have sex with men. *J Viral Hepat* **22**, 535-538 (2015).
114. Zhu, Y.Z., Qian, X.J., Zhao, P. & Qi, Z.T. How hepatitis C virus invades hepatocytes: the mystery of viral entry. *World J Gastroenterol* **20**, 3457-3467 (2014).
115. Kumar, A. *et al.* Structural insights into hepatitis C virus receptor binding and entry. *Nature* **598**, 521-525 (2021).
116. Gerold, G., Moeller, R. & Pietschmann, T. Hepatitis C Virus Entry: Protein Interactions and Fusion Determinants Governing Productive Hepatocyte Invasion. *Cold Spring Harb Perspect Med* **10** (2020).
117. Pileri, P. *et al.* Binding of hepatitis C virus to CD81. *Science* **282**, 938-941 (1998).
118. Scarselli, E. *et al.* The human scavenger receptor class B type I is a novel candidate receptor for the hepatitis C virus. *Embo j* **21**, 5017-5025 (2002).
119. Meertens, L. *et al.* The tight junction proteins claudin-1, -6, and -9 are entry cofactors for hepatitis C virus. *J Virol* **82**, 3555-3560 (2008).
120. Ploss, A. *et al.* Human occludin is a hepatitis C virus entry factor required for infection of mouse cells. *Nature* **457**, 882-886 (2009).
121. Zeisel, M.B., Barth, H., Schuster, C. & Baumert, T.F. Hepatitis C virus entry: molecular mechanisms and targets for antiviral therapy. *Front Biosci (Landmark Ed)* **14**, 3274-3285 (2009).
122. Ludwig, I.S. *et al.* Hepatitis C virus targets DC-SIGN and L-SIGN to escape lysosomal degradation. *J Virol* **78**, 8322-8332 (2004).
123. Kupper, T.S. & Fuhlbrigge, R.C. Immune surveillance in the skin: mechanisms and clinical consequences. *Nat Rev Immunol* **4**, 211-222 (2004).
124. Steinman, R.M. & Cohn, Z.A. Identification of a novel cell type in peripheral lymphoid organs of mice. I. Morphology, quantitation, tissue distribution. *J Exp Med* **137**, 1142-1162 (1973).
125. Martin-Gayo, E. & Yu, X.G. Role of Dendritic Cells in Natural Immune Control of HIV-1 Infection. *Front Immunol* **10**, 1306 (2019).
126. Steinman, R.M. Decisions about dendritic cells: past, present, and future. *Annu Rev Immunol* **30**, 1-22 (2012).
127. Collin, M. & Bigley, V. Human dendritic cell subsets: an update. *Immunology* **154**, 3-20 (2018).
128. Liu, J., Zhang, X., Cheng, Y. & Cao, X. Dendritic cell migration in inflammation and immunity. *Cellular & Molecular Immunology* **18**, 2461-2471 (2021).
129. McWilliam, A.S. *et al.* Dendritic Cells Are Recruited into the Airway Epithelium during the Inflammatory Response to a Broad Spectrum of Stimuli. *Journal of Experimental Medicine* **184**, 2429-2432 (1996).

130. Soloff, A.C. & Barratt-Boyes, S.M. Enemy at the gates: dendritic cells and immunity to mucosal pathogens. *Cell Research* **20**, 872-885 (2010).
131. Sichien, D., Lambrecht, B.N., Williams, M. & Scott, C.L. Development of conventional dendritic cells: from common bone marrow progenitors to multiple subsets in peripheral tissues. *Mucosal Immunology* **10**, 831-844 (2017).
132. Eisenbarth, S.C. Dendritic cell subsets in T cell programming: location dictates function. *Nat Rev Immunol* **19**, 89-103 (2019).
133. Bachem, A. *et al.* Superior antigen cross-presentation and XCR1 expression define human CD11c+CD141+ cells as homologues of mouse CD8+ dendritic cells. *J Exp Med* **207**, 1273-1281 (2010).
134. Cabeza-Cabrerizo, M., Cardoso, A., Minutti, C.M., Pereira da Costa, M. & Reis e Sousa, C. Dendritic Cells Revisited. *Annu Rev Immunol* **39**, 131-166 (2021).
135. Satpathy, A.T., Wu, X., Albring, J.C. & Murphy, K.M. Re(de)fining the dendritic cell lineage. *Nat Immunol* **13**, 1145-1154 (2012).
136. Haniffa, M. *et al.* Human tissues contain CD141hi cross-presenting dendritic cells with functional homology to mouse CD103+ nonlymphoid dendritic cells. *Immunity* **37**, 60-73 (2012).
137. Schlitzer, A. *et al.* IRF4 transcription factor-dependent CD11b+ dendritic cells in human and mouse control mucosal IL-17 cytokine responses. *Immunity* **38**, 970-983 (2013).
138. Kashem, S.W., Haniffa, M. & Kaplan, D.H. Antigen-Presenting Cells in the Skin. *Annu Rev Immunol* **35**, 469-499 (2017).
139. Li, G., Cheng, L. & Su, L. Phenotypic and Functional Study of Human Plasmacytoid Dendritic Cells. *Curr Protoc* **1**, e50 (2021).
140. Siegal, F.P. *et al.* The nature of the principal type 1 interferon-producing cells in human blood. *Science* **284**, 1835-1837 (1999).
141. Cella, M. *et al.* Plasmacytoid monocytes migrate to inflamed lymph nodes and produce large amounts of type I interferon. *Nat Med* **5**, 919-923 (1999).
142. Liu, Y.J. IPC: professional type 1 interferon-producing cells and plasmacytoid dendritic cell precursors. *Annu Rev Immunol* **23**, 275-306 (2005).
143. Schmidt, B., Fujimura, S.H., Martin, J.N. & Levy, J.A. Variations in plasmacytoid dendritic cell (PDC) and myeloid dendritic cell (MDC) levels in HIV-infected subjects on and off antiretroviral therapy. *J Clin Immunol* **26**, 55-64 (2006).
144. Jego, G. *et al.* Plasmacytoid dendritic cells induce plasma cell differentiation through type I interferon and interleukin 6. *Immunity* **19**, 225-234 (2003).
145. Gerosa, F. *et al.* The reciprocal interaction of NK cells with plasmacytoid or myeloid dendritic cells profoundly affects innate resistance functions. *J Immunol* **174**, 727-734 (2005).
146. Farkas, L., Beiske, K., Lund-Johansen, F., Brandtzaeg, P. & Jahnsen, F.L. Plasmacytoid dendritic cells (natural interferon- α/β -producing cells) accumulate in cutaneous lupus erythematosus lesions. *Am J Pathol* **159**, 237-243 (2001).
147. Jahnsen, F.L. *et al.* Experimentally

- induced recruitment of plasmacytoid (CD123high) dendritic cells in human nasal allergy. *J Immunol* **165**, 4062-4068 (2000).
148. Gerlini, G., Mariotti, G., Bianchi, B. & Pimpinelli, N. Massive recruitment of type I interferon producing plasmacytoid dendritic cells in varicella skin lesions. *J Invest Dermatol* **126**, 507-509 (2006).
149. Nakano, H. *et al.* Blood-derived inflammatory dendritic cells in lymph nodes stimulate acute T helper type 1 immune responses. *Nat Immunol* **10**, 394-402 (2009).
150. Sallusto, F. & Lanzavecchia, A. Efficient presentation of soluble antigen by cultured human dendritic cells is maintained by granulocyte/macrophage colony-stimulating factor plus interleukin 4 and downregulated by tumor necrosis factor alpha. *J Exp Med* **179**, 1109-1118 (1994).
151. León, B., López-Bravo, M. & Ardavín, C. Monocyte-derived dendritic cells formed at the infection site control the induction of protective T helper 1 responses against Leishmania. *Immunity* **26**, 519-531 (2007).
152. Albert, M.L., Sauter, B. & Bhardwaj, N. Dendritic cells acquire antigen from apoptotic cells and induce class I-restricted CTLs. *Nature* **392**, 86-89 (1998).
153. Tanaka, H., Demeure, C.E., Rubio, M., Delespesse, G. & Sarfati, M. Human monocyte-derived dendritic cells induce naive T cell differentiation into T helper cell type 2 (Th2) or Th1/Th2 effectors. Role of stimulator/responder ratio. *J Exp Med* **192**, 405-412 (2000).
154. Randolph, G.J., Inaba, K., Robbiani, D.F., Steinman, R.M. & Muller, W.A. Differentiation of phagocytic monocytes into lymph node dendritic cells in vivo. *Immunity* **11**, 753-761 (1999).
155. Cheong, C. *et al.* Microbial stimulation fully differentiates monocytes to DC-SIGN/CD209(+) dendritic cells for immune T cell areas. *Cell* **143**, 416-429 (2010).
156. Marzaioli, V. *et al.* Monocyte-Derived Dendritic Cell Differentiation in Inflammatory Arthritis Is Regulated by the JAK/STAT Axis via NADPH Oxidase Regulation. *Front Immunol* **11**, 1406 (2020).
157. Marzaioli, V. *et al.* CD209/CD14(+) Dendritic Cells Characterization in Rheumatoid and Psoriatic Arthritis Patients: Activation, Synovial Infiltration, and Therapeutic Targeting. *Front Immunol* **12**, 722349 (2021).
158. Dauer, M. *et al.* Mature dendritic cells derived from human monocytes within 48 hours: a novel strategy for dendritic cell differentiation from blood precursors. *J Immunol* **170**, 4069-4076 (2003).
159. Lehtonen, A. *et al.* Differential expression of IFN regulatory factor 4 gene in human monocyte-derived dendritic cells and macrophages. *J Immunol* **175**, 6570-6579 (2005).
160. Skelton, L., Cooper, M., Murphy, M. & Platt, A. Human immature monocyte-derived dendritic cells express the G protein-coupled receptor GPR105 (KIAA0001, P2Y14) and increase intracellular calcium in response to its agonist, uridine diphosphoglucose. *J*

- Immunol* **171**, 1941-1949 (2003).
161. Merad, M., Ginhoux, F. & Collin, M. Origin, homeostasis and function of Langerhans cells and other langerin-expressing dendritic cells. *Nat Rev Immunol* **8**, 935-947 (2008).
162. Zhao, X. *et al.* Vaginal submucosal dendritic cells, but not Langerhans cells, induce protective Th1 responses to herpes simplex virus-2. *J Exp Med* **197**, 153-162 (2003).
163. Lee, J. *et al.* Restricted dendritic cell and monocyte progenitors in human cord blood and bone marrow. *J Exp Med* **212**, 385-399 (2015).
164. Solano-Gálvez, S.G. *et al.* Human Dendritic Cells: Ontogeny and Their Subsets in Health and Disease. *Med Sci (Basel)* **6** (2018).
165. Hoeffel, G. *et al.* Adult Langerhans cells derive predominantly from embryonic fetal liver monocytes with a minor contribution of yolk sac-derived macrophages. *J Exp Med* **209**, 1167-1181 (2012).
166. Merad, M. *et al.* Langerhans cells renew in the skin throughout life under steady-state conditions. *Nat Immunol* **3**, 1135-1141 (2002).
167. Stoitznier, P. *et al.* Visualization and characterization of migratory Langerhans cells in murine skin and lymph nodes by antibodies against Langerin/CD207. *J Invest Dermatol* **120**, 266-274 (2003).
168. Sarrami-Forooshani, R. *et al.* Human immature Langerhans cells restrict CXCR4-using HIV-1 transmission. *Retrovirology* **11**, 52 (2014).
169. Valladeau, J. *et al.* Langerin, a novel C-type lectin specific to Langerhans cells, is an endocytic receptor that induces the formation of Birbeck granules. *Immunity* **12**, 71-81 (2000).
170. Birbeck, M.S., Breathnach, A.S. & Everall, J.D. An Electron Microscope Study of Basal Melanocytes and High-Level Clear Cells (Langerhans Cells) in Vitiligo**From the Chester Beatty Research Institute, Royal Cancer Hospital, London, S.W. 3, and the Departments of Anatomy, and Dermatology, St. Mary's Hospital Medical School (University of London) London, W. 2, England. *Journal of Investigative Dermatology* **37**, 51-64 (1961).
171. Mc Dermott, R. *et al.* Birbeck granules are subdomains of endosomal recycling compartment in human epidermal Langerhans cells, which form where Langerin accumulates. *Mol Biol Cell* **13**, 317-335 (2002).
172. Ribeiro, C.M. *et al.* Receptor usage dictates HIV-1 restriction by human TRIM5 α in dendritic cell subsets. *Nature* **540**, 448-452 (2016).
173. Kawamura, T. *et al.* R5 HIV productively infects Langerhans cells, and infection levels are regulated by compound <i>CCR5</i> polymorphisms. *Proceedings of the National Academy of Sciences* **100**, 8401-8406 (2003).
174. Mbongue, J., Nicholas, D., Firek, A. & Langridge, W. The role of dendritic cells in tissue-specific autoimmunity. *J Immunol Res* **2014**, 857143 (2014).
175. Chang, S.Y., Ko, H.J. & Kweon, M.N. Mucosal dendritic cells shape mucosal immunity. *Exp Mol Med* **46**, e84 (2014).

176. Haniffa, M., Gunawan, M. & Jardine, L. Human skin dendritic cells in health and disease. *J Dermatol Sci* **77**, 85-92 (2015).
177. Banchereau, J. & Steinman, R.M. Dendritic cells and the control of immunity. *Nature* **392**, 245-252 (1998).
178. Pollara, G. *et al.* Dendritic cells in viral pathogenesis: protective or defective? *Int J Exp Pathol* **86**, 187-204 (2005).
179. Li, D. & Wu, M. Pattern recognition receptors in health and diseases. *Signal Transduction and Targeted Therapy* **6**, 291 (2021).
180. Bermejo-Jambrina, M. *et al.* C-Type Lectin Receptors in Antiviral Immunity and Viral Escape. *Front Immunol* **9**, 590 (2018).
181. Geijtenbeek, T.B.H. & Gringhuis, S.I. C-type lectin receptors in the control of T helper cell differentiation. *Nature Reviews Immunology* **16**, 433-448 (2016).
182. Lundberg, K., Rydnert, F., Greiff, L. & Lindstedt, M. Human blood dendritic cell subsets exhibit discriminative pattern recognition receptor profiles. *Immunology* **142**, 279-288 (2014).
183. Kawasaki, T. & Kawai, T. Toll-like receptor signaling pathways. *Front Immunol* **5**, 461 (2014).
184. Pandey, S., Kawai, T. & Akira, S. Microbial sensing by Toll-like receptors and intracellular nucleic acid sensors. *Cold Spring Harb Perspect Biol* **7**, a016246 (2014).
185. Lee, S.M. *et al.* Toll-like receptor 10 is involved in induction of innate immune responses to influenza virus infection. *Proc Natl Acad Sci U S A* **111**, 3793-3798 (2014).
186. Kawai, T. & Akira, S. Toll-like Receptors and Their Crosstalk with Other Innate Receptors in Infection and Immunity. *Immunity* **34**, 637-650 (2011).
187. Kawai, T. & Akira, S. TLR signaling. *Cell Death & Differentiation* **13**, 816-825 (2006).
188. Onomoto, K., Onoguchi, K. & Yoneyama, M. Regulation of RIG-I-like receptor-mediated signaling: interaction between host and viral factors. *Cell Mol Immunol* **18**, 539-555 (2021).
189. Yoneyama, M. *et al.* Shared and Unique Functions of the DExD/H-Box Helicases RIG-I, MDA5, and LGP2 in Antiviral Innate Immunity1. *The Journal of Immunology* **175**, 2851-2858 (2005).
190. Pestka, S., Krause, C.D. & Walter, M.R. Interferons, interferon-like cytokines, and their receptors. *Immunol Rev* **202**, 8-32 (2004).
191. Negishi, H., Taniguchi, T. & Yanai, H. The Interferon (IFN) Class of Cytokines and the IFN Regulatory Factor (IRF) Transcription Factor Family. *Cold Spring Harb Perspect Biol* **10** (2018).
192. Ito, T., Kanzler, H., Duramad, O., Cao, W. & Liu, Y.J. Specialization, kinetics, and repertoire of type 1 interferon responses by human plasmacytoid predendritic cells. *Blood* **107**, 2423-2431 (2006).
193. Saitoh, S.I. *et al.* TLR7 mediated viral recognition results in focal type I interferon secretion by dendritic cells. *Nat Commun* **8**, 1592 (2017).
194. Coccia, E.M. *et al.* Viral infection and Toll-like receptor agonists induce a differential expression of type I and lambda interferons in human plasmacytoid and monocyte-derived

- dendritic cells. *Eur J Immunol* **34**, 796-805 (2004).
195. Schoggins, J.W. Interferon-Stimulated Genes: What Do They All Do? *Annual Review of Virology* **6**, 567-584 (2019).
196. McNab, F., Mayer-Barber, K., Sher, A., Wack, A. & O'Garra, A. Type I interferons in infectious disease. *Nature Reviews Immunology* **15**, 87-103 (2015).
197. Schoggins, J.W. & Rice, C.M. Interferon-stimulated genes and their antiviral effector functions. *Curr Opin Virol* **1**, 519-525 (2011).
198. Chemudupati, M. *et al.* From APOBEC to ZAP: Diverse mechanisms used by cellular restriction factors to inhibit virus infections. *Biochim Biophys Acta Mol Cell Res* **1866**, 382-394 (2019).
199. Montoya, M. *et al.* Type I interferons produced by dendritic cells promote their phenotypic and functional activation. *Blood* **99**, 3263-3271 (2002).
200. Rouzaut, A. *et al.* Dendritic cells adhere to and transmigrate across lymphatic endothelium in response to IFN- α . *Eur J Immunol* **40**, 3054-3063 (2010).
201. De Giovanni, M. *et al.* Spatiotemporal regulation of type I interferon expression determines the antiviral polarization of CD4(+) T cells. *Nat Immunol* **21**, 321-330 (2020).
202. Worbs, T., Hammerschmidt, S.I. & Förster, R. Dendritic cell migration in health and disease. *Nature Reviews Immunology* **17**, 30-48 (2017).
203. Moris, A. *et al.* DC-SIGN promotes exogenous MHC-I-restricted HIV-1 antigen presentation. *Blood* **103**, 2648-2654 (2004).
204. de Witte, L. *et al.* Langerin is a natural barrier to HIV-1 transmission by Langerhans cells. *Nature Medicine* **13**, 367-371 (2007).
205. de Jong, M.A. *et al.* TNF-alpha and TLR agonists increase susceptibility to HIV-1 transmission by human Langerhans cells ex vivo. *J Clin Invest* **118**, 3440-3452 (2008).
206. de Jong, M.A., de Witte, L., Taylor, M.E. & Geijtenbeek, T.B. Herpes simplex virus type 2 enhances HIV-1 susceptibility by affecting Langerhans cell function. *J Immunol* **185**, 1633-1641 (2010).
207. Geijtenbeek, T.B. *et al.* Identification of DC-SIGN, a novel dendritic cell-specific ICAM-3 receptor that supports primary immune responses. *Cell* **100**, 575-585 (2000).
208. Relloso, M. *et al.* DC-SIGN (CD209) Expression Is IL-4 Dependent and Is Negatively Regulated by IFN, TGF- β , and Anti-Inflammatory Agents1. *The Journal of Immunology* **168**, 2634-2643 (2002).
209. Qu, C., Brinck-Jensen, N.-S., Zang, M. & Chen, K. Monocyte-derived dendritic cells: targets as potent antigen-presenting cells for the design of vaccines against infectious diseases. *International Journal of Infectious Diseases* **19**, 1-5 (2014).
210. Kämmerer, U. *et al.* Unique appearance of proliferating antigen-presenting cells expressing DC-SIGN (CD209) in the decidua of early human pregnancy. *Am J Pathol* **162**, 887-896 (2003).
211. Tailleux, L. *et al.* DC-SIGN induction in alveolar macrophages defines privileged target host cells for mycobacteria in patients with tuberculosis. *PLoS Med* **2**, e381 (2005).

212. Soilleux, E.J. *et al.* Constitutive and induced expression of DC-SIGN on dendritic cell and macrophage subpopulations in situ and in vitro. *J Leukoc Biol* **71**, 445-457 (2002).
213. Geijtenbeek, T.B. *et al.* DC-SIGN, a dendritic cell-specific HIV-1-binding protein that enhances trans-infection of T cells. *Cell* **100**, 587-597 (2000).
214. Pöhlmann, S. *et al.* Hepatitis C virus glycoproteins interact with DC-SIGN and DC-SIGNR. *J Virol* **77**, 4070-4080 (2003).
215. Marzi, A. *et al.* DC-SIGN and DC-SIGNR interact with the glycoprotein of Marburg virus and the S protein of severe acute respiratory syndrome coronavirus. *J Virol* **78**, 12090-12095 (2004).
216. Turville, S.G. *et al.* Immunodeficiency virus uptake, turnover, and 2-phase transfer in human dendritic cells. *Blood* **103**, 2170-2179 (2004).
217. Loré, K., Smed-Sörensen, A., Vasudevan, J., Mascola, J.R. & Koup, R.A. Myeloid and plasmacytoid dendritic cells transfer HIV-1 preferentially to antigen-specific CD4+ T cells. *J Exp Med* **201**, 2023-2033 (2005).
218. Trumpfheller, C., Park, C.G., Finke, J., Steinman, R.M. & Granelli-Piperno, A. Cell type-dependent retention and transmission of HIV-1 by DC-SIGN. *International Immunology* **15**, 289-298 (2003).
219. Cormier, E.G. *et al.* L-SIGN (CD209L) and DC-SIGN (CD209) mediate transinfection of liver cells by hepatitis C virus. *Proc Natl Acad Sci U S A* **101**, 14067-14072 (2004).
220. Hamel, R. *et al.* Biology of Zika Virus Infection in Human Skin Cells. *J Virol* **89**, 8880-8896 (2015).
221. Carbaugh, D.L., Baric, R.S. & Lazear, H.M. Envelope Protein Glycosylation Mediates Zika Virus Pathogenesis. *J Virol* **93** (2019).
222. Lempp, F.A. *et al.* Lectins enhance SARS-CoV-2 infection and influence neutralizing antibodies. *Nature* **598**, 342-347 (2021).
223. Thépaut, M. *et al.* DC/L-SIGN recognition of spike glycoprotein promotes SARS-CoV-2 trans-infection and can be inhibited by a glycomimetic antagonist. *PLoS Pathog* **17**, e1009576 (2021).
224. Bracq, L., Xie, M., Benichou, S. & Bouchet, J. Mechanisms for Cell-to-Cell Transmission of HIV-1. *Front Immunol* **9**, 260 (2018).
225. Rodriguez-Plata, M.T. *et al.* The infectious synapse formed between mature dendritic cells and CD4+T cells is independent of the presence of the HIV-1 envelope glycoprotein. *Retrovirology* **10**, 42 (2013).
226. Dong, C., Janas, A.M., Wang, J.H., Olson, W.J. & Wu, L. Characterization of human immunodeficiency virus type 1 replication in immature and mature dendritic cells reveals dissociable cis- and trans-infection. *J Virol* **81**, 11352-11362 (2007).
227. Pohl, C., Shishkova, J. & Schneider-Schaulies, S. Viruses and dendritic cells: enemy mine. *Cell Microbiol* **9**, 279-289 (2007).
228. Peressin, M. *et al.* Efficient transfer of HIV-1 in trans and in cis from Langerhans dendritic cells and macrophages to

- autologous T lymphocytes. *Aids* **28**, 667-677 (2014).
229. McDonald, D. *et al.* Recruitment of HIV and its receptors to dendritic cell-T cell junctions. *Science* **300**, 1295-1297 (2003).
230. Esko, J.D., Kimata, K. & Lindahl, U. Proteoglycans and Sulfated Glycosaminoglycans. In: Varki, A. *et al.* (eds). *Essentials of Glycobiology*. Cold Spring Harbor Laboratory Press Copyright © 2009, The Consortium of Glycobiology Editors, La Jolla, California.: Cold Spring Harbor (NY), 2009.
231. Sarrazin, S., Lamanna, W.C. & Esko, J.D. Heparan sulfate proteoglycans. *Cold Spring Harb Perspect Biol* **3** (2011).
232. Xian, X., Gopal, S. & Couchman, J.R. Syndecans as receptors and organizers of the extracellular matrix. *Cell Tissue Res* **339**, 31-46 (2010).
233. Saunders, S., Jalkanen, M., O'Farrell, S. & Bernfield, M. Molecular cloning of syndecan, an integral membrane proteoglycan. *J Cell Biol* **108**, 1547-1556 (1989).
234. Essner, J.J., Chen, E. & Ekker, S.C. Syndecan-2. *The International Journal of Biochemistry & Cell Biology* **38**, 152-156 (2006).
235. de Witte, L. *et al.* Syndecan-3 is a dendritic cell-specific attachment receptor for HIV-1. *Proc Natl Acad Sci U S A* **104**, 19464-19469 (2007).
236. Kaksonen, M. *et al.* Syndecan-3-deficient mice exhibit enhanced LTP and impaired hippocampus-dependent memory. *Mol Cell Neurosci* **21**, 158-172 (2002).
237. Teng, Y.H., Aquino, R.S. & Park, P.W. Molecular functions of syndecan-1 in disease. *Matrix Biol* **31**, 3-16 (2012).
238. Couchman, J.R. Transmembrane Signaling Proteoglycans. *Annual Review of Cell and Developmental Biology* **26**, 89-114 (2010).
239. Vuong, T.T., Reine, T.M., Sudworth, A., Jenssen, T.G. & Kolset, S.O. Syndecan-4 is a major syndecan in primary human endothelial cells in vitro, modulated by inflammatory stimuli and involved in wound healing. *J Histochem Cytochem* **63**, 280-292 (2015).
240. Smith, M.F., Jr., Novotny, J., Carl, V.S. & Comeau, L.D. Helicobacter pylori and toll-like receptor agonists induce syndecan-4 expression in an NF-kappaB-dependent manner. *Glycobiology* **16**, 221-229 (2006).
241. Okuyama, E. *et al.* Molecular mechanisms of syndecan-4 upregulation by TNF- α in the endothelium-like EAhy926 cells. *J Biochem* **154**, 41-50 (2013).
242. Gopal, S. Syndecans in Inflammation at a Glance. *Front Immunol* **11**, 227 (2020).
243. Bobardt, M.D. *et al.* Syndecan Captures, Protects, and Transmits HIV to T Lymphocytes. *Immunity* **18**, 27-39 (2003).
244. Lefèvre, M., Felmlee, D.J., Parnot, M., Baumert, T.F. & Schuster, C. Syndecan 4 is involved in mediating HCV entry through interaction with lipoviral particle-associated apolipoprotein E. *PLoS One* **9**, e95550 (2014).
245. Bacsá, S. *et al.* Syndecan-1 and syndecan-2 play key roles in herpes simplex virus type-1 infection. *J Gen Virol* **92**, 733-743 (2011).



CHAPTER

2

Transmission of Zika virus by dendritic cell subsets in skin and vaginal mucosa

Julia Eder^{1,2}, Esther Zijlstra-Willems¹, Gerrit Koen³, Neeltje A.
Kootstra^{1,2}, Katja C. Wolthers³, Teunis B. H. Geijtenbeek^{1,2}

¹Amsterdam UMC location University of Amsterdam, Department of
Experimental Immunology, Meibergdreef 9, Amsterdam, The Netherlands

²Amsterdam institute for Infection and Immunity, Amsterdam,
The Netherlands

³Amsterdam UMC location University of Amsterdam, Department of Medical
Microbiology and infection prevention, Meibergdreef 9, Amsterdam,
The Netherlands

Abstract

Zika virus is a member of the Flaviviridae family that has caused recent outbreaks associated with neurological malformations. Transmission of Zika virus occurs primarily via mosquito bite but also via sexual contact. Dendritic cells (DCs) and Langerhans cells (LCs) are important antigen presenting cells in skin and vaginal mucosa and paramount to induce antiviral immunity. To date, little is known about the first cells targeted by Zika virus in these tissues as well as subsequent dissemination of the virus to other target cells. We therefore investigated the role of DCs and LCs in Zika virus infection. Human monocyte derived DCs (moDCs) were isolated from blood and primary immature LCs were obtained from human skin and vaginal explants. Zika virus exposure to moDCs but not skin and vaginal LCs induced Type I Interferon responses. Zika virus efficiently infected moDCs but neither epidermal nor vaginal LCs became infected. Infection of a human full skin model showed that DC-SIGN expressing dermal DCs are preferentially infected over langerin+ LCs. Notably, not only moDCs but also skin and vaginal LCs efficiently transmitted Zika virus to target cells. Transmission by LCs was independent of direct infection of LCs. These data suggest that DCs and LCs are among the first target cells for Zika virus not only in the skin but also the genital tract. The role of vaginal LCs in dissemination of Zika virus from the vaginal mucosa further emphasizes the threat of sexual transmission and supports the investigation of prophylaxes that go beyond mosquito control.

Keywords: Zika virus, vaginal mucosa, Langerhans cells, virus transmission, viral dissemination

Introduction

Zika virus is a mosquito-borne flavivirus containing a single-stranded positive RNA ¹. It belongs to the Flaviviridae family and is closely related to dengue virus (DENV) and West Nile virus (WNV) ². People infected with Zika virus are mostly asymptomatic or experience mild symptoms including fever, arthralgia and a maculopapular rash ^{3,4}. However, Zika virus outbreaks have been associated with severe neuropathologies including microcephaly, congenital deafness and impaired vision, termed Congenital Zika Syndrome in neonates infected *in utero* and Guillain-Barré syndrome in adults ^{5, 6, 7, 8}. Consequently, the World Health Organization (WHO) labeled in 2016 the Zika virus pandemic in South America a public health emergency ⁹. Zika virus is the only Flavivirus that passes the maternal-placental barrier ¹⁰ and infects placental cells that include villous stromal macrophages, i.e. Hofbauer cells, and placental trophoblasts ^{11, 12, 13, 14}. While the exact transmission route for Zika virus over the maternal-fetal barrier is still unclear, physical disruption, and transcytosis have been described *in vitro* ¹⁵ and placental damage observed in animal models ^{16, 17, 18}. Zika virus has further been identified in amniotic fluid and tissues of the developing fetus in infected pregnant women ^{19, 20}. Importantly, Zika virus is also transmitted sexually ^{21, 22, 23, 24, 25, 26}. RNA of Zika virus is present in seminal fluid ^{27, 28} as well as in vaginal fluid ²¹.

Monocytes and Dendritic cells (DCs) are targets for Zika virus infection and might be involved in dissemination of Zika virus ^{29, 30, 31, 32, 33}, as these cells are found in barrier tissues like skin and mucosal surfaces ^{29, 34, 35, 36}. Amongst the DC subsets susceptible to Zika virus are monocyte-derived DCs (moDCs) ^{33, 37}. Zika virus infection of moDCs leads to productive virus replication and secretion ^{31, 33, 34, 38}. DC-SIGN, a C-type lectin receptor (CLR) expressed on DC subsets, facilitates Zika virus binding and infection *in vitro* ³⁹. DC-SIGN is expressed on DCs and macrophages ^{40, 41} and enables infection of viruses like HIV-1 and dengue virus ^{41, 42}. Langerhans cells (LCs), a subset of DCs, are located in the outmost layer of the skin and genital tract ^{43, 44} where they are one of the first cells to encounter and sense viruses ^{45, 46, 47, 48}. However, LCs are also targets for virus infections like HIV-1 ^{49, 50}. In healthy tissue, LCs restrict HIV-1 infection by capture through CLR langerin receptor and subsequent degradation in Birbeck granules ^{51, 52, 53}. The role of LCs in the skin and genital tract during Zika virus infection is still largely unclear.

Here we have investigated the role of DC subsets in skin and vaginal mucosa in Zika virus infection. We observed that Zika virus efficiently infected primary DCs via DC-SIGN, and blocking of the receptor inhibited infection as well as transmission. LCs isolated from human skin or vagina were resistant to Zika virus infection, however LCs efficiently transmitted Zika virus to susceptible target cells. These observations suggest a role for DCs and LCs in the dissemination of Zika virus from site of infection throughout the body. This might be of particular importance during sexual transmission.

Results

moDCs become activated by Zika virus leading to type I interferon responses

Type I IFNs and interferon stimulated genes (ISGs) are important antiviral responses^{54, 55, 56, 57}. Here we investigated whether Zika virus (primary human isolate, Asian lineage) activates moDCs and induces type I IFN responses. We observed upregulation of the co-stimulatory molecules CD80 and CD86 at 24 and 48 hours post inoculation (hpi) (**Figure 1A** and **Sup. Figure 1A**). Antibodies against CLR DC-SIGN blocked Zika virus-induced upregulation of the co-stimulatory markers CD80 and CD86 by Zika virus (**Figure 1A** and **Sup. Figure 1A**). Expression of the maturation marker CD83 was not induced by Zika virus, whereas Poly(I:C), a TLR-3 antagonist, induced low expression of CD83 (**Figure 1A** for single donor representation and the pooled data in **Sup. Figure 1A**). Upregulation of CD80 and CD86 but not CD83 suggests that the cells are not fully matured but activated and primed for antigen presentation. Next we investigated whether Zika virus inoculation of moDCs induces type I IFN responses. Zika virus induced upregulation of IFN beta (IFN β) at 24 hpi and 48 hpi (**Figure 1B** and **Sup. Figure 1A**). Moreover, ISGs Apobec3G, IP10, IRF7 and MXA were induced highest at 24 hpi whereas ISG15 and OAS1 peaked later at 48 hpi (**Figure 1B**). Antibodies against DC-SIGN blocked induction of IFN β , IP10, MXA, ISG15, IRF7, A3G and OAS1, albeit not significantly for A3G and OAS1 at 48 hpi (**Figure 1B**). Blocking viral replication by the viral polymerase inhibitor 7-Deaza-2'-C-Methyladenosine (7DMA) abrogated IFN β and ISG transcription to a similar extent as blocking infection by the blocking antibody against DC-SIGN (**Sup. Figure 1B**). Moreover, heat inactivated Zika virus (inactivated as described previously⁵⁸) did not lead to induction of IFN β or ISGs in moDCs. These data indicate that moDCs sense Zika virus via DC-SIGN, leading to moderate DC maturation and induction of antiviral immunity.

Immature skin LCs are not activated by Zika virus

Immature LCs were isolated by CD1a selection from human skin. Immature skin LCs do not express DC-SIGN but are instead characterized by expressing the CLR langerin^{59, 60, 61}. Following exposure of LCs to Zika virus, LC activation and type I IFN responses was determined. Zika virus did neither induce CD80, CD83 nor CD86 in immature LCs (**Figure 2A** and **Sup. Figure 1B**). Moreover, we did not observe maturation after stimulation with TLR antagonists Poly(I:C) and LTA. However, Zika virus induced ISG15 and IP10, whereas IFN β and other ISGs were not detected (**Figure 2B**). Blocking CLR langerin did not affect LC activation nor type I IFN responses. These data suggest that LCs are not activated by Zika virus

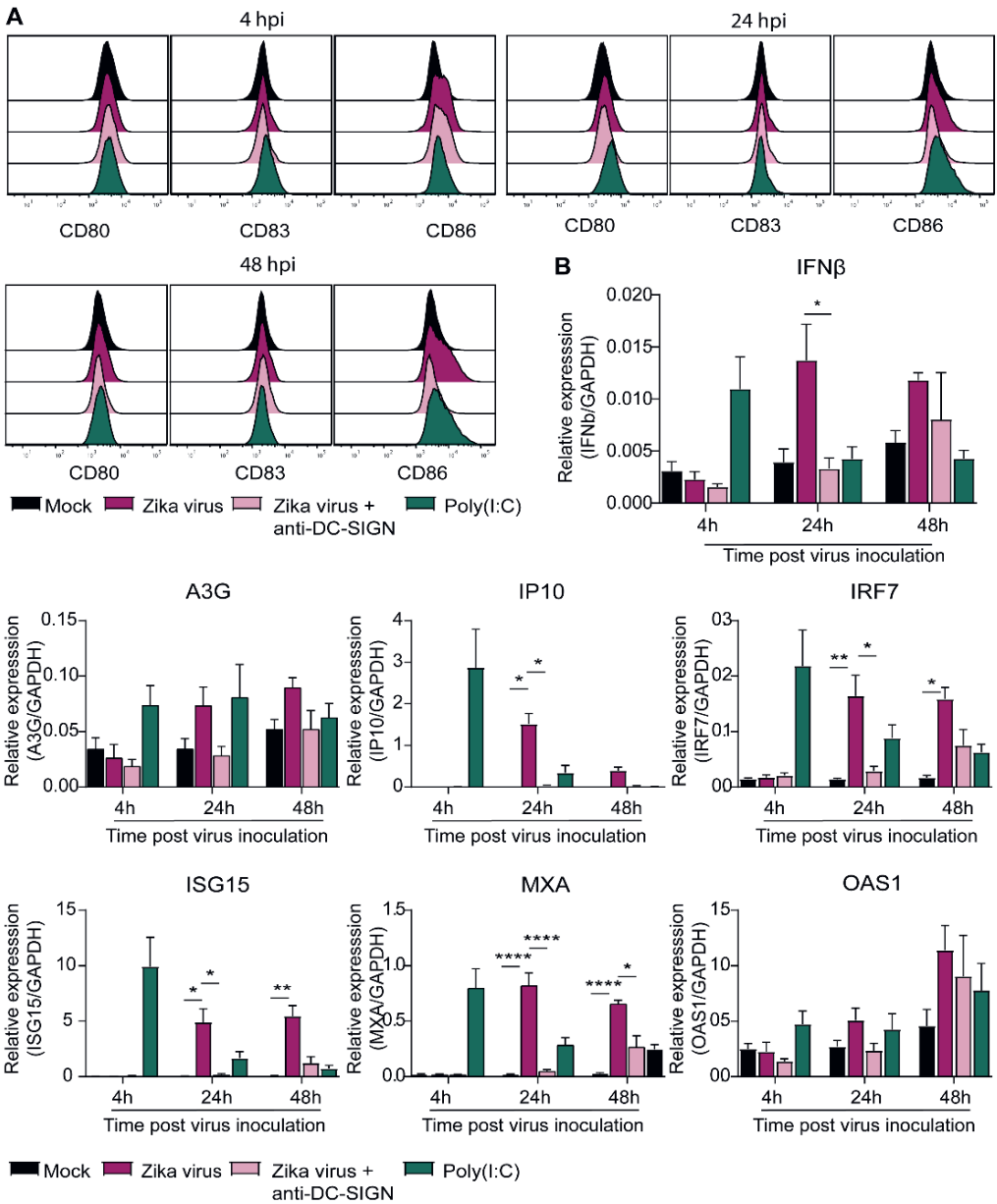


Figure 1 | Zika virus induces activation and interferon responses in monocyte derived DCs. (A) Monocyte derived DCs (moDCs) were pre-incubated with Poly(I:C) or a blocking antibody against DC-SIGN (AZN-D1) before Zika virus was added at a concentration of 850 TCID/ml. Cells were fixed after either 4 hours, 24 hours or 48 hours and expression of activation and maturation markers was measured via flow cytometry (1 representative donor out of 4 individual donors measured in monoplo). (B) moDCs pre-incubated with Poly(I:C) (10 μ g/ml) or AZN-D1 (20 μ g/ml) and subsequently infected with Zika virus (850 TCID/ml) were lysed and expression of IFN β and interferon stimulated genes (ISG) was measured on PCR after 4 hours, 24 hours and 48 hours respectively. Data information: Data show the mean values and error bars are the SEM. Statistical analysis was performed using (B) ordinary one-way ANOVA with Tukey multiple comparison test. * $P \leq 0.05$, ** $P \leq 0.01$, **** $P \leq 0.0001$ ($n=4$ donors measured in monoplo). hpi: hours post inoculation.

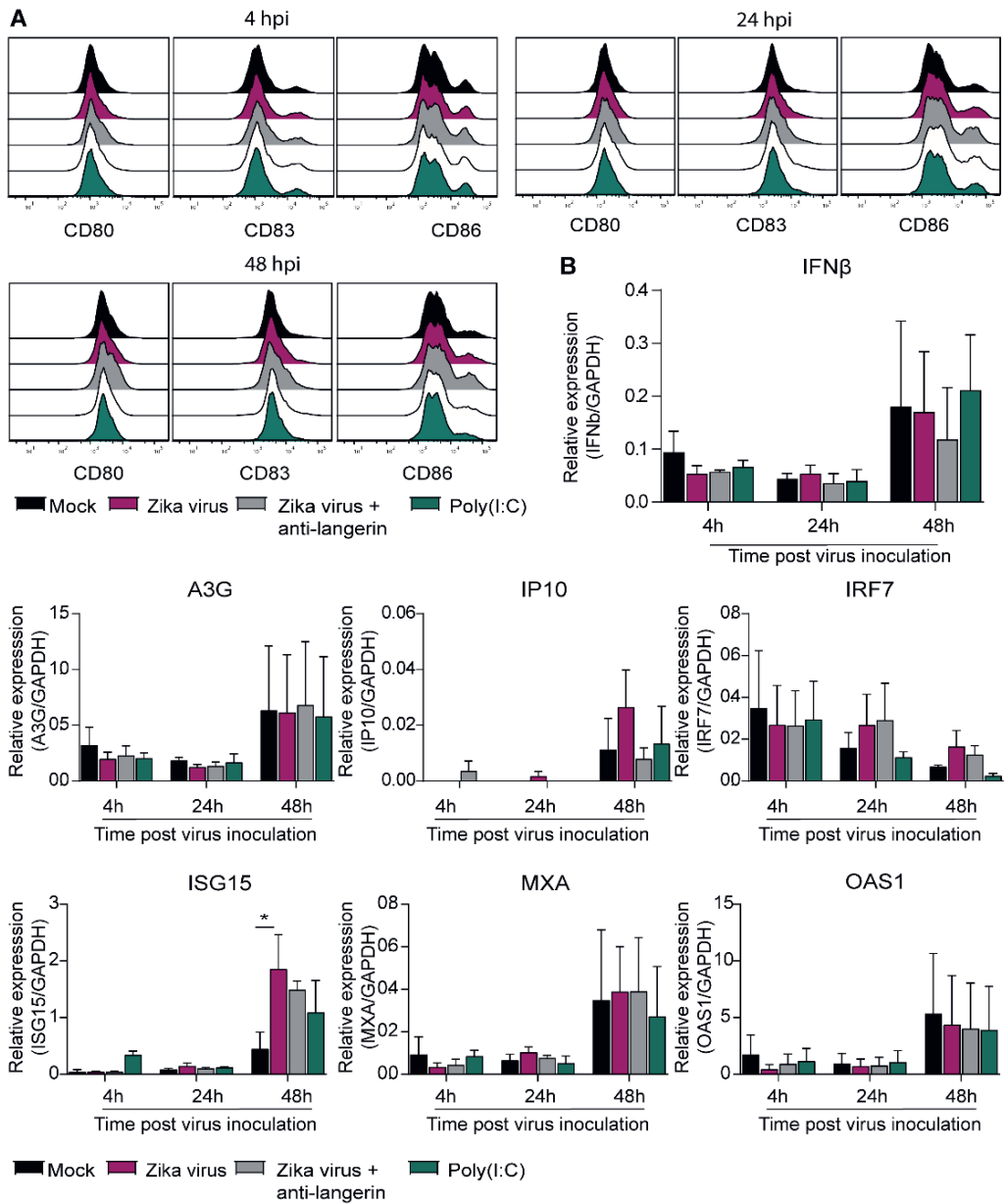


Figure 2 | Zika virus does not induce activation or interferon responses in skin derived LCs. (A) Immature Langerhans cells (LCs) isolated from epidermal skin grafts were pre-incubated with either Poly(I:C) (10 ng/ml), LTA (10 ng/ml), or a blocking antibody against langerin (10E2, 20 μ g/ml) before Zika virus was added at a concentration of (850 TCID/ml). Cells were fixed after either 4 hours, 24 hours or 48 hours and expression of activation and maturation markers was measured via flow cytometry (1 representative out of 3 individual donors measured in mono). (B) Immature LCs pre-incubated with Poly(I:C) or AZN-D1 and subsequently infected with Zika virus (850 TCID/ml) were lysed and expression of IFN β and interferon stimulated genes (ISG) was measured on PCR after 4 hours, 24 hours and 48 hours respectively. Data information: Data show the mean values and error bars are the SEM. Statistical analysis was performed using (B) ordinary two-way ANOVA with Tukey multiple comparison test. *P \leq 0.05, (n=3 donors measured in mono). hpi: hours post inoculation.

DC-SIGN is involved in Zika virus binding and transmission

DC-SIGN and langerin are both important C-type lectins and known attachment receptors for various viruses⁶². Importantly, DC-SIGN has already been shown to bind Zika virus *in vitro*^{39, 63}. Here we investigate whether DC-SIGN and langerin interact with Zika virus. To this end, we employed a Raji cell line selectively expressing either DC-SIGN or langerin (**Figure 3A**). DC-SIGN expressing Raji cells efficiently bound Zika virus in contrast to parental or langerin-expressing Raji cells. Moreover, binding by DC-SIGN-Raji was blocked by antibodies against DC-SIGN but not by isotype antibodies (**Figure 3B**). Next we investigated whether Zika virus binding to DC-SIGN facilitates viral transmission. Notably, DC-SIGN-Raji incubated with Zika virus for 4 hours successfully transmitted Zika virus to target cells in contrast to Langerin-Raji (**Figure 3C**). Mannan, a carbohydrate used to block CLRs, or antibodies against DC-SIGN, but not the isotypes control significantly reduced Zika virus transmission by DC-SIGN Raji, suggesting that DC-SIGN captures and transmits Zika virus (**Figure 3C**). These data strongly suggest that DC-SIGN, in contrast to langerin, is involved in Zika virus binding and transmission.

DC-SIGN+ primary moDCs are susceptible to Zika virus infection and transmission

To determine whether DCs are susceptible to Zika virus infection, moDCs were inoculated with increasing concentrations of Zika virus and expression of viral proteins was measured at different time points after inoculation by flow cytometry. Zika virus infection of moDCs was detected after 8 hpi and increased up to 48 hpi compared to mock infected moDCs (**Figure 4A**). Infection levels increased over time and with higher virus concentration. Cell viability remained constant for 48 hours (**Sup. Figure 2B**). moDCs highly express DC-SIGN (**Sup. Figure 2C**) and antibodies against DC-SIGN blocked infection of moDCs without influencing cell viability (**Figure 4B** and **Sup. Figure 2D**). Soluble mannan also inhibited Zika virus infection of moDCs (**Sup. Figure 2E**). The TAM receptors Tyro3 and AXL, candidate receptors for Zika virus infection⁶⁴, are also expressed on moDCs. Similarly, skin derived LCs highly express Tyro3 but instead of AXL they express MerTK (**Sup. Figure 3A**). Moreover, viral polymerase inhibitor 7DMA blocked moDC infection in a concentration dependent manner 24 hpi and 48 hpi post inoculation (**Figure 4C**). These data indicate that Zika virus productively infects DCs.

We next investigated whether moDCs transmit Zika virus to Zika virus-permissive Vero cells. moDCs were exposed to Zika virus for 4 hours and were co-cultured with Vero cells after washing. Vero cell infection was determined by flow cytometry. Notably, Vero cells became infected by Zika virus (**Figure 4D**). As moDCs were not productively infected after 4 hours, these data suggest that moDCs transmit virus independent of infection. Next we infected moDCs for 48 hours and after washing co-cultured moDCs with Vero cells. Zika virus-

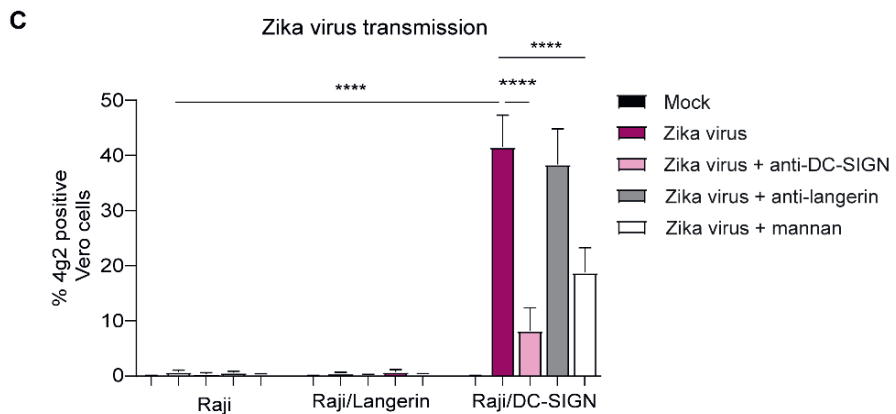
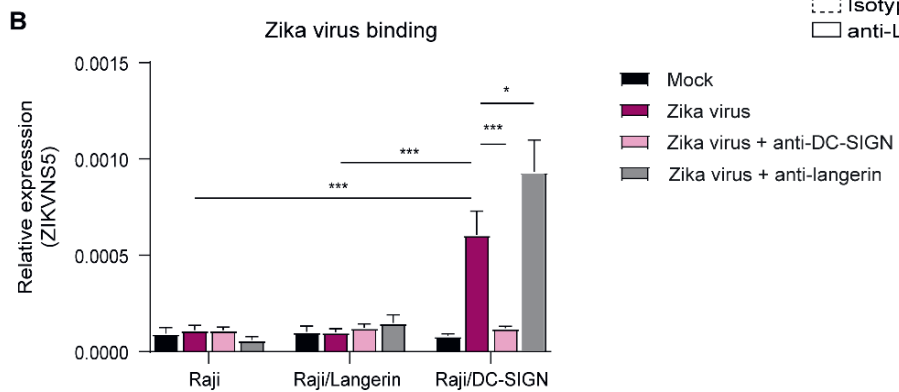
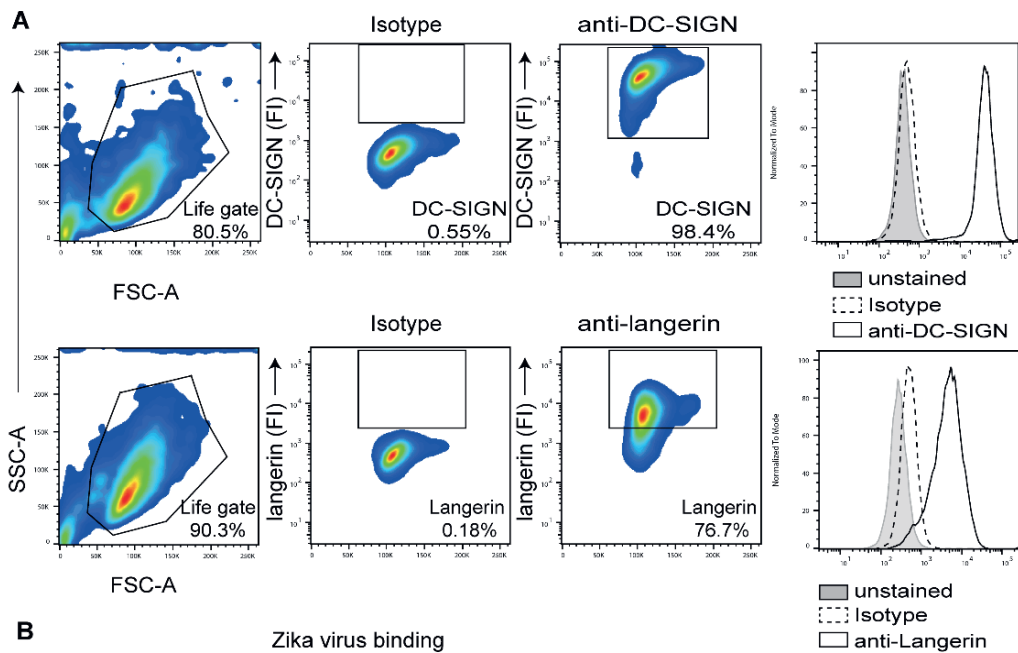


Figure 3. Figure legend on next page

Figure 3 | Zika virus binds to DC-SIGN but not langerin for transmission. (A) Raji cells expressing either DC-SIGN or langerin as measured by flow cytometry (n=1 representative donor). (B) Raji, Raji/SIGN and Raji/Langerin cells were exposed to Zika virus (175 TCID/ml) for 4 hours before measuring binding of Zika virus NS5 protein. Quantification of viral RNA was measured by quantitative real-time PCR. Additionally, cells were pre-incubated with either an anti-DC-SIGN antibody (AZN-D1, 20 µg/ml) or an anti-langerin antibody (10E2, 20 µg/ml) prior to virus inoculation. (C) Raji cells were inoculated with Zika virus (35 TCID/ml) in presence or absence of AZN-D1, 10E2 or mannan for 4 hours. After washing the Raji, the cells were co-cultured with Vero cells for another 2 to 3 days to determine viral transmission. Zika virus infection of Vero cells was measured by flow cytometry (4g2 Flavivirus envelope protein). Data information: Data show the mean values and error bars are the SEM. Statistical analysis was performed using (B) ordinary two-way ANOVA with Tukey's multiple-comparison test. *P≤0.05, ***P≤0.001 (n=4 experiments measured in monoplo). (C) ordinary two-way ANOVA with Tukey's multiple-comparison test. ****P≤0.0001 (n=4 experiments measured in triplicate).

infected moDCs efficiently transmitted Zika virus to Vero cells, and transmission was inhibited by the replication inhibitor 7DMA (**Figure 4E**). 7DMA inhibition decreased but did not block viral transmission at higher inoculum, suggesting that part of the transmission is replication independent. Antibodies against DC-SIGN completely blocked transmission of moDCs treated with Zika virus for 4 or 48 hours (**Figure 4F and G**). These data suggest that Zika virus efficiently infects primary moDCs and that DC-SIGN is involved in infection and transmission of Zika virus by DCs.

Figure 4 | DC-SIGN positive DCs are susceptible to Zika virus infection and can transmit the virus to target cells. (A) moDCs were inoculated with Zika virus for different time points (4, 8, 24, 32 and 48 hours) before infection was measured by flow cytometry (4g2 Flavivirus protein) (n=4 donors measured in duplicates). (B) moDCs in presence or absence of an anti-DC-SIGN antibody (AZN-D1, 20 µg/ml) were exposed to Zika virus (750 TCID/ml) for either 24 or 48 hours. Infection was measured by flow cytometry (4g2 Flavivirus envelope protein). (C) The Zika virus replication inhibitor 7DMA was added to moDCs in different concentrations (5- 25 µM) prior to Zika virus (750 TCID/ml) inoculation. Zika virus infection (4g2 Flavivirus protein) was determined after 24 or 48 hours. (n=2 donors measured in duplicate). (D) moDCs were incubated with Zika virus for 4 hours at 37°C, extensively washed and co-cultured with Vero cells for another 3 days. (n=3 donors measured in triplicates). (E) moDCs pre-incubated with 7DMA were exposed to Zika virus (750 TCID/ml) for 48 hours at 37°C. After washing, the cells were co-cultured with Vero cells. Transmission by moDCs to Vero cells was determined flow cytometry (4g2 Flavivirus envelope protein). (F, G) moDCs in the presence or absence of anti-DC-SIGN antibody (AZN-D1, 20 µg/ ml) were incubated with Zika virus for either 4 hours (F) or 48 hours at 37°C (G). After washing, moDCs were co-cultured with Vero cells and Vero infection was measured by flow cytometry (4g2 Flavivirus envelope protein) (G) n=5 measured in triplicates. Data information: Data show the mean values and error bars are the SEM. (B) ordinary two-way ANOVA with Tukey's multiple-comparison test. **P ≤ 0.01, ***P ≤ 0.001, ****P ≤ 0.0001, (n=4 donors measured in duplicate). (E) ordinary two-way ANOVA with Tukey's multiple-comparison test. *P ≤ 0.05, (n=4 donors measured in triplicate). (F) ordinary two-way ANOVA with Tukey's multiple-comparison test. ****P ≤ 0.0001, (n=5 donors measured in triplicate). (G) ordinary two-way ANOVA with Tukey's multiple-comparison test. **P ≤ 0.01, ****P ≤ 0.0001, (n=5 donors measured in triplicate). Zika virus concentrations are 375, 750 or 2250 TCID/ml. moDC: monocyte derived moDCs.

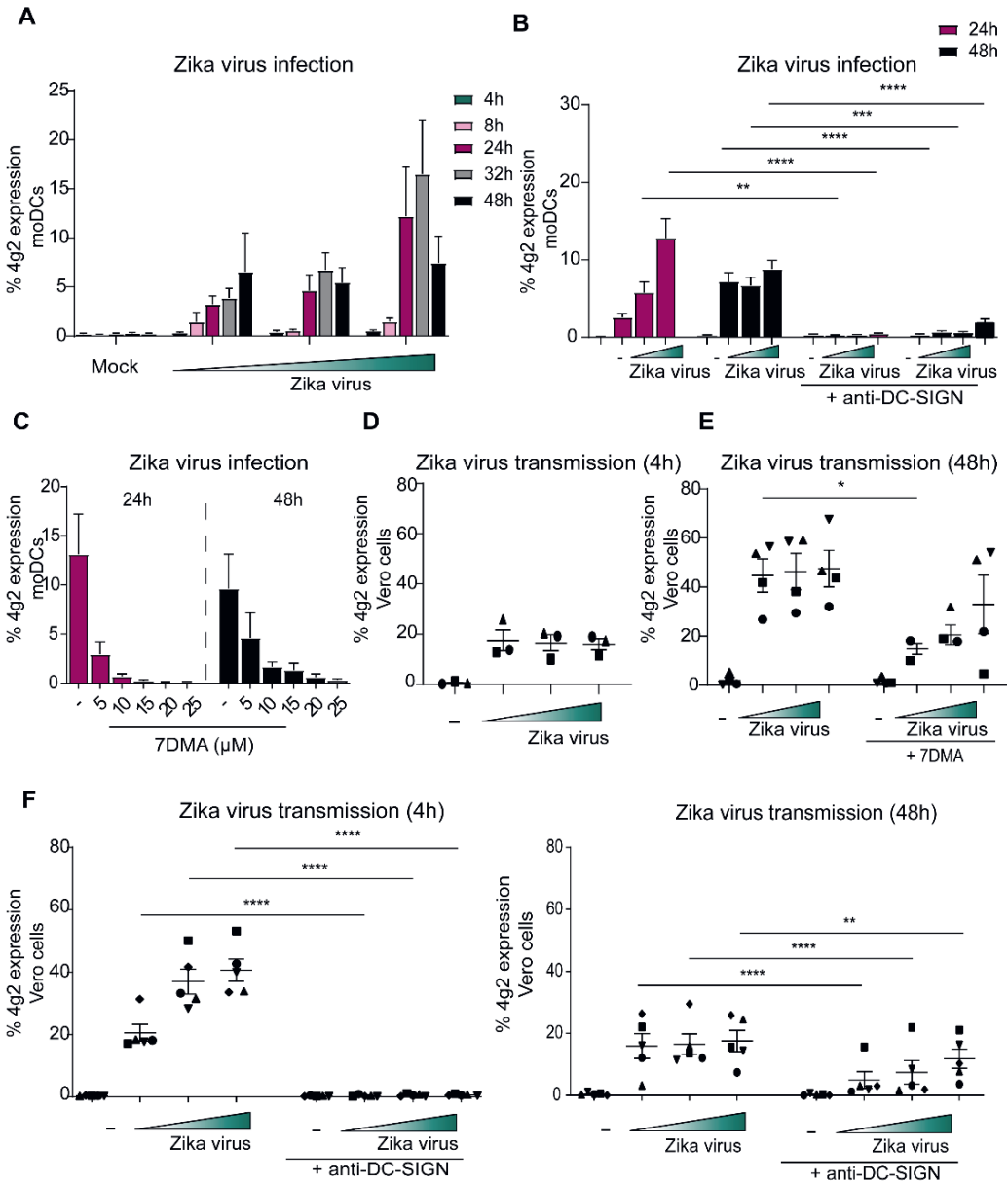


Figure 4. Figure legend on previous page.

Epidermal Langerhans cells transmit Zika virus

Next, immature LCs from human skin were incubated with Zika virus and infection was followed over time. We did not observe any Zika virus-positive LCs at different time points (**Figure 5A**). Moreover, activated LCs isolated after migration from skin sheets, were not

infected by Zika virus (**Figure 5B**). These data suggest that skin-derived LCs are not permissive to Zika virus infection. Importantly, immature skin LCs do not express DC-SIGN but express the CLR langerin and high levels of CD1a (**Figure 5C**). We next incubated immature LCs with Zika virus for 4 hours and co-cultured them with Vero cells. Notably, Vero cells became infected by Zika virus after co-culture with LCs (**Figure 5D**) indicating that skin-derived LCs transmit Zika virus. Transmission was not abrogated by antibodies against langerin, suggesting that langerin is not involved in Zika virus infection nor transmission.

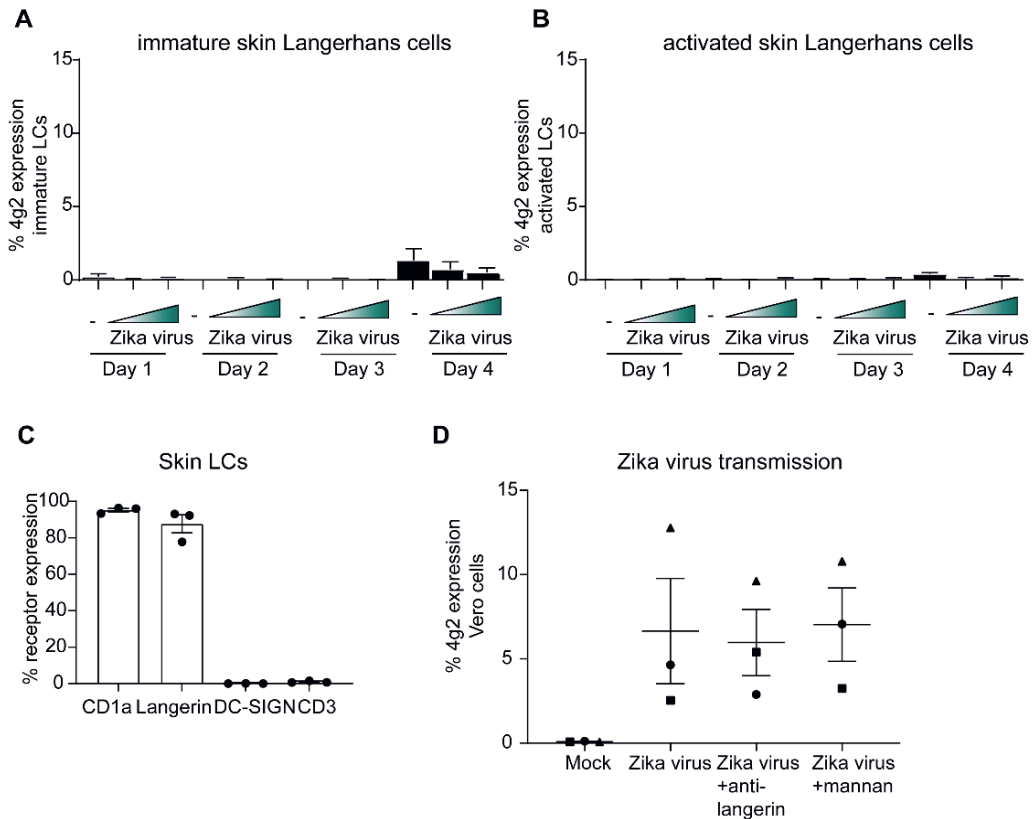


Figure 5 | Skin LCs do not become infected by Zika virus but are involved in viral dissemination through transmission. (A) Immature LCs were isolated from human skin and exposed to Zika virus (750 or 2250 TCID) for up to 4 days. Zika virus infection (4g2 Flavivirus envelope protein) was measured by flow cytometry. (n=4 donors 2 measured in triplicates 2 in monoplo). (B) Activated LCs migrated from epidermal skin sheets after 3 days were exposed to Zika virus (750 or 2250 TCID) for up to 4 days and infection (4g2 Flavivirus envelope protein) was measured by flow cytometry (n=3 donors measured in triplicates). (C) Immature LCs isolated from skin were stained for langerin, CD1a, CD3 and DC-SIGN and expression was measured by flow cytometry (n=3 individual donors). (D) Immature LCs were inoculated with Zika virus (850 TCID/ml) for 4 hours. After thoroughly washing the LCs, they were co-cultured with Vero cells for 3 days. Prior to the addition of Zika virus, skin LCs were incubated with either anti-langerin antibody (10E2, 20 μ g/ml) or mannan (100 μ g/ml). (n=3 donors measured in triplicates). Data information: Data show the mean values and error bars are the SEM. LC: Langerhans cell.

DC subsets in the skin are targeted by Zika virus

We next exposed full skin explants to Zika virus and determined both phenotype and infection of migrated cells. Phenotyping was based on previously described dermal cell markers⁶⁵. After 3 days, migrated cells consisted of CD11c high/HLA-DR⁺ DCs that could further be divided into CD14⁺DC-SIGN⁻ and CD14⁺DC-SIGN⁺ DC subsets. Moreover, we identified a CD11c low/HLA-DR⁺ cell population expressing langerin, suggesting that these are migrated LCs (**Figure 6A-B**). Notably, we observed Zika virus infection in the migrated cells (**Figure 6C**). Further phenotyping revealed that DC-SIGN⁺ dermal cells were more readily infected by Zika virus than langerin⁺ LCs (**Figure 6D-E**). Moreover, Zika virus infected cells highly expressed CD11c (**Sup. Figure 3B**), indicating that these are dermal DCs. Thus our data support a role for DC-SIGN expressing cells as targets for Zika virus infection in skin.

Vaginal LCs transmit Zika virus to target cells

Zika virus can be transmitted sexually^{21, 22, 23, 24, 25, 26}, and therefore vaginal mucosa is an important tissue for viral entry. We isolated vaginal LCs from vaginal mucosa obtained after prolapse surgery and compared these with skin LCs. Vaginal LCs expressed high levels of CD1a and langerin (**Figure 7A**)⁴⁷. Vaginal LCs are highly similar to skin derived LCs in their expression of CD1a and langerin but lack of DC-SIGN (**Figure 7A**). Immature vaginal LCs were not infected by Zika virus after 3 days (**Figure 7B**). Similar to what we observed for skin derived LCs, Zika virus did not induce maturation of vaginal LCs (**Figure 7C**), CD83 expression was not affected by Zika virus.

Notably, vaginal LCs incubated with Zika virus for 4 hours transmitted Zika virus to target cells independent of langerin (**Figure 7D**). These results suggest that LCs in vaginal mucosa transmit Zika virus to target cells and thereby contribute to viral dissemination in the genital tract, regardless of infection.

Figure 6: Dendritic cell subsets in a full skin explant model are susceptible to Zika virus. (A, B) Full skin explants consisting of a dermal and epidermal layer were incubated for 3 days at 37°C during which skin cells crawled out of the tissue and into the medium. (A) Expression of cell surface markers of cells retrieved from full skin explants as measured by flow cytometry. Cells were stained with antibodies against HLA-DR, CD11c, CD14, langerin and DC-SIGN to identify and separate DC subsets (1 representative of n=4 donors measured in triplicates). (B) Pooled data of dermal cells being either CD11c high/HLA-DR⁺ and DC-SIGN⁺ or CD11c low/HLA-DR⁺ and expressing langerin (n=4 donors in triplicates). (C–E) Full skin explants were exposed to Zika virus (1100 TCID₅₀/ml) for 3 days before infection was measured by flow cytometry (n=3 donors measured in triplicates). (C) Zika virus infection (4g2 Flavivirus envelope protein) of full skin explants was determined by flow cytometry. (D) Zika virus positive cells were stained for DC-SIGN and langerin to further determine cell subset infection. Infection of either langerin or DC-SIGN⁺ cells was measured by anti-4G2 Flavivirus envelope protein. Data information: data show the mean values and error bars are the SEM.

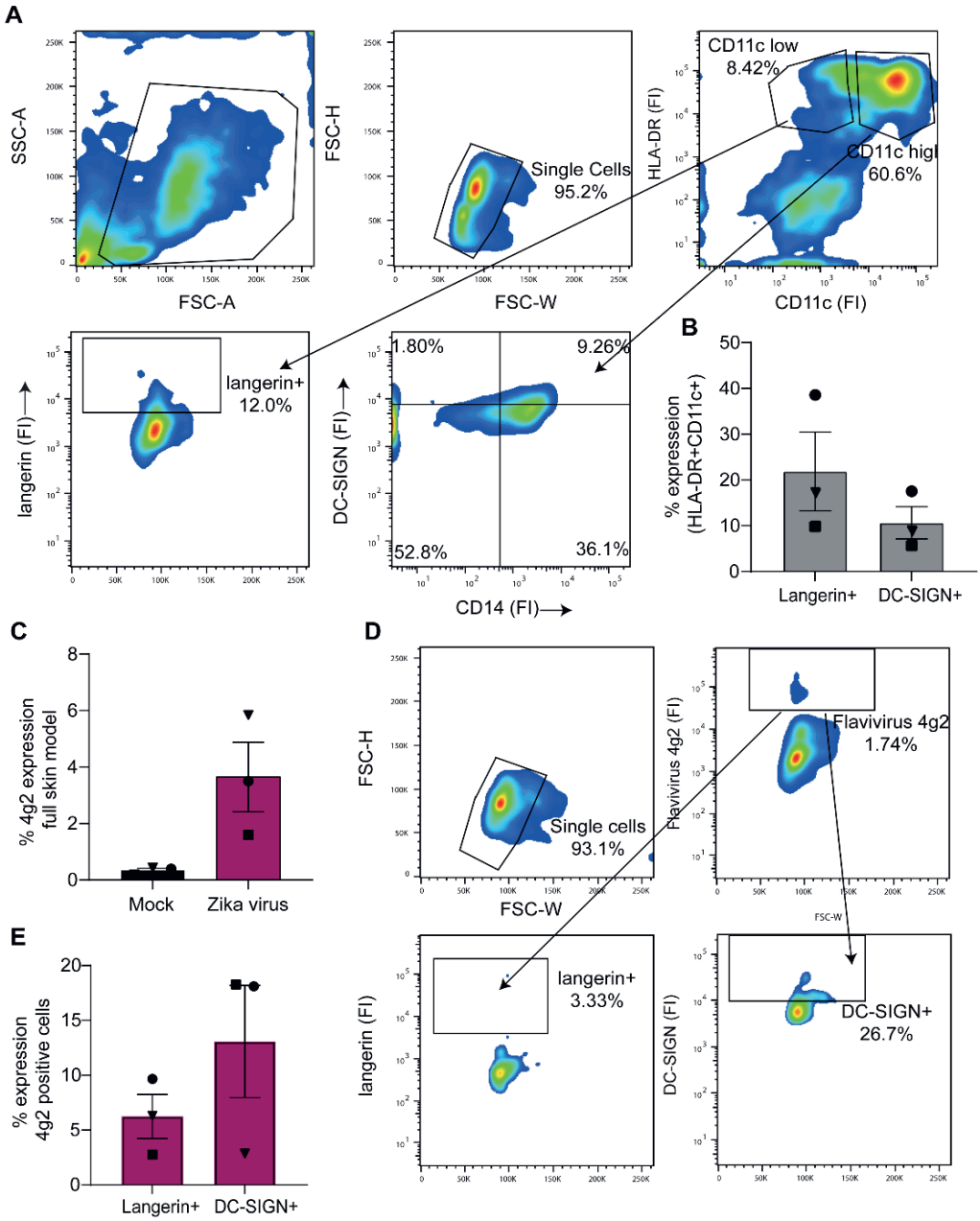


Figure 6. Figure legend on previous page.

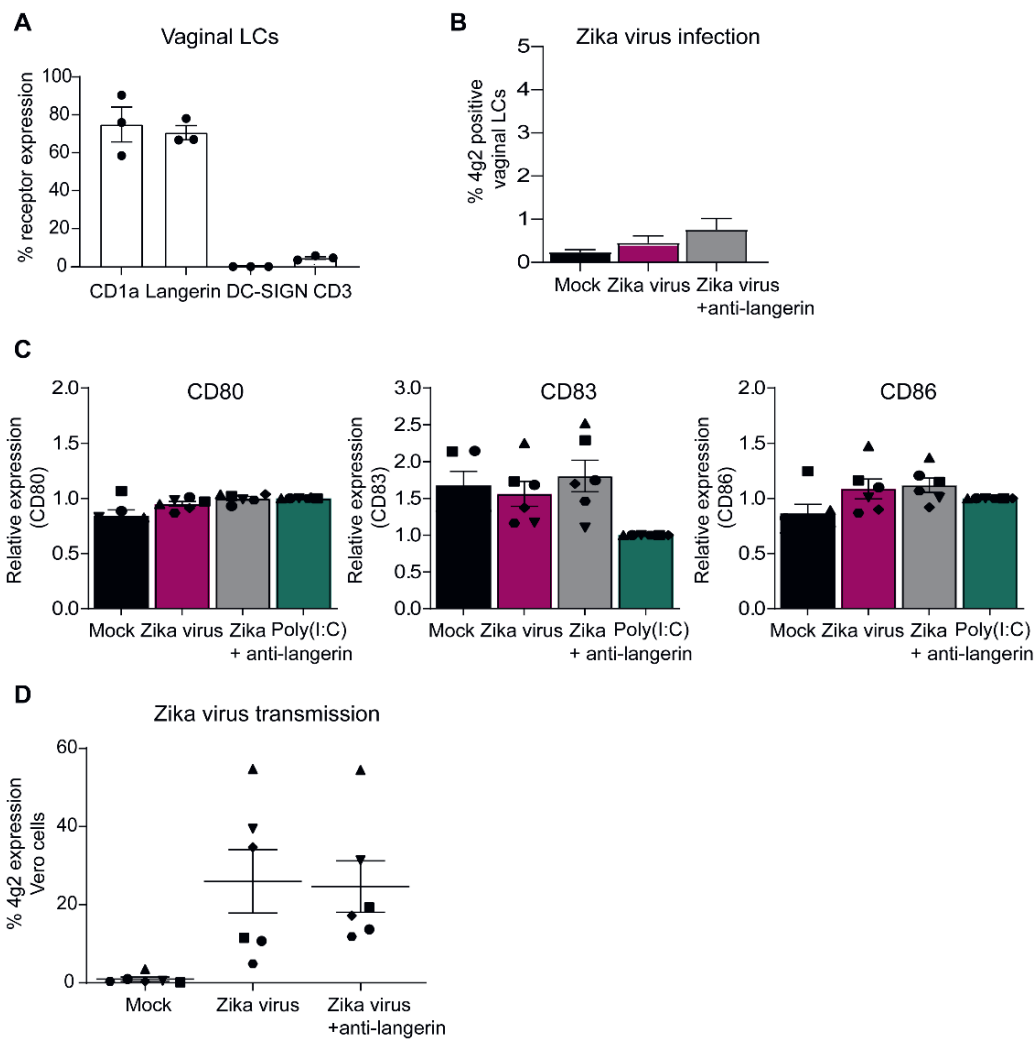


Figure 7 | Vaginal LCs from mucosal tissues transmit Zika virus to target cells independent of infection. (A) Immature LCs isolated from vaginal mucosa were characterized for their high expression of CD1a and langerin and lack of DC-SIGN and CD3, as measured by flow cytometry (n=3 individual vaginal LC donors). (B) Vaginal immature LCs were exposed to Zika virus (850 TCID/ml) for 3 days. Zika virus infection (4g2 Flavivirus envelope protein) was measured by flow cytometry. (n=5 individual donors measured in monoplo). (C) Vaginal immature LCs were pre-incubated with Poly(I:C) (10 ng/ml) or an antibody against langerin (10E2, 20 µg/ml) for 1 hour prior to Zika virus (850 TCID/ml) inoculation. After 24 hours, the expression of activation and maturation markers CD80, CD83 and CD86 were measured by flow cytometry (n=6 donors measured in monoplo). (D) Vaginal immature LCs were inoculated with Zika (850 TCID/ml) virus for 4 hours before the cells were washed extensively and transmitted to Vero cells for co-culture of another 3 days. Prior to Zika virus exposure, the cells were incubated with anti-langerin antibody 10E2 (20 µg/ml). Vero cell infection was measured by anti-4g2 Flavivirus envelope protein on flow cytometry. (D) n=6 donors measured in monoplo). Data information: Data show the mean values and error bars are the SEM.

Discussion

Zika virus continues to circulate endemically in many American and Asian regions^{66, 67, 68}, highlighting the need for better understanding of the virus. Understanding the mechanism of Zika virus infection and transmission are paramount for better prevention and treatment in the future. The (re)emergence of several Flavivirus species in the Americas and Europe (including Zika virus, WNV and YFV) over the past few years suggests that Zika virus could expand to hitherto unaffected areas⁶⁹, and due to climate change conditions more favorable for mosquito breeding and virus replication may persist in these areas⁷⁰.

Little is known about the primary target cells that facilitate Zika virus infection after mosquito bites or sexual contact. Here, we show that different DC subsets are involved in dissemination of Zika virus. Zika virus infected monocyte-derived DC as well as DC subsets in skin, in contrast to epidermal and vaginal LCs. Interestingly, both moDCs and LCs transmitted Zika virus to target cells. Our data strongly suggest that skin and vaginal LCs as well as moDCs are important in viral dissemination of Zika virus. Zika virus stimulation of moDCs lead to a slight increase in the expression of activation markers CD80 and CD86 whereas CD83 was not affected by Zika virus. Moreover, we observed that Zika virus induced type I IFN responses in moDCs after 24 hours, which suggests that infection of moDCs leads to the induction of type I IFN responses similar as observed for dengue virus infection^{71, 72}. As we do not observe induction of type I IFN or ISG at early time points, our data suggest that viral replication is required to induce type I IFN responses and that replication intermediates are sensed. Inhibiting Zika virus replication with the viral polymerase inhibitor 7DMA blocked IFN β transcription 24 hours post inoculation, further indicating that Zika virus infection is important for type I IFN responses. Antibodies against DC-SIGN blocked type I IFN responses as well as infection to a similar extent as the replication inhibitor, supporting that viral replication is a prerequisite for DC activation. Finally, heat-inactivated Zika virus did not induce any type I IFN responses, suggesting that sensing of viral material alone is not sufficient. These data are in line with previous reports that support replicative Zika virus infection of moDCs and induction of type I IFN responses as well as maturation^{32, 38}. Interestingly, Bowen *et. al* suggested that Zika virus blocks IFN β production leading to low maturation and limited type I IFN responses in moDCs following ZIKV infection³¹. Several studies have shown that Zika virus evades antiviral IFN responses. Zika virus NS5 interferes with IFN signaling by inducing degradation of STAT2 proteins^{73, 74, 75}, whereas induction of lipid metabolism has also been suggested to suppress antiviral responses³³. Although we observed that productive infection of moDCs leads to type I IFN responses, we cannot exclude that these responses are limited by Zika virus and might be responsible for the low DC maturation. Moreover, while Zika viruses of the Asian and African lineage do not induce strong maturation and activation in moDCs, IFN induction is nonetheless observed for both lineages³², confirming that Zika virus replication does not completely abrogate type I IFN responses. Further studies are required to understand the

functional consequences on induction of antiviral innate and adaptive immunity to Zika virus by infected DCs.

Conversely, Zika virus did not activate skin derived LCs. Moreover, neither TLR antagonist induced a strong activation, suggesting these cells are difficult to activate. We have shown previously that migration of LCs from epidermal explants induces strong maturation ⁷⁶. However, we observe some induction of ISG15 after 4 hours and 24 hours, indicating that these cells are functional.

While we observed strong binding of Zika virus to cells overexpressing DC-SIGN, we did not observe binding to those expressing langerin. Zika virus binding to DC-SIGN has been described before in different cell lines ^{39, 77, 78} but involvement of other CLR is still largely unclear ⁷⁹. Our data suggest that DC-SIGN is important for Zika virus infection of moDCs isolated from the blood and migrated DCs from a full skin explant model, whereas langerin is not.

Importantly, DC-SIGN expressing cells did not only get infected by Zika virus but also efficiently transmitted Zika virus to target cells, suggesting a role for DC-SIGN in viral dissemination. These data support the notion that Zika virus hijacks DC-SIGN expressing cells for viral dissemination in a process similar to what has been observed previously for other viruses like HIV-1 and recently also SARS-CoV-2 ^{80, 81, 82}. DCs can transmit viruses like HIV-1 via two different pathways: *cis* and *trans*-transmission ⁸³. For *cis*-transmission, DCs are productively infected and new virions are transmitted to target cells ⁸⁴, whereas *trans*-infection refers to the replication independent transfer of virions ⁸³. We observed *cis*-transmission of Zika virus after 48 hours of co-culture with moDCs. Interestingly, we also observed Zika virus transmission by moDCs already after 4 hours of co-culture, where we did not observe infection yet, indicating that Zika virus is transmitted independent of infection. DC-SIGN inhibition abrogated viral dissemination by the *cis* as well as *trans* pathway, suggesting that viral capture via DC-SIGN is crucial for Zika virus infection and transfer. However, block of transmission was strongest during *trans*-infection whereas the protective effect started to wane with longer moDC incubation periods, suggesting that DC-SIGN inhibition is transient. While moDCs efficiently transmitted Zika virus both after 4 hours and 48 hours of incubation, we observed variability in transmission efficacy that are likely attributed to differences in the human primary moDC donors.

Importantly, our data show that DC-SIGN on primary moDCs and skin-derived dermal cells is involved in Zika virus infection and transmission. DC-SIGN expressing cells can be found in many Zika virus target tissues including genital mucosa and the placenta ^{85, 86}, rendering DC-SIGN a promising receptor for preventative approaches against Zika virus.

Importantly, our data describe infection and dissemination of DC-SIGN expressing moDCs with a Zika virus strain of Asian lineage. This strain is the one that was first linked to neurological pathogenicity ⁸⁷ and the strain that is closest related to samples isolated from the outbreak in Brazil ⁸⁸. While there are differences observed in Vero cell and insect cell susceptibility of different Zika virus strains, no such differences were observed in primary

human moDCs³². However, Zika virus from the Asian lineage show higher infection rate in both moDCs and macrophages than a historical African strain³⁸, indicating that moDCs are more susceptible to Asian strain Zika viruses.

LCs, like DCs, migrate to lymph nodes, but are also closely related to macrophages and repopulate locally independent of blood circulation^{44,89}. We observed no Zika virus induced activation of co-stimulatory molecules in epidermal LCs. Interestingly, while LCs did not produce IFN β or most ISGs, there was significant upregulation of IP10 and ISG15 after 48 hours of Zika virus inoculation. Lack of clear IFN β induction might be due to our finding that LCs do not become infected by Zika virus. Neither immature nor activated LCs isolated from skin and vaginal mucosa were infected by Zika virus. Moreover, in a full skin explant model, DC-SIGN expressing cells were preferentially infected over langerin expressing LCs. Notably, we observed that both skin and vaginal LCs transmitted Zika virus to target cells. As we did not observe infection in either of the two cell types, the mode of transmission is likely through *trans*-infection. These data suggest that skin and vaginal LCs might be involved in Zika virus dissemination. The main route of Zika virus transmission is through mosquito bite. We therefore used skin explants from human donor tissue and could verify that DC-SIGN+ cells in the skin become infected with Zika virus. In contrast, langerin expressing cells did not become well infected, supporting their resistance to infection in the skin. However, we observed low levels of langerin expressing cells becoming infected by Zika virus. This is likely contributed to environmental factors present in *in situ* skin explants that are missing in isolated single cell suspension.

Importantly, the female reproductive tract harbors different LC subsets in the epithelial layer of the vagina^{90,91}. LCs we isolated from vaginal mucosa are similar to skin LCs in their co-expression of langerin and CD1a and similarly did not get infected but efficiently transmitted Zika virus to target cells.

Our data strongly suggest that after sexual transmission, Zika virus migrates from the genital tract with the help of LCs. As langerin was not involved in transmission, further studies are required to identify the receptor(s) involved in the transmission of Zika virus by vaginal LCs. In conclusion, DC-SIGN renders primary human DC subsets susceptible to Zika virus infection while also facilitating transmission of infectious virus. Using primary human skin and vaginal mucosa we have uncovered an important role for LCs in the capture and transmission of Zika virus, thereby contributing to viral dissemination and infection. Further investigation into the LC receptors responsible for Zika virus transmission might lead to better understanding and prevention of sexual transmission of Zika virus.

Materials and Methods

Study approval

This study was performed according to the Amsterdam University Medical Centers, location AMC, Medical Ethics Committee guidelines. This study, including the tissue harvesting procedures, was conducted in accordance with the ethical principles set out in the declaration of Helsinki and was approved by the institutional review board of the Amsterdam University Medical Centers and the Ethics Advisory Body of the Sanquin Blood Supply Foundation (Amsterdam, Netherlands). All research was performed in accordance with appropriate guidelines and regulations.

Isolation of monocyte derived Dendritic cells

CD14⁺ monocytes were obtained from buffy coats of healthy volunteer donors (Sanquin blood bank) and differentiated into monocyte derived DCs as described previously⁹². In short, first PBMCs were isolated with lymphoprep. Subsequently, monocytes were collected after percoll gradient steps. Monocytes were cultured in RPMI medium supplemented with 10% FCS, l-glutamine (2 mM, Lonza), penicillin and streptomycin (100 U/mL and 100 µg/mL, respectively, Thermo Fisher) in the presence of GM-CSF (800 U/mL, Invitrogen) and IL-4 (500 U/mL Invitrogen) at 37°C, 5% CO₂ for 6 days to obtain monocyte-derived DCs.

Isolation of Langerhans cells from epidermis

Skin LCs were isolated from human epidermal sheets obtained from healthy donors undergoing corrective plastic surgery. Epidermal sheets were prepared as described previously^{51, 76}. Briefly, skin-grafts consisting of epidermis and dermis were obtained using a dermatome (Zimmer Biomet, Indiana USA). Upon overnight incubation with Dispase II (1 U/mL, Roche Diagnostics), epidermal sheets were separated from dermis, washed and either directly subjected to enzymatic treatment with trypsin and DNase to obtain immature skin LCs or alternatively, cultured in IMDM (Thermo Fischer Scientific, USA) supplemented with 10% FCS, gentamycine (20 µg/mL, Centrafarm, Netherlands), penicilline/streptomycin (10 U/mL and 10 µg/mL, respectively; Invitrogen) for 3 days after to harvest activated LCs. Immature as well as activated skin LCs were purified by ficoll gradient (Axis-shield). Immature skin LCs were further subjugated to CD1a magnetic cell separation (MACS, Miltenyi Biotec). Purity of LCs was routinely verified by flow cytometry using antibodies directed against CD207 (langerin) and CD1a.

Full skin *ex vivo* sheets

Ex vivo sheets of human skin were obtained from healthy donors undergoing corrective

surgery. The top two layers of the skin were prepared as described previously⁵¹. After retrieval of a thin layer (thickness at 12pt) containing both the epidermis and dermis, biopsies with a diameter of 8 mm (Kai medical) were prepared. The biopsies were placed on 500 μ L of IMDM (Thermo Fischer Scientific, USA) supplemented with 10% FCS, gentamycine (20 μ g/mL, Centrafarm, Netherlands), penicilline/streptomycin (10 U/mL and 10 μ g/mL, respectively; Invitrogen). Zika virus was added at a concentration of 1000 TCID/ml after which the sheets were left at 37°C. After 3 days, the sheets were removed and the medium containing the emigrated cells was subjected to further analyses.

Isolation of Langerhans cells from vaginal mucosa

Human vaginal tissue was collected from women undergoing prolapse surgery where excessive vaginal tissue was removed from the anterior or posterior vaginal wall. Surplus stroma was removed from mucosal sheets dissected until a thin layer of submucosa remained and tissue was cut into strips of 5-7 mm. Vaginal tissue strips were incubated overnight at 4 °C in complete medium (Iscoves Modified Dulbecco's Medium (IMDM) of Thermo Fischer Science with L-glutamine 100 mmol/L, 10% FCS, 2500 U/mL penicillin, and 2500 mg/mL streptomycin) supplemented with Dispase II (3 U/mL, Roche Diagnostics). After incubation, the epithelial layer and lamina propria were mechanically split by the use of tweezers. Vaginal epithelial sheets were extensively washed in PBS after which was proceeded with immature LC isolation.

Immature vaginal LCs were obtained after mucosal sheets were cut in small pieces using surgical scissors and incubated for 30 minutes in PBS containing trypsin (0,05%, BD Biosciences) and DNAase I (20 U/mL, Roche Applied Science) to obtain a single cell suspension. Further vaginal LC purification was achieved by ficoll gradient centrifugation (Axis-shield) and CD1a magnetic cell separation (MACS, Miltenyi Biotec).

Cell lines

The African monkey Vero cells (ATCC® CCL-81™) were maintained in MEM with Earle's Salts (Capricorn Scientific, Ebsdorfergrund, Germany) supplemented with 10% fetal calf serum (FCS), L-glutamine and penicillin/streptomycin (10 μ g/mL) as well as non-essential amino acids (NEAA). Culture was maintained at 37C with 5% CO₂. The human B cells, Raji (ATCC® CCL-86™) as well as Raji transfectants stably expressing human DC-SIGN or human langerin created by electroporation⁴¹ were cultured in RPMI 1640 medium (Gibco Life Technologies, Gaithersburg, Md.) containing 10% fetal calf serum (FCS), penicillin/streptomycin (10 μ g/mL). The expression of DC-SIGN and langerin was regularly checked via FACS analysis.

Zika virus production

The following reagent was obtained from the European Virus Archive goes global: Zika virus, strain H/PF/2013 (clinical isolate, Asian lineage), French Polynesia 2013 with Ref-SKU: 001v-EVA1545 and GenBank number KJ776791.2. Vero cells (ATCC® CCL-81™) were inoculated with the Zika virus isolate and used for reproduction of virus stocks. Formation of cytopathic effect (CPE) was closely monitored and after observing a CPE of 4+, supernatant containing the virus was filtered (0.2 µm) and stored at -80C.

Tetrazolium dye colorimetric cell viability (MTT) assay

Viral titers were determined by tissue culture infectious dose (TCID50) on Vero cells by MTT assay. In brief, Vero cells were seeded in a 96 well plate at a cell density of 10.000 cells per well. After 24 hours, cells were inoculated with a 5-fold serial dilution of Zika virus. Cell cytotoxicity was measured 72 hours after infection. MTT solution was added to Vero cells and incubated for 2 hours at 37°C. After removing the MTT solution, MTT solvent containing 4 mM HCL and 1% Nonidet P-40 (NP40) in isopropanol was added to the cells. Homogenous solution was measured at optical density between 580 nm and 655 nm. Loss of MTT staining as determined by spectrometer is indicative of CPE caused by Zika virus infection. The virus titer was determined as TCID50/mL and calculated based on the Reed Muench method⁹³.

Reagents

The following reagents were used: to inhibit Zika virus replication, the viral polymerase inhibitor 7-Deaza-2'-C-Methyladenosine (7DMA) (#ND08351, Carbosynth) as described in⁹⁴. Cells were stimulated with lipopolysaccharide (LPS) Salmonella enterica serotype typhimurium (10 ng/mL, Sigma) or Poly(I:C) (10 µg/mL, Invitrogen).

Zika virus infection

Isolated primary cells as well as cell lines and full skin explants were inoculated with Zika virus at different TCID/ml concentrations. Viral infection was determined after two to three days post inoculation via flow cytometry staining. Zika virus infection was measured with antibodies against either a Flavivirus envelope protein. Viral binding was determined by RT-PCR after 4 hours. Zika virus was heat-inactivated for 60 min at 60°C as described by⁵⁸.

Cell maturation

Monocyte derived DCs, immature skin and immature vaginal LCs were exposed to either Poly(I:C) or LTA (both Invitrogen) at a concentration of 10 µg/ml. Additionally, skin derived LCs were exposed to 1 µM of Motolimod (VTX124 2337, MedChemExpress). Simultaneously,

cells were inoculated with Zika virus at a concentration of 850 TCID/ml with or without the presence of a C-type lectin inhibitor (AZN-D1 for DCs, 10E2 for LCs) or mannan. After 24 hours at 37°C, cells were either fixed to continuing with FACS analysis or lysed for subsequent PCR analysis.

Flow cytometry

Cells were fixed with paraformaldehyde (PFA) and treated with either BSA (extracellular staining) or BSA/Saponin to measure intracellular staining. The following antibodies were used to detect Zika virus: anti-Flavivirus 4g2 mouse IgG2a (NovusBio), anti-Flavivirus 4g2 monoclonal rabbit (Absolute Antibody).

All other antibodies were anti-human: DC-SIGN mouse IgG1 (AZN-D1), , anti-langerin mouse IgG1 (10E2) both in house made, PE conjugated CD207 (langerin), APC conjugated CD1a (BD Biosciences), CD86-FITC (BD Pharmingen), CD80-PE (BD Pharmingen), CD83-APC (BD Pharmingen), DC-SIGN-FITC (R&D systems), CD3-APC/Fire750 (Biolegend), CD11c-APC (Biolegend), PEcy7-HLA-DR (BD Pharmingen), APCcy7-CD14 (BD Biosciences), APCcy7-CD11c (Biolegend), APC-AXL (Thermofisher), PE-MerTK (Thermofisher) and anti-Tyro3 (Thermofisher). For secondary detection the following antibodies were used: AF488-conjugated goat anti-mouse IgG2a (Invitrogen), AF647-conjugated donkey anti-rabbit (Thermofisher), FITC-conjugated goat-anti-mouse IgM (Invitrogen), AF488-conjugated donkey anti-rabbit (Thermofisher).

Flow cytometric analyses were performed on a BD FACS Canto II (BD Biosciences) and data was analysed using FlowJo V10 software (TreeStar).

Zika virus binding

To determine Zika virus binding to C-type lectins DC-SIGN and langerin, Raji cells were seeded at a density of 100.000 cells in 100 µl. Cells were kept in FCS free medium to increase receptor expression prior to virus exposure. Zika virus was added at a concentration of 175 TCID/ml and the cells were left at 4°C for 4 hours. Subsequently, cells were washed extensively to remove any unbound virus before lysis with AVL buffer. RNA was isolated with the QIAamp Viral RNA Mini Kit (Qiagen) according to the manufacturer's protocol.

Transmission assays and co-culture

Raji cells were exposed to 35 TCID/ml Zika virus for 4 hours. DC-SIGN or langerin receptors were blocked prior to virus inoculation antibodies against AZN-D1 or 10E2 for 1 hour at 37°C. Primary DCs were exposed to ZIVK with 425, 850 or 2550 TCID/ml. Skin or vaginal immature LCs were exposed to 805 TCID/ml of Zika virus. Prior to virus inoculation, DC-SIGN or langerin receptors were blocked with antibodies against AZN-D1 or 10E2 respectively in

certain conditions. Infection was determined after incubation with the virus for multiple days and assessed by flow cytometry. Additionally, primary cells were stimulated with LPS or Poly(I:C) for 24h before infection. Virus transmission to Vero target cells was determined by incubating Raji, DCs or LCs with Zika virus for either 4h or 48h. After, cells were washed extensively to remove unbound virus and subsequently co-cultured with Vero cells for 3 days. To assess Zika virus transmission, infection of Vero cells was measured by flow cytometry.

RNA isolation and quantitative Real Time-PCR

Viral RNA in cells was isolated using the QIAamp Viral RNA Mini Kit (Qiagen) according to the manufacturers protocol. cDNA was subsequently synthesized with the M-MLV reverse-transcriptase kit (Promega). cDNA samples were diluted 1 in 5 before further application. Cellular mRNA of cells not exposed to virus was isolated with an mRNA Capture kit (Roche) and cDNA was synthesized with a reverse-transcriptase kit (Promega). PCR amplification for all targets was performed in the presence of SYBR green in a 7500 Fast Realtime PCR System (ABI). Specific primers were designed with Primer Express 2.0 (Applied Biosystems). Primer sequences used for mRNA expression were for gene product: GAPDH, forward primer (CCATGTTTCGTCATGGGTGTG), reverse primer (GGTGCTAA GCAGTTGGTGGTG). For gene product Zika virus-NS5, forward primer (CTTGTGGCTGCTGCGGAGGTCA), reverse primer (AACACGCTTAACAAAGCACTC GTGGTGGGAGCAAACGGAATT) as described previously⁹⁵. For gene product IFN β , forward primer (ACAGACTTACAGGTTACCTCCGAAAC), reverse primer (CATCTGCTGGTTGAAGAATGCTT); for OAS1, forward primer (TGCGCTCAGCTTCGTACTION), reverse primer (GGTGGAGAACTCGCCCTCTT); APOBEC3G, forward primer (TTGAGCCTTGAATAATCTGCC), reverse primer (TCGAGTGTCTGAGAATCTCCCC); MXA, forward primer (TTCAGCACCTGATGGCCTATC), reverse primer (GTACGTCTGGAGCATGAAGAACTG); IRF7, forward primer (GCTCCCCACGCTATACCATCTAC), reverse primer (GCCAGGGTCCAGTTCAC); IP10, forward primer (CGCTGTACCTGCATCAGCAT), reverse primer (CATCTTCTCACCTTCTTTTCA); for ISG15, forward primer (TTTGCCAGTACAGGAGCTTGTG), reverse primer (GGGTGATCTGCGCCTTCA). The normalized amount of target mRNA was calculated from the Ct values obtained for both target and household mRNA with the equation $Nt = 2Ct (GAPDH) - Ct(target)$.

Cell viability assay

MTT solution was added to Vero cells and incubated for 2 hours at 37°C. After removing the MTT solution, MTT solvent containing 4 mM HCL and 1% Nonidet P-40 (NP40) in isopropanol was added to the cells. Homogenous solution was measured at optical density between 580 nm and 655 nm. For cell viability check with the CellTiter-Glo[®] Luminescent Cell Viability

Assay (Promega), cells were mixed with the buffer in a 1:1 ratio. The cells were treated according to the manufacturers protocol and measured with a luminometer.

Statistics

All results are presented as mean \pm SEM and were analyzed by GraphPad Prism 8 software (GraphPad Software Inc.). A two-tailed, parametric Student's *t*-test for unpaired observation, Mann-Whitney tests (differences between different donors, that were not normally distributed) was performed. For unpaired, non-parametric observations a one-way ANOVA or two-way ANOVA test with post hoc analysis (Tukey's or Dunnet's) were performed. Statistical significance was set at * $P < 0.05$, ** $P < 0.01$ *** $P < 0.001$ **** $P < 0.0001$.

Data availability statement

The original contributions presented in the study are included in the article/Supplementary Material. Further inquiries can be directed to the corresponding author.

Author contributions

JE conceived and designed experiments. JE and EZW performed the experiments, acquired data and analyzed data. JE, NK and TBHG interpreted data and contributed to scientific discussion. GK, NK and KCW provided essential research materials. GK helped with experiments and data acquisition. JE and TBHG wrote the manuscript with input from all listed authors. TBHG perceived of the original study idea and was involved in all aspects of the study. All authors approved the final version of the manuscript. The corresponding author vouches for the completeness and accuracy of the data.

Funding

This research was funded through a European Research Council (Advanced grant 670424).

Conflict of interest

The authors have no conflicts of interest to disclose.

Acknowledgments

We would like to thank Ad van Nuenen for continued support in and outside the ML-III laboratory.

References

1. Musso, D. & Gubler, D.J. Zika Virus. *Clinical microbiology reviews* **29**, 487-524 (2016).
2. Zanoluca, C. & Dos Santos, C.N. Zika virus - an overview. *Microbes Infect* **18**, 295-301 (2016).
3. Duffy, M.R. *et al.* Zika virus outbreak on Yap Island, Federated States of Micronesia. *The New England journal of medicine* **360**, 2536-2543 (2009).
4. Musso, D., Nilles, E.J. & Cao-Lormeau, V.M. Rapid spread of emerging Zika virus in the Pacific area. *Clin Microbiol Infect* **20**, 0595-596 (2014).
5. Mlakar, J. *et al.* Zika Virus Associated with Microcephaly. *The New England journal of medicine* **374**, 951-958 (2016).
6. Heymann, D.L. *et al.* Zika virus and microcephaly: why is this situation a PHEIC? *Lancet (London, England)* **387**, 719-721 (2016).
7. Krauer, F. *et al.* Zika Virus Infection as a Cause of Congenital Brain Abnormalities and Guillain-Barre Syndrome: Systematic Review. *PLoS medicine* **14**, e1002203 (2017).
8. Musso, D., Ko, A.I. & Baud, D. Zika Virus Infection - After the Pandemic. *The New England journal of medicine* **381**, 1444-1457 (2019).
9. WHO. WHO statement on the first meeting of the International Health Regulations (2005) (IHR 2005) Emergency Committee on Zika virus and observed increase in neurological disorders and neonatal malformations. . 2016.
10. Carrera, J., Trenerry, A.M., Simmons, C.P. & Mackenzie, J.M. Flavivirus replication kinetics in early-term placental cell lines with different differentiation pathways. *Virology* **18**, 251 (2021).
11. El Costa, H. *et al.* ZIKA virus reveals broad tissue and cell tropism during the first trimester of pregnancy. *Sci Rep* **6**, 35296 (2016).
12. Rosenberg, A.Z., Yu, W., Hill, D.A., Reyes, C.A. & Schwartz, D.A. Placental Pathology of Zika Virus: Viral Infection of the Placenta Induces Villous Stromal Macrophage (Hofbauer Cell) Proliferation and Hyperplasia. *Arch Pathol Lab Med* **141**, 43-48 (2017).
13. Aagaard, K.M. *et al.* Primary Human Placental Trophoblasts are Permissive for Zika Virus (ZIKV) Replication. *Sci Rep* **7**, 41389 (2017).
14. Tabata, T. *et al.* Zika Virus Targets Different Primary Human Placental Cells, Suggesting Two Routes for Vertical Transmission. *Cell Host Microbe* **20**, 155-166 (2016).
15. Chiu, C.F. *et al.* The Mechanism of the Zika Virus Crossing the Placental Barrier and the Blood-Brain Barrier. *Front Microbiol* **11**, 214 (2020).
16. Szaba, F.M. *et al.* Zika virus infection in immunocompetent pregnant mice causes fetal damage and placental pathology in the absence of fetal infection. *PLoS Pathog* **14**, e1006994 (2018).
17. Martinot, A.J. *et al.* Fetal Neuropathology in Zika Virus-Infected Pregnant Female Rhesus Monkeys. *Cell*

- 173**, 1111-1122.e1110 (2018).
18. Hirsch, A.J. *et al.* Zika virus infection in pregnant rhesus macaques causes placental dysfunction and immunopathology. *Nat Commun* **9**, 263 (2018).
 19. Santos, G.R. *et al.* Histopathologic Changes in Placental Tissue Associated With Vertical Transmission of Zika Virus. *Int J Gynecol Pathol* **39**, 157-162 (2020).
 20. Martines, R.B. *et al.* Notes from the Field: Evidence of Zika Virus Infection in Brain and Placental Tissues from Two Congenitally Infected Newborns and Two Fetal Losses--Brazil, 2015. *MMWR. Morbidity and mortality weekly report* **65**, 159-160 (2016).
 21. Counotte, M.J. *et al.* Sexual transmission of Zika virus and other flaviviruses: A living systematic review. *PLoS medicine* **15**, e1002611 (2018).
 22. Davidson, A., Slavinski, S., Komoto, K., Rakeman, J. & Weiss, D. Suspected Female-to-Male Sexual Transmission of Zika Virus - New York City, 2016. *MMWR. Morbidity and mortality weekly report* **65**, 716-717 (2016).
 23. Deckard, D.T. *et al.* Male-to-Male Sexual Transmission of Zika Virus--Texas, January 2016. *MMWR. Morbidity and mortality weekly report* **65**, 372-374 (2016).
 24. D'Ortenzio, E. *et al.* Evidence of Sexual Transmission of Zika Virus. *The New England journal of medicine* **374**, 2195-2198 (2016).
 25. Hills, S.L. *et al.* Transmission of Zika Virus Through Sexual Contact with Travelers to Areas of Ongoing Transmission - Continental United States, 2016. *MMWR. Morbidity and mortality weekly report* **65**, 215-216 (2016).
 26. Duggal, N.K. *et al.* Frequent Zika Virus Sexual Transmission and Prolonged Viral RNA Shedding in an Immunodeficient Mouse Model. *Cell reports* **18**, 1751-1760 (2017).
 27. Mead, P.S. *et al.* Zika Virus Shedding in Semen of Symptomatic Infected Men. *The New England journal of medicine* **378**, 1377-1385 (2018).
 28. Musso, D. *et al.* Detection of Zika virus RNA in semen of asymptomatic blood donors. *Clin Microbiol Infect* **23**, 1001.e1001-1001.e1003 (2017).
 29. Yang, D. *et al.* STAT2-dependent restriction of Zika virus by human macrophages but not dendritic cells. *Emerg Microbes Infect* **10**, 1024-1037 (2021).
 30. Michlmayr, D., Andrade, P., Gonzalez, K., Balmaseda, A. & Harris, E. CD14(+)CD16(+) monocytes are the main target of Zika virus infection in peripheral blood mononuclear cells in a paediatric study in Nicaragua. *Nat Microbiol* **2**, 1462-1470 (2017).
 31. Bowen, J.R. *et al.* Zika Virus Antagonizes Type I Interferon Responses during Infection of Human Dendritic Cells. *PLoS Pathog* **13**, e1006164 (2017).
 32. Vielle, N.J. *et al.* Silent infection of human dendritic cells by African and Asian strains of Zika virus. *Sci Rep* **8**, 5440 (2018).
 33. Branche, E. *et al.* SREBP2-dependent lipid gene transcription enhances the infection of human dendritic cells by Zika virus. *Nat Commun* **13**, 5341 (2022).
 34. García-Nicolás, O., Lewandowska, M.,

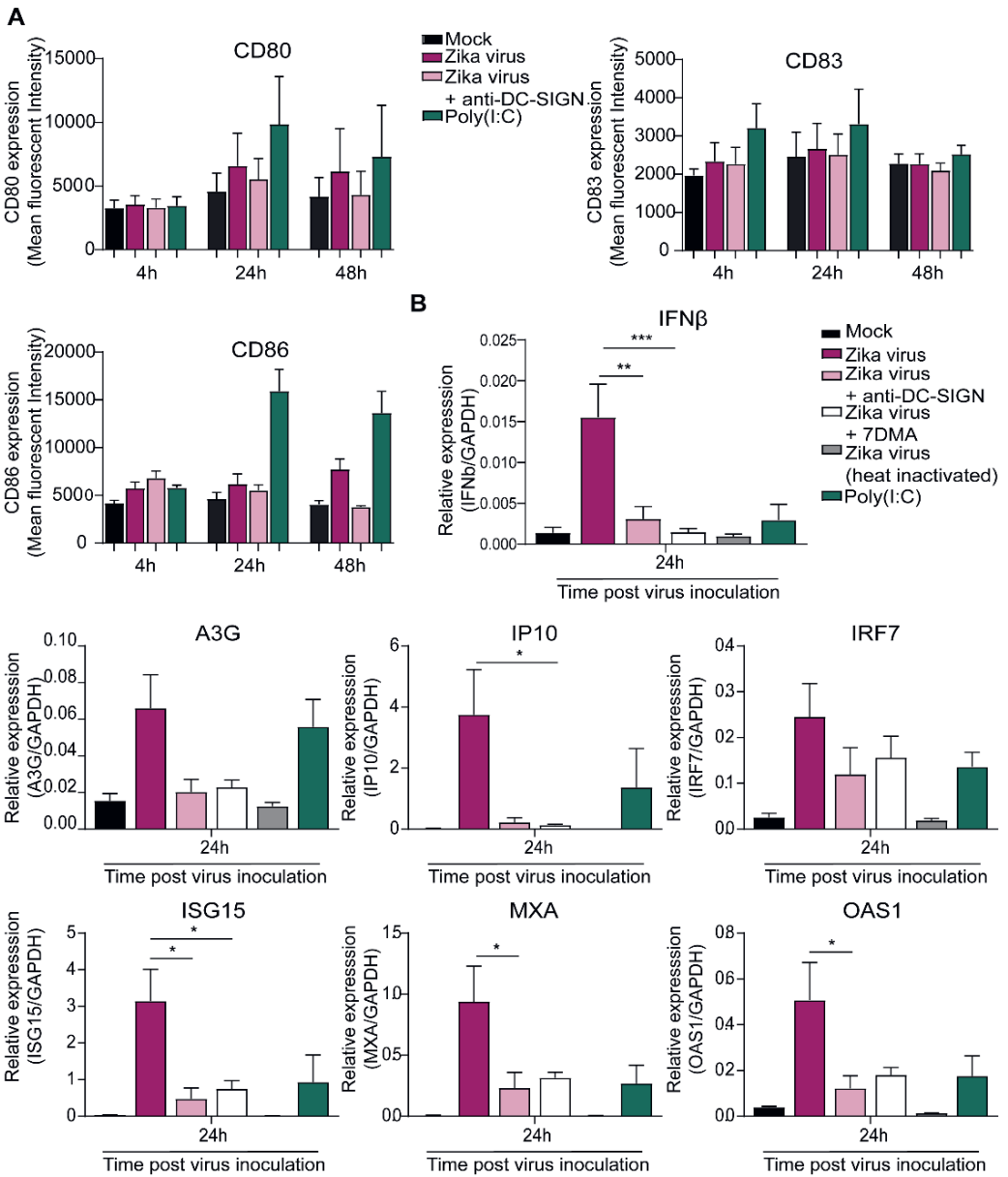
- Ricklin, M.E. & Summerfield, A. Monocyte-Derived Dendritic Cells as Model to Evaluate Species Tropism of Mosquito-Borne Flaviviruses. *Front Cell Infect Microbiol* **9**, 5 (2019).
35. Schmid, M.A., Diamond, M.S. & Harris, E. Dendritic cells in dengue virus infection: targets of virus replication and mediators of immunity. *Front Immunol* **5**, 647 (2014).
36. Schmid, M.A. & Harris, E. Monocyte recruitment to the dermis and differentiation to dendritic cells increases the targets for dengue virus replication. *PLoS Pathog* **10**, e1004541 (2014).
37. Sun, X. *et al.* Transcriptional Changes during Naturally Acquired Zika Virus Infection Render Dendritic Cells Highly Conducive to Viral Replication. *Cell reports* **21**, 3471-3482 (2017).
38. Österlund, P. *et al.* Asian and African lineage Zika viruses show differential replication and innate immune responses in human dendritic cells and macrophages. *Sci Rep* **9**, 15710 (2019).
39. Hamel, R. *et al.* Biology of Zika Virus Infection in Human Skin Cells. *J Virol* **89**, 8880-8896 (2015).
40. Soilleux, E.J. DC-SIGN (dendritic cell-specific ICAM-grabbing non-integrin) and DC-SIGN-related (DC-SIGNR): friend or foe? *Clin Sci (Lond)* **104**, 437-446 (2003).
41. Geijtenbeek, T.B. *et al.* DC-SIGN, a dendritic cell-specific HIV-1-binding protein that enhances trans-infection of T cells. *Cell* **100**, 587-597 (2000).
42. Tassaneeritthep, B. *et al.* DC-SIGN (CD209) mediates dengue virus infection of human dendritic cells. *J Exp Med* **197**, 823-829 (2003).
43. Clayton, K., Vallejo, A.F., Davies, J., Sirvent, S. & Polak, M.E. Langerhans Cells-Programmed by the Epidermis. *Front Immunol* **8**, 1676 (2017).
44. Merad, M., Ginhoux, F. & Collin, M. Origin, homeostasis and function of Langerhans cells and other langerin-expressing dendritic cells. *Nat Rev Immunol* **8**, 935-947 (2008).
45. van den Berg, L.M. *et al.* Langerhans Cell-Dendritic Cell Cross-Talk via Langerin and Hyaluronic Acid Mediates Antigen Transfer and Cross-Presentation of HIV-1. *J Immunol* **195**, 1763-1773 (2015).
46. West, H.C. & Bennett, C.L. Redefining the Role of Langerhans Cells As Immune Regulators within the Skin. *Front Immunol* **8**, 1941 (2017).
47. Hertoghs, N. *et al.* Sexually transmitted founder HIV-1 viruses are relatively resistant to Langerhans cell-mediated restriction. *PLoS One* **14**, e0226651 (2019).
48. Hladik, F. *et al.* Initial events in establishing vaginal entry and infection by human immunodeficiency virus type-1. *Immunity* **26**, 257-270 (2007).
49. Cunningham, A.L., Carbone, F. & Geijtenbeek, T.B. Langerhans cells and viral immunity. *Eur J Immunol* **38**, 2377-2385 (2008).
50. Wu, S.J. *et al.* Human skin Langerhans cells are targets of dengue virus infection. *Nat Med* **6**, 816-820 (2000).
51. de Witte, L. *et al.* Langerin is a natural barrier to HIV-1 transmission by Langerhans cells. *Nat Med* **13**, 367-371

- (2007).
52. Ribeiro, C.M. *et al.* Receptor usage dictates HIV-1 restriction by human TRIM5 α in dendritic cell subsets. *Nature* **540**, 448-452 (2016).
 53. van den Berg, L.M. *et al.* Caveolin-1 mediated uptake via langerin restricts HIV-1 infection in human Langerhans cells. *Retrovirology* **11**, 123 (2014).
 54. Yan, N. & Chen, Z.J. Intrinsic antiviral immunity. *Nat Immunol* **13**, 214-222 (2012).
 55. Schoggins, J.W. Interferon-Stimulated Genes: What Do They All Do? *Annu Rev Virol* **6**, 567-584 (2019).
 56. Schoggins, J.W. *et al.* A diverse range of gene products are effectors of the type I interferon antiviral response. *Nature* **472**, 481-485 (2011).
 57. Soto, J.A. *et al.* The Role of Dendritic Cells During Infections Caused by Highly Prevalent Viruses. *Front Immunol* **11**, 1513 (2020).
 58. Chida, A.S. *et al.* Comparison of Zika virus inactivation methods for reagent production and disinfection methods. *Journal of Virological Methods* **287**, 114004 (2021).
 59. Soilleux, E.J. & Coleman, N. Langerhans cells and the cells of Langerhans cell histiocytosis do not express DC-SIGN. *Blood* **98**, 1987-1988 (2001).
 60. Ebner, S. *et al.* Expression of C-type lectin receptors by subsets of dendritic cells in human skin. *International Immunology* **16**, 877-887 (2004).
 61. de Witte, L., Nabatov, A. & Geijtenbeek, T.B. Distinct roles for DC-SIGN $^{+}$ -dendritic cells and Langerhans cells in HIV-1 transmission. *Trends Mol Med* **14**, 12-19 (2008).
 62. Bermejo-Jambrina, M. *et al.* C-Type Lectin Receptors in Antiviral Immunity and Viral Escape. *Front Immunol* **9**, 590 (2018).
 63. Routhu, N.K. *et al.* Glycosylation of Zika Virus is Important in Host-Virus Interaction and Pathogenic Potential. *Int J Mol Sci* **20** (2019).
 64. Hastings, A.K. *et al.* TAM Receptors Are Not Required for Zika Virus Infection in Mice. *Cell reports* **19**, 558-568 (2017).
 65. Fehres, C.M. *et al.* In situ Delivery of Antigen to DC-SIGN $^{+}$ CD14 $^{+}$ Dermal Dendritic Cells Results in Enhanced CD8 $^{+}$ T-Cell Responses. *J Invest Dermatol* **135**, 2228-2236 (2015).
 66. Honein, M.A., Cetron, M.S. & Meaney-Delman, D. Endemic Zika virus transmission: implications for travellers. *Lancet Infect Dis* **19**, 349-351 (2019).
 67. Yadav, P.D. *et al.* Zika a Vector Borne Disease Detected in Newer States of India Amidst the COVID-19 Pandemic. *Front Microbiol* **13**, 888195 (2022).
 68. Jesus, M.C.S. *et al.* Silent circulation of Zika and dengue virus in *Aedes aegypti* (Diptera: Culicidae) during a non-epidemic year in the state of Sergipe, northeastern Brazil. *Trans R Soc Trop Med Hyg* **116**, 924-929 (2022).
 69. Gould, E., Pettersson, J., Higgs, S., Charrel, R. & de Lamballerie, X. Emerging arboviruses: Why today? *One Health* **4**, 1-13 (2017).
 70. Benitez, M.A. Climate change could affect mosquito-borne diseases in Asia. *Lancet (London, England)* **373**, 1070 (2009).
 71. Sprokholt, J.K. *et al.* RIG-I-like Receptor

- Triggering by Dengue Virus Drives Dendritic Cell Immune Activation and T(H)1 Differentiation. *J Immunol* **198**, 4764-4771 (2017).
72. Sprockholt, J.K. *et al.* RIG-I-like receptor activation by dengue virus drives follicular T helper cell formation and antibody production. *PLoS Pathog* **13**, e1006738 (2017).
 73. Kumar, A. *et al.* Zika virus inhibits type-I interferon production and downstream signaling. *EMBO Rep* **17**, 1766-1775 (2016).
 74. Hertzog, J. *et al.* Infection with a Brazilian isolate of Zika virus generates RIG-I stimulatory RNA and the viral NS5 protein blocks type I IFN induction and signaling. *Eur J Immunol* **48**, 1120-1136 (2018).
 75. Grant, A. *et al.* Zika Virus Targets Human STAT2 to Inhibit Type I Interferon Signaling. *Cell Host Microbe* **19**, 882-890 (2016).
 76. Sarrami-Forooshani, R. *et al.* Human immature Langerhans cells restrict CXCR4-using HIV-1 transmission. *Retrovirology* **11**, 52 (2014).
 77. Ramos-Soriano, J. & Rojo, J. Glycodendritic structures as DC-SIGN binders to inhibit viral infections. *Chem Commun (Camb)* **57**, 5111-5126 (2021).
 78. Carbaugh, D.L., Baric, R.S. & Lazear, H.M. Envelope Protein Glycosylation Mediates Zika Virus Pathogenesis. *J Virol* **93** (2019).
 79. Agrelli, A., de Moura, R.R., Crovella, S. & Brandão, L.A.C. ZIKA virus entry mechanisms in human cells. *Infect Genet Evol* **69**, 22-29 (2019).
 80. Bermejo-Jambrina, M. *et al.* Infection and transmission of SARS-CoV-2 depend on heparan sulfate proteoglycans. *Embo j* **40**, e106765 (2021).
 81. Ganesh, L. *et al.* Infection of specific dendritic cells by CCR5-tropic human immunodeficiency virus type 1 promotes cell-mediated transmission of virus resistant to broadly neutralizing antibodies. *J Virol* **78**, 11980-11987 (2004).
 82. Engering, A., Van Vliet, S.J., Geijtenbeek, T.B. & Van Kooyk, Y. Subset of DC-SIGN(+) dendritic cells in human blood transmits HIV-1 to T lymphocytes. *Blood* **100**, 1780-1786 (2002).
 83. Dong, C., Janas, A.M., Wang, J.H., Olson, W.J. & Wu, L. Characterization of human immunodeficiency virus type 1 replication in immature and mature dendritic cells reveals dissociable cis- and trans-infection. *J Virol* **81**, 11352-11362 (2007).
 84. Bracq, L., Xie, M., Benichou, S. & Bouchet, J. Mechanisms for Cell-to-Cell Transmission of HIV-1. *Front Immunol* **9**, 260 (2018).
 85. Yang, S.W. *et al.* DC-SIGN expression in Hofbauer cells may play an important role in immune tolerance in fetal chorionic villi during the development of preeclampsia. *J Reprod Immunol* **124**, 30-37 (2017).
 86. Reyes, L. & Golos, T.G. Hofbauer Cells: Their Role in Healthy and Complicated Pregnancy. *Front Immunol* **9**, 2628 (2018).
 87. Oehler, E. *et al.* Zika virus infection complicated by Guillain-Barre syndrome--case report, French Polynesia, December 2013. *Euro*

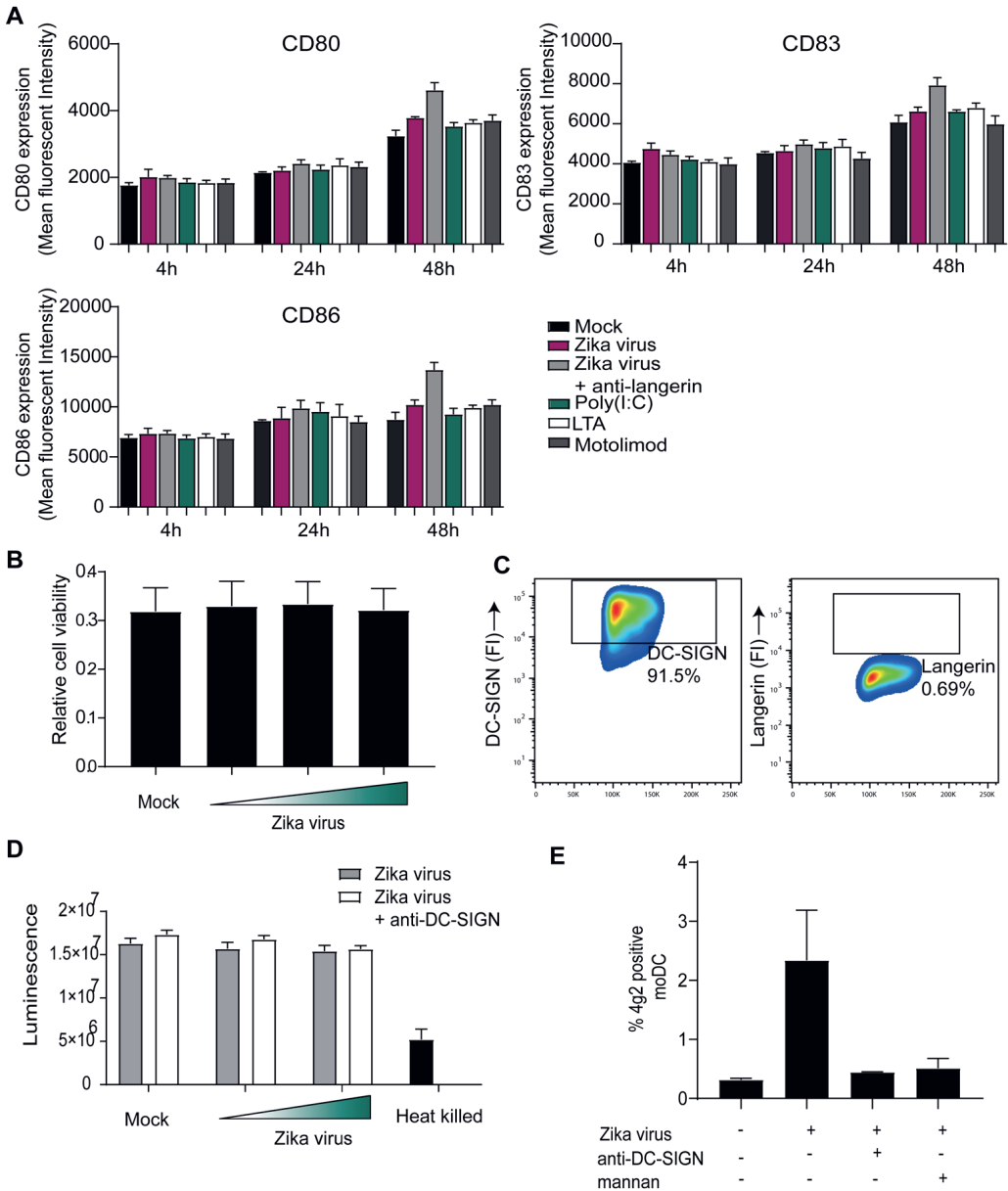
- surveillance : bulletin Europeen sur les maladies transmissibles = European communicable disease bulletin* **19** (2014).
88. Musso, D. Zika Virus Transmission from French Polynesia to Brazil. *Emerg Infect Dis* **21**, 1887 (2015).
89. Doebel, T., Voisin, B. & Nagao, K. Langerhans Cells - The Macrophage in Dendritic Cell Clothing. *Trends Immunol* **38**, 817-828 (2017).
90. Wira, C.R., Fahey, J.V., Sentman, C.L., Pioli, P.A. & Shen, L. Innate and adaptive immunity in female genital tract: cellular responses and interactions. *Immunol Rev* **206**, 306-335 (2005).
91. Duluc, D. *et al.* Transcriptional fingerprints of antigen-presenting cell subsets in the human vaginal mucosa and skin reflect tissue-specific immune microenvironments. *Genome Med* **6**, 98 (2014).
92. Mesman, A.W. *et al.* Measles virus suppresses RIG-I-like receptor activation in dendritic cells via DC-SIGN-mediated inhibition of PP1 phosphatases. *Cell Host Microbe* **16**, 31-42 (2014).
93. REED, L.J. & MUENCH, H. A SIMPLE METHOD OF ESTIMATING FIFTY PER CENT ENDPOINTS¹². *American Journal of Epidemiology* **27**, 493-497 (1938).
94. Zmurko, J. *et al.* The Viral Polymerase Inhibitor 7-Deaza-2'-C-Methyladenosine Is a Potent Inhibitor of In Vitro Zika Virus Replication and Delays Disease Progression in a Robust Mouse Infection Model. *PLoS Negl Trop Dis* **10**, e0004695-e0004695 (2016).
95. Lu, C.Y. *et al.* The Rescue and Characterization of Recombinant, Microcephaly-Associated Zika Viruses as Single-Round Infectious Particles. *Viruses* **11** (2019)

Supplementary material



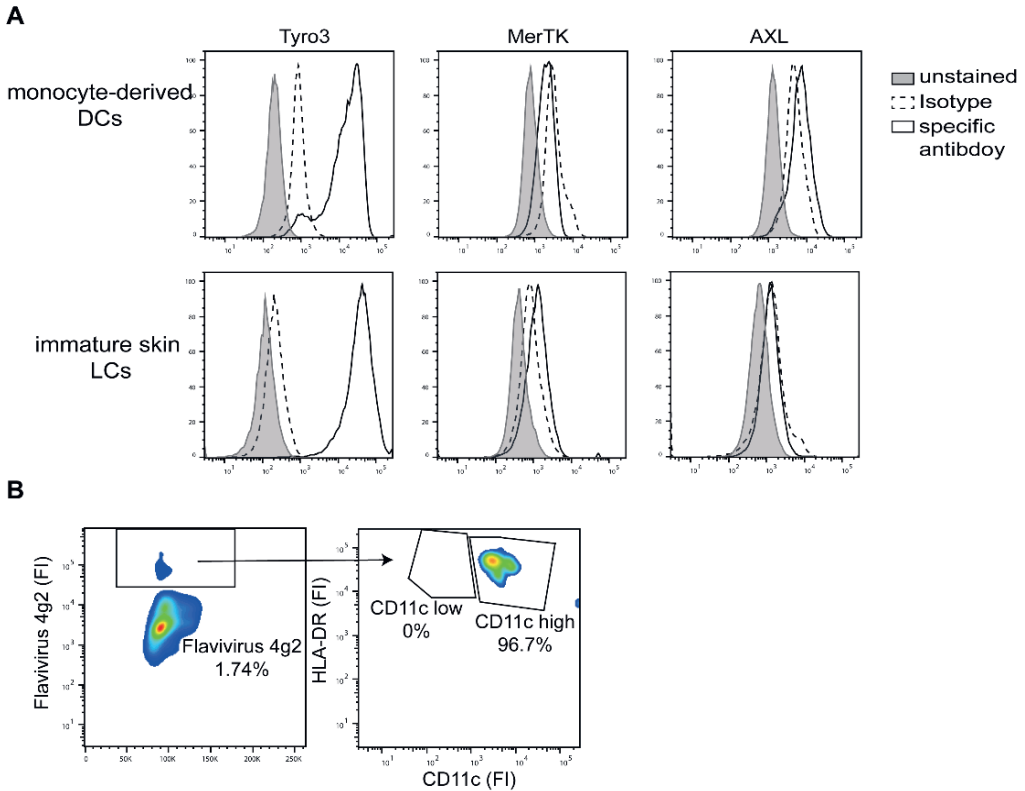
Supplemental Figure 1 | (A) Monocyte derived DCs (moDCs) were pre-incubated with Poly(I:C) or a blocking antibody against DC-SIGN (AZN-D1) before Zika virus was added at a concentration of 850 TCID₅₀/ml. Cells were fixed after either 4 hours, 24 hours or 48 hours and expression of activation and maturation markers CD80, CD83 and CD86 was measured via flow cytometry (n=4 donors measured in mono). (B) moDCs were pre-incubated with the Zika virus viral polymerase inhibitor 7DMA (20 µg/ml), pre-incubated with Poly(I:C) or a blocking antibody against DC-SIGN (AZN-D1) before Zika virus or heat inactivated Zika virus was added to the cells. Expression of maturation and activation markers was measured via flow cytometry after 24 hours post inoculation (n=4 donors) ▶

► measured in mono). Data information: Data show the mean values and error bars are the SEM. (B) Statistical analysis was performed with an ordinary One-way-ANOVA and a Tukey's multiple comparison. * $P \leq 0.05$, ** $P \leq 0.01$, *** $P \leq 0.001$



Supplemental Figure 2 | (A) Immature skin derived LCs were pre-incubated with Poly(I:C), LTA, Motolimod or a blocking antibody against langerin (10E2) before Zika virus was added at a concentration of 850 TCID₅₀/ml. Cells were fixed after either 4 hours, 24 hours or 48 hours and expression of activation and maturation markers was measured via flow cytometry (n=3 donors measured in mono). (B) Monocyte derived DCs (moDCs) were incubated with Zika virus for 48 hours before cell viability was measured by MTT assay (n=3 donors in duplicates). ►

► (C) moDCs were characterized for their expression of DC-SIGN and lack of langerin. Cell receptor expression was measured via flow cytometry (n=2 donors in duplicates). (D) moDCs were pre-incubated with a blocking antibody against DC-SIGN prior to Zika virus inoculation. After 48 hours, cell viability was measured with a CellGlow assay (n=3 donors measured in duplicates). (E) moDCs were pre-incubated with the carbohydrate mannan or a blocking antibody against DC-SIGN (AZN-D1) before Zika virus was added at a concentration of 850 TCID₅₀/ml. Cells were fixed after 48 hours and infection was measured via flow cytometry with a 4g2 Flavivirus antibody (n=2 donors measured in mono).



Supplemental Figure 3 | (A) Expression of TAM receptors (Tyro3, AXL, MerTK) was measured on moDCs and skin derived immature LCs via flow cytometry. (1 representative donor of n=2 moDC and n=3 LC donors). (B) Expression of CD11c was measured in dermal cells crawled out of full skin explants that were infected with Zika virus. (1 representative donor of n=3)



CHAPTER

3

Immune activation of vaginal human Langerhans cells increases susceptibility to HIV-1 infection

Nienke H van Teijlingen¹, Julia Eder^{1,2}, Ramin Sarrami-Forooshani³,
Esther M Zijlstra-Willems^{1,2}, Jan-Paul WR Roovers⁴, Elisabeth van
Leeuwen⁴, Carla MS Ribeiro^{1,2*}, Teunis BH Geijtenbeek^{1,2*}

¹Amsterdam UMC location Academic Medical Center, Experimental
Immunology, Meibergdreef 9, Amsterdam, The Netherlands

²Amsterdam institute for Infection & Immunity, Amsterdam, The Netherlands

³ATMP Department, Breast Cancer Research Center, Motamed Cancer
Institute, ACECR, P.O. BOX: 15179/64311, Tehran, Iran

⁴Amsterdam UMC location Academic Medical Center, Obstetrics and
Gynaecology, Meibergdreef 9, Amsterdam, The Netherlands

*these authors contributed equally to this work

Published in Sci Rep. 2023 Feb 25;13(1):3283.

doi: 10.1038/s41598-023-30097-x.

Abstract

Vaginal inflammation increases the risk for sexual HIV-1 transmission but underlying mechanisms remain unclear. In this study we assessed the impact of immune activation on HIV-1 susceptibility of primary human vaginal Langerhans cells (LCs). Vaginal LCs isolated from human vaginal tissue expressed a broad range of TLRs and became activated after exposure to both viral and bacterial TLR ligands. HIV-1 replication was restricted in immature vaginal LCs as only low levels of infection could be detected. Notably, activation of immature vaginal LCs by bacterial TLR ligands increased HIV-1 infection, whereas viral TLR ligands were unable to induce HIV-1 replication in vaginal LCs. Furthermore, mature vaginal LCs transmitted HIV-1 to CD4 T cells. This study emphasizes the role for vaginal LCs in protection against mucosal HIV-1 infection, which is abrogated upon activation. Moreover, our data suggest that bacterial STIs can increase the risk of HIV-1 acquisition in women.

Introduction

HIV-1/AIDS remains the leading cause of death for African women of reproductive age and these women are more than two times as likely to become HIV-1 infected compared to their male peers^{1,2}. In women, the major route of infection is sexual transmission via the vaginal mucosa³. Vaginal mucosal tissue protects women against environmental cues such as invading pathogens, mechanical stress (i.e. intercourse), and constant exposure to commensal microbiota^{4,5}. Vaginal mucosa can be divided into two major compartments; the epithelial layer and the sub epithelial lamina propria. The epithelial layer consists of non-keratinized stratified squamous epithelial cells and harbours only a few specific immune cells. In contrast, the lamina propria is composed of connective tissue and is rich in immune cells^{6,7}.

The vaginal epithelium is the first compartment to become exposed to HIV-1 upon sexual transmission and constitutes a physical barrier to viral particles by its multi-layers, tight junctions, and secreted mucus. Although not as extensively as the lamina propria, the epithelial layer is equipped with various local immune players^{6,8}. Besides antimicrobial peptides (i.e. LL-37 and defensins) and immunoglobulins (i.e. IgA and IgG), the epithelial layer contains T cells and Langerhans cells (LCs)^{6,8,9}. LCs embody a subtype of antigen presenting cells (APCs) that play a central role in mucosal immunology and distinctively express the C-type lectin receptor langerin^{10,11}. In the vaginal epithelium, LCs are resident immune cells that express HIV-1 entry receptors^{12,13,14,15}. LCs are part of the dendritic cell lineage but also share close traits with macrophages through a common precursor¹⁶. Moreover, LCs are tissue resident and repopulate locally independent of blood circulation¹⁷. During HIV-1 infection, LCs can be both protective or detrimental¹⁸. Immature LCs exert anti-viral properties *in vitro* as they restrict infection with low doses of HIV-1 through capture by langerin and subsequent internalization and TRIM5 α /autophagy-mediated degradation^{19,20,21}. However, LCs can also be productively infected by HIV-1 through their CD4 and CCR5 receptors^{15,22}. Moreover, recent studies identified new cell populations that are closely related to “classic” LCs^{23,24,25}. Vaginal epithelial dendritic cells (VEDCs) are characterized by their CD1a and langerin expression but harbor no Birbeck granules²³. Epidermal CD11c+ DCs are CD1a positive but express low levels of langerin^{23,25}. Compared to classic LCs, these cells are more permissive to HIV-1 infection and transmission^{23,25}. While inflammatory responses by LCs and other immune cells are beneficial and required to effectively eliminate sexually transmitted infections (STIs), vaginal inflammation prior to HIV-1 exposure paradoxically increases the risk of HIV-1 acquisition^{26,27,28,29}. Local vaginal inflammation not only hampers the barrier function of vaginal epithelium, but also activates LCs leading to attenuation of their protective role in HIV-1 infection^{14,20,30}. Inflammatory stimuli increase the ability of skin LCs to capture and transmit HIV-1 while also enhancing the replicative potential of HIV-1 in LCs³⁰. Interestingly, agonists to the Toll-like receptor (TLR) 2 enhance susceptibility of LCs to HIV-1, suggesting that gram+ bacteria might be

responsible for enhanced infection and transmission of HIV-1³¹. Recently, we have shown that the vaginal bacterium *Prevotella timonensis* enhances HIV-1 capture as well as transmission by LCs, providing further evidence that bacterial species can influence HIV-1 susceptibility of target cells³². Moreover, elevated levels of pro-inflammatory cytokines can recruit activated CD4 T cells from the lamina propria, supplying additional HIV-1 target cells³³.

Our current study uses physiologically important immature human LCs freshly isolated from vaginal mucosa and shows that they restrict HIV-1 infection and pose a barrier to sexual HIV-1 transmission in women. In contrast, mature vaginal LCs were efficiently infected by HIV-1 and largely transmitted HIV-1 to CD4 T cells. Notably, exposure to bacterial, but not viral, TLR ligands enhanced HIV-1 infection and transmission of immature vaginal LCs. Thus, this study supports a role for human vaginal LCs in protection against HIV-1 and suggests that activation of vaginal LCs by bacteria increases sexual HIV-1 susceptibility in women.

Results

Vaginal LC purification

To obtain immature and mature LCs from vaginal epithelium, a combination of mechanical and enzymatic methods was used (**Figure. 1A**). Epithelial sheets were separated from the lamina propria and submucosal stroma using surgical scissors and subsequent overnight incubation with the enzyme Dispase II. Smooth separation after Dispase II incubation could only be secured when stromal layers were thin and cut strips did not exceed a width of 7 mm. Immature LCs were immediately isolated from epithelial sheets using enzymatic digestion. For mature vaginal LCs, epithelial sheets were cultured for several days and emigrated CD1a⁺ were harvested. Both immature and mature vaginal LCs were purified using density gradient isolation and subsequent positive CD1a selection with MACS. After two rounds of CD1a selection, the immature isolation protocol resulted in an immature LC purity, defined as CD1a⁺ and langerin^{high} expressing cells of 79.1% (ranging 63.9-90.0%, **Figure. 1B** and **Supplemental Figure. 1A**). One CD1a selection round resulted in 55.5 % immature LC purity (range 23.7-78.0%, **Figure. 1B**). For the mature LC model, cell purity accounted for 53.6% (1st CD1a selection round, range 37.8-68.5%, **Figure 1C**) and 70.5% (2nd CD1a selection round, range 63.3-73.3%, **Figure. 1C**). Isolation of vaginal cells as described in **Figure 1** resulted in a consistent purity of CD1a positive cells stably above 85% (**Supplemental Figure. 1B**). The CD1a positive cells highly expressed HLA-DR, CD11b, E-cadherin and Mucin-1. The co-purified/isolated CD1a negative fraction was slightly enriched for CCR5, but no particular cell type could be identified as specific markers for vaginal epithelial cells were not available (data not shown). Both enzymatically isolated and emigrated CD1a⁺ cells expressed langerin, suggesting that these are LCs. The LCs were

purified from vaginal epithelium using a combination of mechanical and enzymatic methods, resulting in CD1a⁺/langerin high purities up to ~80%.

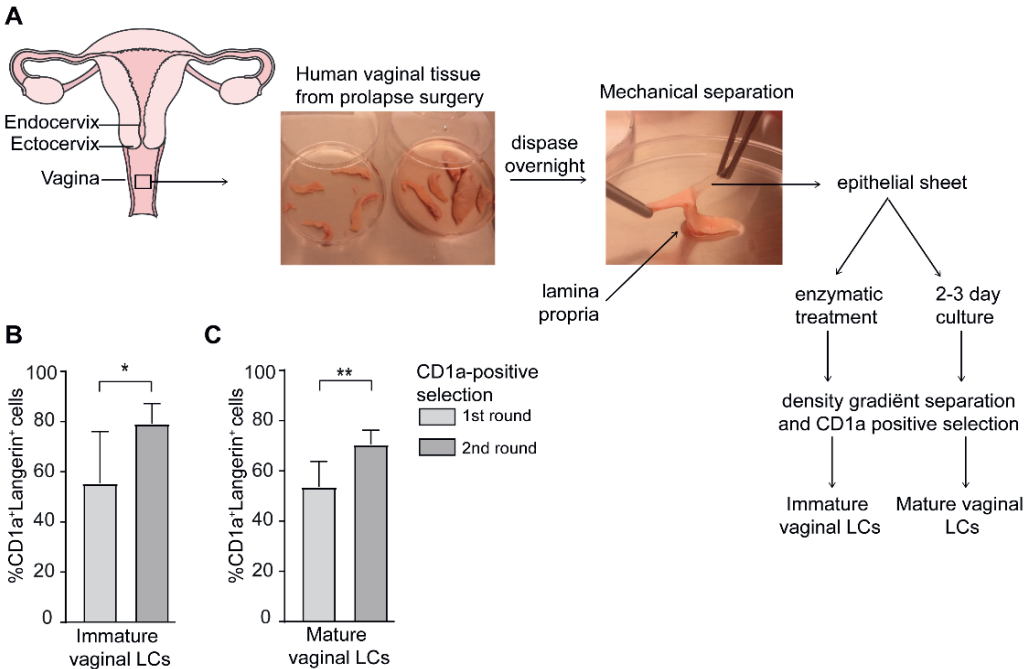


Figure 1 | Vaginal LC purification. (A) schematic model and pictures of isolation procedures used to obtain immature and mature vaginal LCs from primary human vaginal tissue. Images were adopted from Servier Medical Art by Servier (<http://www.servier.com/Powerpoint-image-bank>) and modified by the authors under the following terms: CREATIVE COMMONS Attribution 3.0 Unported (CC BY 3.0); (B-C) vaginal LC purity (% CD1a⁺/Langerin^{high} cells) after immature (B, N=7) and mature (C, N=6) isolation procedure. * $p < 0,05$, ** $p < 0,01$, two-tailed t-test, data are mean \pm SD.

Emigrated mature vaginal LCs express lower levels of langerin and higher levels of CD86

Both immature and mature CD1a⁺ LCs were analysed for expression of CD4, CCR5, langerin and CD86 by flow cytometry. As described previously, HIV-1 receptor CD4 and HIV-1 co-receptor CCR5 were detected on immature and mature vaginal LCs (**Figure. 2A and B**)^{12, 34}. CCR5 was higher expressed by mature LCs, whereas CD4 expression was similar on both immature and mature LCs isolated from the same vaginal mucosa explants (**Figure. 2**). Both immature and mature LCs expressed langerin, a C-type lectin receptor involved in HIV-1 binding and TRIM5 α /autophagy-mediated degradation^{20, 21} (**Figure. 2**). Notably, langerin expression was substantially decreased in mature vaginal LCs compared to immature LCs (**Figure. 2**), similar to what we have previously observed in skin derived LCs³⁵. Mature LCs

expressed higher levels of co-stimulatory molecule CD86 (**Figure. 2**), indicating the increased capacity to prime naïve T cells. Taken together, vaginal LCs express several surface receptors involved in the initial interaction between LCs and HIV-1.

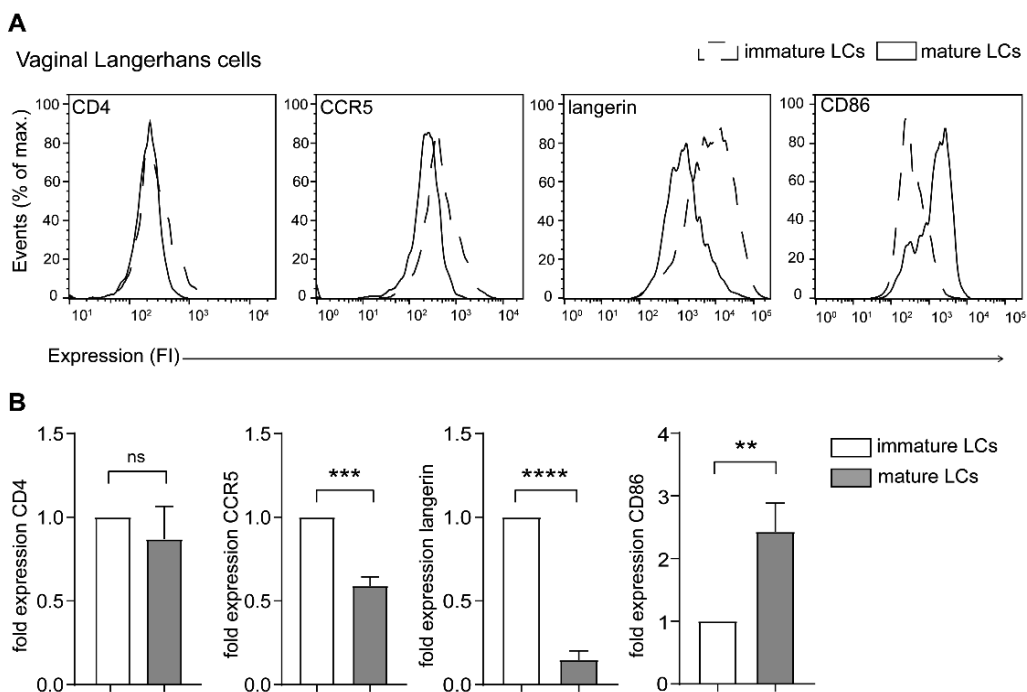


Figure 2 | Immature and mature vaginal LCs display a differential phenotype. (A), representative plots of the expression of LC receptors involved in the interaction with HIV-1 (CD4, CCR5, langerin) and T cells (CD86) on immature and mature vaginal LCs as determined by flow cytometry. (B, N=3) pooled data from 3 separate donors of immature and mature vaginal LCs (CD1a+) for the expression of CD4, CCR5, langerin and CD86. ** $p < 0.01$, *** $p < 0.001$, unpaired t-test, data are mean \pm SD.

Vaginal LCs express functional viral and bacterial TLRs

To investigate the ability of vaginal LCs to respond to bacterial and viral ligands, we determined their TLR expression profile. Vaginal LCs expressed all major TLRs, except TLR9 (**Figure. 3A**). Strikingly, TLR4 could be detected, whereas epidermal LCs lack the expression of this bacteria-sensing TLR³⁶. Importantly, we sorted immature vaginal LCs into CD1a positive and CD1a negative fractions and only detected TLR4 on the CD1a positive cells (**Supplemental Figure. 1C**). To test the functionality of TLRs expressed by vaginal LCs, we exposed immature vaginal LCs (CD1a+ and langerin^{high}) to TLR ligands and analysed upregulation of co-stimulatory molecule CD86 as measure of TLR activation. Stimulation of immature vaginal LCs with bacterial ligands for TLR1/2 (Pam3CSK4) or TLR4 (LPS) resulted in a significantly increased expression of CD86 (**Figure. 3B and C**). The most extensive

increase in CD86 expression was induced by viral TLR3 ligand Poly(I:C) (**Figure. 3B and D**). Levels of CD86 expression after stimulation with these activating TLR ligands were similar to the level of CD86 expression of emigrated mature LCs (**Figure. 2B**). TLR7/8 ligand R848 induced CD86 upregulation similar to Poly(I:C) but did not reach significance (p -value = 0.186). When stimulating the cells with Lipid A, key domain of LPS³⁷, we observed similar upregulation of CD86 expression compared to LPS (**Supplemental Figure. 1D**). Furthermore, co-treatment with Polymyxin B sulfate, a potent antibiotic used to inhibit LPS³⁸, decreased the LPS-induced CD86 expression (**Supplemental Figure. 1D**), supporting that LPS moiety is responsible for this cell maturation. Next, we wanted to examine the full co-stimulatory potential of vaginal LCs after TLR triggering. In addition to CD86, vaginal LCs were assessed for their ability to upregulate co-stimulatory molecules CD80 and CD83 in response to stimulation with Poly(I:C) and LPS (**Figure 3D**). CD80 was upregulated both after Poly(I:C) and LPS stimulation, in accordance with CD86 (**Figure. 3D**). However, the expression of CD83 was similar between immature and mature LCs (**Figure. 3D**), suggesting these LCs are not fully matured but able to present antigens. We also investigated whether receptors important for HIV-1 infection of LCs, i.e. CD4, CCR5, and Langerin, were affected by LC activation through TLRs (**Figure. 3E**). Neither CD4 nor CCR5 were affected by TLR stimulation with Poly(I:C) or LPS (**Figure. 3E**). These results contrast with CCR5 downregulation we observed upon LC maturation through migration (**Figure. 2A and B**), suggesting that activation after TLR stimulation induces a different LC phenotype. Importantly, langerin was significantly downregulated after TLR stimulation (**Figure. 3E**). Taken together, these results indicate that immature vaginal LCs harbour functional TLRs and therefore can respond to bacteria as well as viruses. Moreover, stimulation with TLR ligands leads to an activated LC phenotype that can prime LCs for antigen presentation as well as support HIV-1 infection.

Immature vaginal LCs efficiently capture HIV-1 gp120 via langerin

We next investigated the interaction of HIV-1 with immature and mature vaginal LCs using a fluorescent HIV-1 gp120-coated bead-binding assay. HIV-1 gp120 efficiently interacted with immature vaginal LCs, resulting in ~60% binding (**Figure. 4A and C**). HIV-1 gp120 binding to immature vaginal LCs was significantly decreased by a langerin-blocking antibody as well as by mannan, a mannosylated carbohydrate structure known for its binding to langerin. Mature LCs have a decreased langerin expression (**Figure. 2B**) and captured HIV-1 gp120 less efficiently (~20%, **Figure. 4B and D**) compared to immature LCs. Neither anti-langerin nor mannan could significantly block HIV-1 gp120 binding to mature vaginal LCs. Moreover, HIV-1 gp120 binding to immature vaginal LCs was only marginally decreased after blocking CD4 or CCR5 in comparison to the decrease observed with anti-langerin (**Figure. 4E**), suggesting that these receptors are less involved in the binding of HIV-1 to immature vaginal LCs. As expected, anti-DC-SIGN antibodies did not decrease binding.

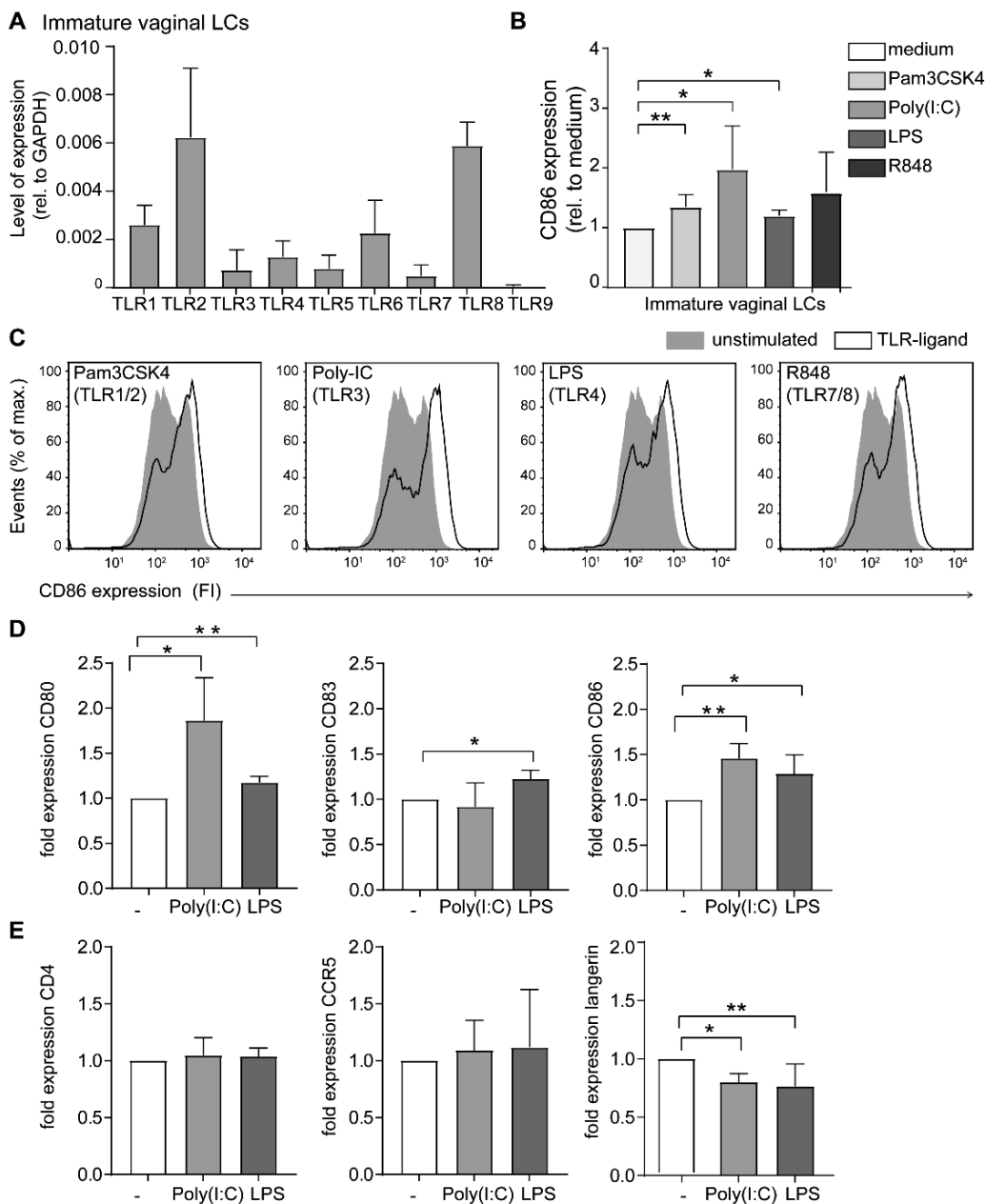


Figure 3 | Vaginal LCs express functional viral and bacterial TLRs. (A) TLR expression levels of immature vaginal LCs (CD1a+, Langerin^{high}) as determined by RT-PCR (N=4); (B) relative maturation (MFI CD86 'TLR-ligand' / MFI CD86 'medium') of immature LCs exposed to TLR-ligands (N=4-6); * $p < 0.05$, ** $p < 0.01$, two-tailed t -test, data are mean \pm SD; (C) representative histograms of CD86 upregulation on immature vaginal LCs (CD1a+, Langerin^{high}) in response to TLR-ligands as determined by flow cytometry (unstimulated – filled grey histogram; TLR-ligand – black line). (D, N=5, N=4 and N=5 respectively) pooled data of expression of CD80, CD83 and CD86 on separated donors after stimulation with either LPS or Poly-I:C; (E, N=6) pooled data of separate donors for expression of CD4, CCR5 and langerin; * $p < 0.05$, ** $p < 0.01$, two-tailed t -test, data are mean \pm SD.

These results strongly suggest that langerin expressed on immature vaginal LCs efficiently captures HIV-1 gp120, and thereby considered a major HIV-1 binding receptor on LCs ²⁰. However, mature LCs have decreased langerin expression (**Figure. 2B**), suggesting that other receptors (i.e. CD4 and CCR5) play a role in virus binding and subsequent infection.

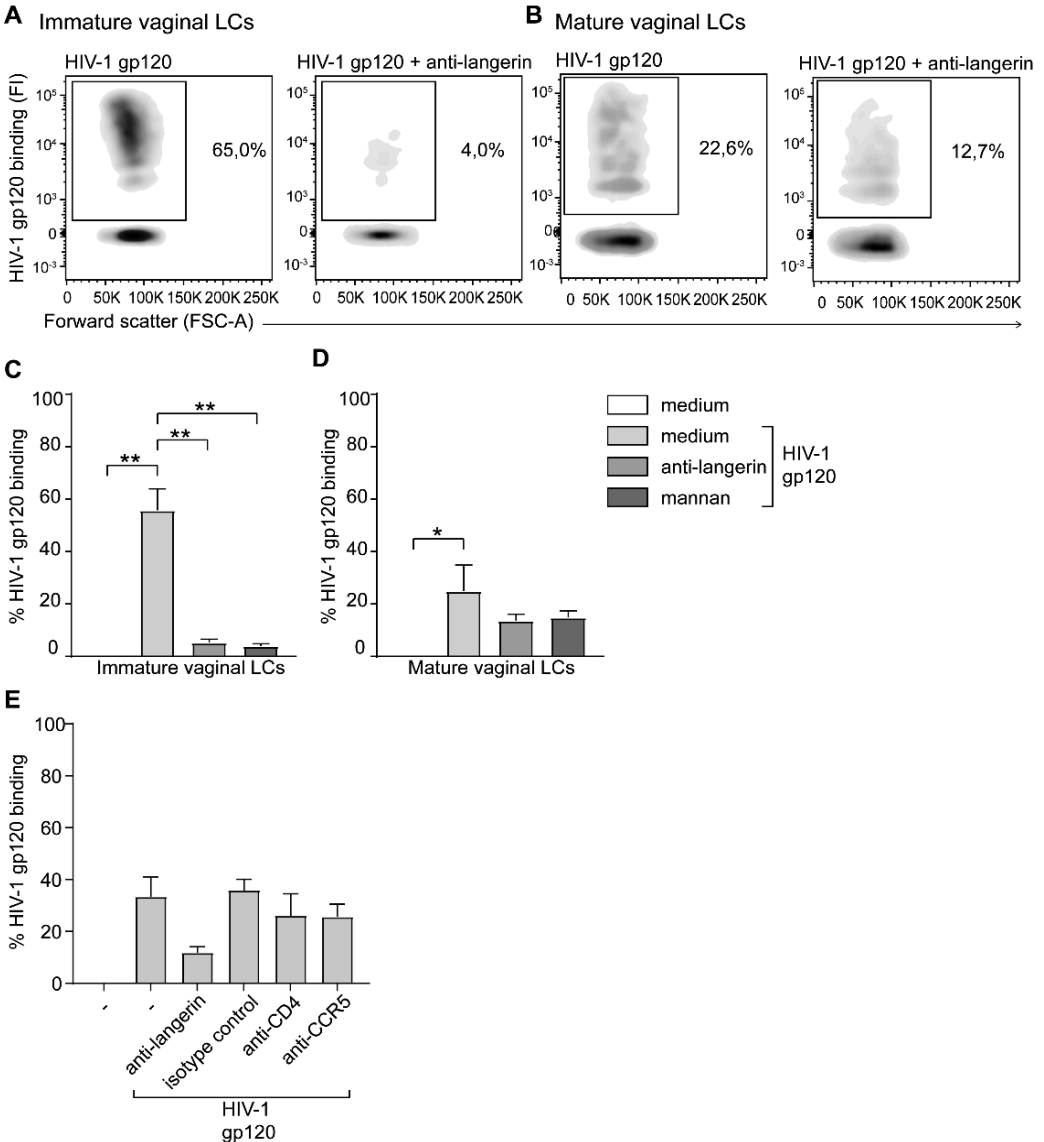


Figure 4 | Immature vaginal LCs efficiently engage HIV-1 through langerin. (A-B) representative flow cytometry plots of HIV-1 gp120 binding to immature (A) and mature (B) vaginal (CD1a+, Langerin^{high}) left untreated or pre-treated with anti-langerin; C-D), pooled HIV-1 gp120 binding data (% HIV-1-gp120+) of immature (C, N=3) and mature (D, N=3) vaginal LCs pre-treated with medium, anti-langerin, or mannan; * $p < 0,05$, ** $p < 0,01$, two-tailed t -test; (E, N=2) GP120 binding (% HIV-1-gp120+) on immature vaginal LCs in the presence or absence of anti-langerin (10E2), anti-DC-SIGN (D1, isotype control), anti-CD4 or anti-CCR5 blocking antibody; data are mean \pm SD.

Mature vaginal Langerhans cells become highly infected by HIV-1 and bacterial TLR ligands abrogate HIV-1 restriction in vaginal LCs

LCs form a protective barrier against HIV-1 infection^{10, 19, 20, 21}. As shown for skin-derived LCs, the antiviral properties can be attenuated when LCs are subjected to immune activation; instead of targeting HIV-1 for degradation, LCs become productively infected^{19, 20, 21}. Here we investigated the levels of HIV-1 infection of immature as well as of mature vaginal LCs (CD1a+ and langerin^{high}) after a 5-day exposure to various HIV-1 strains. Immature vaginal LCs showed low levels of HIV-1 infection after exposure to different HIV-1 strains NL4.3-Bal, SF162, and JR-CSF. Infection levels (% p24+ of CD1a positive cell fraction) varied from 1.3 to 6.6 % (**Figure. 5A**). In contrast, higher levels of HIV-1 infection were observed in mature CD1a positive vaginal LCs (**Figure. 5B**). HIV-1 infection levels of mature cells varied more compared to immature vaginal LCs, ranging from 4.3 to 51.7 %, and were clearly higher for the PBMC produced HIV-1 strains SF162 and JR-CSF (~43.2 and ~36.3%) than for NL4.3-Bal (~11.1%).

Additionally, vaginal immature LCs were stimulated with various TLR ligands to investigate their influence on the HIV-1 restrictive function of immature vaginal LCs. Immature vaginal LCs were stimulated overnight with Pam3CSK4, poly(I:C), LPS, and R848, and subsequently infected with HIV-1 (SF162). Notably, the bacterial ligand Pam3CSK4 (TLR1/2) and LPS (TLR4) specifically increased the infection levels in vaginal immature LCs (**Figure 5C**). Stimulation with viral ligands Poly(I:C) (TLR3) and R848 (TLR 7/8), which efficiently activated immature vaginal LCs (**Figure. 3B and C**), did not result in increased HIV-1 infection compared to unstimulated LCs (**Figure 5C**). Infection levels in Pam3CSK4- and LPS-stimulated LCs (max 3.6-fold increase), however, did not reach the magnitude of HIV-1 infection observed in the mature vaginal cell model (12.5-fold increase; **Figure. 5B**). These data indicate that immature vaginal LCs are poorly susceptible to R5-tropic HIV-1, whereas mature vaginal LCs are efficiently infected by R5-tropic HIV-1 strains. Moreover, our findings suggest that bacterial co-infections increase HIV-1 susceptibility by abrogating the restriction of HIV-1 infection in immature vaginal LCs.

Mature vaginal Langerhans cells effectively transmit HIV-1 to target cells

Next, we investigated the ability of both immature and mature vaginal LCs to transmit HIV-1 to target cells. First, vaginal LCs were exposed to HIV-1 for 2 days, allowing productive infection of LCs, then washed extensively and subsequently co-cultured with PHA/IL2-activated CD4 T cells in a 1:2 ratio for 3 days. Transmission of HIV-1 (SF162) by immature vaginal LCs was low (~3.3%, **Figure. 5D**). In contrast, mature vaginal LCs efficiently transmitted HIV-1 to CD4 T cells, resulting in infection levels of ~47.3% in CD4 T cells after co-culture. Thus, mature vaginal LCs are productively infected with HIV-1 resulting in

abundant HIV-1 transmission to target CD4 T cells. During sexual transmission of HIV-1, multiple viral strains are present in the genital tract. However, typically only one strain, termed transmitted founder (T/F) virus, establishes infection^{39, 40}. Vaginal LCs are more susceptible to T/F viruses than to their chronic HIV-1 counterparts, exhibiting increased infection⁴¹. We therefore incubated LPS-activated vaginal LCs with the HIV-1 T/F virus Ch058 and co-cultured them with susceptible target cells and determined transmission after several days (**Figure. 5E**). Although we observed donor differences, LPS-activated LCs showed a trend in increased HIV-1 transmission, indicating that activation of vaginal mucosa by bacteria can enhance HIV-1 transmission by vaginal LCs.

Discussion

HIV-1/AIDS is still a global health problem and sexual transmission is the major route of infection^{2, 42}. Vaginal STIs compose a risk for acquisition of HIV-1 and previous studies point out immune activation as being the mediating factor^{26, 27, 28, 29}. More specifically, TLR ligation has been suggested to affect susceptibility of LCs in vaginal mucosa and enhance sexual transmission of HIV-1³¹.

Here we have investigated primary human vaginal LCs in the context of immune activation. Skin-derived LCs do not express TLR4^{36, 43} and, notably, here we show that vaginal LCs express TLR4 and this affects HIV-1 infection. Immune activation in *ex vivo* culture of immature mucosal sheets or direct activation of immature vaginal LCs by bacterial TLR ligands including LPS enhanced HIV-1 infection as well as transmission to CD4 T cells. These data indicate that vaginal LCs might be more susceptible to HIV-1 in the presence of gram-negative bacteria observed in bacterial vaginosis.

LCs are considered a potential target for HIV-1 as they express entry receptors CD4 and CCR5, as shown in this report and previous studies^{12, 34}. HIV-1 binding to CD4 and CCR5 leads to fusion of the viral envelope with the target cell membrane. However, expression of langerin by LCs forms an infection barrier; langerin efficiently captures HIV-1 and targets the virus to a TRIM5 α /autophagy-mediated degradation process^{20, 21}. Viral scavenging by langerin is thought to prevent HIV-1 infection of LCs but also prevents infection of surrounding cells. This protective effect depends on various factors such as viral load as well as expression of langerin. Therefore, at high concentrations LCs can become infected by HIV-1. Importantly, while immature monocyte-derived LCs are poorly susceptible to HIV-1 infection, the chance for infection increases in their mature counterparts⁴⁴. We show that immature vaginal LCs, directly isolated from fresh vaginal tissue, are poorly susceptible to HIV-1 infection. This is in accordance with studies from our group using immature LCs isolated from skin^{14, 20} or vaginal mucosa⁴¹. As well as studies on vaginal explants that report no productive HIV-1 infection in vaginal LCs^{9, 45}. In line with these studies, we detected low HIV-1 infection in immature vaginal LCs. However, we observed high levels of infection in vaginal LCs that were activated through *ex vivo* culturing prior to HIV-1

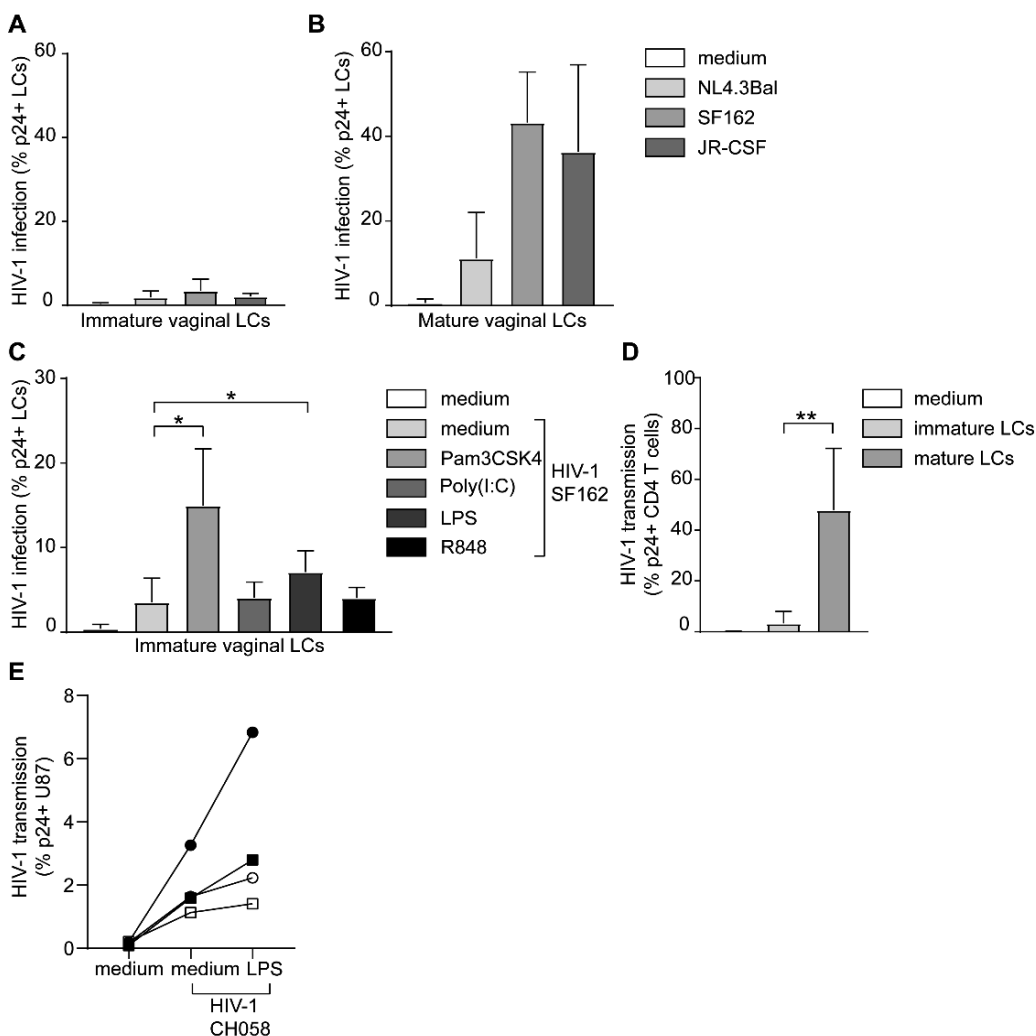


Figure 5 | Bacterial TLR-ligands increase HIV-1 infection in vaginal LCs and activated vaginal LCs transmit HIV-1 to target cells. (A-B) HIV-1 (NL4.3Bal, SF162, JR-CSF) infection of immature (A, N=3-10) and activated (B, N=2-5) vaginal LCs (CD1a+, Langerin^{high}) as measured by double staining for intracellular p24 and CD1a, and analyzed by flow cytometry; (C) HIV-1 (SF162) infection in immature vaginal LCs pre-stimulated with TLR-ligands, N=4-7 * $p < 0,05$, two-tailed t -test, (D) HIV-1 (SF162) transmission from immature and mature vaginal LCs to CD4 T cells after co-culture, N=3-5, ** $p < 0.01$, two-tailed t -test, (E, N=4) HIV-1 Transmitted Founder virus (CH058) transmission by immature vaginal LCs to CD4/CCR5 expressing U87 cells with or without prior stimulation or LPS for 30 minutes, data are mean \pm SD.

exposure. This increased HIV-1 susceptibility might be explained by decreased expression of langerin, as we observed lower levels of langerin expression and a decreased capacity to bind gp120 coated beads by mature LCs compared to their immature counterparts. Interestingly, we still observe some gp120 binding to mature LCs after langerin block,

suggesting that other receptors might be involved. Our data suggest that CD4 and CCR5 are not involved in the gp120 binding as antibodies against these receptors do not abrogate gp120 binding by immature LCs. It is possible that heparan sulfate proteoglycans are involved in the remaining gp120 binding by mature LCs³⁵.

Recently, new subsets of langerin expressing cells were described in the skin and vaginal mucosa^{23, 24, 25}. In the vaginal mucosa, CD1a+ and langerin+ epithelial DCs were suggested to become infected by HIV-1 due to their lack of Birbeck granules²³ while epidermal CD11c+ DCs described in the epidermis and anogenital tissues were more susceptible to HIV-1 than LCs²⁵. With our isolation method we obtained cells that expressed high levels of both CD1a and langerin while also expressing CD4 and CCR5. High expression of langerin and low susceptibility to HIV-1 suggests that we are looking at classic LCs. Another LC subset, termed LC2, was recently identified in the epidermis and differs phenotypically and functionally from classical LCs (LC1)²⁴. As of now, there is no evidence of an LC2 population in vaginal mucosa and further research into their localization is needed.

LCs from skin do not express TLR4 and are unresponsive to LPS^{36, 46}. As human skin is an extensive and important organ, this unresponsiveness might be a mechanism contributing to the tolerance to bacterial commensals which prevents unnecessary inflammation⁴⁶. Strikingly, our data strongly suggest that vaginal LCs are fully equipped with TLR1-8, including TLR4. Whereas, we did not observe any TLR4 expression in CD1a negative sorted vaginal cell fraction nor skin immature LCs (**Supplemental Figure 1C** and data not shown). These data imply that vaginal LCs are able to recognize vaginal co-infections caused by viruses as well as bacteria.

By exposing immature vaginal LCs to TLR ligands we obtained an activated phenotype with increased levels of co-stimulatory molecules CD80 and CD86. Interestingly, CD83 did not increase in expression upon stimulation with either TLR ligand, suggesting the cells are not fully matured but activated and primed for antigen presentation. Notably, we observed stronger downregulation of langerin in emigrated LCs, suggesting that the TLR-activated LCs are less mature than emigrated LCs. This is further supported by finding that emigrated LCs were more efficient in HIV-1 transmission than TLR-activated LCs.

Only bacterial TLR ligands Pam3CSK4 and LPS increased HIV-1 infection in immature vaginal LCs. Strikingly, Poly(I:C) exposure resulted in high LC activation, but low HIV-1 infection of vaginal LCs, in line with previous reports in LCs from skin and in a monocyte-derived LC model³¹. Viral TLR3 ligand Poly(I:C), might induce an antiviral interferon response in vaginal LCs, which further preserves the anti-HIV-1 function of vaginal LCs. In previous reports, the activation of TLR3 by viral agonists and viral stomatitis virus resulted in the release of type I IFN and IFN inducible chemokines CXCL9 and CXCL11, inducing an antiviral response in LC-like DCs⁴⁷. However, as both chemokines are potent T cell attractants, this could also lead to an influx of T cells in the tissue, indirectly increasing the risk of HIV-1 acquisition in these tissues. These findings suggest that specific TLR-induced signalling pathways and immune activation programs can render vaginal LCs susceptible to HIV-1.

We have recently identified a role for *P. timonensis*, a gram negative bacterium highly enriched in vaginal dysbiosis, in enhancing of HIV-1 susceptibility. Exposure to *P. timonensis* highly increased uptake of HIV-1 by vaginal LCs and protected the virus from degradation, highlighting an important role for the vaginal microbiome in HIV-1 infection and transmission³². LCs are antigen presenting cells that closely interact with HIV-1 target cells (i.e. CD4 T cells) after activation and migration to a lymph node in order to direct immune responses, making them ideal first target cells for HIV-1 infection. Considering this characteristic of LCs, we have performed co-cultures of infected and extensively washed vaginal LCs with CD4 T cells to address their HIV-1 transmission capacity. Mature vaginal LCs transmitted HIV-1 efficiently to CD4 T cells, whereas immature vaginal LCs exerted their restrictive function also in these co-cultures as transmission by immature LCs to CD4 T cells was low. For freshly isolated skin-derived LCs, we have shown that langerin prevents HIV-1 transmission in immature LCs whereas mature LCs are more efficient in HIV-1 transfer due to lower langerin expression²⁰. Moreover, other factors (e.g. the complement system in semen) can increase HIV-1 transmission by LCs, bypassing langerin mediated restriction⁴⁸. Similarly, LCs found in human foreskin can become infected and transmit HIV-1 to T cells via conjugate formation⁴⁹. However, it should be noted that the last study used virus-infected cells whereas most other studies worked with cell-free virus. Factors such as timing, viral load, cell origin and isolation methods might account for the divergence in the results. On the contrary, others suggest that langerin is involved in both uptake and transfer of HIV-1 from LCs to T cells and that langerin block prevents transmission⁵⁰, indicating that the role of langerin is not fully elucidated yet. Moreover, immature skin LCs stimulated with Pam3CSK4 increased capture and subsequent *trans*-infection of HIV-1 to T cells³⁰. However, the role of Pam3CSK4 in enhancing infection of target cells with RSV and HIV-1, has been suggested to be independent of TLR activation and instead a result of increased binding⁵¹. While our data suggest that decreased langerin expression is involved in increased susceptibility of TLR-activated LCs, it is possible that other receptors are involved in infection and transmission. A set of receptors that might be involved in HIV-1 transmission irrespective of immune activation are Syndecans. These Heparan sulfate proteoglycans have been shown to aid HIV-1 infection of DCs⁵² as well as facilitate transmission of HCV by LCs, counteracting langerin restriction³⁵. HIV-1 T/F viruses are the strains that establish infection in the genital tract during mucosal transmission⁵³. Immature LCs from both skin and vaginal mucosa are significantly more susceptible to T/F viruses than their chronic, laboratory adapted strains⁴¹. It is still not entirely clear what factors determine their superior infection³⁹. T/F viruses are characterized by their higher resistance to type I interferons compared to chronic HIV-1 strains, suggesting that antiviral environments lead to selective pressure for these strains to prevail⁵⁴.

Using primary human vaginal mucosa as well as different HIV-1 strains and isolates, we have shown that immature LCs highly expressing CD1a and langerin are poorly susceptible to HIV-1 infection and transmission in the vagina. These data indicate that immature vaginal

LCs form a natural barrier against sexual HIV-1 transmission in women. Strikingly, bacterial ligands activated vaginal LCs, and activation increased HIV-1 infection and subsequent transmission to CD4 T cells. Thus, our study strongly suggests that bacterial pathogens can abrogate HIV-1 restriction by vaginal LCs, thereby increasing vaginal HIV-1 susceptibility. Furthermore, our data emphasize the importance for prevention of vaginal immune activation in the development of novel strategies against HIV-1/AIDS in women.

Methods

Tissue samples

Human vaginal tissue was collected from women undergoing vaginal surgery for pelvic organ prolapse in which excessive vaginal tissue was removed of the anterior or posterior vaginal wall. This study, including the tissue harvesting procedures, was approved by the Medical Ethics Review Committee of the Academic Medical Center (AMC) of Amsterdam. All research was performed in accordance with relevant guidelines and regulations. Vaginal tissue was freshly processed for each experiment. Surplus stroma was dissected until a thin layer of submucosa remained and tissue was cut into strips of 5-7 mm. Vaginal tissue strips were incubated overnight at 4 °C in complete medium (Iscoves Modified Dulbecco's Medium (IMDM) of Thermo Fischer Science with L-glutamine 100 mmol/L, 10% FCS, 2500 U/mL penicillin, and 2500 mg/mL streptomycin) supplemented with Dispase II (3 U/mL, Roche Diagnostics). After incubation, the epithelial layer and lamina propria were mechanically split by the use of tweezers. Vaginal epithelial sheets were extensively washed in PBS after which was proceeded with immature LC isolation or the *ex vivo* culture protocol.

Immature vaginal Langerhans cells

Epithelial sheets were cut in small pieces using surgical scissors and incubated for 10 minutes in PBS containing trypsin (0,05%, BD Biosciences) and DNAase I (20 U/mL, Roche Applied Science) to obtain a single cell suspension. Short incubation times (customized per donor, max. 10 minutes) were used to preserve cell viability and surface marker integrity. After inactivation of trypsin with FCS and thorough resuspension, cells were filtered and washed in complete medium. Further vaginal LC purification was achieved by ficoll gradient centrifugation (Axis-shield) and CD1a magnetic cell separation (MACS, Miltenyi Biotec). The resulting cell population expressed high CD1a and langerin. Cells were routinely checked for CD1a and langerin before being used for functional experiments.

Mature vaginal Langerhans cells

Vaginal epithelial sheets were incubated in complete medium in 6-wells plates and migratory cells were collected after 3 days. Similar to immature LCs, further purification was accomplished using ficoll gradient centrifugation (Axis shield) and two rounds of CD1a magnetic cell separation (Miltenyi Biotec).

Phenotyping LCs by flow cytometry

Immature and mature LCs were phenotyped using CD1a-APC (BD Pharmingen), langerin-PE (Novocastra), CD86-FITC (BD Pharmingen), CD80-PE (BD Pharmingen), CD83-APC (BD Pharmingen), CD4-AF488 (Biolegend), CD195 (CCR5)-PE (BD Pharmingen) and unlabeled CXCR4 (R&D systems) for which secondary detection with Goat-anti-Mouse-A488 (Invitrogen) was used. HIV-1 infection and transmission samples were stained for CD1a-APC (LC marker), CD3-PerCP (T cell marker), and p24-PE (HIV-1 envelope protein, Beckman Coulter). Immature vaginal LCs were further sorted with a FacsARIA 3 laser sorter (BD Biosciences) after staining for CD1a-APC into CD1a positive and CD1a negative fractions. Samples were analysed using FACSCanto II flow cytometers (BD Biosciences) and data analysis was carried out with FlowJo V10.

TLR expression profile detection with RT-PCR

mRNA was isolated using mRNA Capture kit (Roche Life Sciences) and cDNA was synthesized with Reverse Transcription System (Promega). Amplification and real-time quantification was performed by PCR with SYBR Green according to manufacturer's guidelines for the ABI 7500 Fast PCR detection system (Applied biosciences). The normalized amount of TLR mRNA (N_t) was calculated from the C_t values obtained for both TLR and household (GAPDH) mRNA with the equation $N_t = 2^{C_t(\text{GAPDH}) - C_t(\text{TLR})}$.

TLR stimulations

Immature LCs were incubated overnight in complete medium supplemented with Pam3CSK4 (5 ug/mL, Invivogen), Poly(I:C) (10 ug/mL, Invivogen), LPS (10 ng/mL, SIGMA), R848 (10 ug/mL, Invivogen), Lipid A, diphosphoryl from Escherichia coli F583 (10 ng/ml, Sigma), LPS + Polymyxin B Sulfate (PMB) (25 ug/ml, Enzolifesciences) or Lipid A + PMB (25 ug/ml) respectively. LCs were either analyzed by flow cytometry for upregulation of co-stimulatory molecule CD86, or were infected with SF162 (multiplicity of infection (MOI) 0.1).

HIV-1 gp120 binding to langerin

TransFluorSpheres (Molecular Probes, Eugene, OR) were coated with purified HIV-1 gp120 envelope protein as described previously. HIV-1 gp120-bead-binding studies were also performed as described previously⁵⁵. In short, vaginal LCs were pre-incubated with anti-langerin (10E2), mannan anti-DC-SIGN (AZN-D1), anti-CD4, anti-CCR5 or left untreated, after which HIV-1 gp120-coated beads were added and binding capacity was assessed using flow cytometry.

Cells

The langerin expressing U87 cells stably expressing CD4 and wild-type CCR5 co-receptor (obtained through the NIH AIDS Reagent Program, Division of AIDS, NIAID, NIH: U87 CD4+CCR5+ cells) were cultured in Iscove's Modified Dulbecco's Medium (Thermo Fischer Scientific, USA) supplemented with 10% fetal calf serum (FCS), L-glutamine and penicillin/streptomycin (10 µg/mL) as described previously²¹.

Viruses, HIV-1 infection and transmission

R5 tropic HIV-1 strains NL4.3-Bal, JR-CSF, and SF162, were used in LC infection experiments and these viruses were generated as described previously¹⁹. For additional transmission experiments and infection studies using TLR ligands, SF162 and NL4.3Bal virus was used. Moreover, the HIV-1 Transmitted/Founder (T/F) virus CH058 was used for transmission from immature vaginal LCs to U87. CH058 was generated as previously described⁴¹. Immature and mature LCs were infected with a MOI of 0.1 and HIV-1 infection was assessed by flow cytometry at day 5 after infection by intracellular p24 staining. To determine transmission of HIV-1 from LCs to T cells, infected LCs were washed extensively at day 2 of infection and were subsequently co-cultured with allogeneic PHA/IL-2 activated CD4 T cells for 3 days. Infection levels in CD4 T cells were measured to assess HIV-1 transmission by vaginal LCs. Additionally, vaginal immature LCs were stimulated with LPS or PamC3K for 24h (NL43Bal) or 30 min (Ch058) before infection. After 2 days, cells were washed extensively and co-cultured with U87 to determine transmission to these target cells. After 3 days of co-culture, vaginal LCs were washed away and infection in U87 cells was measured by flow cytometry.

Data availability

The datasets generated during and/or analysed during the current study are available from the corresponding author on reasonable request.

Author contributions

NHvT designed, performed and interpreted most experiments and prepared the manuscript. JE and RSF helped design, perform and interpret experiments. JE edited the manuscript and figures. EZW performed and analysed some experiments. JPWRR helped with tissue collection and participated in discussion on the data and writing the manuscript. EvL participated in discussion on the data and writing the manuscript. CMSR and TBHG supervised all aspects of the project.

Funding

This work was supported by the AMC PhD Scholarship, Dutch Research Council (NWO, <http://www.nwo.nl/>) VENI grant 863.13.025, NWO VICI grant 918.10.619, and the European Research Council (<https://erc.europa.eu/>) Advanced Grant 670424. The funders had no role in study design, data collection and analysis, decision to publish, or preparation of the manuscript. The datasets generated during and/or analysed during the current study are available from the corresponding author on reasonable request.

Conflict of interest

The author(s) declare no competing interests.

References

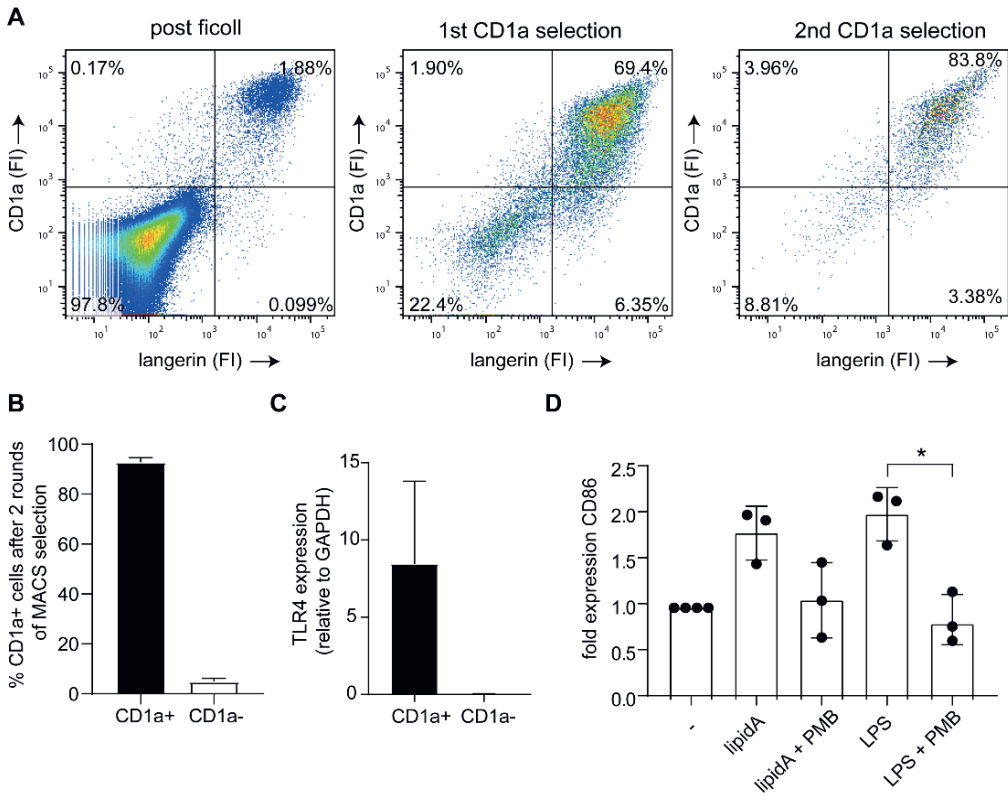
1. UNAIDS. We've got the power — Women, adolescent girls and the HIV response; 2020.
2. UNAIDS. Global AIDS update 2016. 2016.
3. NIH. HIV and Women. 2021 August 13, 2021 [cited 2022 06-07-2022] Available from: <https://hivinfo.nih.gov/understanding-hiv/fact-sheets/hiv-and-women#:~:text=The%20most%20common%20way%20that,is%20riskier%20than%20insertive%20sex.>
4. Zhou, J.Z., Way, S.S. & Chen, K. Immunology of Uterine and Vaginal Mucosae: (Trends in Immunology 39, 302-314, 2018). *Trends Immunol* **39**, 355 (2018).
5. Lacroix, G., Gouyer, V., Gottrand, F. & Desseyn, J.L. The Cervicovaginal Mucus Barrier. *Int J Mol Sci* **21** (2020).
6. Hickey, D.K., Patel, M.V., Fahey, J.V. & Wira, C.R. Innate and adaptive immunity at mucosal surfaces of the female reproductive tract: stratification and integration of immune protection against the transmission of sexually transmitted infections. *J Reprod Immunol* **88**, 185-194 (2011).
7. Lee, S.K., Kim, C.J., Kim, D.J. & Kang, J.H. Immune cells in the female reproductive tract. *Immune Netw* **15**, 16-26 (2015).
8. Kyongo, J.K. *et al.* Searching for lower female genital tract soluble and cellular biomarkers: defining levels and predictors in a cohort of healthy Caucasian women. *PLoS One* **7**, e43951 (2012).
9. Hladik, F. *et al.* Initial events in establishing vaginal entry and infection by human immunodeficiency virus type-1. *Immunity* **26**, 257-270 (2007).
10. de Jong, M.A. & Geijtenbeek, T.B. Langerhans cells in innate defense against pathogens. *Trends Immunol* **31**, 452-459 (2010).
11. van der Vlist, M. & Geijtenbeek, T.B. Langerin functions as an antiviral receptor on Langerhans cells. *Immunol Cell Biol* **88**, 410-415 (2010).
12. Duluc, D. *et al.* Functional diversity of human vaginal APC subsets in directing T-cell responses. *Mucosal Immunol* **6**, 626-638 (2013).
13. Hladik, F. & McElrath, M.J. Setting the stage: host invasion by HIV. *Nat Rev Immunol* **8**, 447-457 (2008).
14. Sarrami-Forooshani, R. *et al.* Human immature Langerhans cells restrict CXCR4-using HIV-1 transmission. *Retrovirology* **11**, 52 (2014).
15. Kawamura, T. *et al.* Candidate microbicides block HIV-1 infection of human immature Langerhans cells within epithelial tissue explants. *J Exp Med* **192**, 1491-1500 (2000).
16. Hoeffel, G. *et al.* Adult Langerhans cells derive predominantly from embryonic fetal liver monocytes with a minor contribution of yolk sac-derived macrophages. *J Exp Med* **209**, 1167-1181 (2012).
17. Merad, M. *et al.* Langerhans cells renew in the skin throughout life under steady-state conditions. *Nat Immunol* **3**, 1135-1141 (2002).
18. Cunningham, A.L., Carbone, F. &

- Geijtenbeek, T.B. Langerhans cells and viral immunity. *Eur J Immunol* **38**, 2377-2385 (2008).
19. van den Berg, L.M. *et al.* Caveolin-1 mediated uptake via langerin restricts HIV-1 infection in human Langerhans cells. *Retrovirology* **11**, 123 (2014).
 20. de Witte, L. *et al.* Langerin is a natural barrier to HIV-1 transmission by Langerhans cells. *Nat Med* **13**, 367-371 (2007).
 21. Ribeiro, C.M. *et al.* Receptor usage dictates HIV-1 restriction by human TRIM5 α in dendritic cell subsets. *Nature* **540**, 448-452 (2016).
 22. Kawamura, T. *et al.* R5 HIV productively infects Langerhans cells, and infection levels are regulated by compound CCR5 polymorphisms. *Proc Natl Acad Sci U S A* **100**, 8401-8406 (2003).
 23. Pena-Cruz, V. *et al.* HIV-1 replicates and persists in vaginal epithelial dendritic cells. *J Clin Invest* **128**, 3439-3444 (2018).
 24. Liu, X. *et al.* Distinct human Langerhans cell subsets orchestrate reciprocal functions and require different developmental regulation. *Immunity* **54**, 2305-2320.e2311 (2021).
 25. Bertram, K.M. *et al.* Identification of HIV transmitting CD11c(+) human epidermal dendritic cells. *Nat Commun* **10**, 2759 (2019).
 26. Mlisana, K. *et al.* Symptomatic vaginal discharge is a poor predictor of sexually transmitted infections and genital tract inflammation in high-risk women in South Africa. *J Infect Dis* **206**, 6-14 (2012).
 27. Masson, L. *et al.* Genital inflammation and the risk of HIV acquisition in women. *Clin Infect Dis* **61**, 260-269 (2015).
 28. Haaland, R.E. *et al.* Inflammatory genital infections mitigate a severe genetic bottleneck in heterosexual transmission of subtype A and C HIV-1. *PLoS Pathog* **5**, e1000274 (2009).
 29. Laga, M. *et al.* Non-ulcerative sexually transmitted diseases as risk factors for HIV-1 transmission in women: results from a cohort study. *Aids* **7**, 95-102 (1993).
 30. de Jong, M.A. *et al.* TNF-alpha and TLR agonists increase susceptibility to HIV-1 transmission by human Langerhans cells ex vivo. *J Clin Invest* **118**, 3440-3452 (2008).
 31. Ogawa, Y. *et al.* Gram-positive bacteria enhance HIV-1 susceptibility in Langerhans cells, but not in dendritic cells, via Toll-like receptor activation. *Blood* **113**, 5157-5166 (2009).
 32. van Teijlingen, N.H. *et al.* Vaginal bacterium *Prevotella timonensis* turns protective Langerhans cells into HIV-1 reservoirs for virus dissemination. *Embo j* **41**, e110629 (2022).
 33. Anahtar, M.N. *et al.* Cervicovaginal bacteria are a major modulator of host inflammatory responses in the female genital tract. *Immunity* **42**, 965-976 (2015).
 34. Zaitseva, M. *et al.* Expression and function of CCR5 and CXCR4 on human Langerhans cells and macrophages: implications for HIV primary infection. *Nat Med* **3**, 1369-1375 (1997).
 35. Nijmeijer, B.M. *et al.* Syndecan 4 Upregulation on Activated Langerhans Cells Counteracts Langerin Restriction to Facilitate Hepatitis C Virus Transmission.

- Front Immunol* **11**, 503 (2020).
36. Flacher, V. *et al.* Human Langerhans cells express a specific TLR profile and differentially respond to viruses and Gram-positive bacteria. *J Immunol* **177**, 7959-7967 (2006).
 37. Steimle, A., Autenrieth, I.B. & Frick, J.S. Structure and function: Lipid A modifications in commensals and pathogens. *Int J Med Microbiol* **306**, 290-301 (2016).
 38. Cardoso, L.S. *et al.* Polymyxin B as inhibitor of LPS contamination of *Schistosoma mansoni* recombinant proteins in human cytokine analysis. *Microb Cell Fact* **6**, 1 (2007).
 39. Nijmeijer, B.M. & Geijtenbeek, T.B.H. Negative and Positive Selection Pressure During Sexual Transmission of Transmitted Founder HIV-1. *Front Immunol* **10**, 1599 (2019).
 40. Joseph, S.B., Swanstrom, R., Kashuba, A.D. & Cohen, M.S. Bottlenecks in HIV-1 transmission: insights from the study of founder viruses. *Nat Rev Microbiol* **13**, 414-425 (2015).
 41. Hertoghs, N. *et al.* Sexually transmitted founder HIV-1 viruses are relatively resistant to Langerhans cell-mediated restriction. *PLoS One* **14**, e0226651 (2019).
 42. Haase, A.T. Targeting early infection to prevent HIV-1 mucosal transmission. *Nature* **464**, 217-223 (2010).
 43. van der Aar, A.M. *et al.* Langerhans cells favor skin flora tolerance through limited presentation of bacterial antigens and induction of regulatory T cells. *J Invest Dermatol* **133**, 1240-1249 (2013).
 44. Kawamura, T., Qualbani, M., Thomas, E.K., Orenstein, J.M. & Blauvelt, A. Low levels of productive HIV infection in Langerhans cell-like dendritic cells differentiated in the presence of TGF-beta1 and increased viral replication with CD40 ligand-induced maturation. *Eur J Immunol* **31**, 360-368 (2001).
 45. Ballweber, L. *et al.* Vaginal langerhans cells nonproductively transporting HIV-1 mediate infection of T cells. *J Virol* **85**, 13443-13447 (2011).
 46. van der Aar, A.M. *et al.* Loss of TLR2, TLR4, and TLR5 on Langerhans cells abolishes bacterial recognition. *J Immunol* **178**, 1986-1990 (2007).
 47. Renn, C.N. *et al.* TLR activation of Langerhans cell-like dendritic cells triggers an antiviral immune response. *J Immunol* **177**, 298-305 (2006).
 48. Nijmeijer, B.M. *et al.* HIV-1 subverts the complement system in semen to enhance viral transmission. *Mucosal Immunol* **14**, 743-750 (2021).
 49. Zhou, Z. *et al.* HIV-1 efficient entry in inner foreskin is mediated by elevated CCL5/RANTES that recruits T cells and fuels conjugate formation with Langerhans cells. *PLoS Pathog* **7**, e1002100 (2011).
 50. Nasr, N. *et al.* Inhibition of two temporal phases of HIV-1 transfer from primary Langerhans cells to T cells: the role of langerin. *J Immunol* **193**, 2554-2564 (2014).
 51. Nguyen, D.T. *et al.* The synthetic bacterial lipopeptide Pam3CSK4 modulates respiratory syncytial virus infection independent of TLR activation. *PLoS Pathog* **6**, e1001049 (2010).
 52. de Witte, L. *et al.* Syndecan-3 is a

- dendritic cell-specific attachment receptor for HIV-1. *Proc Natl Acad Sci U S A* **104**, 19464-19469 (2007).
53. Keele, B.F. *et al.* Identification and characterization of transmitted and early founder virus envelopes in primary HIV-1 infection. *Proc Natl Acad Sci U S A* **105**, 7552-7557 (2008).
54. Fenton-May, A.E. *et al.* Relative resistance of HIV-1 founder viruses to control by interferon-alpha. *Retrovirology* **10**, 146 (2013).
55. Sprokholz, J.K., Hertoghs, N. & Geijtenbeek, T.B. Flow Cytometry-Based Bead-Binding Assay for Measuring Receptor Ligand Specificity. *Methods Mol Biol* **1390**, 121-129 (2016).

Supplementary material



Supplemental figure 1 | (A, one representative donor) CD1a and langerin expression of cells isolated from vaginal mucosa after ficoll, 1st CD1a MACS selection, 2nd CD1a MACS selection. (B, N=8) improved isolation of CD1a positive immature vaginal LCs after two MACS selection steps. (C, N=4) TLR4 expression on immature vaginal LCs after sorting into CD1a positive and CD1a negative fractions. Expression was determined by real time quantitative PCR and values are depicted normalized to GAPDH. (D, N=3) expression of CD86 on immature vaginal LCs after stimulation with Lipid A, LPS, PMB or a combination thereof. * $p < 0,05$, two-tailed t-test; data are mean \pm SD



CHAPTER

4

SARS-CoV-2 infection activates dendritic cells via cytosolic receptors rather than extracellular TLRs

Lieve E.H. van der Donk¹, Julia Eder¹, John L. van Hamme¹, Philip J.M. Brouwer², Mitch Brinkkemper², Ad C. van Nuenen¹, Marit J. van Gils², Rogier W. Sanders^{2,3}, Neeltje A. Kootstra¹, Marta Bermejo-Jambrina^{1*}, Teunis B.H. Geijtenbeek^{1*}

¹Department of Experimental Immunology, Amsterdam institute for Infection and Immunity, Amsterdam University Medical Centers, University of Amsterdam, Meibergdreef 9, Amsterdam, The Netherlands.

²Department of Medical Microbiology, Amsterdam institute for Infection and Immunity, Amsterdam University Medical Centers, University of Amsterdam, Meibergdreef 9, Amsterdam, The Netherlands.

³Department of Microbiology and Immunology, Weill Medical College of Cornell University, New York, NY 10021, USA.

*These authors contributed equally to this work.

Abstract

Severe acute respiratory syndrome coronavirus 2 (SARS-CoV-2) causes coronavirus disease 2019 (COVID-19), an infectious disease characterized by strong induction of inflammatory cytokines, progressive lung inflammation and potentially multi-organ dysfunction. It remains unclear how SARS-CoV-2 infection leads to immune activation. The Spike (S) protein of SARS-CoV-2 has been suggested to trigger Toll-like receptor 4 (TLR4) and thereby activate immunity. Here, we have investigated the role of TLR4 in SARS-CoV-2 infection and immunity. Neither exposure of isolated S protein, SARS-CoV-2 pseudovirus nor primary SARS-CoV-2 isolate induced TLR4 activation in a TLR4-expressing cell line. Human monocyte-derived dendritic cells (DCs) express TLR4 but not angiotensin converting enzyme 2 (ACE2), and DCs were not infected by SARS-CoV-2. Notably, neither S protein nor SARS-CoV-2 induced DC maturation or cytokines, indicating that both S protein and SARS-CoV-2 virus particles do not trigger extracellular TLRs including TLR4. Ectopic expression of ACE2 in DCs led to efficient infection by SARS-CoV-2 and, strikingly, efficient type I interferon (IFN) and cytokine responses. These data strongly suggest that not extracellular TLRs but intracellular viral sensors are key players in sensing SARS-CoV-2. These data imply that SARS-CoV-2 escapes direct sensing by TLRs, which might underlie the lack of efficient immunity to SARS-CoV-2 early during infection.

Key words: SARS-CoV-2, dendritic cells, Toll-like receptor 4, innate immune response, intracellular viral sensors

Abbreviations: severe acute respiratory syndrome coronavirus 2 (SARS-CoV-2); coronavirus disease 19 (COVID-19); pattern recognition receptor (PRR); Spike (S); Toll-like receptor (TLR); dendritic cells (DCs); angiotensin converting enzyme 2 (ACE2); interferon (IFN); interleukin (IL); lipopolysaccharide (LPS).

Introduction

Severe acute respiratory syndrome coronavirus 2 (SARS-CoV-2) is a novel coronavirus that causes coronavirus disease 2019 (COVID-19) ¹. COVID-19 emerged in 2019 in Wuhan, China ², and has since spread globally causing a pandemic. The symptoms of COVID-19 vary amongst individuals, ranging from mild respiratory symptoms to severe lung injury, multi-organ dysfunction and death ^{3, 4, 5, 6}. Increasing evidence suggests that disease severity depends not solely on viral infection, but also on an excessive host proinflammatory response, whereby high concentrations of proinflammatory cytokines result in an unfavorable immune response and induce tissue damage ^{7, 8}. The events leading to excessive proinflammatory responses are not completely understood. Therefore, it is necessary to elucidate the mechanisms that are triggered by SARS-CoV-2 to induce innate and adaptive immune responses.

Innate immune cells express pattern recognition receptors (PRRs) that recognize pathogen-associated molecular patterns (PAMPs) and subsequently orchestrate an immune response against pathogens ⁹. Dendritic cells (DCs) are essential immune cells that function as a bridge between innate and adaptive immunity. DCs express various PRR families such as Toll-like receptors (TLRs) and cytosolic RIG-I-like receptors (RLRs) that are triggered upon virus interaction or infection ¹⁰. DCs are therefore essential during SARS-CoV-2 infection to sense infection and instruct T and B cells for efficient antiviral immune responses. However, it is unclear whether and how SARS-CoV-2 is sensed by DCs.

SARS-CoV-2 Spike (S) protein uses angiotensin converting enzyme 2 (ACE2) ^{11, 12} as receptor for infection. However, besides interacting with ACE2, recent *in silico* analyses suggest that the Spike (S) protein could also potentially interact with members of the TLR family, in particular TLR4 ^{13, 14}. TLR4 is abundantly expressed on DCs ^{15, 16}, and therefore TLR4 signaling could be involved in induction of pro-inflammatory mediators. Other studies using cell lines and SARS-CoV-2 S protein support a potential interaction of TLR4 with the S protein ^{17, 18, 19}. However, it remains unclear whether infectious SARS-CoV-2 virus is sensed by TLR4 and whether this interaction induces DC activation and initiation of immunity.

Here, we have investigated how SARS-CoV-2 is sensed by human DCs. Neither recombinant S protein, SARS-CoV-2 pseudovirus nor a primary SARS-CoV-2 isolate induced immunity in TLR4-expressing cell lines or DCs, indicating that TLR4 or other extracellular TLRs are not involved in SARS-CoV-2 infection. However, ectopic expression of ACE2 on DCs led to infection by SARS-CoV-2 and induction of type I interferon (IFN) and cytokines. These data imply that intracellular PRRs rather than transmembrane TLRs are involved in instigating an immune response against SARS-CoV-2.

Results

SARS-CoV-2 S protein does not trigger TLR4

To assess whether TLR4 acts as a sensor of S protein of SARS-CoV-2, we treated a TLR4-expressing HEK293 cell line (293/TLR4) with SARS-CoV-2 recombinant S protein or S nanoparticles²⁰ and determined activation by measuring interleukin (IL)-8. Neither S protein nor S nanoparticles induced IL-8 secretion by 293/TLR4 cells, in contrast to the positive control lipopolysaccharide (LPS) (**Figure 1A**). The parental 293 cells did not induce IL-8 upon treatment with S protein or S nanoparticle and LPS. These data suggest that S protein of SARS-CoV-2 does not trigger TLR4. Primary monocyte-derived DCs express TLR4 but also other TLRs²¹. We therefore exposed primary human DCs to SARS-CoV-2 S nanoparticles and assessed cytokine production by qPCR. Treatment of DCs with S nanoparticles did neither induce type I interferon (IFN) nor cytokines (**Figure 1B-E**). The positive control LPS induced IFN- β (**Figure 1B**) and the interferon-stimulated gene (ISG) APOBEC3G (A3G) (**Figure 1C**) as well as cytokines IL-6 and IL-10 (**Figure 1D, E**). These data strongly suggest that S protein from SARS-CoV-2 does not trigger extracellular TLRs on DCs.

SARS-CoV-2 virus particles do not trigger TLR4

To assess whether TLR4 plays a role in SARS-CoV-2 entry and replication, we ectopically expressed ACE2 on 293 and 293/TLR4 cell lines and infected the cells with SARS-CoV-2 pseudovirus that expresses the full-length S glycoprotein from SARS-CoV-2 and contains a luciferase reporter gene²². Infection was determined by measuring luciferase activity. SARS-CoV-2 pseudovirus infected ACE2-positive 293 and 293/TLR4 cells but not the parental 293 and 293/TLR4 cells (**Figure 2A**). TLR4 expression did not affect infection, as infection was comparable between 293/ACE2 and 293/TLR4/ACE2 cells. Next we investigated whether SARS-CoV-2 pseudovirus activates TLR4. SARS-CoV-2 pseudovirus neither induced IL-8 in parental 293 nor in 293/TLR4 cells (**Figure 2B**). Moreover, ACE2 expression did not induce activation as exposure of ACE2-positive 293 and 293/TLR4 cells to SARS-CoV-2 pseudovirus did not lead to IL-8 production (**Figure 2B**). These data further support the findings that S protein from SARS-CoV-2 does not trigger TLR4 and also show that ACE2 does not affect TLR4 signaling. Next, we performed a serial dilution with a primary SARS-CoV-2 isolate (hCoV-19/Italy) on 293 and 293/TLR4 cells to determine whether high virus concentrations are able to induce TLR4. Neither 293 nor 293/TLR4 cells expressed IL-8 upon exposure to the primary SARS-CoV-2 isolate, suggesting that high virus concentrations do not trigger TLR4 (**Figure 2C**). Next, we treated either ACE2-positive or -negative 293 and 293/TLR4 cells with the primary SARS-CoV-2 isolate and determined infection and activation. Infection was determined by measuring virus particles in the supernatant by qPCR. As expected, both 293/ACE2 and 293/TLR4/ACE2 cells were productively infected at

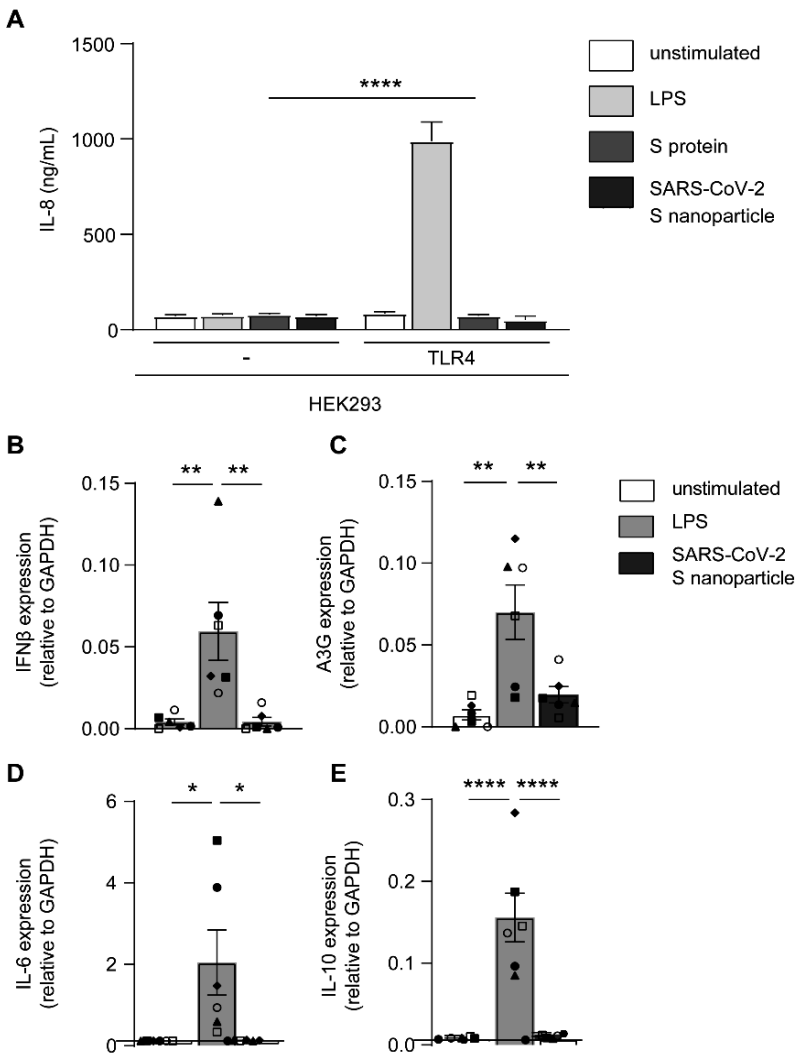


Figure 1 | S protein and SARS-CoV-2 S nanoparticle do not trigger TLR4. (A) 293 cells or 293/TLR4 cells were exposed to LPS, SARS-CoV-2 S protein or S nanoparticles for 24h. IL-8 production was determined by ELISA. (B-E) Primary dendritic cells were exposed to LPS or SARS-CoV-2 S nanoparticles for 8h. Expression of IFN β (B), A3G (C), IL-6 (D) and IL-10 (E) was determined with qPCR. Data show the mean values and SEM. Statistical analysis was performed using (A) two-way ANOVA with Šidák's multiple comparisons test, or (B-E) one-way ANOVA with Tukey's multiple comparisons test. Data represent six replicates obtained in three separate experiments (A), or experiments performed with six donors in three independent experiments, with each symbol representing a different donor (B-E). ****p<0.0001, ***p<0.001; **p<0.01; *p<0.05.

similar levels by SARS-CoV-2, in contrast to ACE2-negative 293 and 293/TLR4 cells (cutoff Ct values >30), (**Figure 2D**). Neither ACE2-positive nor -negative 293 and 293/TLR4 cells expressed any IL-8 upon exposure to the primary SARS-CoV-2 isolate (**Figure 2E**). These data strongly suggest that TLR4 does not sense infectious SARS-CoV-2 virus particles.

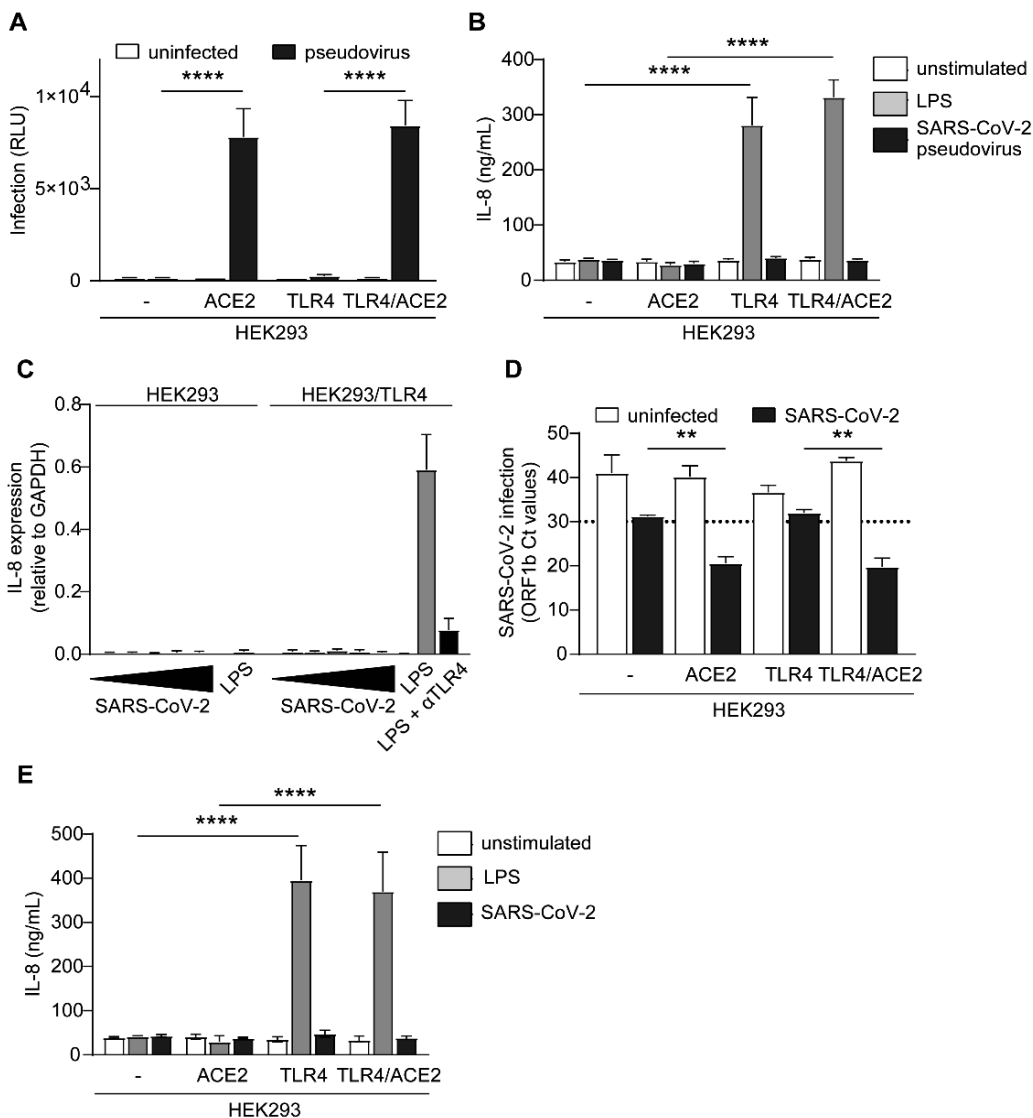


Figure 2 | SARS-CoV-2 virus particles do not trigger TLR4. (A-B) ACE2-positive and -negative 293 and 293/TLR4 cells were exposed to SARS-CoV-2 pseudovirus and infection was determined after 3 days by measuring luciferase activity (A), and IL-8 production was measured after 24h by ELISA (B). (C) 293 and 293/TLR4 cells were exposed to increasing titers of SARS-CoV-2, or LPS in the absence or presence of anti-TLR4 antibodies, and IL-8 production was determined after 24h by qPCR. Increasing titers are indicated by a bar, ranging from TCID100 (narrow) to TCID100.000 (wide). (D-E) ACE2-positive and -negative 293 and 293/TLR4 cells were exposed to a primary SARS-CoV-2 isolate and infection was determined after 24h by measuring the viral gene ORF1b expression in supernatant by qPCR (D) and IL-8 production was measured after 24h by ELISA (E). Data show the mean values and SEM. Statistical analysis was performed using two-way ANOVA with Šidák's (A) or Tukey's (B, D-E) multiple comparisons test. Data represent nine replicates obtained in three separate experiments (A-B), or three separate experiments (C-E). ****p<0.0001; **p<0.01. RLU = relative light units.

Infectious SARS-CoV-2 does not activate DCs

Subsequently, we examined whether SARS-CoV-2 pseudovirus induces DC maturation and cytokine production. DCs do not express ACE2 and we have previously shown that SARS-CoV-2 pseudovirus does not infect DCs^{23, 24}. We investigated the maturation and cytokine production by DCs stimulated with SARS-CoV-2 pseudovirus. Exposure of DCs to SARS-CoV-2 pseudovirus did neither induce expression of costimulatory markers CD80 and CD86 nor maturation marker CD83, in contrast to LPS (**Figure 3A-D, Supplemental Figure 1**). Moreover, SARS-CoV-2 pseudovirus did not induce any cytokines, in contrast to LPS (**Figure 3E-H**). These data indicate that the S protein expressed by SARS-CoV-2 pseudovirus does not activate DCs. Next, we exposed DCs to a primary SARS-CoV-2 isolate and determined DC maturation and cytokine production. We have previously shown that DCs do not become infected by primary SARS-CoV-2²³. Exposure of DCs to the primary SARS-CoV-2 isolate did neither induce expression of CD80, CD86 nor CD83, whereas LPS induced expression of CD83 and CD86 (**Figure 4A-C**). Next we investigated cytokine induction by DCs after exposure to primary SARS-CoV-2 isolate or agonists for extracellular TLRs (TLR1/2, TLR2/6, TLR4, and TLR5). LPS, flagellin and LTA induced type I IFN responses as well as cytokines, whereas Pam3CSK4 only induced cytokines (**Figure 4D-G**). However, exposure of

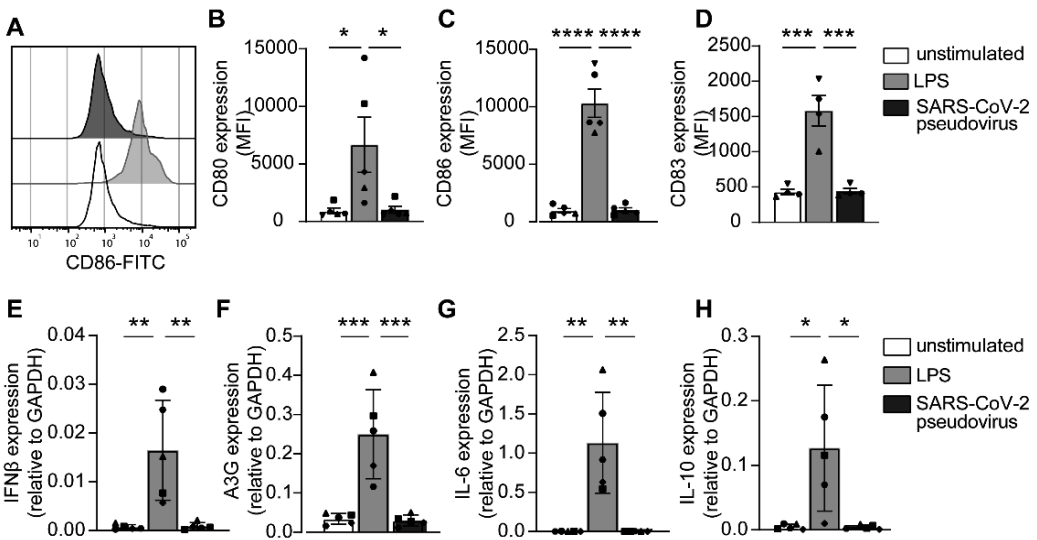


Figure 3 | SARS-CoV-2 pseudovirus does not activate dendritic cells. (A-D) Primary DCs were exposed to LPS or SARS-CoV-2 pseudovirus and maturation and cytokine production was determined after 24h and 6h respectively. (A) Representative histogram of CD86 expression. (B-D) Cumulative flow cytometry data of CD80 (B), CD86 (C), and CD83 (D) expression. (E-H) mRNA levels of IFN β (E), A3G (F), IL-6 (G) and IL-10 (H) were determined with qPCR. Data show the mean values and SEM. Statistical analysis was performed using one-way ANOVA with Tukey's multiple comparisons test. Data represent five donors analyzed in three separate experiments (B-C, E-H), or four donors analyzed in two separate experiments (D), with each symbol representing a different donor. **** $p < 0.0001$; *** $p < 0.001$; ** $p < 0.01$; * $p < 0.05$. MFI = mean fluorescence intensity.

DCs to the primary SARS-CoV-2 isolate did not lead to induction of type I IFN responses nor cytokines (**Figure 4D-G**). Therefore, these data strongly indicate that primary SARS-CoV-2 virus particles are not sensed by any extracellular PRRs on DCs such as TLR2, TLR4, and TLR5. Although SARS-CoV-2 did not directly activate DCs, we investigated whether DCs become activated indirectly by SARS-CoV-2-infected cells. Therefore, DCs were co-cultured with SARS-CoV-2 infected VeroE6 cells and DC activation was determined. Strikingly, co-culture of DCs with SARS-CoV-2-infected, but not uninfected VeroE6 cells induced expression of costimulatory molecules CD80 and CD86 (**Figure 4H-K**). These data support a role for indirect activation of DCs by infected cells during SARS-CoV-2 infection.

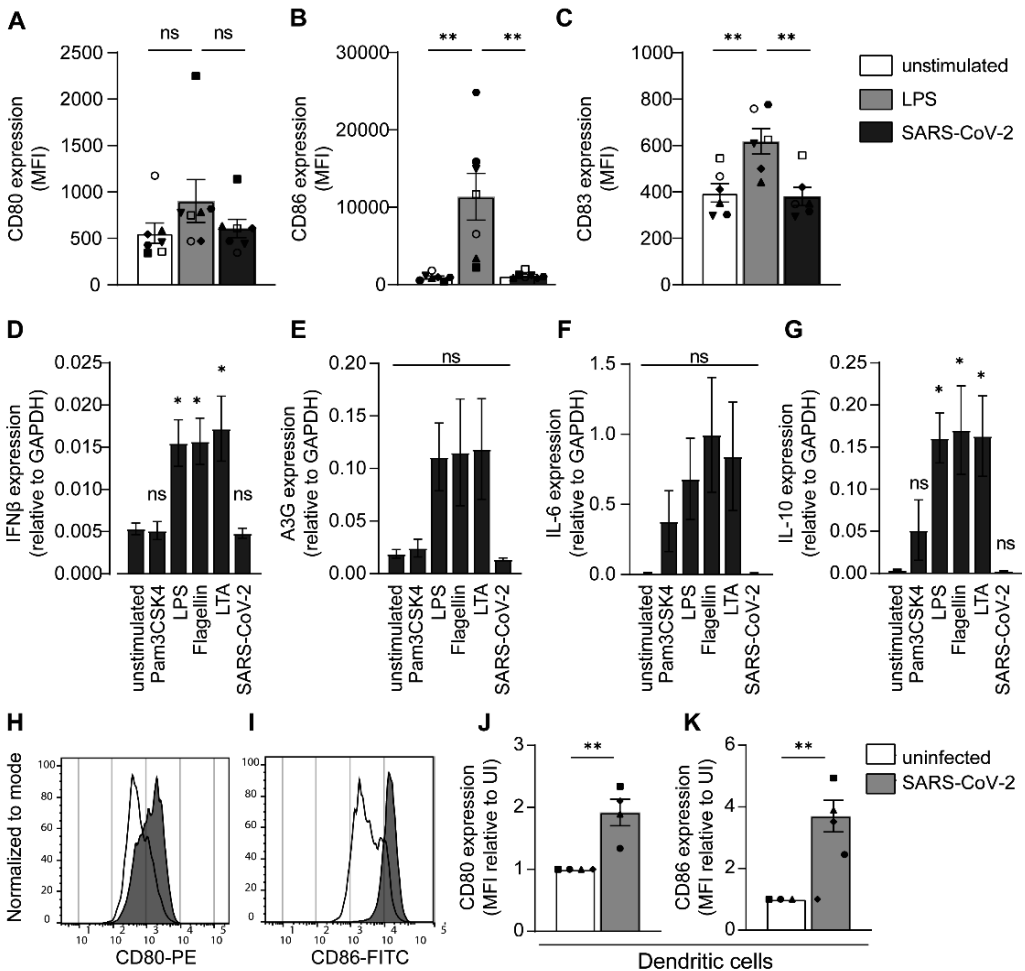


Figure 4. Figure legend on next page.

Figure 4 | Primary SARS-CoV-2 isolate does not activate dendritic cells. (A-C) Primary DCs were exposed to LPS or primary SARS-CoV-2 isolate and DC maturation was measured after 24h by flow cytometry. Cumulative flow cytometry data of CD80 (A), CD86 (B), and CD83 (C) expression. (D-G) Primary DCs were exposed to different TLR agonists or primary SARS-CoV-2 isolate and mRNA levels of IFN β (D), A3G (E), IL-6 (F) and IL-10 (G) were determined with qPCR. (D-G) Data are compared to the unstimulated condition. (H-K) Primary DCs were co-cultured with VeroE6 cells infected by SARS-CoV-2 and DC maturation was determined after 24h by measuring expression of CD80 and CD86. (H-I) Representative histograms of CD80 (H) and CD86 (I) expression. (J-K) Cumulative flow cytometry data of CD80 (J) and CD86 (K) expression. Data is relative to the uninfected condition (UI). Data show the mean values and SEM. Statistical analysis was performed using one-way ANOVA with Tukey's multiple comparisons test (A-G), or using an unpaired student's *t*-test (J-K). Data represent seven donors (A-B) or six donors (C) analyzed in four experiments; or five donors analyzed in three separate experiments (D-G); or four donors analyzed in two separate experiments (J-K), with each symbol representing a different donor. ***p*<0.01; **p*<0.05; ns = non-significant. MFI = mean fluorescence intensity; UI = uninfected.

Ectopic ACE2 expression on DCs results in SARS-CoV-2 infection and immune activation

Next, we investigated whether infection of DCs after ectopic expression of ACE2 with primary SARS-CoV-2 isolate would induce immune responses. DCs do not express ACE2, but transfection with ACE2 plasmid resulted in ACE2 mRNA and surface expression (**Figure 5A-C**). Next, both DCs and ACE2-expressing DCs were exposed to the primary SARS-CoV-2 isolate for 24h in presence or absence of blocking antibodies against ACE2. ACE2-expressing DCs were infected by SARS-CoV-2 and infection was blocked by antibodies against ACE2 (**Figure 5D**). Notably, infection of DCs with SARS-CoV-2 induced transcription of IFN- β (**Figure 5E**) as well as the ISG A3G (**Figure 5F**). Infection also induced pro-inflammatory cytokine IL-6 (**Figure 5G**). Both type I IFN responses and IL-6 were abrogated by blocking infection using ACE2 antibodies. Although the transfection procedure itself slightly activates DCs, SARS-CoV-2 infection significantly increased DC activation, which was abrogated by blocking ACE2. These data strongly suggest that DC activation of ACE2-expressing DCs is due to SARS-CoV-2 infection.

It has been described that TLR4 not only induces signaling pathways from the plasma membrane, but could also be internalized to the endosomal pathway to induce alternative signaling²⁵. To investigate whether ACE2-mediated internalization of SARS-CoV-2 triggers endosomal TLR4, we blocked TLR4 upon infection. Both DCs and ACE2-expressing DCs were exposed to the primary SARS-CoV-2 isolate in presence or absence of blocking antibodies against TLR4 and ACE2. ACE2-expressing DCs were infected by SARS-CoV-2 and both infection and IFN- β production was blocked by antibodies against ACE2, but not by antibodies against TLR4 (**Figure 5H-I**), suggesting that endosomal TLR4 triggering is not involved in the observed SARS-CoV-2-induced immune activation. Moreover, higher concentrations of the primary SARS-CoV-2 isolate did not induce type I IFN responses in DCs compared to ACE2-expressing DCs (**Figure 5J**). Taken together, these data strongly indicate that infection is required to induce cytokine responses by DCs and suggest that intracellular

PRRs rather than extracellular TLRs are involved in sensing SARS-CoV-2 and instigating immune responses against SARS-CoV-2.

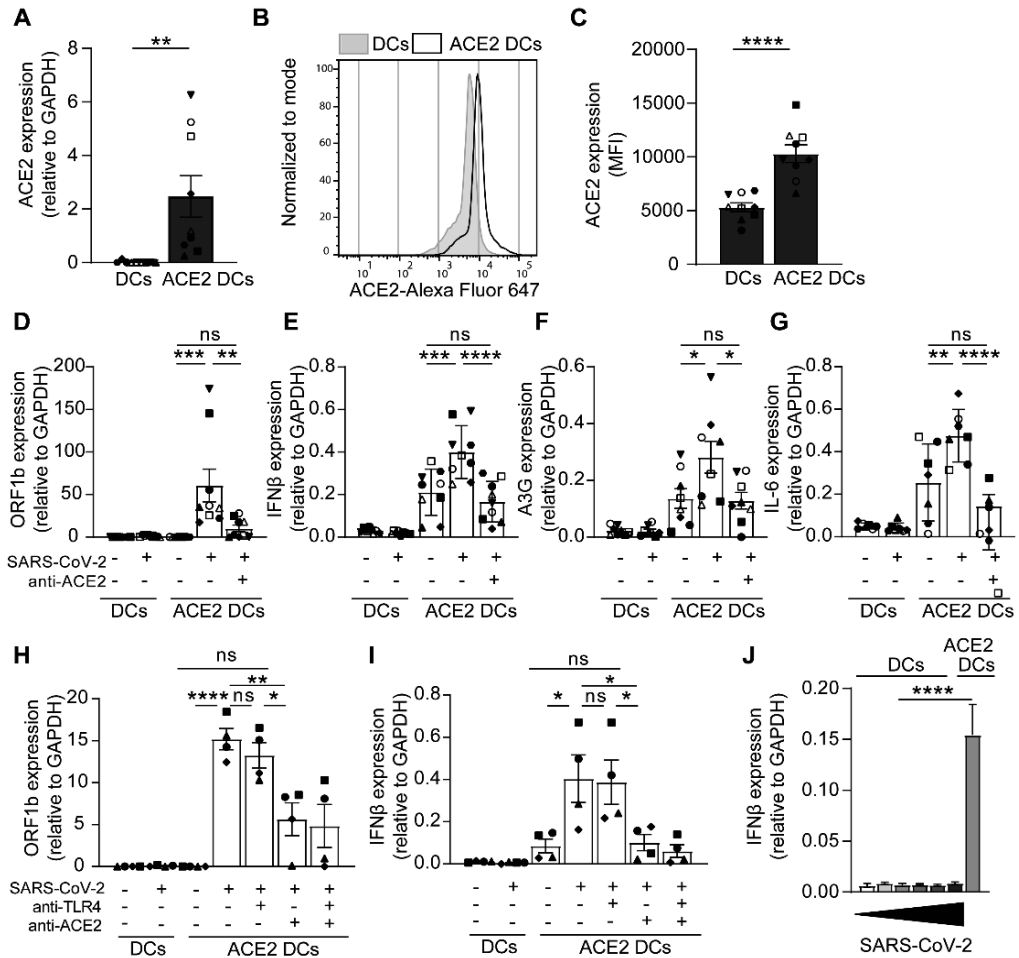


Figure 5 | Ectopic expression of ACE2 on DCs results in infection and induction of immune responses. (A-C) Ectopic expression of ACE2 on primary DCs was determined by qPCR and flow cytometry. (A) Cumulative qPCR data of ACE2 expression on DCs. (B) Representative histogram of ACE2 expression on DCs. (C) Cumulative flow cytometry data of ACE2 expression. (D-G) ACE2-positive and -negative DCs were exposed to primary SARS-CoV-2 isolate in presence or absence of blocking antibodies against ACE2. Infection (D) and mRNA levels of IFNβ (E), A3G (F), and IL-6 (G) were determined with qPCR. (H-I) ACE2-positive and -negative DCs were exposed to primary SARS-CoV-2 isolate in presence of blocking antibodies against TLR4 and ACE2. Infection (H) and mRNA levels of IFNβ (I) were determined with qPCR. (J) ACE2- negative DCs were exposed to increasing titers of primary SARS-CoV-2 isolate for 24h and compared to ACE2-positive DCs infected with TCID1000, and mRNA levels of IFN-β were determined by qPCR. Increasing titers are indicated by a bar, ranging from TCID100 (narrow) to TCID100.000 (wide). Data show the mean values and SEM. Statistical analysis was performed using (A, C) unpaired student's t-test or (D-I) one-way ANOVA with Tukey's multiple comparisons test. Data represent nine donors (A, C-F) or seven donors (G) obtained in five separate experiments, or four donors (H-J) obtained in two separate experiments, with each symbol representing a different donor. ****p<0.0001; ***p<0.001; **p<0.01; *p<0.05; ns = non-significant. MFI = mean fluorescence intensity.

Discussion

SARS-CoV-2 has established itself as a contagious human respiratory pathogen, which can trigger a robust inflammatory cytokine response⁸. However, it remains largely unknown whether innate immune receptors are involved in the onset of immune responses against SARS-CoV-2. TLR4 has been suggested to play a role in sensing SARS-CoV-2 and inducing a strong immune response^{13, 14}. Here, our data suggest that SARS-CoV-2 by itself is not recognized by TLR4, as neither a TLR4-expressing 293 cell line nor primary DCs were activated by exposure to recombinant S protein, SARS-CoV-2 pseudovirus or primary SARS-CoV-2 virus particles. Ectopic expression of ACE2 on primary DCs allowed infection with primary SARS-CoV-2. Notably, productive infection of ACE2-positive DCs induced type I IFN and cytokine responses, which were abrogated by blocking ACE2. Our data therefore suggest that SARS-CoV-2 virus particles are not sensed by extracellular TLRs, including TLR4, but that infection via ACE2 is required.

Other studies have reported that SARS-CoV-2 S protein triggers TLR4, and also TLR2 and TLR6 are suggested to interact with the S protein^{13, 14, 17, 18, 19, 26}. However, neither a TLR4-expressing 293 cell line nor primary DCs were activated by recombinant S proteins. It is possible that contamination during the purification process of recombinant proteins might induce activation and explain the differences. Therefore, we have also investigated immune activation by SARS-CoV-2 pseudovirus and infectious primary SARS-CoV-2 isolates. However, neither TLR4-expressing 293 cells nor primary DCs were activated by pseudovirus or a primary isolate of SARS-CoV-2, even at high virus concentrations. Therefore, our data strongly suggest that S protein expressed by SARS-CoV-2 does not trigger TLR4. Differences between our findings and those published might be due to different S protein preparations, purity of recombinant proteins or cell models. Most studies have used cell lines whereas we have used primary monocyte-derived DCs, which express high levels of TLR4, and are sensitive to TLR4 agonists. Monocyte-derived DCs are present in human lung^{27, 28} and monocytes infiltrating the lungs can differentiate into monocyte-derived DCs after pathogen exposure^{29, 30}, which further supports the relevance of monocyte-derived DCs to study TLR4 function in SARS-CoV-2 infection.

Monocyte-derived DCs do not express ACE2²⁴ and did not become infected by SARS-CoV-2, suggesting that the inability of primary SARS-CoV-2 to activate DCs strongly implies that SARS-CoV-2 is not sensed by TLR4 or other extracellular PRRs. Notably, ectopically expressing ACE2 on DCs led to infection and the production of cytokines, indicating that replication of SARS-CoV-2 triggers cytosolic sensors. Indeed, studies suggest that intracellular viral sensors such as RIG-I or MDA5 are involved in SARS-CoV-2 infection^{31, 32, 33}. Our data therefore support an important role for infection by SARS-CoV-2 in inducing immune activation and imply that infection of immune cells, such as antigen presenting cells (APCs), is essential to induction of immunity. Therefore, it is important to identify ACE2-positive DC subsets and macrophages, since these APCs could be sensitive to

infection and thereby orchestrate adaptive immunity. However, in the absence of DC infection, epithelial cell infection and subsequent inflammation and tissue damage might account for initial immune activation as release of PAMPs and DAMPs by these infected cells might activate ACE2-negative DCs³⁴. Notably, co-culture of DCs with SARS-CoV-2-infected cells led to activation of DCs, supporting a role for indirect activation of DCs by infected cells. It remains unclear whether these secondary signals are able to correctly instruct DCs and this might underlie the strong inflammatory responses observed during COVID-19. Our finding that SARS-CoV-2 is not recognized by TLR4 might therefore be an escape mechanism leading to inefficient DC activation and subsequent aberrant inflammatory responses. It has been suggested that worsening of disease in COVID-19 patients coincides with the activation of the adaptive immune response, 1-2 weeks after infection⁸. Since DCs have a bridging function to activate the adaptive immune response, it is important to study DCs in the context of COVID-19. Our research suggests that ACE2-negative DCs are not properly activated by infectious SARS-CoV-2. Moreover, our data suggest that SARS-CoV-2 is able to escape from extracellular TLRs that are one of the most important PRR families crucial for induction of innate and adaptive immunity, and further research will show whether the lack of TLR activation underlies observed inflammation during COVID-19.

Materials and methods

Cell lines

The Simian kidney cell line VeroE6 (ATCC® CRL-1586™) was maintained in CO₂ independent medium (Gibco Life Technologies, Gaithersburg, Md.) supplemented with 10% fetal calf serum (FCS), 2mM L-glutamine and penicillin/streptomycin. Culture was maintained at 37°C without CO₂.

Human embryonic kidney cells (HEK293) were maintained in IMDM (Gibco) supplemented with 10% FCS and 1% penicillin/streptomycin (Invitrogen). HEK293 cells stably transfected with TLR4 cDNA (HEK/TLR4) were a kind gift from D. T. Golenbock¹⁵. HEK293 and HEK/TLR4 cells were transiently transfected with pcDNA3.1(-)hACE2 (Addgene plasmid #1786) to generate HEK/ACE2 or HEK/TLR4/ACE2 cell lines. Transfection was performed using Lipofectamine LTX and PLUS reagent (Invitrogen) according to the manufacturer's protocol. After 24h, cells were split and seeded into flat-bottom 96-well plates (Corning) and left to attach for 24h, before performing further experiments. Cultures were maintained at 37°C and 5% CO₂. Before infection with the SARS-CoV-2 isolate (described below), media was exchanged for CO₂-independent media, since infection with a SARS-CoV-2 primary isolate occurs under CO₂ negative conditions. Human ACE2-expressing cell lines were analyzed for ACE2 expression via quantitative real-time PCR.

Primary cells

This study was performed in accordance with the ethical principles set out in the declaration of Helsinki and was approved by the institutional review board of the Amsterdam University Medical Centers, location AMC Medical Ethics Committee and the Ethics Advisory Body of Sanquin Blood Supply Foundation (Amsterdam, Netherlands). Human CD14⁺ monocytes were isolated from the blood from healthy volunteer donors (Sanquin blood bank) and subsequently differentiated into monocyte-derived dendritic cells (DCs). The isolation from buffy coats was done by density gradient centrifugation on Lymphoprep (Nycomed) and Percoll (Pharmacia). After separation by Percoll, the isolated monocytes were cultured in RPMI 1640 (Gibco) supplemented with 10% FCS, 2mM L-glutamin (Invitrogen) and 10 U/mL penicillin and 100 µg/mL streptomycin, containing the cytokines IL-4 (500 U/mL) and GM-CSF (800 U/mL) (both Gibco) for differentiation into DCs. After 4 days of differentiation, DCs were seeded at 1×10^6 /mL in a 96-well plate (Greiner), and after 2 days of recovery, DCs were stimulated or infected as described below.

Alternatively, monocyte-derived DCs that were transfected with hACE2 were seeded at 0.5×10^6 cells/mL in a 6-well plate and transfection was performed with Lipofectamine LTX and PLUS reagents (Invitrogen) according to the manufacturer's instructions for primary cells. After 24h, cells were seeded at 1×10^6 /mL in a 96-well plate and after 24h of recovery, they were infected with primary SARS-CoV-2 isolate.

SARS-CoV-2 pseudovirus production

For production of single-round infection viruses, human embryonic kidney 293T/17 cells (ATCC, CRL-11268) were co-transfected with an adjusted HIV-1 backbone plasmid (pNL4-3.Luc.R-S-) containing previously described stabilizing mutations in the capsid protein (PMID: 12547912) and firefly luciferase in the *nef* open reading frame (1.35 µg) and pSARS-CoV-2 expressing SARS-CoV-2 S protein (0.6 µg) (GenBank; MN908947.3)²². Transfection was performed in 293T/17 cells using genejuice (Novagen, USA) transfection kit according to manufacturer's protocol. At day 3 or day 4, pseudotyped SARS-CoV-2 virus particles were harvested and filtered over a 0.45 µm nitrocellulose membrane (SartoriusStedim, Gottingen, Germany). SARS-CoV-2 pseudovirus productions were quantified by p24 ELISA (Perkin Elmer Life Sciences).

SARS-CoV-2 (primary isolate) virus production

The following reagent was obtained from Dr. Maria R. Capobianchi through BEI Resources, NIAID, NIH: SARS-Related Coronavirus 2, Isolate Italy-INMI1, NR-52284, originally isolated January 2020 in Rome, Italy. VeroE6 cells (ATCC® CRL-1586™) were inoculated with the SARS-CoV-2 isolate and used for reproduction of virus stocks. Cytopathic effect formation was closely monitored and virus supernatant was harvested after 48h. Tissue culture

infectious dose (TCID₅₀) was determined on VeroE6 cells by MTT assay 48h after infection. Loss of MTT staining as determined by spectrometer is indicative of cell death. The virus titer was determined as TCID₅₀/mL and calculated based on the Reed Muench method³⁵, as described before²³.

Stimulation and infection

HEK293 and transfected derivatives were left unstimulated or stimulated for 24h with 10 ng/mL lipopolysaccharide (LPS) from *Salmonella* (Sigma), 10 µg/mL isolated S protein, 10 µg/mL S nanoparticle, or with pseudotyped or authentic SARS-CoV-2, as specified below. DCs were left unstimulated, or stimulated with 10 µg/ml Pam3CSK4 (Invivogen), 10 ng/mL LPS from *Salmonella typhosa* (Sigma), 10 µg/mL flagellin from *Salmonella typhimurium* (Invivogen), 10 µg/mL lipoteichoic acid (LTA) from *Staphylococcus aureus* (Invivogen), pseudotyped virus or SARS-CoV-2. Blocking of ACE2 or TLR4 was performed with 8 µg/mL anti-ACE2 (R&D systems) or 10 µg/mL anti-TLR4 (clone 7E3, Hycult) for 30 min at 37°C before adding stimuli. Monocyte-derived DCs do not express ACE2 and are therefore not infected. Therefore, pseudovirus stimulation was performed for 6h, after which the cells were lysed for mRNA analysis of cytokine production. DCs ectopically expressing ACE2 were stimulated for 24h with virus before the cells were lysed for mRNA analysis of cytokine production. Also, cells were stimulated for 24h and fixed for 30 min with 4% paraformaldehyde, after which the expression of maturation markers was assessed with flow cytometry. For the pseudovirus infection assays, HEK293 or 293/TLR4 cell lines and DCs were exposed to 95 ng/mL and 191.05 ng/mL of SARS-CoV-2 pseudovirus, respectively. Viral protein production was quantified after 3 days at 37°C by measuring luciferase reporter activity. Luciferase activity was measured using the Luciferase assay system (Promega, USA) according to manufacturer's instructions. For the primary SARS-CoV-2 infection assays, HEK293 or HEK/TLR4 cell lines and DCs were exposed to the SARS-CoV-2 isolate (hCoV-19/Italy) at different TCIDs (100 and 1000; MOI 0.0028-0.028) for 24h at 37°C. After 24h, cell supernatant was taken and DCs were lysed for isolation of viral RNA. Also, the HEK293/ACE2 and HEK/TLR4/ACE2 cell lines were exposed to the SARS-CoV-2 isolate (hCoV-19/Italy) at TCID 100 (MOI 0.0028) for 24h at 37°C. After 24h, the cells were washed 3 times and new media was added. After 48h, cell supernatant was harvested and the cells were lysed to investigate productive infection.

RNA isolation and quantitative real-time PCR

Cells exposed to SARS-CoV-2 pseudovirus were lysed and mRNA was isolated with the mRNA Catcher™ PLUS Purification Kit (ThermoFisher). Subsequently, cDNA was synthesized with a reverse-transcriptase kit (Promega). RNA of cells exposed to SARS-CoV-2 WT was isolated with the QIAamp Viral RNA Mini Kit (Qiagen) according to the manufacturer's protocol.

cDNA was synthesized with the M-MLV reverse-transcriptase kit (Promega) and diluted 1 in 5 in DNase/RNase-free water before further application. PCR amplification was performed in the presence of SYBR green (ThermoFisher) in a 7500 Fast Realtime PCR System (ABI). Specific primers were designed with Primer Express 2.0 (Applied Biosystems). The ORF1b primers used were as described before ³⁶. The normalized amount of target mRNA was calculated from the Ct values obtained for both target and household mRNA with the equation $Nt = 2^{Ct(GAPDH) - Ct(target)}$. The following primers were used: GAPDH: F_CCATGTTTCGT CATGGGTGTG; R_GGTGCTAAGCAGTTGGTGGTG; TLR4: F_CTGCAATGGATCAAGGACCAG; R_CCATTCGTTCAACTCCACCA; ACE2: F_GGACCCAGGAAATGTTTCAGA; R_GGCTGCAGAAAGT GACATGA; ORF1b: F_TGGGGTTTTACAGGTAACCT; R_AACACGCTTAACAAAGCACTC; IL-8: F_TGAGAGTGGACCACACTGCG; R_TCTCCACAACCCTCTGCACC; IFNB: F_ACAGACTTACAGGTT ACCTCCGAAAC; R_CATCTGCTGGTTGAAGAATGCTT; APOBEC3G: F_TTGAGCCTTGAATAAT CTGCC; R_TCGAGTGTCTGAGAATCTCCCC; IL-6: F_TGCAATAACCACCCCTGACC; R_TGCGCAGA ATGAGATGAGTTG; IL-10: F_GAGGCTACGGCGCTGTCAT; R_CCACGGCCTTGCTCTTGT

ELISA

Cell supernatants were harvested after 24h of stimulation and secretion of IL-8 was measured by ELISA (eBiosciences) according to the manufacturer's instructions. OD450 nm values were measured using a BioTek Synergy HT. Supernatant containing SARS-CoV-2 pseudovirus was inactivated with 0.1% triton and supernatant containing SARS-CoV-2 was inactivated with 1% triton before performing ELISA.

Flow cytometry

For cell surface staining, cells were incubated in 0.5% PBS-BSA (phosphate-buffered saline containing 0.5% bovine serum albumin (BSA; Sigma-Aldrich)) containing antibodies for 30 min at 4°C. Single-cell measurements were performed on a FACS Canto flow cytometer (BD Biosciences) and FlowJo V10 software (TreeStar) was used to analyze the data. The antibody clones used are: CD86 (2331 (FUN-1), BD Pharmingen), CD80 (L307.4, BD Pharmingen), CD83 (HB15e, BD Pharmingen), ACE2 (AF933, R&D systems), goat-IgG (AB-2535864, ThermoFisher Scientific), donkey-anti-goat (A-21447, ThermoFisher Scientific). For each experiment, live cells were gated on FSC and SSC and analyzed further with the markers mentioned (**Supplemental Figure 1**). The authors adhered to the guidelines for the use of flow cytometry and cell sorting in immunological studies ³⁷.

Statistics

Graphpad Prism v8 (GraphPad Software) was used to generate all graphs and for statistical analyses. Statistics were performed using a Student's *t* test for pairwise comparisons.

Multiple comparisons within groups were performed using an RM one-way analysis of variance (ANOVA) with a Tukey's multiple comparisons test, or two-way ANOVA with a Tukey's or Šidák's multiple comparisons test where indicated. $p < 0.05$ were considered statistically significant.

Data availability

The data that support the findings of this study are available from the corresponding authors upon reasonable request.

Ethics approval statement

This study was performed in accordance with the ethical principles set out in the declaration of Helsinki and was approved by the institutional review board of the Amsterdam University Medical Centers, location AMC Medical Ethics Committee and the Ethics Advisory Body of Sanquin Blood Supply Foundation (Amsterdam, Netherlands).

Author Contributions

LEHvdD and MBJ designed experiments; LEHvdD, MBJ, JE, and JLvH performed the experiments; PJMB, MB, ACvN, NAK, MJvG and RWS contributed essential research materials and scientific input. LEHvdD, MBJ and TBHG analyzed and interpreted data; LEHvdD, MBJ and TBHG wrote the manuscript with input from all listed authors. TBHG supervised all aspects of this study.

Conflict of interest

All authors declare no commercial or financial conflicts of interest

Acknowledgements

This research was funded by the Netherlands Organisation for Health Research and Development together with the Stichting Proefdiervrij (ZonMW MKMD COVID-19 grant nr. 114025008 to TBHG) and European Research Council (Advanced grant 670424 to TBHG), and two COVID-19 grants from the Amsterdam institute for Infection & Immunity (to TBHG, RWS, and MJvG). LEHvdD was supported by the Netherlands Organization for Scientific Research (NWO) (Grant number: 91717305). This study was also supported by NWO through a Vici grant (to RWS), and by the Bill & Melinda Gates Foundation through the Collaboration for AIDS Vaccine Discovery (CAVD), grant INV-002022 (to RWS).

References

- Zhu N, Zhang D, Wang W, Li X, Yang B, Song J, et al. A Novel Coronavirus from Patients with Pneumonia in China, 2019. *N Engl J Med.* 2020;382(8):727-33.
- Li Q, Guan X, Wu P, Wang X, Zhou L, Tong Y, et al. Early Transmission Dynamics in Wuhan, China, of Novel Coronavirus-Infected Pneumonia. *N Engl J Med.* 2020;382(13):1199-207.
- Harrison AG, Lin T, Wang P. Mechanisms of SARS-CoV-2 Transmission and Pathogenesis. *Trends Immunol.* 2020;41(12):1100-15.
- Wang D, Hu B, Hu C, Zhu F, Liu X, Zhang J, et al. Clinical Characteristics of 138 Hospitalized Patients With 2019 Novel Coronavirus-Infected Pneumonia in Wuhan, China. *JAMA.* 2020;323(11):1061-9.
- Wiersinga WJ, Rhodes A, Cheng AC, Peacock SJ, Prescott HC. Pathophysiology, Transmission, Diagnosis, and Treatment of Coronavirus Disease 2019 (COVID-19): A Review. *JAMA.* 2020;324(8):782-93.
- Yuki K, Fujiogi M, Koutsogiannaki S. COVID-19 pathophysiology: A review. *Clin Immunol.* 2020;215:108427.
- Mangalmurti N, Hunter CA. Cytokine Storms: Understanding COVID-19. *Immunity.* 2020;53(1):19-25.
- Tay MZ, Poh CM, Renia L, MacAry PA, Ng LFP. The trinity of COVID-19: immunity, inflammation and intervention. *Nat Rev Immunol.* 2020;20(6):363-74.
- Akira S, Uematsu S, Takeuchi O. Pathogen recognition and innate immunity. *Cell.* 2006;124(4):783-801.
- Freer G, Matteucci D. Influence of dendritic cells on viral pathogenicity. *PLoS Pathog.* 2009;5(7):e1000384.
- Hoffmann M, Kleine-Weber H, Schroeder S, Kruger N, Herrler T, Erichsen S, et al. SARS-CoV-2 Cell Entry Depends on ACE2 and TMPRSS2 and Is Blocked by a Clinically Proven Protease Inhibitor. *Cell.* 2020;181(2):271-80 e8.
- Letko M, Marzi A, Munster V. Functional assessment of cell entry and receptor usage for SARS-CoV-2 and other lineage B betacoronaviruses. *Nat Microbiol.* 2020;5(4):562-9.
- Bhattacharya M, Sharma AR, Mallick B, Sharma G, Lee SS, Chakraborty C. Immunoinformatics approach to understand molecular interaction between multi-epitopic regions of SARS-CoV-2 spike-protein with TLR4/MD-2 complex. *Infect Genet Evol.* 2020;85:104587.
- Choudhury A, Mukherjee S. In silico studies on the comparative characterization of the interactions of SARS-CoV-2 spike glycoprotein with ACE-2 receptor homologs and human TLRs. *J Med Virol.* 2020;92(10):2105-13.
- Chow JC, Young DW, Golenbock DT, Christ WJ, Gusovsky F. Toll-like receptor-4 mediates lipopolysaccharide-induced signal transduction. *J Biol Chem.* 1999;274(16):10689-92.
- Visintin A, Mazzoni A, Spitzer JH, Wyllie DH, Dower SK, Segal DM. Regulation of Toll-like receptors in human monocytes and dendritic cells. *J Immunol.* 2001;166(1):249-55.

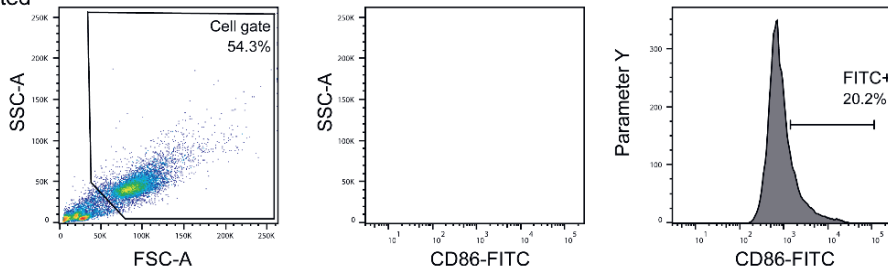
17. Aboudounya MM, Holt MR, Heads RJ. SARS-CoV-2 Spike S1 glycoprotein is a TLR4 agonist, upregulates ACE2 expression and induces pro-inflammatory M₁ macrophage polarisation. *bioRxiv*. 2021;2021.08.11.455921.
18. Shirato K, Kizaki T. SARS-CoV-2 spike protein S1 subunit induces pro-inflammatory responses via toll-like receptor 4 signaling in murine and human macrophages. *Heliyon*. 2021;7(2):e06187.
19. Zhao Y, Kuang M, Li J, Zhu L, Jia Z, Guo X, et al. SARS-CoV-2 spike protein interacts with and activates TLR4. *Cell Res*. 2021;31(7):818-20.
20. Brouwer PJM, Brinkkemper M, Maisonnasse P, Dereuddre-Bosquet N, Grobben M, Claireaux M, et al. Two-component spike nanoparticle vaccine protects macaques from SARS-CoV-2 infection. *Cell*. 2021;184(5):1188-200 e19.
21. Kawai T, Akira S. Toll-like receptors and their crosstalk with other innate receptors in infection and immunity. *Immunity*. 2011;34(5):637-50.
22. Brouwer PJM, Caniels TG, van der Straten K, Snitselaar JL, Aldon Y, Bangaru S, et al. Potent neutralizing antibodies from COVID-19 patients define multiple targets of vulnerability. *Science*. 2020;369(6504):643-50.
23. Bermejo-Jambrina M, Eder J, Kaptein TM, van Hamme JL, Helgers LC, Vlaming KE, et al. Infection and transmission of SARS-CoV-2 depends on heparan sulfate proteoglycans. *bioRxiv*. 2021;2020.08.18.255810.
24. Song X, Hu W, Yu H, Zhao L, Zhao Y, Zhao X, et al. Little to no expression of angiotensin-converting enzyme-2 on most human peripheral blood immune cells but highly expressed on tissue macrophages. *Cytometry A*. 2020.
25. Kagan JC, Su T, Horng T, Chow A, Akira S, Medzhitov R. TRAM couples endocytosis of Toll-like receptor 4 to the induction of interferon-beta. *Nat Immunol*. 2008;9(4):361-8.
26. Zheng M, Karki R, Williams EP, Yang D, Fitzpatrick E, Vogel P, et al. TLR2 senses the SARS-CoV-2 envelope protein to produce inflammatory cytokines. *Nat Immunol*. 2021;22(7):829-38.
27. Baharom F, Thomas S, Rankin G, Lepzien R, Pourazar J, Behndig AF, et al. Dendritic Cells and Monocytes with Distinct Inflammatory Responses Reside in Lung Mucosa of Healthy Humans. *J Immunol*. 2016;196(11):4498-509.
28. Baharom F, Rankin G, Blomberg A, Smed-Sorensen A. Human Lung Mononuclear Phagocytes in Health and Disease. *Front Immunol*. 2017;8:499.
29. Landsman L, Varol C, Jung S. Distinct differentiation potential of blood monocyte subsets in the lung. *J Immunol*. 2007;178(4):2000-7.
30. Osterholzer JJ, Chen GH, Olszewski MA, Curtis JL, Huffnagle GB, Toews GB. Accumulation of CD11b+ lung dendritic cells in response to fungal infection results from the CCR2-mediated recruitment and differentiation of Ly-6Chigh monocytes. *J Immunol*. 2009;183(12):8044-53.
31. Thorne LG, Reuschl AK, Zuliani-Alvarez L, Whelan MVX, Turner J, Noursadeghi M,

- et al. SARS-CoV-2 sensing by RIG-I and MDA5 links epithelial infection to macrophage inflammation. *EMBO J.* 2021:e107826.
32. Yang D, Geng T, Harrison AG, Wang P. Differential roles of RIG-I-like receptors in SARS-CoV-2 infection. *bioRxiv.* 2021.
33. Yin X, Riva L, Pu Y, Martin-Sancho L, Kanamune J, Yamamoto Y, et al. MDA5 Governs the Innate Immune Response to SARS-CoV-2 in Lung Epithelial Cells. *Cell Rep.* 2021;34(2):108628.
34. Campana P, Parisi V, Leosco D, Bencivenga D, Della Ragione F, Borriello A. Dendritic Cells and SARS-CoV-2 Infection: Still an Unclarified Connection. *Cells.* 2020;9(9).
35. Reed LJ, Muench H. A simple method of estimating fifty per cent endpoints. *American journal of epidemiology.* 1938;27(3):493-7.
36. Chu DKW, Pan Y, Cheng SMS, Hui KPY, Krishnan P, Liu Y, et al. Molecular Diagnosis of a Novel Coronavirus (2019-nCoV) Causing an Outbreak of Pneumonia. *Clin Chem.* 2020;66(4):549-55.
37. Cossarizza A, Chang HD, Radbruch A, Abrignani S, Addo R, Akdis M, et al. Guidelines for the use of flow cytometry and cell sorting in immunological studies (third edition). *Eur J Immunol.* 2021;51(12):2708-3145.

Supplementary material

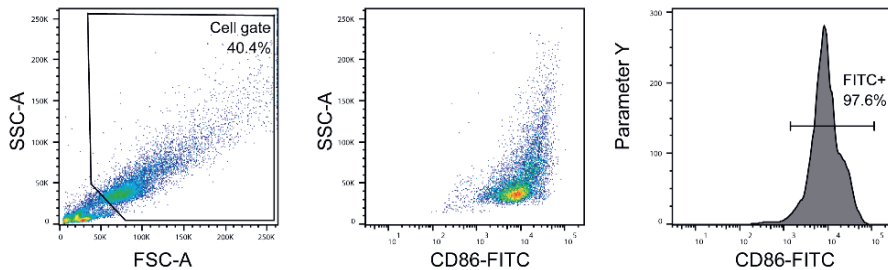
A

Unstimulated



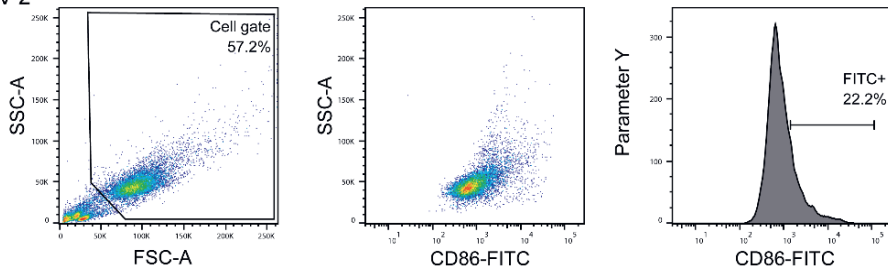
B

LPS



C

SARS-CoV-2



Supplemental Figure 1 | Dendritic cell gating strategy. After exposure to different stimuli, dendritic cells were harvested, fixed, and stained with antibodies against various markers and analyzed by flow cytometry. (A-C) Representative flow cytometry plots of one donor stimulated with medium (A), LPS (B), or SARS-CoV-2 (C). The percentage of selected cells is depicted in the upper right corner of the dot plot, and the expression of CD86 was plotted in a histogram. Histograms show the percentages of CD86-FITC-positive cells.



CHAPTER

5

Syndecan 4 upregulation on activated Langerhans cells counteracts langerin restriction to facilitate Hepatitis C virus transmission

Bernadien M. Nijmeijer¹, Julia Eder¹, Catharina J. M. Langedijk¹, Tanja M. Kaptein¹, Sofie Meeussen², Pascale Zimmermann^{2,3}, Carla M.S. Ribeiro¹, Teunis B. H. Geijtenbeek¹

¹Department of Experimental Immunology, Amsterdam Infection and Immunity Institute, Amsterdam University Medical Centers, University of Amsterdam, Amsterdam, The Netherlands

²Department of Human Genetics, KU Leuven, Leuven, Belgium

³Centre de Recherche en Cancérologie de Marseille, Equipe labellisée Ligue 2018, Aix-Marseille Université, Inserm, CNRS, Institut Paoli Calmettes, Marseille France

Abstract

Sexually transmitted Hepatitis C virus (HCV) infections and high reinfections are a major concern amongst men who have sex with men (MSM) living with HIV-1 and HIV-negative MSM. Immune activation and/or HIV-1 coinfection enhance HCV susceptibility via sexual contact, suggesting that changes in immune cells or factors are involved in increased susceptibility. Activation of anal mucosal Langerhans cells (LCs) has been implicated in increased HCV susceptibility as activated but not immature LCs efficiently retain and transmit HCV to other cells. However, the underlying molecular mechanism of transmission remains unclear. Here we identified the Heparan Sulfate Proteoglycan Syndecan 4 as the molecular switch, controlling HCV transmission by LCs. Syndecan 4 was highly upregulated upon activation of LCs and interference with Heparan Sulfate Proteoglycans or silencing of Syndecan 4 abrogated HCV transmission. These data strongly suggest that Syndecan 4 mediates HCV transmission by activated LCs. Notably, our data also identified the C-type lectin receptor langerin as a restriction factor for HCV infection and transmission. Langerin expression abrogated HCV infection in HCV permissive cells, whereas langerin expression on the Syndecan 4 expressing cell line strongly decreased HCV transmission to a target hepatoma cell line. These data suggest that the balanced interplay between langerin restriction and Syndecan 4 transmission determines HCV dissemination. Silencing of langerin enhanced HCV transmission whereas silencing Syndecan 4 on activated LCs decreased transmission. Blocking Heparan Sulfate Proteoglycans abrogated HCV transmission by LCs *ex vivo* identifying Heparan Sulfate Proteoglycans and Syndecan 4 as potential targets to prevent sexual transmission of HCV. Thus, our data strongly suggest that interplay between receptors promotes or restricts transmission and further indicate that Syndecan 4 is the molecular switch controlling HCV susceptibility after sexual contact.

Keywords: Langerhans cells, Hepatitis C virus, Heparan Sulfate Proteoglycans, Heparan Sulfates, Syndecan 4, langerin, viral dissemination

Introduction

Viral hepatitis is responsible for an estimated 1.3 million deaths from acute infection, hepatitis-related liver cancer and cirrhosis in 2015¹. Hepatitis C virus (HCV) infections accounts for almost 30% of these deaths¹. In the mid-2000s HCV infection emerged in men who have sex with men (MSM)^{2,3,4,5} likely due to sexual contact^{6,7,8,9}. Although directly acting antiviral (DAA) treatment is very effective in clearing HCV¹⁰, the high reinfection rates amongst MSM who cleared HCV spontaneously or who were successfully treated^{11,12,13} underscores the need for a better understanding of the mechanisms involved in sexual transmission of HCV. As new HCV infections were typically found in MSM living with human immunodeficiency virus type 1 (HIV-1), it was suggested that the HIV-1 status is an important risk factor for sexually acquired HCV^{8,9,11,14}. However, recent studies suggest that sexual transmission of HCV also occurs in HIV-1-negative MSM eligible for or using pre-exposure prophylaxis (PrEP), indicating that HIV-1 infection status is not the only factor affecting susceptibility^{15,16,17}. Potential mechanisms for increased rates of sexual transmission of HCV among MSM may include high-risk practices⁴ and unprotected mucosal traumatic sex leading to rectal bleeding¹⁸ which could lead to disruption of the mucosal integrity allowing HCV to cross the epithelial barrier to either directly enter the blood stream or indirectly via immune cells promoting sexual transmission of HCV. We have previously shown an important role for Langerhans cells (LCs) in HCV transmission during HIV-1 coinfection but also upon immune activation¹⁹.

LCs reside in mucosal tissues and are therefore among the first immune cells to encounter viruses, they are thought to be involved in sexual transmission of HIV-1^{20,21,22}. Interestingly, LC function in HIV-1 infection depends on their activation state^{20,21,22}. Immature LCs have been shown to restrict HIV-1 infection via the C-type lectin receptor langerin (CD207)^{20,21}. Langerin is highly expressed by immature LCs and capture of HIV-1 by langerin leads to viral internalization into Birbeck granules. Virus fusion triggers degradation of HIV-1 via E3-ubiquitin ligase tri-partite-containing motif 5 α (TRIM5 α) mediated autophagic degradation, thereby preventing infection of LCs^{20,21}. Upon LC activation, as can occur during genital coinfections, LCs lose their protective function, become infected by HIV-1 and efficiently transmit HIV-1 to T cells, thereby promoting HIV-1 dissemination²².

Primary LCs are also present at mucosal sites of the foreskin and within the anal tissue^{19,23}, the primary entry site of sexually transmitted HCV. Interestingly, under normal conditions LCs are refractory to HCV but upon HIV-1 infection or when activated LCs are able to retain HCV, facilitating transmission to target cells¹⁹. These data suggest that activation of LCs in MSM might allow the virus to penetrate mucosal tissues and establish dissemination via the blood or lymph²⁴. Thus, the activation state of the LCs dictates HCV susceptibility but the molecular mechanism deciding the fate of the virus are unknown. Therefore we have investigated the molecular mechanism involved in HCV susceptibility during sexual contact. Syndecans are known to function as attachment receptors to facilitate HIV-1 transmission

^{25, 26}. Syndecans are transmembrane heparan sulfate proteoglycans (HSPGs) expressed on the surfaces of human cells that possess heparan sulfate glycosaminoglycan chains ²⁷. They are classified into members of the Syndecan family that consist of Syndecan 1, Syndecan 2, Syndecan 3 and Syndecan 4 ^{28, 29}. Sexually transmitted viruses such as HIV-1, herpes simplex virus type 1 and 2 (HSV-1 and HSV-2) and human papillomavirus (HPV) interact with heparan sulfates on Syndecans to mediate binding and internalization to host cells to promote infection and spread to other cells ^{30, 31, 32, 33, 34, 35}. HCV also interacts with heparan sulfates on Syndecan 1 and Syndecan 4 which can facilitate attachment and infection in cell lines ^{36, 37}.

Here our data show that upon activation LCs acquire the ability to retain and transmit HCV using HSPGs. Further analyses showed that the major HSPG involved is specific Syndecan 4. Strikingly, Syndecan 4 induction upon activation of LCs counteracts langerin restriction of HCV infection and transmission. Ectopic expression of langerin on the Syndecan 4 expressing cell line enhanced HCV capture but decreased HCV transmission to a target hepatoma cell line Huh7.5. Moreover, silencing langerin on Mutz-LCs enhanced HCV transmission which strongly support a restrictive role for langerin in mucosal HCV transmission. Together our data strongly suggest that activated LCs upregulate Syndecan 4 to capture HCV via their heparan sulfate chains and exploit them as in *trans*-receptors to infect hepatocytes. This transmission mechanism implicates that the balanced interplay between langerin and Syndecan 4 on activated LCs dictates HCV susceptibility after sexual contact. Therapeutical interventions targeting Syndecan 4 on mucosal LCs could represent a novel strategy to counteract LC-mediated dissemination of HCV.

Results

Heparan sulfate proteoglycans promote HCV transmission

As HSPGs are known receptors for HCV on hepatocytes ^{36, 37} we investigated the role of heparan sulfates in LC-mediated HCV transmission. Immature and activated LCs were isolated and their phenotype was verified ²⁰ (**Supplemental Figure S1**). Activated in contrast to immature LCs expressed high levels of heparan sulfates on their cell surface (**Figure 1A** and **1B**). Next we blocked the heparan sulfate binding places on HCV using heparin to investigate their role in transmission. Notably, heparin treatment of pseudotyped HCV (HIV-1 NL4.3Δenv pseudotyped with HCV env glycoproteins E1 and E2) blocked HCV transmission by activated LCs (**Figure 1C**). Immature LCs did not transmit HCV to target cells (**Figure 1C**), even though both, immature and activated LCs captured HCV (**Figure 1D**). Moreover, heparin treatment of both pseudotyped HCV genotype 1a strain pHCV_H77_E1_E2 and replicative HCV genotype 2a strain (JFH1-AM120-RLuc) blocked HCV transmission in the *ex vivo* transmission model (**Figure 1E** and **Figure 1F**) confirming a role for heparan sulfates on *ex vivo* LCs in HCV transmission. Next we removed heparan sulfates

from activated LCs by enzymatic digestion to investigate the involvement of HSPGs. Enzymatic treatment of activated LCs with heparinase decreased the expression of heparan sulfates on the cell surface (**Figure 1G**). Notably, heparan sulfate removal resulted in a significant decrease of HCV transmission, compared to untreated LCs (**Figure 1H**). These data strongly suggest that HSPGs expressed by LCs, mediate HCV transmission.

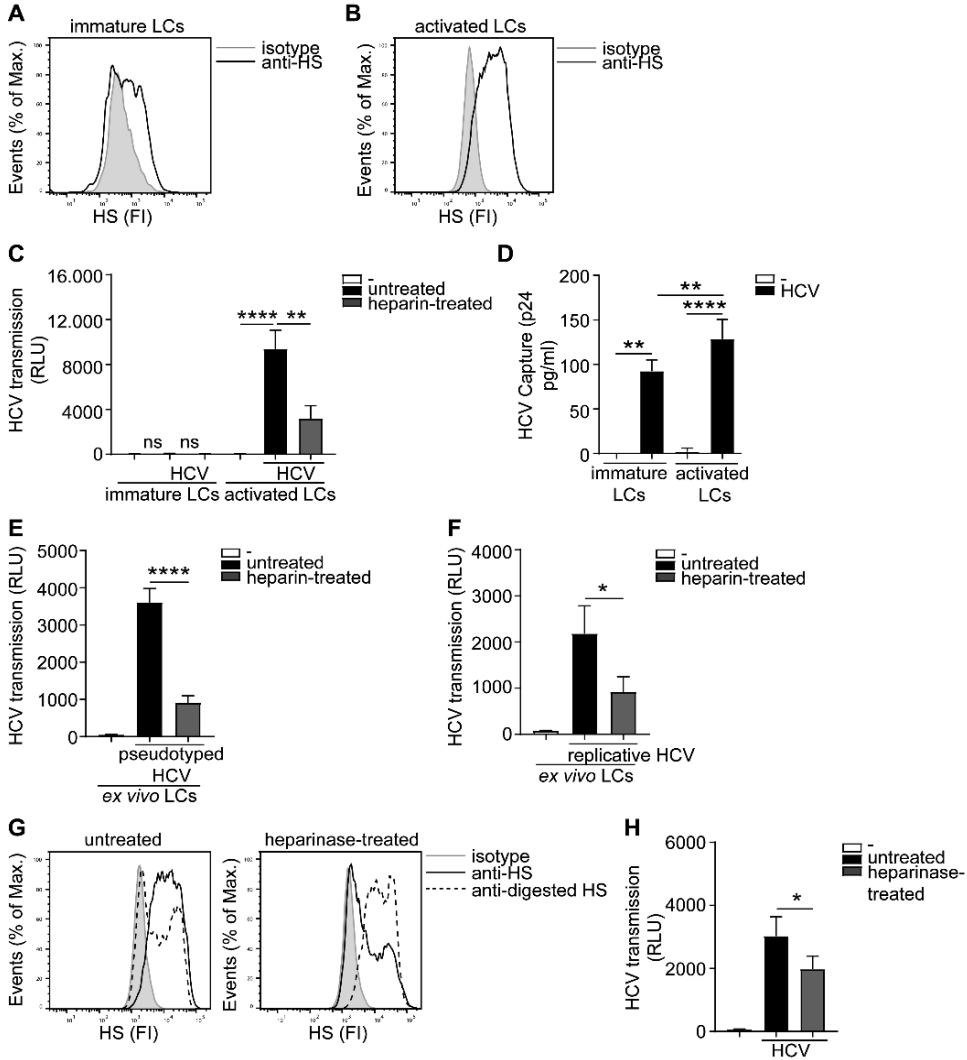


Figure 1. Figure legend on next page.

Figure 1 | Heparan sulfate proteoglycans promote HCV transmission. (A-B) Immature and activated LCs express heparan sulfates. One representative donor out of 3 is depicted. (C) Pseudotyped HCV was pre-incubated with heparin (250U) and transmission by LCs to Huh7.5 cells was determined. (D) Immature and activated LCs were exposed to pseudotyped HCV, lysed and binding was quantified by p24 ELISA. (E-F) *Ex vivo* tissue was cultured in medium for 24 hours and subsequently exposed to either medium or (E) heparin (500U) pre-incubated pseudotyped HCV or pseudotyped HCV for another 24 hours and transmission by LCs to Huh7.5 cells was determined. (F) heparin (500U) pre-incubated replicative HCV or replicative HCV for another 24 hours and transmission by LCs to Huh7.5 cells was determined. (G) Activated LCs were left untreated or treated with heparinase for 2 hours and heparan sulfate expression was determined. One representative donor out of 3 is depicted. (H) Activated LCs were left untreated or treated with heparinase for 2 hours, washed, exposed to pseudotyped HCV and transmission by LCs to Huh7.5 cells was determined. Error bars are the mean \pm SD of (C) immature LCs n=3 donors measured in triplo or activated LCs n=3 donors measured in triplo. (D) immature LCs n=3 donors measured in duplo or activated LCs n=7 donors measured in duplo. (E) n=3 donors measured in quadruplo. (F) n=4 donors measured in quadruplo. (H) n=3 donors measured in quadruplo. ns = not significant, *p< 0.05, **p< 0.01, ***p< 0.0001 by two-tailed, unpaired, non-parametric, Mann-Whitney test. LCs: Langerhans cells, HS: heparan sulfates, FI: fluorescent intensity, RLU: relative light units, HCV: Hepatitis C virus.

Syndecan 4 facilitates HCV transmission

Next we assessed the potential role for HSPGs to serve as HCV transmission receptors. We investigated the ability of human B cell line Namalwa expressing the different Syndecans (**Figure 2A**) to transmit HCV. Only the cell-line expressing Syndecan 4 was able to transmit replicative HCV genotype 2a strain to target cells (**Figure 2B**). Similarly, Syndecan 4 also efficiently transmitted pseudotyped HCV in contrast to the other Syndecans (**Figure 2C**). These data strongly suggest that HCV specifically interacts with Syndecan 4 for transmission. Next we examined the role of heparan sulfates in HCV transmission by Syndecan 4 cells using not only unfractionated heparin, but also several low molecular weight (LMW) heparins. Pseudotyped HCV was exposed to either unfractionated heparin or LMW heparins dalteparin, tinzaparin and enoxaparin and HCV transmission was determined. The different LMW heparins inhibited transmission by Syndecan 4 to a similar extent as unfractionated heparin (**Figure 2D**), strongly suggesting that heparan sulfates on Syndecan 4 are important for the interaction with HCV. Finally we inhibited heparan sulfate biosynthesis by PNP-Xyl treatment. Syndecan 4 cells were left untreated or cultured in the presence of 1.0mM or 2.5mM PNP-Xyl for 72 hours. The cell viability was not affected at these concentrations (data not shown). PNP-Xyl treatment decreased heparan sulfate expression on the cell surface of Syndecan 4 cells (**Figure 2E**), and abrogated HCV transmission in a concentration dependent manner (**Figure 2F**). Thus, our data strongly suggest that Syndecan 4 in contrast to the other Syndecans is a specific receptor for HCV transmission.

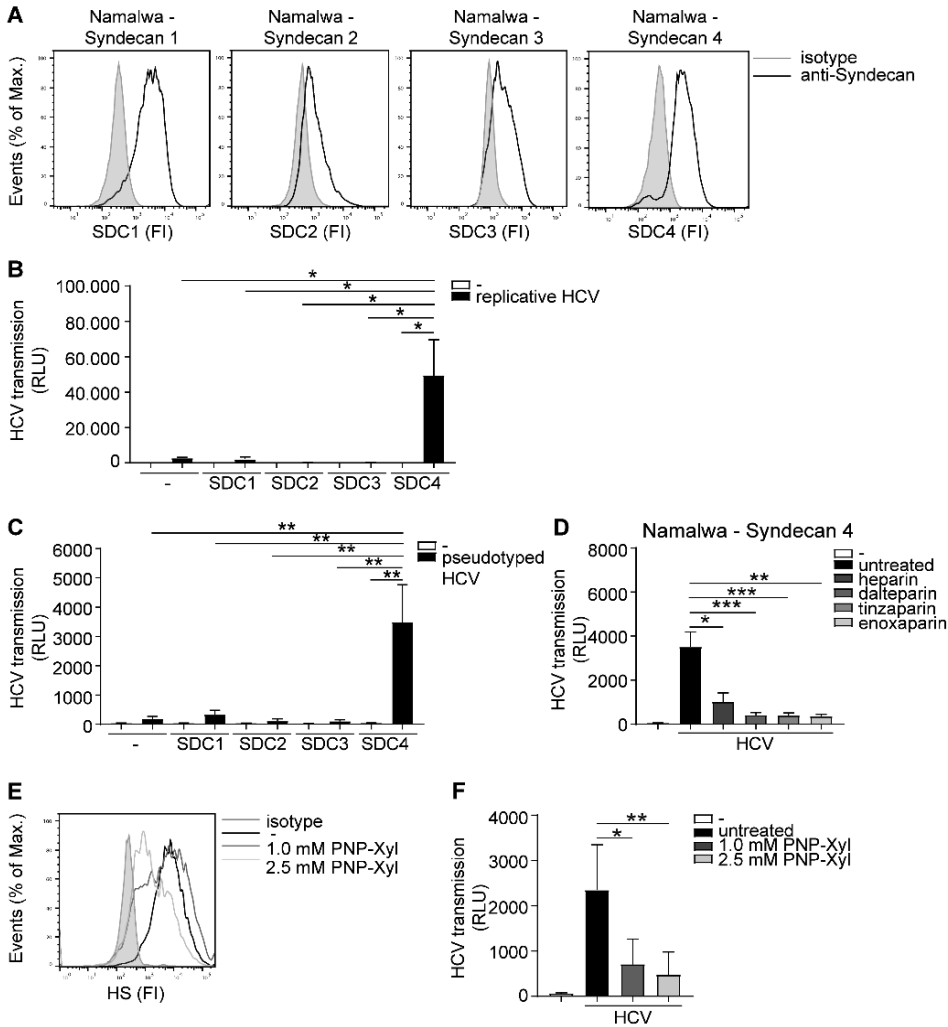


Figure 2 | Syndecan 4 facilitates HCV transmission. (A) Different Syndecan cell lines express Syndecan 1-4, on the cell surface determined by flow cytometry. One representative experiment out of 2 is depicted. (B-C) Different Syndecan cell lines were exposed to (B) replicative HCV or (C) pseudotyped HCV (B-C) and transmission by LCs to Huh7.5 cells was determined. (D) Pseudotyped HCV was pre-incubated with unfractionated heparin (500U) or dalteparin (500U) or tinzaparin (500U) or enoxaparin (500U) and transmission by LCs to Huh7.5 cells was determined. (E) Syndecan 4 cells were cultured in the presence of PNP-Xyl inhibitor for 72 hours and heparan sulfate surface expression was determined by flow cytometry. One representative donor out of 3 is depicted. (F) Syndecan 4 cells were cultured in the presence of PNP-Xyl inhibitor for 72 hours, harvested, exposed to pseudotyped HCV and transmission by Syndecan 4 cells to Huh7.5 cells was determined. Error bars are the mean \pm SD of (B) one representative donor measured in quadruplo. (C) one representative donor out of 3 measured in quadruplo. (D) n=5 experiments (medium and HCV) or n=3 experiments (heparin, dalteparin, tinzaparin, enoxaparin) measured in triplo or quadruplo. (F) n=5 experiments measured in quadruplo. *p < 0.05, **p < 0.01, ***p < 0.001, by two-tailed, unpaired, parametric, Student t-test. SDC1: Syndecan 1, SDC2: Syndecan 2, SDC3: Syndecan 3, SDC4: Syndecan 4, PNP-Xyl: p-Nitrophenyl- β -d-xylopyranoside, HS: heparan sulfates, FI: fluorescent intensity, RLU: relative light units, HCV: Hepatitis C virus

Activated LCs transmit HCV via Syndecan 4

Next we investigated the Syndecan 4 expression on primary LCs. Activated LCs expressed higher levels of Syndecan 4 than immature LCs from the same donor (**Figure 3A**). In order to investigate the role of Syndecan 4 in transmission by LCs, Syndecan 4 was silenced in primary activated LCs by RNA interference (**Figure 3B** and **Figure 3C**). Silencing Syndecan 4 did not interfere with the expression of other Syndecans or langerin (**Supplemental Figure S2**). Syndecan 4 silencing strongly decreased HCV transmission by activated LCs compared to the non-targeting control (**Figure 3D**). Thus, our data indicate that Syndecan 4 expression is upregulated upon activation of LCs and thereby facilitates HCV transmission to hepatocytes.

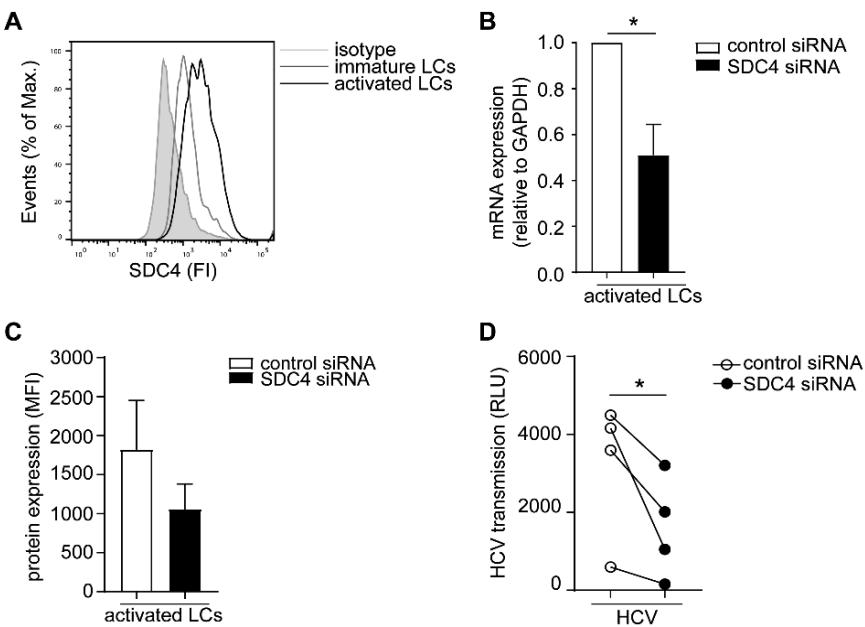


Figure 3 | Activated LCs transmit HCV via Syndecan 4. (A) Immature and activated LCs express Syndecan 4 on the cell surface. One representative donor out of 2 is depicted. (B) Syndecan 4 silencing was confirmed by real-time PCR. mRNA expression was normalized to GAPDH and set at 1 in cells treated with control siRNA. (C) Cell surface expression of Syndecan 4 after silencing determined by flow cytometry. (D) Activated LCs were transfected with non-target control or Syndecan 4 siRNA and after 72 hours exposed to pseudotyped HCV and transmission by LCs to Huh7.5 cells was determined. Error bars are the mean \pm SD of (B) $n=4$ donors, (C) $n=3$ donors (D) $n=4$ donors measured in triplo or quadruplo. * $p < 0.05$, by two-tailed, paired, parametric, Student t-test. LCs: Langerhans cells, SDC4: Syndecan 4, HS: heparan sulfates, FI: fluorescent intensity, MFI: mean fluorescent intensity, RLU: relative light units, HCV: Hepatitis C virus

Langerin restricts HCV infection

LCs specifically express the CLR langerin that has a protective role in HIV-1 dissemination by restricting HIV-1 infection and transmission^{20, 21}. Immature LCs expressed high levels of langerin, which is downregulated upon activation of LCs (**Figure 4A**)³⁸. Nothing is known about the role of langerin in HCV infection. The Huh7.5 cell line does not express langerin on the cell surface (**Supplemental Figure S3**). Therefore, we ectopically expressed langerin on the HCV susceptible Huh7.5 cell line (**Figure 4B**) and investigated its function in infection. Notably, infection of langerin-expressing Huh7.5 cells by pseudotyped HCV was significantly lower compared to Huh7.5 cells (**Figure 4C**). Moreover, langerin expression also decreased infection of Huh7.5 with replicative HCV (**Figure 4D**). Huh7.5 cells and Huh7.5-langerin cells exhibit similar growth (**Supplemental Figure S4**), suggesting the observed differences resulted from a decrease in infection. These data strongly suggest that langerin restricts pseudotyped as well as replicative HCV infection.

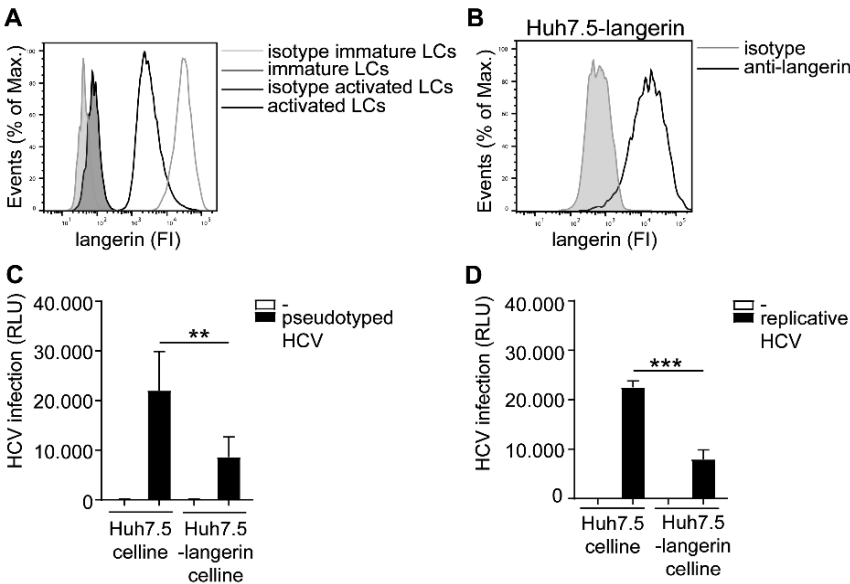


Figure 4 | Langerin restricts HCV infection. (A) Immature and activated LCs from the same donor express langerin. One representative donor out of 3 is depicted. (B) Huh7.5-langerin cell line was transduced with lentiviruses expressing sequences coding human langerin. Surface expression was determined by flow cytometry. One representative experiment is depicted. (C-D) Huh7.5 cell line or Huh7.5-langerin cell line was infected with (C) pseudotyped HCV or (D) replicative HCV (C-D) and cell line infection was determined. Error bars are the mean \pm SD of (C) $n=6$ experiments measured in triplo or quadruplo. (D) $n=3$ experiments measured in triplo. ** $p < 0.01$, *** $p < 0.001$, by two-tailed, unpaired, parametric, Student t-test. FI: fluorescent intensity, RLU: relative light units, HCV: Hepatitis C virus

The interplay between langerin and Syndecan 4 determines HCV transmission

To investigate the interplay between langerin and Syndecan 4, the Syndecan 4 Namalwa cell line was transduced with langerin (**Figure 5A**). Ectopic expression of langerin on the SDC4 cell line did not affect the overall expression of HS or the cell surface SDC4 expression of the cell lines (**Supplemental Figure S5**). Ectopic expression of langerin increased HCV capture by langerin-expressing Syndecan 4 cells (**Figure 5B**). Strikingly, langerin expression significantly inhibited Syndecan 4-mediated HCV transmission (**Figure 5C**). These data strongly suggest that langerin and Syndecan 4 have opposite roles in HCV transmission; Syndecan 4 promotes HCV transmission whereas langerin counteracts Syndecan 4 driven HCV transmission. Next we investigated the interplay between both receptors on LCs. As silencing of langerin on primary LCs is challenging, we have used Mutz-derived LCs as a validated model to study LC-mediated virus transmission^{21, 39}. Mutz-LCs have a more activated phenotype than immature LCs, therefore express intermediate levels of langerin³⁹. Concomitantly, we could confirm that Mutz-LCs also express both HSPGs and Syndecan 4 (**Figure 5D and 5E**). Mutz-LCs efficiently transmitted HCV to hepatocytes in a heparan sulfate-dependent manner, since heparin inhibited HCV transmission (**Figure 5F**). Langerin silencing in Mutz-LCs significantly increased HCV transmission (**Figure 5G, 5H and 5I**). Our data strongly suggest that langerin counteracts Syndecan 4-mediated transmission by LCs and therefore expression of langerin and Syndecan 4 control HCV restriction or transmission, respectively.

Discussion

Sexually acquired Hepatitis C virus predominantly occurs amongst MSM living with HIV-1^{2, 3, 4, 5, 6, 7, 9} but also increasing cases of sexually acquired HCV have been reported amongst HIV-1 negative MSM eligible for or on PrEP^{15, 16, 17, 40, 41, 42}. Therefore, a better understanding of the mechanisms involved in sexual transmission of HCV are needed. Immature LCs reside in the anal mucosa and are among the first cells to encounter HCV upon receptive anal intercourse¹⁹. We have previously shown that immature LCs are not able to transmit HCV but that either HIV-1 infection or immune activation changes the function of these LCs as activated as well as HIV-1 infected LCs retain HCV for transmission to target cells¹⁹. Here we identified an important novel role for Syndecan 4 on activated LCs in HCV transmission. Syndecan 4 is upregulated on activated LCs facilitating HCV transmission. Moreover, we have identified a HCV restrictive role for the C-type lectin receptor langerin that is highly expressed by immature LCs and downregulated by activated LCs. Our data indicate that the interplay between langerin and Syndecan 4 on LCs controls HCV transmission and the increased expression of Syndecan 4 and simultaneous downregulation of langerin after

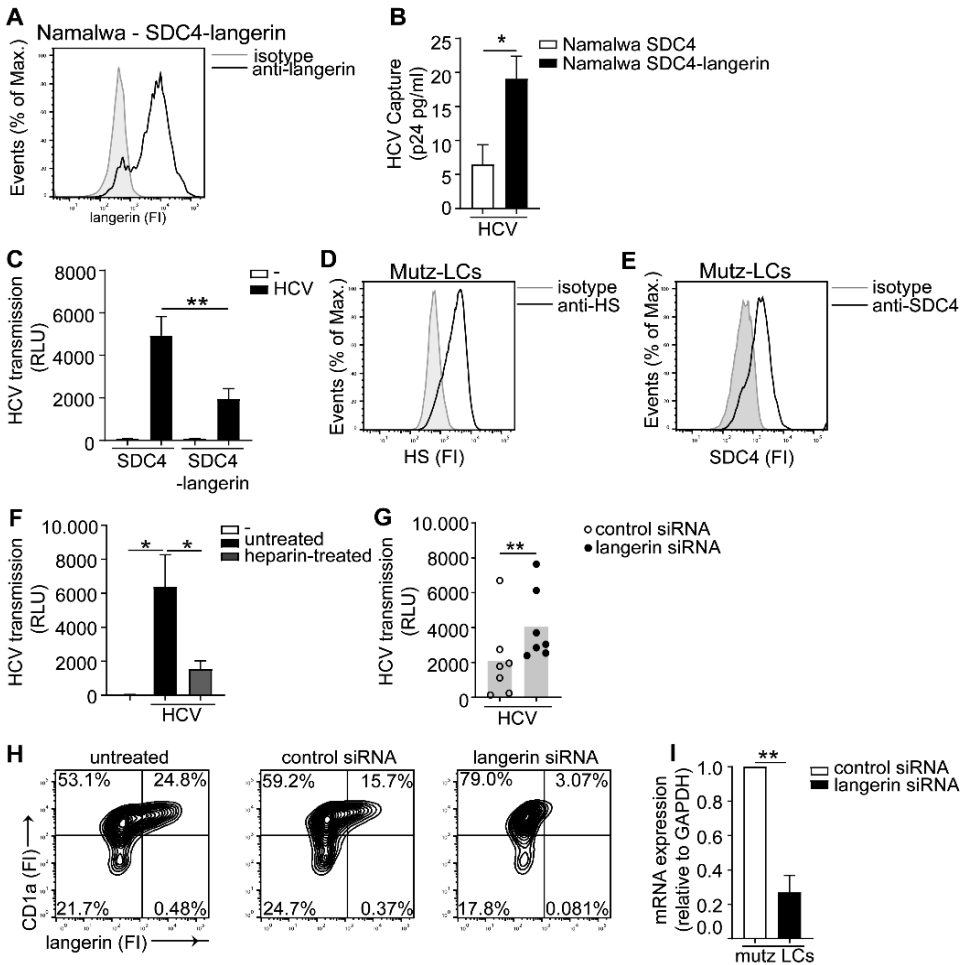


Figure 5 | The interplay between langerin and Syndecan 4 determines HCV transmission. (A) Syndecan 4-langerin cell line express langerin on the cell surface determined by flow cytometry. One representative experiment is depicted. (B) Syndecan 4 cell line or Syndecan 4-langerin cell line, were exposed to pseudotyped HCV, lysed and binding was quantified by p24 ELISA. (C) Syndecan 4 cell line or Syndecan 4-langerin cell line, were exposed to pseudotyped HCV and transmission by LCs to Huh7.5 cells was determined. (D-E) Mutz-LCs express (D) heparan sulfates (E) Syndecan 4 (D-E) on the cell surface as determined by flow cytometry. One representative donor is depicted. (F) Pseudotyped HCV was pre-incubated with heparin (500U) and transmission by Mutz LCs to Huh7.5 cells was determined. (G) Mutz-LCs were transfected with non-target control or langerin siRNA or left untreated and after 72 hours exposed to pseudotyped HCV and transmission by LCs to Huh7.5 cells was determined. (H) Mutz-LCs were transfected with non-target control or langerin siRNA or left untreated and after 72 hours silencing was confirmed by flow cytometry. One representative donor is depicted. (I) Mutz-LCs were transfected with non-target control or langerin siRNA or and after 72 hours silencing was confirmed by real-time PCR. mRNA expression was normalized to GAPDH and set at 1 in cells treated with control siRNA. Error bars are the mean \pm SD of (B) n=3 experiments measured in duplo. (C) n=4 experiments measured in quadruplo. (B-C-I) *p < 0.05, **p < 0.01, by two-tailed, unpaired, parametric, Student t-test. Error bars are the mean \pm SD of (F) one representative donor out of 2, measured in quadruplo. (G) n=7 donors measured in triplio. (I) n=2 donors (F-G) *p < 0.05, **p < 0.01, by two-tailed, unpaired, non-parametric, Mann-Whitney test. LCs: Langerhans cells, SDC4: Syndecan 4, HS: heparan sulfates, FI: fluorescent intensity, RLU: relative light units, HCV: Hepatitis C virus.

activation of LCs might be the molecular switch allowing HCV transmission during sexual contact.

HSPGs are well known for their function as internalizing receptors or co-receptors⁴³. Many other viruses including, HIV-1⁴⁴, herpesvirus⁴⁵, human papillomavirus⁴⁶, human cytomegalovirus⁴⁷, adenovirus⁴⁸, dengue virus⁴⁹ and vaccinia virus⁵⁰ use HSPG as initial binding target for transfer to a secondary receptor allowing fusion. Heparin treatment of both HCV genotype 1a as well as HCV genotype 2a blocked HCV transmission by *ex vivo* LCs, suggesting that HSPGs expressed by LCs mediate HCV transmission and that the observed effect is observed in multiple HCV genotypes. Moreover, Syndecan 3 has been shown to be involved in HIV-1 transmission by macrophages and DCs by supporting HIV-1 attachment, retaining viral infectivity and subsequent transmission to target cells^{25, 26, 51}. Initial attachment of HCV to target cells occurs via interaction with virion associated component apolipoprotein E (apoE)⁵² or HCV envelope proteins E1 and E2 and HSPGs^{53, 54}. Especially Syndecan 1 and Syndecan 4 have shown to be important attachment receptors for HCV on the surface of hepatocytes thereby facilitating infection^{36, 37}. We observed that of the different members of the Syndecan family, Syndecan 4 exclusively transmitted HCV to target cells, which was abrogated when HCV was exposed to unfractionated heparin or LMW heparins. Also, culturing Syndecan 4 cells in the presence of a heparan sulfate biosynthesis inhibitor PNP-Xyl^{55, 56, 57, 58} dose-dependently decreased HCV transmission to target cells. These data strongly suggest that the heparan sulfate or proteoglycan backbone of Syndecan 4 is different from the other Syndecans and functions as an important receptor for HCV transmission. Syndecan 4-mediated transmission of HCV was independent of infection as the B cell-line expressing Syndecan 4 was not infected with HCV (data not shown). Previously, we have shown that HCV transmission by activated LCs is also independent of infection¹⁹. Silencing of Syndecan 4 on activated LCs decreased HCV transmission, our data confirms the importance of Syndecan 4 as attachment receptor for HCV on activated LCs, mediating HCV dissemination. In this study we have used the HCV replicon system in Huh7.5 cells to generate replication competent virus particles. In the different models we have used the Huh7.5 cells as target cells for transmission. Several studies have shown that hepatocytes can be infected by replicative HCV suggesting that these cells can also be used. However, primary hepatocytes retain RIG-I which would limit replication and make detection more difficult due to innate antiviral responses. Even though this study is conducted with hepatoma cell lines, Syndecan 4 is also expressed by other cells including primary hepatocytes and thereby its specific ability to transmit HCV might also be involved in virus spread in the liver via hepatocytes *in vivo*.

Activation of LCs strongly increased expression of heparan sulfates and Syndecan 4. These data suggest that Syndecan 4 has an important role in LC function not only for virus capture but also for their mobilization from mucosal sites and subsequent migration to lymphoid tissues. LCs have the ability to migrate from mucosal sites to lymphoid organs to present captured virions to permissive cells^{59, 60, 61}. Syndecans have been shown to play a role in cell

migration and adhesion by mediating interaction of the heparan sulfate chains with various extracellular matrix proteins^{62,63}. Interestingly, *ex vivo* LCs upregulate Syndecan 4 during maturation, which functionally regulates cell motility^{62,64} and our data strongly suggest that *ex vivo* LCs required Syndecan 4 for HCV transmission. Thus, upregulation of Syndecan 4 on LCs might have an important role in cellular function such as migration but is hijacked by HCV to allow dissemination during sexual contact. The retention of HCV by LCs might allow entry of virus into the blood or into lymphoid tissues where LCs might transfer the virus to other cells leading to dissemination to the liver²⁴. Syndecan 4 induction confers activated LCs with the ability to transmit HCV but our data suggest that this is not the only mechanism. Immature LCs express high levels of the CLR langerin, which is downregulated upon activation. Langerin is well known for its restrictive function in HIV-1 dissemination. HIV-1 capture via langerin, leads to TRIM5 α -mediated autophagic degradation of HIV-1, thereby restricting virus transmission^{20,21}. Human TRIM5 α is a host restriction factor that restricts retrovirus infection after fusion⁶⁵ and similarly, in LCs, fusion of HIV-1 triggers TRIM5 α -dependent autophagy restricting HIV-1 infection²¹. Little is known about other viruses that are restricted by langerin. Notably, here we have identified langerin as a restriction factor for HCV infection and transmission.

Ectopic expression of langerin on a HCV susceptible cells decreased infection of both replicative HCV as well as pseudotyped HCV. Pseudotyped HCV consists of the HCV E1 and E2 envelope glycoproteins and the HIV-1 NL4.3 Δ env backbone which could explain routing for TRIM5 α -mediated autophagic degradation²¹. As langerin restriction of HIV-1 depends on TRIM5 α binding to the HIV-1 capsid, it is likely that pseudotyped HCV is restricted via TRIM5 α -mediated autophagy. However, infection of replicative HCV strain was also restricted by langerin strongly suggesting that the restriction by langerin is relevant to HCV but the mechanism of this restriction is still unknown. Recently, it was shown that TRIM5 α restricts specific viruses from the Flaviviridae family via proteosomal degradation⁶⁶, suggesting that other degradation pathways could be involved in langerin-mediated restriction of HCV. Further studies are required to confirm the uptake route for HCV in LCs. Interestingly, langerin also prevented HCV transmission by Syndecan 4-positive cell-lines as well as Mutz-LCs and this transmission is independent of infection. Thus, these data suggest that langerin also restricts transmission of HCV independent of fusion as we have shown previously that HCV does not infect LCs. It is possible that langerin routes HCV into langerin-induced Birbeck granules that prevent transmission or that the virus is degraded via either proteosomal degradation or autophagy, but this has yet to be further investigated.

Our data show that the interplay between Syndecan 4 and langerin on LCs controls the ability to transmit HCV by LCs. Syndecan 4 mediates transmission that is counteracted by langerin. Therefore the expression levels of both proteins are important. Immature LCs expressed low levels of Syndecan 4 whereas these cells express high levels of langerin and this might be important in preventing HCV transmission. In contrast, activation of LCs induced Syndecan 4 expression and simultaneously decreased langerin, suggesting that the

change in expression patterns underlies the ability of activated LCs to transmit HCV. These data suggest that blocking Syndecan 4 function *in vivo* might limit HCV transmission in high risk populations.

Although the availability of highly effective directly acting antivirals (DAA) ¹⁰ created optimism towards HCV elimination, the incidence of acute HCV has not declined consistently due to high reinfection rates amongst MSM ^{11, 12, 13}. Disruption of the mucosal integrity allowing HCV to cross the epithelial barrier to either directly enter the blood stream or indirectly via immune cells may promote sexual transmission of HCV since a sufficient quantity of HCV is shed into the rectum upon sexual contact ⁶⁷. Our data strongly suggest an important role for both langerin and Syndecan 4 in HCV transmission by LCs. Activation of LCs leads to upregulation of Syndecan 4 which counteracts langerin restriction to facilitate viral dissemination after sexual contact. Heparin and LMW heparins could be interesting candidates to protect against sexual transmission of HCV. This concept has been investigated already in the context of other STIs such as HSV-1 and HSV-2, and HPV ^{30, 68, 69, 70}. Interestingly, in the *ex vivo* tissue explant model where LCs reside in their natural microenvironment, blocking heparan sulfate interaction with HCV using heparin resulted in an abrogation of HCV transmission. Further investigation into the role of attachment receptors in HCV transmission would contribute to the understanding of sexual transmission of HCV in MSM.

Materials and Methods

Antibodies and reagents

The following antibodies were used (all anti-human): Heparan Sulfate (clone F58-10E4) (Amsbio), digested Heparan (clone F69-3G10) (Amsbio), Syndecan 1 (DL-101) (Santa Cruz), Syndecan 2-FITC (H-7) (Santa Cruz), Syndecan 3 (M-300) (Santa Cruz), Syndecan 4 (clone F94-8G3), CD207-PE (langerin) mouse IgG1 (#IM3577) (BeckmanCoulter, USA), CD1a-APC mouse IgG1 (BD Biosciences, San Jose, CA, USA) CD1a-PE (clone SK9) mouse IgG2b (BD Bioscience), HLA-B27-FITC (clone HLA-ABC-m3), mouse IgG2a (Abcam), HLA-DR-FITC (clone G46-6), mouse IgG2b (BD Bioscience), CD80-PE, mouse IgG1 (BD Pharmingen), CD83-PE, mouse IgG1 (eBioscience), CD86-FITC, mouse IgG1 (BD Pharmingen), FITC-conjugated goat-anti-mouse IgM (#31992) (Invitrogen), AF488-conjugated goat-anti-mouse IgG1 (#A21121) (Invitrogen), AF488-conjugated donkey-anti-mouse IgG2b (Invitrogen).

The following reagents were used: Unfractionated (UF) heparin, 5.000 I.E./ml (LEO). Low Molecular Weight (LMW) heparins: dalteparin, 10.000 IE anti-Xa/ml (Pfizer), tinzaparin, 10.000 IE anti-X1/0.5ml (LEO), enoxaparin, 100 mg/ml (Sanofi). 4-Nitrophenyl β -D-xylopyranoside (PNP-Xyl, 2001-96-9) (SigmaAldrich). Heparinase III from *Flavobacterium heparium*, EC 4.2.2.8, Batch 010, (Amsbio). 123Count eBeads, REF# 01-1234-42, LOT# E133305, 1.011.000 eBeads/ml (eBioscience).

Plasmids and Viruses

The following plasmids were provided by Dr. Takaji Wakita at Tokyo Metropolitan Institute of Neuroscience: Genotype 2a HCV genomic RNA clone pJFH1 (APP1025)⁷¹, pNL4.3.Luc_Δenv provided by Dr. N.R. Landau⁷², pHCV_H77_E1_E2(AF009606) Dr. Joe Grove (Addgene)⁷³. For single-round infection assay, human embryonic kidney 293T/17 cells (ATCC, CRL-11268) were co-transfected with pNL4.3.Luc_Δenv, containing firefly luciferase gene at the *nef* position (1.35ug) and genotype 1a pHCV_H77_E1_E2(AF009606) (0.6ug). Transfection was performed in 293T/17 cells using genejuice (Novagen, USA) transfection kit according to manufacturer's protocol. At day 3 or day 4, pseudotyped HCV virus particles were harvested and filtered over 0.45 μm nitrocellulose membrane (SartoriusStedim, Gottingen, Germany). Replicative JFH1-AM120-Rluc *in vitro* transcribed RNA, containing a luciferase reporter gene, was generated according to manufacturer's instructions (Ambion MEGAscript-kit, ThermoFisher, USA) and electroporated into Huh7.5 cells as previously described⁷⁴. Virus particles were harvested on day 8 and, TCID50s were determined. The TCID50 of HCV ranged from 2 x10³ to 4x10³.

Cell lines

The human B cell line Namalwa (ATCC, CRL-1432) and Namalwa cells stably expressing human Syndecan 1, Syndecan 2, Syndecan 3, Syndecan 4 (described earlier, laboratory Prof. Zimmermann⁷⁵) were maintained in RPMI 1640 medium (Gibco Life Technologies, Gaithersburg, Md.) containing 10% fetal calf serum (FCS). The expression of the different Syndecans was validated by flow cytometry using core protein-specific antibodies directed against the different Syndecans. Huh7.5 (human hepatocellular carcinoma) cell line were provided by dr. Charles M. Rice⁷⁶. Cells were maintained in Dulbecco modified Eagle medium (Gibco Life Technologies, Gaithersburg, Md.) containing 10% fetal calf serum (FCS) and penicillin/streptomycin. Medium was supplemented with 1mM HEPES buffer (Gibco Life Technologies, Gaithersburg, Md.). Mutz-LCs were differentiated from CD34⁺ human AML cell line Mutz3 progenitors in the presence of GM-CSF (100 ng/ml, Invitrogen), TGF-β (10 ng/ml, R&Dsystems) and TNF-α (2.5 ng/ml), R&Dsystems) and cultured as described before³⁹. Cell surface expression of heparan sulfates and Syndecan 4 on Mutz-LCs was verified by flow cytometry using antibodies directed against CD1a, CD207 and respectively heparan sulfate or Syndecan 4. Flow cytometric analyses were performed on a BD FACS Canto II (BD Biosciences). Data was analyzed using FlowJo vX.0.7 software (TreeStar).

Huh7.5 and Namalwa cell line langerin transduction

Langerin expression plasmid pcDNA3.1 were obtained from Life Technologies and subcloned into lentiviral construct pWPXLd (Addgene). HIV-1-based lentiviruses were

produced by co-transfection of 293T cells with the lentiviral vector construct, the packaging construct (pPAX2, Addgene) and vesicular stomatitis virus glycoprotein envelope (pMD2.G, Addgene) as described previously⁷⁷. Huh7.5 cell line or Namalwa Syndecan 4 cell line were transduced with HIV-1-based lentiviruses expressing sequences coding human wild-type langerin. Subsequently cells were sorted using a FACS Aria (BD) based on CD207-PE mouse IgG1 (#IM3577). Ectopic expression of langerin was confirmed by flow cytometry.

***Ex vivo* model and primary LC isolation**

Epidermal sheets were prepared as described previously^{20, 38}. Briefly, skin-grafts were obtained using a dermatome (Zimmer Biomet, Indiana USA). After incubation with Dispase II (1 U/ml, Roche Diagnostics), epidermal sheets were separated from dermis, washed, cut in 1 cm² and cultured in Iscoves Modified Dulbeccos's Medium (IMDM, Thermo Fischer Scientific, USA) supplemented with 10% FCS, gentamicin (20 µg/ml, Centrafarm, Netherlands), penicillin/streptomycin (10 U/ml and 10 µg/ml, respectively; Invitrogen). Activated LCs were generated as described before²⁰. Briefly, obtained epidermal sheets were separated from dermis, washed and cultured in IMDM (Thermo Fischer Scientific, USA) supplemented with 10% FCS, gentamicin (20 µg/ml, Centrafarm, Netherlands), penicillin/streptomycin (10 U/ml and 10 µg/ml, respectively; Invitrogen) for 3 days and activated LCs were harvested. Immature LC-enriched epidermal single-cell suspensions were generated as described before^{20, 38}. Briefly, epidermal sheets were incubating in PBS containing DNase I (20 units/ml; Roche Applied Science) and trypsin 0.05% (Beckton Dickinson, USA). Single-cell suspension was layered on Ficoll gradient (Axis-shield) and immature LCs were purified using CD1a microbeads (Miltenyi Biotec, Germany). LCs were routinely 85% to 98% pure and expressed high levels of Langerin and CD1a²². Cell surface expression of heparan sulfates on primary LCs was verified by flow cytometry using antibodies directed against CD207 (langerin) and CD1a and heparan sulfates for immature LCs and CD1a and heparan sulfates for activated LCs.

Transmission assays and co-culture

Namalwa cell line (1.0x10⁶ cells/ml, 100ul per well) or Namalwa Syndecan 1-4 cell line (1.0x10⁶ cells/ml, 100ul per well) or immature LCs (8.0x10⁵ cells/ml and 1.0x10⁶ cells/ml LCs, 100ul per well) or activated LCs (1.0x10⁶ cells/ml LCs, 100ul per well) were exposed to replicative HCV genotype 2a strain containing a luciferase reporter gene (JFH1-AM120-Rluc) or pseudotyped HCV (HIV-1 NL4.3Δenv pseudotyped with HCV env glycoproteins E1 and E2) pre-incubated with 250U or 500U UF heparin or LMW heparins either for 4 or 24 hours, harvested, extensively washed to remove unbound virus and co-cultured with Huh7.5 for 3 or 5 days at 37°C and analyzed for luciferase reporter activity. Luciferase activity (relative light units (R.L.U.)) was measured using the Luciferase assay system (Promega, USA) or

Reporter gene assay system (Britelite plus, PerkinElmer) according to manufacturer's instructions. For the *ex vivo* transmission model epidermal sheets were culture for 24 hours and exposed to medium or UF heparin pre-incubated replicative HCV or pseudotyped HCV for another 24 hours. After 48 hours cells were harvested, extensively washed to remove unbound virus and co-cultured with Huh7.5 for 5 days at 37°C, transmission was determined by luciferase reporter activity. Luciferase activity (relative light units (R.L.U.)) was measured using the Luciferase assay system (Promega, USA) or Reporter gene assay system (Britelite plus, PerkinElmer) according to manufacturer's instructions.

RNA interference

MUTZ-LCs and primary LCs were silenced by electroporation with Neon Transfection System (ThermoFischer Scientific). The siRNA were specific for langerin (10 μM siRNA, M-013059-01, SMARTpool; Dharmacon), siRNA Syndecan 4 (10 μM siRNA, M-003706-01-0005, SMARTpool; Dharmacon) or non-targeting siRNA (D-001206-13, SMARTpool; Dharmacon) as control. Silencing of the targets was verified by real-time PCR, flow cytometry. Cells were used for experiment 72 hours after silencing. Silencing of the targets was verified by real-time PCR or flow cytometry.

RNA isolation and quantitative real-time PCR

mRNA was isolated with an mRNA Capture kit (Roche) and cDNA was synthesized with a reverse-transcriptase kit (Promega) and PCR amplification was performed in the presence of SYBR green in a 7500 Fast Realtime PCR System (ABI). Specific primers were designed with Primer Express 2.0 (Applied Biosystems). Primer sequences used for mRNA expression were for gene product: GAPDH, forward primer (CCATGTTTCGTCATGGGTGTG), reverse primer (GGTGCTAA GCAGTTGGTGGTG). For gene product: langerin, forward primer (CACAGTGGCATTCTGGAGTCC), reverse primer (CCACCCCTCCCACTTTAACC). For gene product: Syndecan 4, forward primer (AGGTGTCAATGTCCAGCACTGTG) reverse primer (AGCAGTAGGATCAGGAAGACGGC). The normalized amount of target mRNA was calculated from the Ct values obtained for both target and household mRNA with the equation $Nt = 2^{Ct(GAPDH) - Ct(target)}$. For relative mRNA expression, control siRNA sample was set at 1 for each donor.

Biosynthesis inhibition and enzymatic treatment

Namalwa Syndecan 4 cell line were cultured in the presence of 1.0mM or 2.5mM PNP-Xyl for 72 hours to inhibit HSPG biosynthesis and used in subsequent experiments. The expression of cell surface heparan sulfates was assessed by flow cytometry using antibodies directed against heparan sulfates. 1.0×10^6 cells/ml were treated in D-PBS/0.25% BSA with

140 miliunits heparinase III (Amsbio) for 2 hours at 25°C, washed and used in subsequent experiments. Enzymatic digestion was verified by flow cytometry using antibodies directed against heparan sulfates and digested heparan sulfates.

Statistics

A two-tailed, parametric Student's *t*-test for paired observations (differences within the same donor) or unpaired observation (differences between different donors) was performed. For unpaired, non-parametric observations a Mann-Whitney test was performed. Statistical analyses were performed using GraphPad Prism 7 software and significance was set at * $P < 0.05$, ** $P < 0.01$ *** $P < 0.001$ **** $P < 0.0001$.

Study approval

Human skin tissue was obtained from healthy donors undergoing corrective abdominal surgery in accordance with our institutional guidelines. This study was approved by the Medical Ethics Review Committee of the Amsterdam University Medical Centers, location Academic Medical Center (AMC), Amsterdam, the Netherlands, reference number: W15_089 # 15.0103. All samples were handled anonymously.

Author Contributions

B.M.N. performed and designed the research study, analyzed the data, wrote the paper. J.E. performed the research study and analyzed the data. C.J.M.L. performed the research study and analyzed the data. T.K. performed the research study. S.M. contributed essential material. P.Z. contributed essential material. C.M.S.R. designed the research study and contributed essential material. T.B.H.G. was involved in all aspects of the study. All authors contributed to the manuscript, read and approved the submitted version.

Funding

This work was supported by Aidsfonds [P-11118], European Research Council, Advanced grant [670424] and Dutch Scientific organization NWO [VIDI 91718331]. The funders had no role in study design, data collection and analysis, decision to publish, or preparation of the manuscript.

Conflict of interest

All authors declare that they have no competing interests.

Acknowledgments

We are grateful to the Boerhaave Medical Centre (Amsterdam, The Netherlands) and A. Knottenbelt (Flevo clinic Almere, The Netherlands) for the provision of human skin tissues.

References

1. WHO, W.H.O. Global hepatitis report, 2017; 2017 19 April 2017. Report No.: Licens CC BY-NA-SA 30IGO. 2017;67. .
2. Wandeler, G., Dufour, J.F., Bruggmann, P. & Rauch, A. Hepatitis C: a changing epidemic. *Swiss Med Wkly* **145**, w14093 (2015).
3. Jordan, A.E. *et al.* Prevalence of hepatitis C virus infection among HIV+ men who have sex with men: a systematic review and meta-analysis. *Int J STD AIDS* **28**, 145-159 (2017).
4. Danta, M. *et al.* Recent epidemic of acute hepatitis C virus in HIV-positive men who have sex with men linked to high-risk sexual behaviours. *Aids* **21**, 983-991 (2007).
5. Matthews, G.V., Hellard, M., Kaldor, J., Lloyd, A. & Dore, G.J. Further evidence of HCV sexual transmission among HIV-positive men who have sex with men: response to Danta *et al.* *Aids* **21**, 2112-2113 (2007).
6. CDC. Sexual transmission of hepatitis C virus among HIV-infected men who have sex with men--New York City, 2005-2010. *MMWR Morb Mortal Wkly Rep* **60**, 945-950 (2011).
7. van de Laar, T.J., Matthews, G.V., Prins, M. & Danta, M. Acute hepatitis C in HIV-infected men who have sex with men: an emerging sexually transmitted infection. *Aids* **24**, 1799-1812 (2010).
8. van de Laar, T.J. *et al.* Increase in HCV incidence among men who have sex with men in Amsterdam most likely caused by sexual transmission. *J Infect Dis* **196**, 230-238 (2007).
9. Danta, M. & Rodger, A.J. Transmission of HCV in HIV-positive populations. *Curr Opin HIV AIDS* **6**, 451-458 (2011).
10. Naggie, S. *et al.* Ledipasvir and Sofosbuvir for HCV in Patients Coinfected with HIV-1. *N Engl J Med* **373**, 705-713 (2015).
11. Hagan, H., Jordan, A.E., Neurer, J. & Cleland, C.M. Incidence of sexually transmitted hepatitis C virus infection in HIV-positive men who have sex with men. *Aids* **29**, 2335-2345 (2015).
12. Lambers, F.A. *et al.* Alarming incidence of hepatitis C virus re-infection after treatment of sexually acquired acute hepatitis C virus infection in HIV-infected MSM. *Aids* **25**, F21-27 (2011).
13. Ingiliz, P. *et al.* HCV reinfection incidence and spontaneous clearance rates in HIV-positive men who have sex with men in Western Europe. *J Hepatol* **66**, 282-287 (2017).
14. Wandeler, G. *et al.* Hepatitis C virus infections in the Swiss HIV Cohort Study: a rapidly evolving epidemic. *Clin Infect Dis* **55**, 1408-1416 (2012).
15. van de Laar, T.J., Paxton, W.A., Zorgdrager, F., Cornelissen, M. & de Vries, H.J. Sexual transmission of hepatitis C virus in human immunodeficiency virus-negative men who have sex with men: a series of case reports. *Sex Transm Dis* **38**, 102-104 (2011).
16. Volk, J.E., Marcus, J.L., Phengrasamy, T. & Hare, C.B. Incident Hepatitis C Virus Infections Among Users of HIV Preexposure Prophylaxis in a Clinical

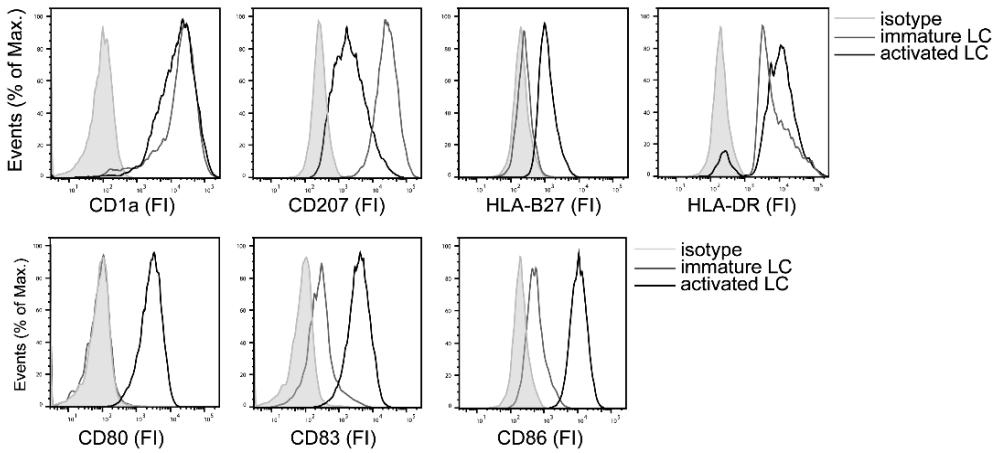
- Practice Setting. *Clin Infect Dis* **60**, 1728-1729 (2015).
17. McFaul, K. *et al.* Acute hepatitis C infection in HIV-negative men who have sex with men. *J Viral Hepat* **22**, 535-538 (2015).
 18. Schmidt, A.J. *et al.* Trouble with bleeding: risk factors for acute hepatitis C among HIV-positive gay men from Germany--a case-control study. *PLoS One* **6**, e17781 (2011).
 19. Nijmeijer, B.M. *et al.* HIV-1 exposure and immune activation enhance sexual transmission of Hepatitis C virus by primary Langerhans cells. *J Int AIDS Soc* **22**, e25268 (2019).
 20. de Witte, L. *et al.* Langerin is a natural barrier to HIV-1 transmission by Langerhans cells. *Nat Med* **13**, 367-371 (2007).
 21. Ribeiro, C.M. *et al.* Receptor usage dictates HIV-1 restriction by human TRIM5 α in dendritic cell subsets. *Nature* **540**, 448-452 (2016).
 22. de Jong, M.A. *et al.* TNF-alpha and TLR agonists increase susceptibility to HIV-1 transmission by human Langerhans cells *ex vivo*. *J Clin Invest* **118**, 3440-3452 (2008).
 23. Preza, G.C. *et al.* Antigen-presenting cell candidates for HIV-1 transmission in human distal colonic mucosa defined by CD207 dendritic cells and CD209 macrophages. *AIDS Res Hum Retroviruses* **30**, 241-249 (2014).
 24. Nijmeijer, B.M., Koopsen, J., Schinkel, J., Prins, M. & Geijtenbeek, T.B. Sexually transmitted hepatitis C virus infections: current trends, and recent advances in understanding the spread in men who have sex with men. *J Int AIDS Soc* **22 Suppl 6**, e25348 (2019).
 25. de Witte, L. *et al.* Syndecan-3 is a dendritic cell-specific attachment receptor for HIV-1. *Proc Natl Acad Sci U S A* **104**, 19464-19469 (2007).
 26. Bobardt, M.D. *et al.* Syndecan captures, protects, and transmits HIV to T lymphocytes. *Immunity* **18**, 27-39 (2003).
 27. Prydz, K. & Dalen, K.T. Synthesis and sorting of proteoglycans. *J Cell Sci* **113 Pt 2**, 193-205 (2000).
 28. Saunders, S., Jalkanen, M., O'Farrell, S. & Bernfield, M. Molecular cloning of syndecan, an integral membrane proteoglycan. *J Cell Biol* **108**, 1547-1556 (1989).
 29. Couchman, J.R. Syndecans: proteoglycan regulators of cell-surface microdomains? *Nat Rev Mol Cell Biol* **4**, 926-937 (2003).
 30. Tiwari, V., Maus, E., Sigar, I.M., Ramsey, K.H. & Shukla, D. Role of heparan sulfate in sexually transmitted infections. *Glycobiology* **22**, 1402-1412 (2012).
 31. Zhang, Y.J. *et al.* Envelope-dependent, cyclophilin-independent effects of glycosaminoglycans on human immunodeficiency virus type 1 attachment and infection. *J Virol* **76**, 6332-6343 (2002).
 32. De Francesco, M.A., Baronio, M. & Poesi, C. HIV-1 p17 matrix protein interacts with heparan sulfate side chain of CD44v3, syndecan-2, and syndecan-4 proteoglycans expressed on human activated CD4+ T cells affecting tumor necrosis factor alpha and interleukin 2 production. *J Biol Chem* **286**, 19541-

- 19548 (2011).
33. Karasneh, G.A., Ali, M. & Shukla, D. An important role for syndecan-1 in herpes simplex virus type-1 induced cell-to-cell fusion and virus spread. *PLoS One* **6**, e25252 (2011).
 34. Shukla, D. & Spear, P.G. Herpesviruses and heparan sulfate: an intimate relationship in aid of viral entry. *J Clin Invest* **108**, 503-510 (2001).
 35. Johnson, K.M. *et al.* Role of heparan sulfate in attachment to and infection of the murine female genital tract by human papillomavirus. *J Virol* **83**, 2067-2074 (2009).
 36. Shi, Q., Jiang, J. & Luo, G. Syndecan-1 serves as the major receptor for attachment of hepatitis C virus to the surfaces of hepatocytes. *J Virol* **87**, 6866-6875 (2013).
 37. Lefèvre, M., Felmler, D.J., Parnot, M., Baumert, T.F. & Schuster, C. Syndecan 4 is involved in mediating HCV entry through interaction with lipoviral particle-associated apolipoprotein E. *PLoS One* **9**, e95550 (2014).
 38. Sarrami-Forooshani, R. *et al.* Human immature Langerhans cells restrict CXCR4-using HIV-1 transmission. *Retrovirology* **11**, 52 (2014).
 39. de Jong, M.A. *et al.* Mutz-3-derived Langerhans cells are a model to study HIV-1 transmission and potential inhibitors. *J Leukoc Biol* **87**, 637-643 (2010).
 40. Hoornenborg, E. *et al.* MSM starting preexposure prophylaxis are at risk of hepatitis C virus infection. *Aids* **31**, 1603-1610 (2017).
 41. Cotte, L. *et al.* Hepatitis C virus incidence in HIV-infected and in preexposure prophylaxis (PrEP)-using men having sex with men. *Liver Int* (2018).
 42. Charre, C. *et al.* Hepatitis C virus spread from HIV-positive to HIV-negative men who have sex with men. *PLoS One* **13**, e0190340 (2018).
 43. Bartlett, A.H. & Park, P.W. Proteoglycans in host-pathogen interactions: molecular mechanisms and therapeutic implications. *Expert Rev Mol Med* **12**, e5 (2010).
 44. Mondor, I., Ugolini, S. & Sattentau, Q.J. Human immunodeficiency virus type 1 attachment to HeLa CD4 cells is CD4 independent and gp120 dependent and requires cell surface heparans. *J Virol* **72**, 3623-3634 (1998).
 45. Shieh, M.T., WuDunn, D., Montgomery, R.I., Esko, J.D. & Spear, P.G. Cell surface receptors for herpes simplex virus are heparan sulfate proteoglycans. *J Cell Biol* **116**, 1273-1281 (1992).
 46. de Witte, L. *et al.* Binding of human papilloma virus L1 virus-like particles to dendritic cells is mediated through heparan sulfates and induces immune activation. *Immunobiology* **212**, 679-691 (2007).
 47. Compton, T., Nowlin, D.M. & Cooper, N.R. Initiation of human cytomegalovirus infection requires initial interaction with cell surface heparan sulfate. *Virology* **193**, 834-841 (1993).
 48. Summerford, C. & Samulski, R.J. Membrane-associated heparan sulfate proteoglycan is a receptor for adeno-associated virus type 2 virions. *J Virol* **72**, 1438-1445 (1998).

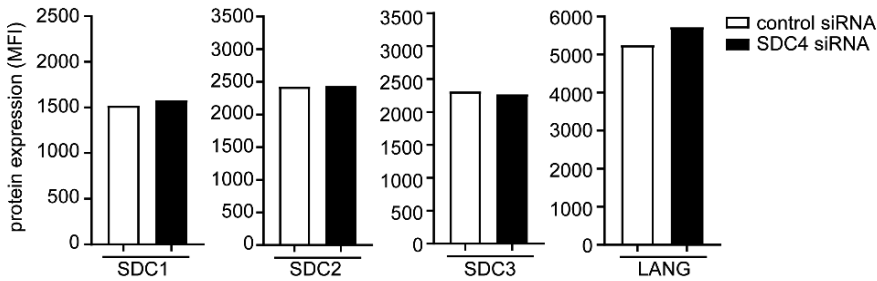
49. Chen, Y. *et al.* Dengue virus infectivity depends on envelope protein binding to target cell heparan sulfate. *Nat Med* **3**, 866-871 (1997).
50. Chung, C.S., Hsiao, J.C., Chang, Y.S. & Chang, W. A27L protein mediates vaccinia virus interaction with cell surface heparan sulfate. *J Virol* **72**, 1577-1585 (1998).
51. Saphire, A.C., Bobardt, M.D., Zhang, Z., David, G. & Gallay, P.A. Syndecans serve as attachment receptors for human immunodeficiency virus type 1 on macrophages. *J Virol* **75**, 9187-9200 (2001).
52. Xu, Y. *et al.* Characterization of hepatitis C virus interaction with heparan sulfate proteoglycans. *J Virol* **89**, 3846-3858 (2015).
53. Barth, H. *et al.* Cellular binding of hepatitis C virus envelope glycoprotein E2 requires cell surface heparan sulfate. *J Biol Chem* **278**, 41003-41012 (2003).
54. Germe, R. *et al.* Cellular glycosaminoglycans and low density lipoprotein receptor are involved in hepatitis C virus adsorption. *J Med Virol* **68**, 206-215 (2002).
55. Okayama, M., Kimata, K. & Suzuki, S. The influence of p-nitrophenyl beta-D-xyloside on the synthesis of proteochondroitin sulfate by slices of embryonic chick cartilage. *J Biochem* **74**, 1069-1073 (1973).
56. Schwartz, N.B., Galligani, L., Ho, P.L. & Dorfman, A. Stimulation of synthesis of free chondroitin sulfate chains by beta-D-xylosides in cultured cells. *Proc Natl Acad Sci U S A* **71**, 4047-4051 (1974).
57. Morriss-Kay, G.M. & Crutch, B. Culture of rat embryos with beta-D-xyloside: evidence of a role for proteoglycans in neurulation. *J Anat* **134**, 491-506 (1982).
58. Thompson, H.A. & Spooner, B.S. Proteoglycan and glycosaminoglycan synthesis in embryonic mouse salivary glands: effects of beta-D-xyloside, an inhibitor of branching morphogenesis. *J Cell Biol* **96**, 1443-1450 (1983).
59. Kissenpfennig, A. *et al.* Dynamics and function of Langerhans cells in vivo: dermal dendritic cells colonize lymph node areas distinct from slower migrating Langerhans cells. *Immunity* **22**, 643-654 (2005).
60. Niedecken, H., Lutz, G., Bauer, R. & Kreysel, H.W. Langerhans cell as primary target and vehicle for transmission of HIV. *Lancet* **2**, 519-520 (1987).
61. Kawamura, T., Kurtz, S.E., Blauvelt, A. & Shimada, S. The role of Langerhans cells in the sexual transmission of HIV. *J Dermatol Sci* **40**, 147-155 (2005).
62. Midwood, K.S., Valenick, L.V., Hsia, H.C. & Schwarzbauer, J.E. Coregulation of fibronectin signaling and matrix contraction by tenascin-C and syndecan-4. *Mol Biol Cell* **15**, 5670-5677 (2004).
63. Saoncella, S. *et al.* Syndecan-4 signals cooperatively with integrins in a Rho-dependent manner in the assembly of focal adhesions and actin stress fibers. *Proc Natl Acad Sci U S A* **96**, 2805-2810 (1999).
64. Averbek, M. *et al.* Switch in syndecan-1 and syndecan-4 expression controls maturation associated dendritic cell motility. *Exp Dermatol* **16**, 580-589 (2007).
65. Stremlau, M. *et al.* Specific recognition

- and accelerated uncoating of retroviral capsids by the TRIM5 α restriction factor. *Proc Natl Acad Sci U S A* **103**, 5514-5519 (2006).
66. Chiramel, A.I. *et al.* TRIM5 α Restricts Flavivirus Replication by Targeting the Viral Protease for Proteasomal Degradation. *Cell Rep* **27**, 3269-3283.e3266 (2019).
67. Foster, A.L. *et al.* Shedding of Hepatitis C Virus Into the Rectum of HIV-infected Men Who Have Sex With Men. *Clin Infect Dis* **64**, 284-288 (2017).
68. Christensen, N.D. *et al.* Papillomavirus microbicidal activities of high-molecular-weight cellulose sulfate, dextran sulfate, and polystyrene sulfonate. *Antimicrob Agents Chemother* **45**, 3427-3432 (2001).
69. Gandhi, N.S. & Mancera, R.L. Heparin/heparan sulphate-based drugs. *Drug Discov Today* **15**, 1058-1069 (2010).
70. Nyberg, K. *et al.* The low molecular weight heparan sulfate-mimetic, PI-88, inhibits cell-to-cell spread of herpes simplex virus. *Antiviral Res* **63**, 15-24 (2004).
71. Kato, T. *et al.* Sequence analysis of hepatitis C virus isolated from a fulminant hepatitis patient. *J Med Virol* **64**, 334-339 (2001).
72. Connor, R.I., Chen, B.K., Choe, S. & Landau, N.R. Vpr is required for efficient replication of human immunodeficiency virus type-1 in mononuclear phagocytes. *Virology* **206**, 935-944 (1995).
73. Kolykhalov, A.A. *et al.* Transmission of hepatitis C by intrahepatic inoculation with transcribed RNA. *Science* **277**, 570-574 (1997).
74. Liu, S., Xiao, L., Nelson, C. & Hagedorn, C.H. A cell culture adapted HCV JFH1 variant that increases viral titers and permits the production of high titer infectious chimeric reporter viruses. *PLoS One* **7**, e44965 (2012).
75. Zhang, Z., Coomans, C. & David, G. Membrane heparan sulfate proteoglycan-supported FGF2-FGFR1 signaling: evidence in support of the "cooperative end structures" model. *J Biol Chem* **276**, 41921-41929 (2001).
76. Lindenbach, B.D. *et al.* Complete replication of hepatitis C virus in cell culture. *Science* **309**, 623-626 (2005).
77. Arrighi, J.F. *et al.* DC-SIGN-mediated infectious synapse formation enhances X4 HIV-1 transmission from dendritic cells to T cells. *J Exp Med* **200**, 1279-1288 (2004).

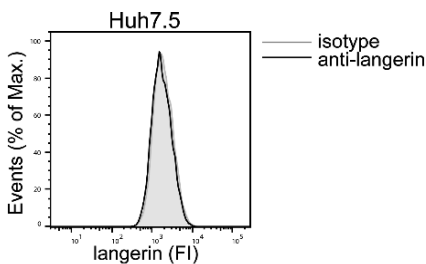
Supplementary material



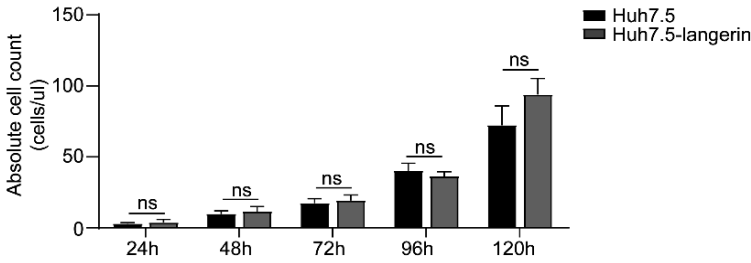
Supplementary Figure S1 | LCs downregulated langerin and upregulate activation markers upon activation. Immature and activated LCs from the same donor were isolated and stained with antibodies against CD2a, CD207, HLA-B27, CD80, CD83, CD86. Surface expression was determined by flow cytometry. One representative donor is depicted. LC: Langerhans cell, FI: fluorescent intensity



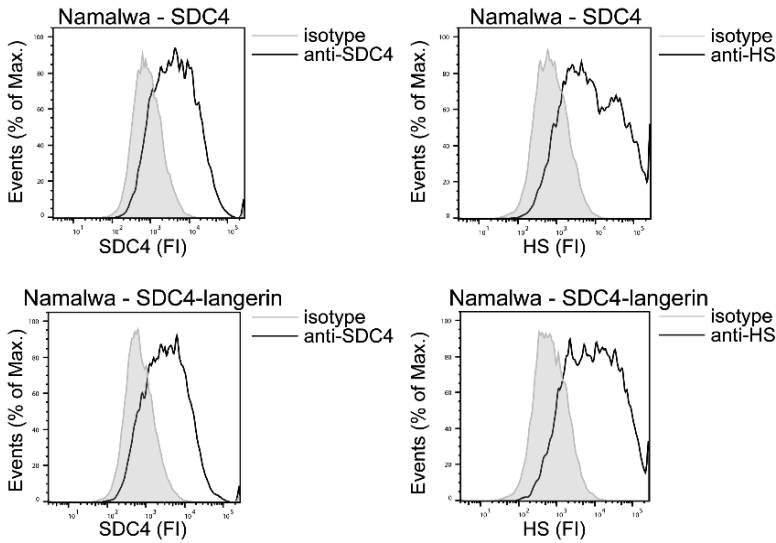
Supplementary Figure S2 | Syndecans and langerin expression on activated LCs after silencing. Activated LCs were transfected with non-target control or Syndecan 4 siRNA and after 72 hours cell surface expression of relevant markers was determined by flow cytometry. One representative donor is depicted. MFI: mean fluorescent intensity, SDC1: Syndecan 1, SDC2: Syndecan 2, SDC3: Syndecan 3, SDC4: Syndecan 4, LANG: Langerin



Supplementary Figure S3 | The Huh7.5 cell lines does not express langerin. Huh7.5 cells were stained with an antibody against langerin and surface expression was determined by flow cytometry. One representative experiment is depicted. FI: fluorescent intensity



Supplementary Figure S4 | Huh7.5 and Huh7.5-langerin cell lines exhibit similar growth. 5.0×10^4 cells/ml were seeded and after T=24h, T=48h, T=72h, T=96h and T=120h harvested, incubated with counting beads and absolute cell count was assessed by flow cytometry. One representative experiment measured in quadruplicate is depicted. Ns = not significant by two-tailed, unpaired, parametric, Student t-test



Supplementary Figure S5 | HS and SDC4 expression on the SDC4 cell line is not altered after langerin transduction. SDC4 cell line without langerin or transduced with lentiviruses expressing sequences coding human langerin were stained with antibodies against HS or SDC4 and surface expression was determined by flow cytometry. One experiment is depicted. FI: fluorescent intensity, HS: Heparan sulfate, SDC4: Syndecan 4



CHAPTER

6

Infection and transmission of SARS-CoV-2 depend on heparan sulfate proteoglycans

Julia Eder^{1*}, Marta Bermejo-Jambrina^{1*}, Tanja M. Kaptein¹, John L. van Hamme¹, Leanne C. Helgers¹, Killian E. Vlaming¹, Philip J.M. Brouwer², Ad C. van Nuenen¹, Marcel Spaargaren³, Godelieve J. de Bree⁴, Bernadien M. Nijmeijer¹, Neeltje A. Kootstra¹, Marit J. van Gils², Rogier W. Sanders^{2,5}, Teunis B. H. Geijtenbeek¹

¹Department of Experimental Immunology, Amsterdam institute for Infection and Immunity, Amsterdam University Medical Centers, University of Amsterdam, Meibergdreef 9, Amsterdam, The Netherlands.

²Department of Medical Microbiology, Amsterdam institute for Infection and Immunity, Amsterdam University Medical Centers, University of Amsterdam, Meibergdreef 9, Amsterdam, The Netherlands.

³Department of Pathology, Lymphoma and Myeloma Center Amsterdam (LYMMCARE), Cancer Center Amsterdam (CCA), Amsterdam University Medical Centers, University of Amsterdam, Meibergdreef 9, Amsterdam, The Netherlands.

⁴Department of Internal Medicine, Amsterdam institute for Infection and Immunity, Amsterdam University Medical Centers, University of Amsterdam, Meibergdreef 9, Amsterdam, The Netherlands.

⁵Department of Microbiology and Immunology, Weill Medical College of Cornell University, New York, NY 10021, USA.

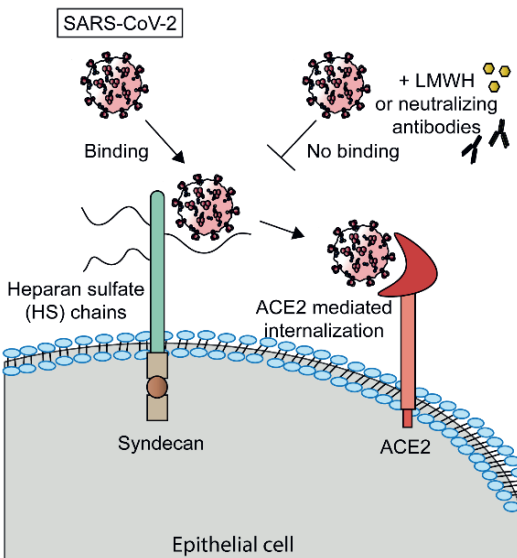
*These authors contributed equally.

*Published in EMBO J. 2021 Oct 18;40(20):e106765.
doi: 10.15252/embj.2020106765. Epub 2021 Sep 23.*

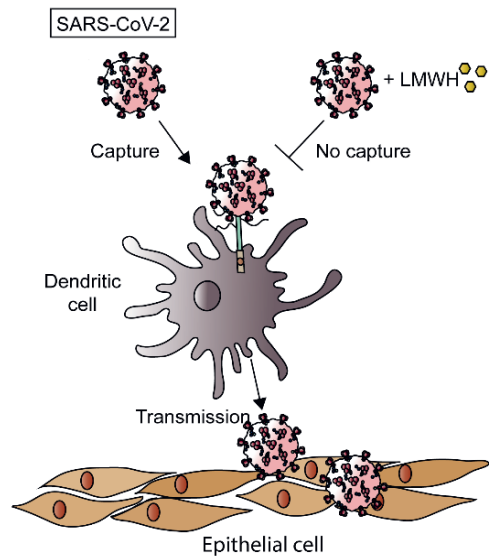
Abstract

The current pandemic caused by severe acute respiratory syndrome coronavirus-2 (SARS-CoV-2) and outbreaks of new variants highlight the need for preventive treatments. Here we identified heparan sulfate proteoglycans as attachment receptors for SARS-CoV-2. Notably, neutralizing antibodies against SARS-CoV-2 isolated from COVID-19 patients interfered with SARS-CoV-2 binding to heparan sulfate proteoglycans, which might be an additional mechanism of antibodies to neutralize infection. SARS-CoV-2 binding to and infection of epithelial cells was blocked by low molecular weight heparins (LMWH). Although dendritic cells (DCs) and mucosal Langerhans cells (LCs) were not infected by SARS-CoV-2, both DC subsets efficiently captured SARS-CoV-2 via heparan sulfate proteoglycans, and transmitted the virus to ACE2-positive cells. Notably, human primary nasal cells were infected by SARS-CoV-2 and infection was blocked by pre-treatment with LMWH. These data strongly suggest that heparan sulfate proteoglycans are important attachment receptors facilitating infection and transmission, and support the use of LMWH as prophylaxis against SARS-CoV-2 infection.

SARS-CoV-2 binds Heparan sulfates (HS) and is blocked by Low molecular weight heparins (LMWH)



SARS-CoV-2 is captured and transmitted by dendritic cells and is blocked by LMWH



Keywords: SARS-CoV-2 / Heparan sulfate proteoglycans / epithelial cells / dendritic cells / low molecular weight heparins

Introduction

Severe acute respiratory syndrome coronavirus 2 (SARS-CoV-2) emerged in Wuhan, China in late 2019 and can cause coronavirus disease 2019 (COVID-19), an influenza-like disease ranging from mild respiratory symptoms to severe lung injury, multi organ failure and death^{1,2,3}. SARS-CoV-2 spread quickly and has caused a pandemic with a severe impact on global health and world economy^{4,5}. SARS-CoV-2 is transmitted predominantly via large droplets expelled from the upper respiratory tract through sneezing and coughing^{6,7} and is subsequently taken up via mucosal surfaces of the nose, mouth and eyes⁸. SARS-CoV-2 infects epithelial cells in the respiratory tract, such as ciliated mucus secreting bronchial epithelial cells and type 1 pneumocytes in the lung, as well as epithelial cells in the gastrointestinal tract^{9,10}. For more than a year lockdown strategies and social distancing have been used to mitigate viral spread but due to negative socioeconomic consequences these are not feasible long-term solutions^{11,12}. Currently, several COVID-19 vaccines have been developed and worldwide vaccination programs have been initiated¹³, which aim to curb and stop the pandemic. However, immunocompromised individuals as well as people on immunosuppressive drugs are potentially less protected by vaccinations^{14,15}. Moreover, current vaccine candidates might be less effective against new SARS-CoV-2 variants^{16,17}. Thus, there is a need for protective strategies specifically targeting SARS-CoV-2 to prevent further dissemination.

SARS-CoV-2 belongs to the betacoronaviruses, a family that also includes SARS-CoV and MERS-CoV¹⁸. The coronavirus Spike (S) protein is a class I fusion protein that mediates virus entry^{19,20}. The S protein consist of two subunits; S1 directly engages via its receptor-binding domain (RBD) with host surface receptors^{21,22} and S2 mediates fusion between virus and cell membrane^{23,24}. SARS-CoV-2 uses angiotensin-converting enzyme 2 (ACE2) as its main receptor^{18,25}. ACE2 is a type I integral membrane protein abundantly expressed on epithelial cells lining the respiratory tract²⁶ but also the ileum, esophagus and liver²⁷ and ACE2 expression dictates SARS-CoV-2 tropism¹⁰. However, it remains unclear whether SARS-CoV2 requires other receptors for virus entry. Neutralizing monoclonal antibodies against SARS-CoV-2 have been identified that are directed not only at the RBD but also outside the RBD²⁸, suggesting that other mechanisms of neutralization or other (co-)receptors might be involved.

Heparan sulfates are expressed by most cells including epithelial cells as heparan sulfate proteoglycans and these have been shown to interact with viruses such as HIV-1, HCV, Sindbis virus and also SARS-CoV^{29,30,31,32,33}. Recently, it was shown that the S protein of SARS-CoV-2 interacts with heparan sulfates, which might be required for infection^{34,35}.

Here we show that the heparan sulfate proteoglycans are important for infection of polarized epithelial cells as well as primary nasal cells with SARS-CoV-2. Infection is inhibited by heparin and low molecular weight heparins (LMWH). Mucosal dendritic cell subsets captured SARS-CoV-2 via heparan sulfate proteoglycans. The different DC subsets did not

become infected but transmitted SARS-CoV-2 to ACE2-positive cells, which might facilitate virus dissemination. Our findings suggest that heparan sulfate proteoglycans function as attachment receptors for SARS-CoV-2 and LMWH can be used as prophylactics against SARS-CoV-2 or prevent dissemination early after infection.

Results

SARS-CoV-2 pseudovirus binds to heparan sulfates expressed by cells.

We incubated Huh7.5 cells that express ACE2 (**Figure EV1A**) with SARS-CoV-2 pseudovirus, which consists of HIV-1 particles pseudotyped with SARS-CoV-2 S protein²⁸. Virus binding was determined by measuring HIV-1 p24 binding by ELISA. SARS-CoV-2 pseudovirus attached to Huh7.5 cells, which was blocked by anti-ACE2 antibodies (anti-ACE2) as well as by neutralizing antibodies from COVID-19 patients²⁸ (**Figure 1A**). Unfractionated (UF) heparin inhibited binding of SARS-CoV-2 pseudovirus to Huh7.5 cells comparable to the neutralizing or anti-ACE2 antibodies (**Figure 1A**). Enzymatic removal of heparan sulfates on the cell surface by Heparinase treatment decreased SARS-CoV-2 virus binding (**Figure 1B** and **Figure EV1B**). Exostosin-1 (EXT1) knockdown decreased expression of heparan sulfates on the cell surface³⁶ (**Figure 1C**). SARS-CoV-2 pseudovirus attached to XG1 cells, which was blocked by UF Heparin, whereas knockdown of EXT1 abrogated SARS-CoV-2 pseudovirus binding (**Figure 1D**). These data suggest that heparan sulfates are important for attachment of SARS-CoV-2 to cells.

Low molecular weight heparins inhibit SARS-CoV-2 infection

To determine the effect of UF Heparin on SARS-CoV-2 infection, we infected Huh7.5 cells with SARS-CoV-2 pseudovirus, expressing the luciferase reporter gene, and determined infection by measuring luciferase reporter activity. UF Heparin blocked infection in a dose-dependent manner (**Figure 2A**). Low molecular weight heparin (LMWH) have replaced UF heparin in the clinic as anti-coagulant treatment due to their smaller size and superior pharmacological properties³⁷. LMWH enoxaparin blocked SARS-CoV-2 pseudovirus infection in a dose dependent manner to similar levels as UF Heparin (**Figure 2A**) without affecting cell viability of Huh7.5 cells (**Figure EV1C**). Not only enoxaparin but also other clinically approved LMWH blocked binding of SARS-CoV-2 pseudovirus to Huh7.5 cells (**Figure 2B**). The different LMWH also blocked infection of Huh7.5 cells with SARS-CoV-2 pseudovirus to a similar extent as enoxaparin (**Figure 2C**).

Next we investigated whether ACE2 is required for infection in presence of heparan sulfates. Human kidney epithelial 293T cells were not susceptible to SARS-CoV-2 pseudovirus whereas ectopic expression of ACE2 rendered these cells susceptible to SARS-CoV-2

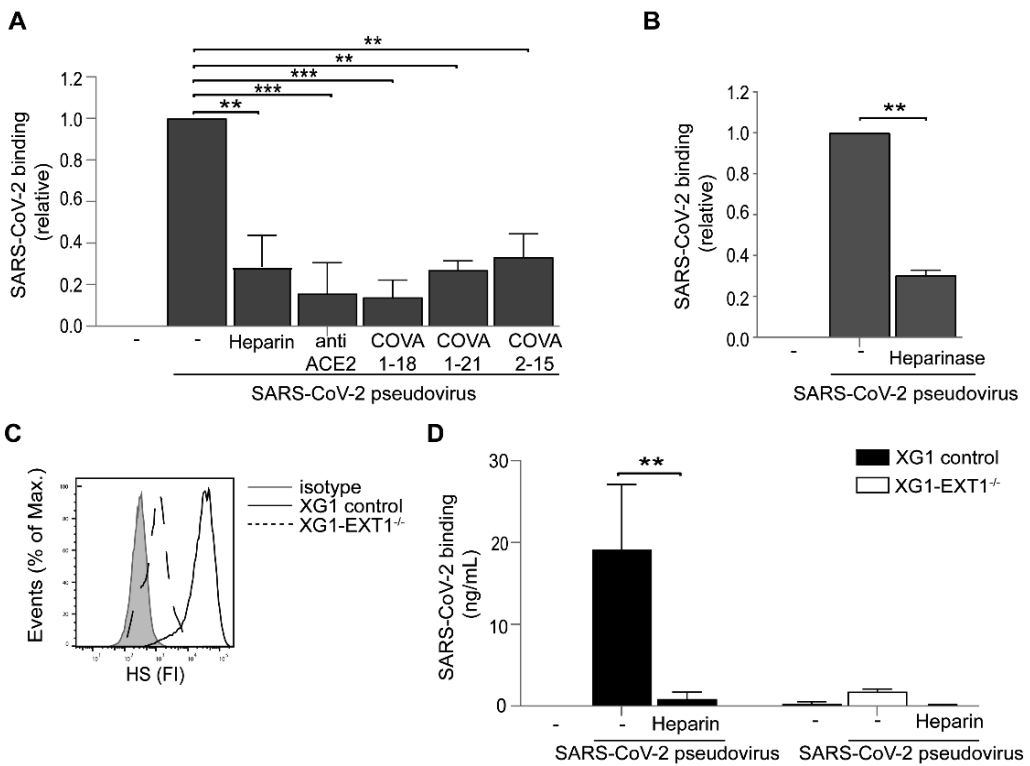


Figure 1 | SARS-CoV-2 pseudovirus binds to heparan sulfates. (A) Huh7.5 cells were pre-incubated with neutralizing antibody to ACE2 and SARS-CoV-2 pseudovirus was pre-incubated with patient isolated mAb COVA1-18, COVA1-21 and COVA2-15 (10 μ g/mL) or UF heparin (250 IU/mL) for 30 min at 37°C. SARS-CoV-2 pseudovirus alone or with blocks was added to the cells for 4h at 4°C and binding was determined by ELISA. (B) Heparan sulfates were removed from Huh7.5 cells by enzymatic treatment with heparinase III for 1 hour at 37°C, then washed, and exposed to SARS-CoV-2 pseudovirus for 4h at 4°C. Treated and untreated cells were subsequently lysed and binding was determined by ELISA. (C) Flow cytometry analysis of cell surface expression of heparan sulfates (HS) in control transduced cells or upon CRISPR/Cas9-mediated EXT1 KO (EXT1^{-/-}). (D) Control and EXT1^{-/-} XG1 cells were exposed to SARS-CoV-2 pseudovirus or SARS-CoV-2 pseudovirus pre-treated with 250 IU/mL UF heparin for 30 min at 37°C. After incubation for 4h at 4°C, cells were lysed and binding was measured by ELISA. Data information: Data show the mean values and error bars are the SEM. Statistical analysis was performed using (A) ordinary one-way ANOVA with Tukey multiple-comparison test. * $P \leq 0.05$, ** $P \leq 0.01$, *** $P \leq 0.001$ (n=3), (B) unpaired Student's t-test with Welch's correction. * $P \leq 0.05$, ** $P \leq 0.01$ (n=3), (D) two-way ANOVA with Dunnett's multiple-comparison test. * $P \leq 0.05$, ** $P \leq 0.01$ (n=3).

pseudovirus (**Figure 2D** and **Figure EV1D** and **EV1E**). Infection was abrogated by both LMWH enoxaparin and UF heparin to a similar level as antibodies against ACE2 (**Figure 2D**). The combination of ACE2 antibodies and LMWH enoxaparin or UF heparin blocked infection of 293T-ACE2 cells (**Figure 2D**). These data suggest that heparan sulfates act as attachment receptors that allow the virus to bind to cells, facilitating infection via ACE2. Next we investigated whether pre-incubation of SARS-CoV-2 with LWMH prevents ACE2 binding. The primary SARS-CoV-2 isolate (hCoV-19/Italy) interacted with immobilized ACE2 and, notably,

pretreatment of the virus with LMWH did not affect ACE2 binding (**Figure EV1F**). These data suggest that LMWH prevent virus attachment but do not affect the interaction with ACE2. Simian Vero E6 cells are highly susceptible to SARS-CoV-2, which causes severe cytopathic effects (CPE) ¹ and therefore we investigated the role of LMWH upon SARS-CoV-2 infection by measuring the cytopathic effects. Infection of VeroE6 with a primary SARS-CoV-2 isolate (hCoV-19/Italy) caused severe CPE as cell viability decreased (**Figure 2E**), which was counteracted by LMWH enoxaparin in a concentration dependent manner. These data support an important role for heparan sulfates in ACE2-dependent infection of cells with SARS-CoV-2.

SARS-CoV-2 infection of polarized epithelial cells is blocked by UF heparin and LMWH

The colorectal adenocarcinoma Caco-2 and bronchial adenocarcinoma Calu-3 cells represent models for human intestinal and respiratory epithelial cells, respectively ^{38, 39}. Both cell lines were cultured on microporous filters with an air liquid interface to achieve a polarized monolayer and polarization was monitored by transepithelial electrical resistance (TEER). TEER increased over time to confirm that the cells are polarized after culture of more than 14 days (**Figure 3A**). Undifferentiated Caco-2 and Calu-3 expressed low levels of ACE2 but polarization of the cells highly increased ACE2 expression (**Figure 3B**). SARS-CoV-2 pseudovirus bound to both polarized Caco-2 and Calu-3 cells and binding was significantly

Figure 2 | Low molecular weight heparins inhibit SARS-CoV-2 infection. (A) Huh7.5 cells were exposed to SARS-CoV-2 pseudovirus directly or after pre-treatment with different concentrations (0.0001, 0.001, 0.1, 0.5, 1, 5, 50, 100, 250 IU/mL) of UF heparin or LMWH enoxaparin for 30 min at 37°C. Infection was determined by luciferase reporter activity after 5 days. (B) SARS-CoV-2 pseudovirus was pre-incubated for 30 min at 37°C with UF heparin (250 IU/mL) or LMWHs tinzaparin (250 IU/mL) or dalteparin (250 IU/mL) or LMWH enoxaparin (250 IU/mL) or nadroparin (250 IU/mL). Huh7.5 were exposed to the SARS-CoV-2 pseudovirus, alone or treated with different LMWHs for 4 hours at 4°C, washed, lysed and binding was determined by ELISA. (C) SARS-CoV-2 pseudovirus was pre-incubated for 30 min at 37°C with UF heparin (250 IU/mL) or LMWHs tinzaparin (250 IU/mL) or dalteparin (250 IU/mL) or LMWH enoxaparin (250 IU/mL) or nadroparin (250 IU/mL). Huh7.5 cells were infected with SARS-CoV-2 pseudovirus in presence or absence of different LMWHs and infection was determined after 5 days by luciferase reporter activity. (D) 293T cells expressing ACE2 were infected with SARS-CoV-2 in presence or absence of antibodies against ACE2, UF heparin (250 IU/mL) or LMWH enoxaparin (250 IU/mL) and infection was determined after 3 days by luciferase reporter activity. (E) VeroE6 cells were infected with SARS-CoV-2 isolate (hCoV-19/Italy; 100 TCID₅₀/mL) previously treated with serial dilutions of LMWH enoxaparin. Cell viability was determined by using an MTT assay (n=3 donors measured in triplicate). Data information: Data show the mean values and error bars are the SEM. Statistical analysis was performed using (A) ordinary one-way ANOVA with Dunnett's multiple-comparison test. *P≤0.05, **P≤0.01, ***P≤0.001, ****P≤0.0001 (n=3 donors measured in triplicate). (B) ordinary one-way ANOVA with Tukey's multiple-comparison test (n=3 donors measured in triplicate), (C) ordinary one-way ANOVA with Dunnett's multiple-comparison test. *P≤0.05, **P≤0.01, ***P≤0.001, ****P≤0.0001 (n=3 donors measured in triplicate), (D) ordinary one-way ANOVA with Dunnett's multiple-comparison test. *P≤0.05, **P≤0.01 (n=3 measured in triplicates). RLU: relative light units.

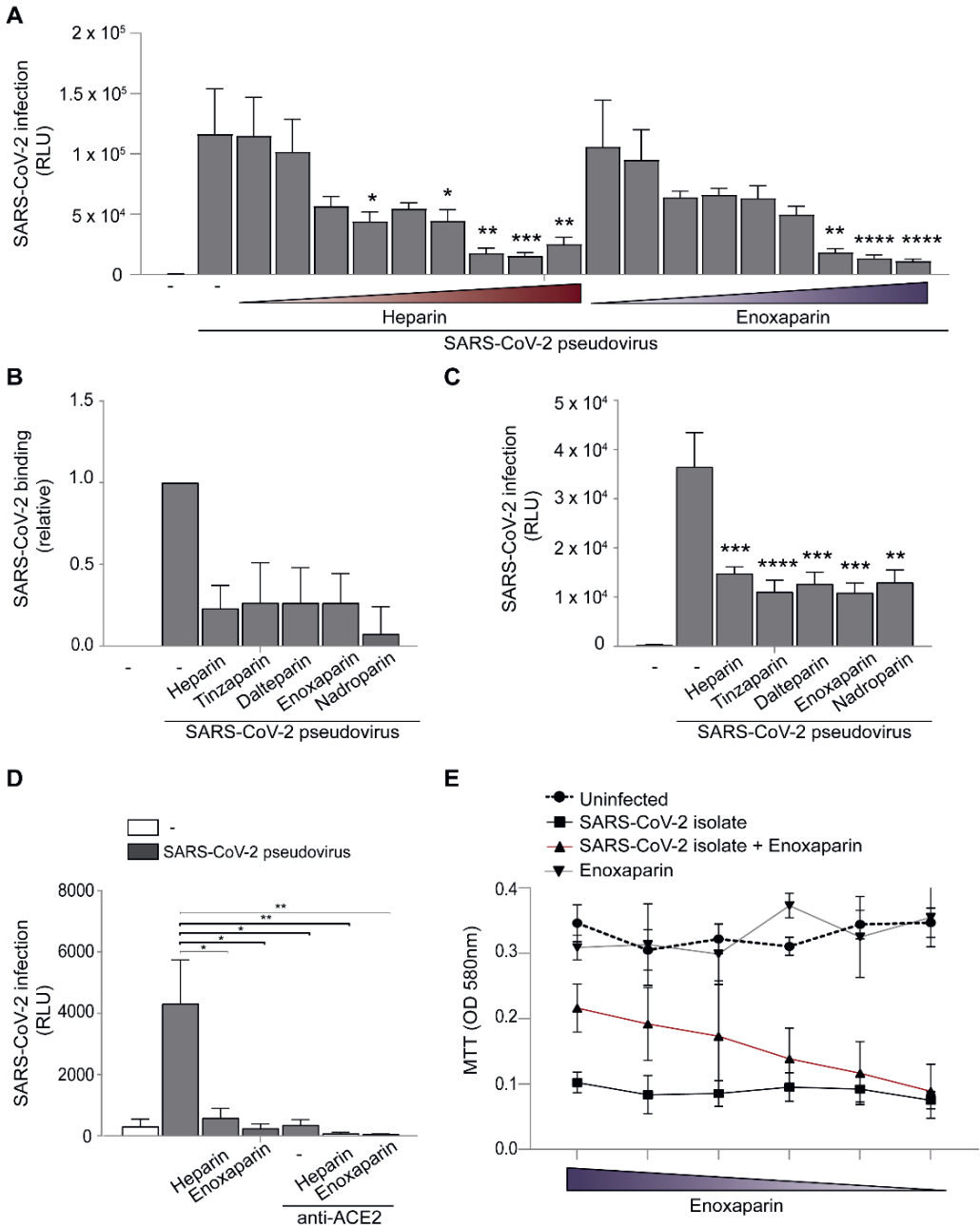


Figure 2. Figure legend on previous page.

blocked by LMWH to similar levels as antibodies against ACE2 (**Figure 3C and D**). The combination of an antibody against ACE2 and LMWH enoxaparin did not further decrease binding. We next infected polarized Calu-3 cells with the primary SARS-CoV-2 isolate for 24 hours, washed and after another 24 hours determined productive infection. Infection was determined by measuring SARS-CoV-2 ORF1b transcripts present during infection in cells but also in virus particles. Calu-3 polarized cells were productively infected by the SARS-CoV-2 isolate as shown by the SARS-CoV-2 ORF1b viral transcripts in the cell-lysates, and the secretion of SARS-CoV-2 virus particles in the supernatant (**Figure 3E and F** as well as **EV3A and EV3B**). Cell viability was not affected by infection as checked by GAPDH expression. Notably, productive infection of Calu-3 cells was inhibited by LMWH to a similar level as ACE2 antibodies (**Figure 3E and F** as well as **EV3A and EV3B**). These data suggest that heparan sulfates are required for binding and infection of polarized respiratory epithelial cells with SARS-CoV-2 pseudovirus as well as primary SARS-CoV-2 isolate.

Figure 3 | SARS-CoV-2 infection of polarized epithelial cells is blocked by UF heparin and LMWH. (A) Barrier integrity was analysed by TEER measurements of Caco-2 and Calu-3 over a period of 20 days (n=3 donors measured in quadruplicates). (B) ACE2 cell surface expression on Caco-2 and Calu-3 was determined by quantitative real-time PCR. (C, D) SARS-CoV-2 binding was measured in polarized Caco-2 (C) and Calu-3 (D) cells in presence or absence of antibodies against ACE2 (cell incubation), and UF heparin (250 IU/mL) or LMWH enoxaparin (250 IU/mL) (virus incubation). (E) Polarized Calu-3 were inoculated with 0.5 TCID₅₀/mL of a SARS-CoV-2 isolate (hCoV-19/Italy) either directly or in presence of antibodies against ACE2 or upon pre-treatment with LMWH enoxaparin (250 IU/mL) for 30 min at 37°C. Virus was detected by lysing after 48 hours through quantitative real-time PCR of viral RNA (E) and virus production was determined by detection of viral RNA in supernatant using quantitative real-time PCR (F). Data information: Data show the mean values and error bars are the SEM. Statistical analysis was performed using (B) ordinary one-way ANOVA with Tukey's multiple-comparison test. *P≤0.05, **P≤0.01 (n=5 Caco-2 donors measured in monoplo), *p=0.0460 (n=5 Calu-3 donors measured in monoplo), (C, D) ordinary one-way ANOVA with Tukey's multiple-comparison test. *P≤0.05, **P≤0.01, ***P≤0.001, ****P≤0.0001 (C) (n=3 Caco-2 donors measured in triplicate), (D)(n=3 Calu-3 donors measured in triplicate), (E, F) ordinary one-way ANOVA with Tukey's multiple-comparison test. *P≤0.05, **P≤0.01, ***P≤0.001, ****P≤0.0001 (n=3 donors measured in monoplo). TEER: Transepithelial electrical resistance.

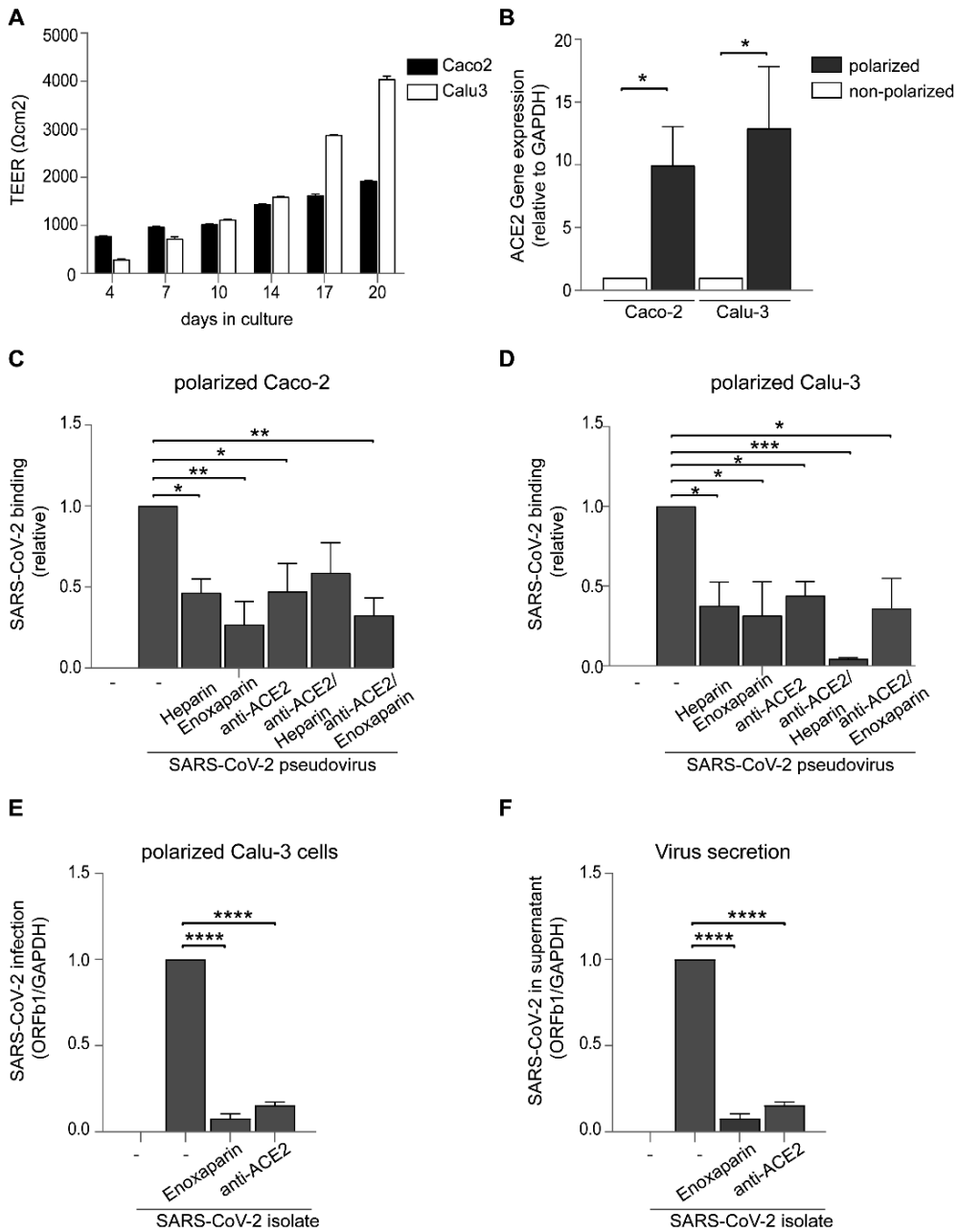


Figure 3. Figure legend on previous page.

Heparan sulfate proteoglycans Syndecan 1 and 4 are important for SARS-CoV-2 binding

The heparan sulfate proteoglycan family of Syndecans are particularly important in facilitating cell adhesion of several viruses^{33, 40}. Therefore, we used the Namalwa B cell-line that ectopically expressed Syndecan 1 or Syndecan 4 (**Figure EV2A-EV2C**) as these Syndecans are expressed by epithelial cells^{41, 42}. Namalwa cells did not express ACE2 (**Figure EV1A**). Syndecan 1 and Syndecan 4 expressing Namalwa cells bound more efficiently with SARS-CoV-2 pseudovirus than the parental Namalwa cells (**Figure 4A**). Both UF heparin and LMWH enoxaparin blocked the interaction of Syndecan 1- and -4 expressing cells with SARS-CoV-2 pseudovirus (**Figure 4A**). Moreover, Syndecan 1-expressing cells did not interact with control pseudovirus lacking the SARS-CoV-2 S protein neither did LMWH enoxaparin affect the interaction (**Figure EV2D**). Similarly, control pseudovirus did not interact with Huh7.5 cells (**Figure EV2D**). These data suggest that the interaction of Syndecans with SARS-CoV-2 is specific and depends on the S protein.

Next we measured binding of primary SARS-CoV-2 to Syndecan expressing cells. The primary SARS-CoV-2 isolate attached to both Syndecan 1 and Syndecan 4 expressing cells and LMWH enoxaparin blocked binding to background levels similar to those observed for the parental control cells (**Figure 4B and EV3B**). Cell viability was unaffected as determined by GAPDH expression. These data indicate that Syndecan 1 and 4 are important heparan sulfate proteoglycans involved in SARS-CoV-2 binding and infection.

Neutralizing antibodies against SARS-CoV-2 interfere with SARS-CoV-2 binding to Syndecan 1

Several antibodies against SARS-CoV-2 were isolated from COVID-19 patients and some of these were potent neutralizing antibodies against SARS-CoV-2 that target the RBD (COVA1-15, COVA1-18) as well as the non-RBD (COVA1-21) of the S protein²⁸. Therefore, we investigated whether antibodies against SARS-CoV-2 interfere with the interaction of heparan sulfates with SARS-CoV-2. We treated SARS-CoV-2 pseudovirus with different S-protein targeting antibodies and measured virus binding to ACE2-negative Syndecan 1-positive Namalwa cells. Notably, only the three neutralizing antibodies against SARS-CoV-2, COVA-1-15, 1-18 and 1-21 blocked the interaction of SARS-CoV-2 pseudovirus with Syndecan 1 in a concentration dependent manner and to similar levels as observed for LMWH (**Figure 5A**). In contrast, non-neutralizing antibodies did not inhibit virus binding (**Figure 5A**). Next we determined the ability of the S protein antibodies to block binding of the primary SARS-CoV-2 isolate to ACE2-negative Syndecan 1-expressing Namalwa. Similar as observed for SARS-CoV-2 pseudovirus, the three neutralizing COVA antibodies blocked the interaction of the SARS-CoV-2 isolate with Syndecan 1, whereas non-neutralizing antibody COVA-1-27 did not block binding (**Figure 5B and EV3C**). These data strongly

suggest that neutralizing RBD and non-RBD antibodies against SARS-CoV-2 interfere with SARS-CoV-2 binding to heparan sulfate proteoglycans and that this binding is facilitated by the SARS-CoV-2 S protein.

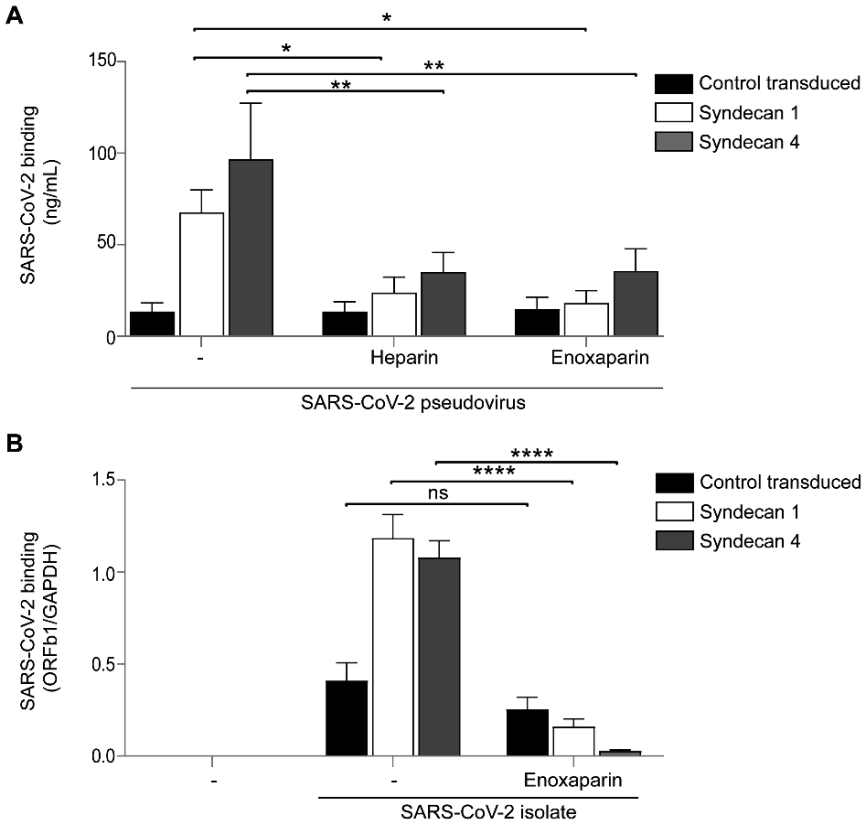


Figure 4 | Heparan sulfate proteoglycans Syndecan 1 and 4 are important for SARS-CoV-2 binding. (A) Namalwa cells ectopically expressing either Syndecan 1 or 4 were exposed to either SARS-CoV-2 pseudovirus alone or SARS-CoV-2 pseudovirus pre-treated with UF heparin (250 IU/mL) or LMWH enoxaparin (250 IU/mL) for 30 min at 37°C. Binding was measured after 4 hours at 4°C by ELISA. (B) SARS-CoV-2 isolate (hCoV-19/Italy) was pre-incubated with LMWH enoxaparin (250 IU/mL) for 30 min at 37°C. Namalwa cells expressing Syndecan 1 and 4 were exposed to either SARS-CoV-2 isolate (100 TCID₅₀/mL) or SARS-CoV-2 isolate (100 TCID₅₀/mL) pre-treated with LMWH enoxaparin (250 IU/mL) for 4 hours at 4°C and binding was determined by quantitative real-time PCR. Data show the mean values and error bars are the SEM. Statistical analysis was performed using (A) 2way-ANOVA with Dunnett's multiple-comparison test. *P≤0.05, **P≤0.01 (n = 7), (B) 2way-ANOVA with Sidak's multiple-comparison test. *P≤0.05, **P≤0.01, ***P≤0.001, ****P≤0.0001 (n = 3 measured in triplicate).

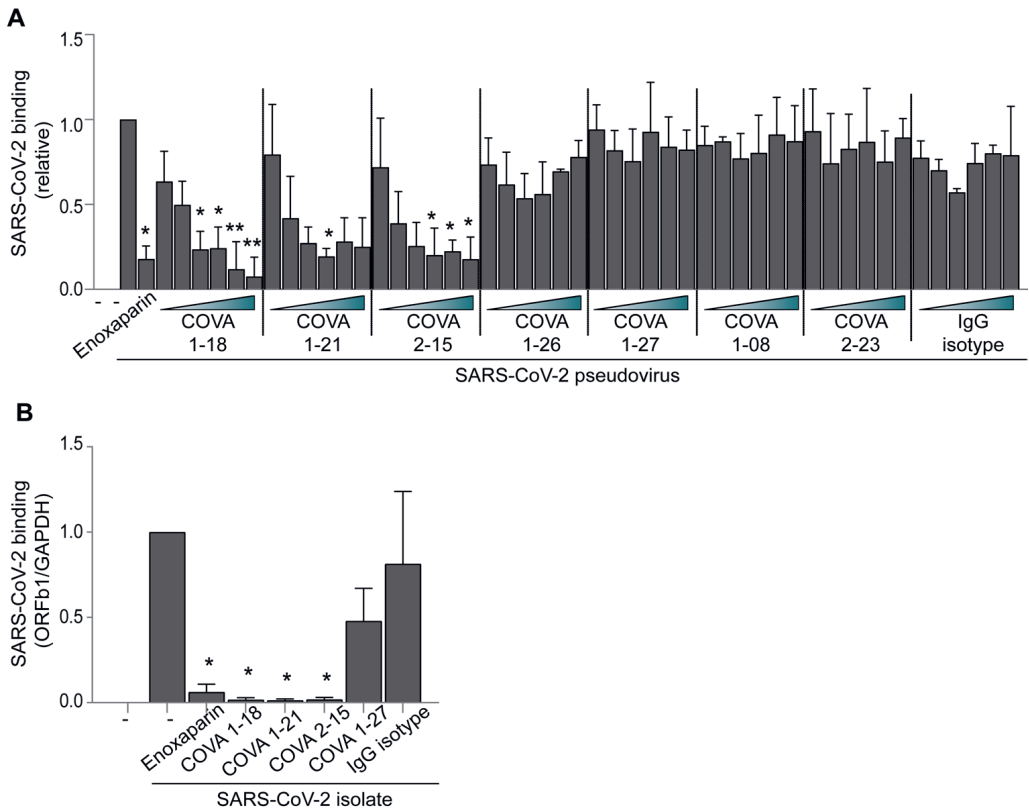


Figure 5 | Neutralizing antibodies against SARS-CoV-2 interfere with SARS-CoV-2 binding to Syndecan 1. (A) SARS-CoV-2 pseudovirus was pre-treated with LMWH enoxaparin (250 IU/mL), or different neutralizing antibodies against SARS-CoV-2 (COVA1-18, COVA1-21 and COVA2-15) and a human IgG1 isotype control at concentrations of 100 pg/mL, 500 pg/mL, 1 ng/mL, 5 ng/mL, 10 ng/mL and 50 ng/mL for 30 min at 37°C. Binding of pseudovirus to Syndecan 1 expressing cells in absence or presence of LMWH enoxaparin or antibodies was determined by ELISA. (B) SARS-CoV-2 isolate (hCoV-19/Italy) was pre-treated for 30 min at 37°C with either LMWH enoxaparin (250 IU/mL) or one of the following neutralizing antibodies (COVA1-18, 1-21 and 2-15), a non-neutralizing antibody (COVA1-27) or a human IgG1 isotype control, all at the concentration of 1 pg/mL. SARS-CoV-2 isolate alone or with blocks was added at a concentration of 100 TICD/mL. Detection of virus binding to Syndecan 1 expressing Namalwa was measured by quantitative real-time PCR. Data information: Data show the mean values and error bars are the SEM. Statistical analysis was performed using (A) ordinary one-way with Dunnett's multiple-comparison test. * $P \leq 0.05$, ** $P \leq 0.01$ ($n=3$), (B) ordinary one-way with Tukey's multiple-comparison test. * $P \leq 0.05$, ** $P \leq 0.01$ ($n=2$ measured in duplicates).

SARS-CoV-2 targets dendritic cells for dissemination

SARS-CoV-2 infects cells in nasal mucosa, lung and the intestinal tract but mechanisms for dissemination of the virus from the respiratory to the intestinal tract remain unclear.

Mucosal DC subsets might be involved in promoting local infection of epithelial cells in these tissues through capture as well as virus dissemination as these antigen presenting cells after

activation migrate to the lymphoid tissues to present antigens to T cells. We therefore investigated whether SARS-CoV-2 infects different mucosal DC subsets and whether DCs can transmit the virus to other cells. We differentiated monocytes to DCs, which is a model for submucosal DC, and also isolated primary human Langerhans cells (LCs) from skin^{43, 44} as this DC subset resides in squamous mucosa of different tissues including nasal and intestinal mucosa^{45, 46}. Both monocyte-derived DCs and primary LCs efficiently bound SARS-CoV-2 pseudovirus and binding was inhibited by UF heparin as well as LMWH enoxaparin (**Figure 6A and B**). Notably, neither DCs nor LCs were infected by SARS-CoV-2 pseudovirus (**Figure 6C**), which is due to the absence of ACE2 expression on both subsets (**Figure 6D**). These data suggest that primary DC subsets capture SARS-CoV-2 via heparan sulfate proteoglycans but this does not lead to infection. Different DC subsets transmit HIV-1 to target cells independent of productive infection^{44, 47, 48}. We therefore incubated both DCs and LCs with SARS-CoV-2 pseudovirus and after washing away unbound virus, co-cultured the DC subsets with susceptible ACE2 expressing Huh7.5 cells (**Figure 6E**). Notably, co-culture of both virus-exposed DC subsets with Huh7.5 cells led to infection of the latter, as determined by luciferase reporter activity and infection was blocked by pre-treatment of pseudovirus with UF heparin and LMWH enoxaparin (**Figure 6F and G**). Next, DCs and LCs were incubated with the primary SARS-CoV-2 isolate and after extensive washing added to ACE2 positive Huh7.5 cells. Infection of Huh7.5 cells was determined by quantitative PCR after removing leftover DCs or LCs. Notably, both SARS-CoV-2-exposed DCs and LCs transmitted the virus to Huh7.5 cells as shown by infection of Huh7.5 cells, and transmission was inhibited by LMWH enoxaparin (**Figure 6H and I** as well as **EV4A and EV4B**). These data suggest that both DCs and LCs efficiently capture SARS-CoV-2 via heparan sulfate proteoglycans and transmit the virus to ACE2 expressing target cells, which could be involved in virus dissemination from mucosal sites to lymphoid tissues.

SARS-CoV-2 attaches to and infects primary nasal cells via heparan sulfate proteoglycans

Nasal epithelium is an important target for SARS-CoV-2 infection. Higher viral loads are detected in nasal and nasopharyngeal swabs compared to throat swabs^{49, 50}. Here we isolated nasal cells from healthy volunteers by brushing the inside of the nasal cavity. Epithelial cells are a major component of the isolated cells as shown by high percentage of cells positive for the epithelial cell marker EpCAM (**Figure 7A**). Also hematopoietic cells were present in the nasal cell fraction as shown by the expression of the hematopoietic cell marker CD45 (**Figure 7A**). Next we analyzed Syndecan 1 and 4 transcripts in the nasal fraction as well as expression of ACE2. Especially high levels of Syndecan 1 transcripts were identified in the nasal fraction compared to those observed for polarized Calu-3 cells (**Figure 7B and EV5A**). ACE2 transcript were also detected, suggesting that SARS-CoV-2 could directly infect nasal cells (**Figure 7B and EV5A**)⁵¹. We first investigated binding of

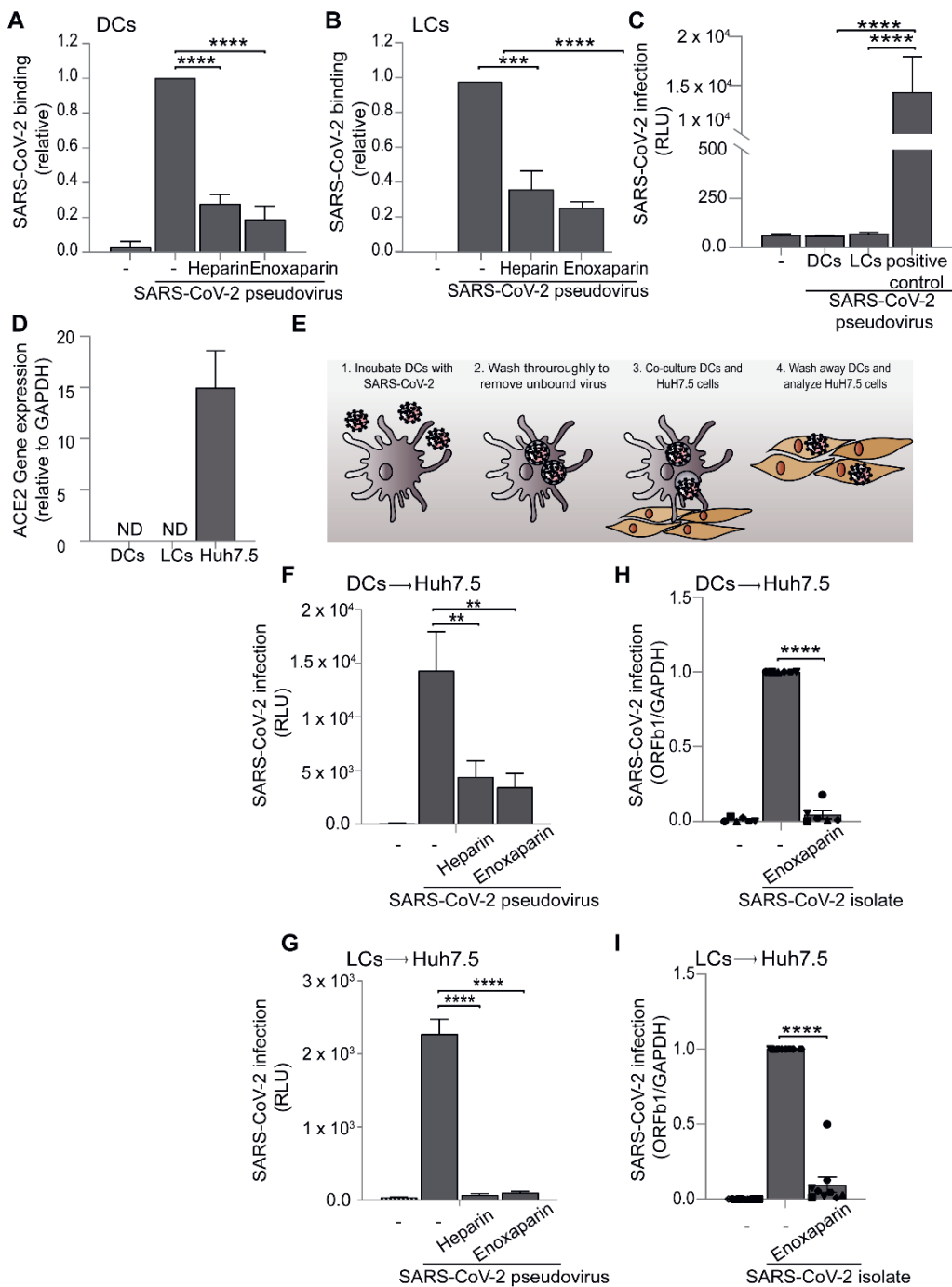


Figure 6. Figure legend on next page.

Figure 6 | SARS-CoV-2 targets dendritic cells for dissemination. (A, B) SARS-CoV-2 binding to monocyte-derived DCs (A) or primary LCs (B) in absence or presence of UF heparin (250 IU/mL) or LMWH enoxaparin (250 IU/mL). (C) DCs and LCs were infected with SARS-CoV-2 pseudovirus and infection was determined after 5 days by measuring luciferase reporter activity. As positive controls Huh7.5 cells were infected. (D) ACE2 cell surface expression on DCs, LCs and Huh7.5. Representative data for an experiment repeated more than three times with similar results (n=3 in duplicates). (E) Graphical overview of the cell-to-cell viral transmission assay. (F, G) DCs (F) and LCs (G) were pre-incubated with SARS-CoV-2 pseudovirus for 4 hours at 37°C in presence or absence of UF heparin (250 IU/mL) or LMWH enoxaparin (250 IU/mL), extensively washed and co-cultured with Huh7.5 cells. Transmission by DCs or LCs to Huh7.5 cells was determined by luciferase reporter activity. (H, I) SARS-CoV-2 isolate (hCoV-19/Italy) was pre-treated with LMWH enoxaparin (250 IU/mL) for 30 min at 37°C. DCs (H) and LCs (I) were exposed to either the untreated or pre-treated SARS-CoV-2 isolate (100 TCID₅₀/mL) for 24h, washed thoroughly and co-cultured with Huh7.5 cells. Quantification of viral RNA was measured by quantitative real-time PCR. Data information: Data show the mean values and error bars are the SEM. (A, B) ordinary one-way ANOVA with Tukey's multiple-comparison test. *P≤0.05, **P≤0.01, ***P≤0.001, ****P≤0.0001 (A) (n=4), (B) (n=4), (C) ordinary one-way ANOVA with Tukey's multiple-comparison test. *P≤0.05, **P≤0.01, ***P≤0.001, ****P≤0.0001 (n=4 measured in triplicate), (F) ordinary one-way ANOVA with Dunnett's multiple-comparison test. *P≤0.05, **P≤0.01 (n=4 measured in triplicate), (G) ordinary one-way ANOVA with Tukey's multiple-comparison test. *P≤0.05, **P≤0.01, ***P≤0.001, ****P≤0.0001 (n=3 measured in triplicate). (H, I) ordinary one-way ANOVA with Tukey's multiple-comparison test. *P≤0.05, **P≤0.01, ***P≤0.001, ****P≤0.0001 (H) (n=3 in duplicates), (I) (n=4 in duplicates). DCs: Dendritic cells, LCs: Langerhans cells, RLU: relative light units, ND: Not determined.

primary SARS-CoV-2 isolate to the nasal cells. SARS-CoV-2 attached to the nasal cells from different donors and binding was blocked by LMWH enoxaparin (**Figure 7C** and **EV5B**). Primary nasal cells were exposed to SARS-CoV-2 and cultured for 24 hours. Viability was not affected as measured by GAPDH expression. Notably, we observed high levels of SARS-CoV-2 ORF1b in cell-lysates (**Figure 7D** and **EV5C**). Infection was inhibited by ACE2 block and, importantly, LMWH treatment blocked infection of SARS-CoV-2 as shown by decreased ORF1b in cell-lysate (**Figure 7D** and **EV5C**). These data suggest that heparan sulfate proteoglycans expressed by the nasal epithelium are involved in SARS-CoV-2 binding and infection.

Discussion

SARS-CoV-2 interacts with ACE2 to infect cells. Recent studies suggest that heparan sulfates might interact with S protein to enhance viral attachment^{34, 35}. Moreover, Clausen *et al.* show that heparan sulfate binding to SARS-CoV-2 facilitates ACE2 interactions³⁴. Here we show that heparan sulfate proteoglycans on primary epithelial cells and primary dendritic cell subsets interact with both pseudotyped and primary SARS-CoV-2. We have identified Syndecan 1 and 4 as important attachment receptors for SARS-CoV-2. Interestingly, neutralizing antibodies against SARS-CoV-2 prevented the interaction of SARS-CoV-2 with Syndecan 1, suggesting that antibodies targeting the interaction of SARS-CoV-2 with heparan sulfates might also neutralize infection similarly to what was shown for antibodies against ACE2. Moreover, we identified a role for heparan sulfate proteoglycans during

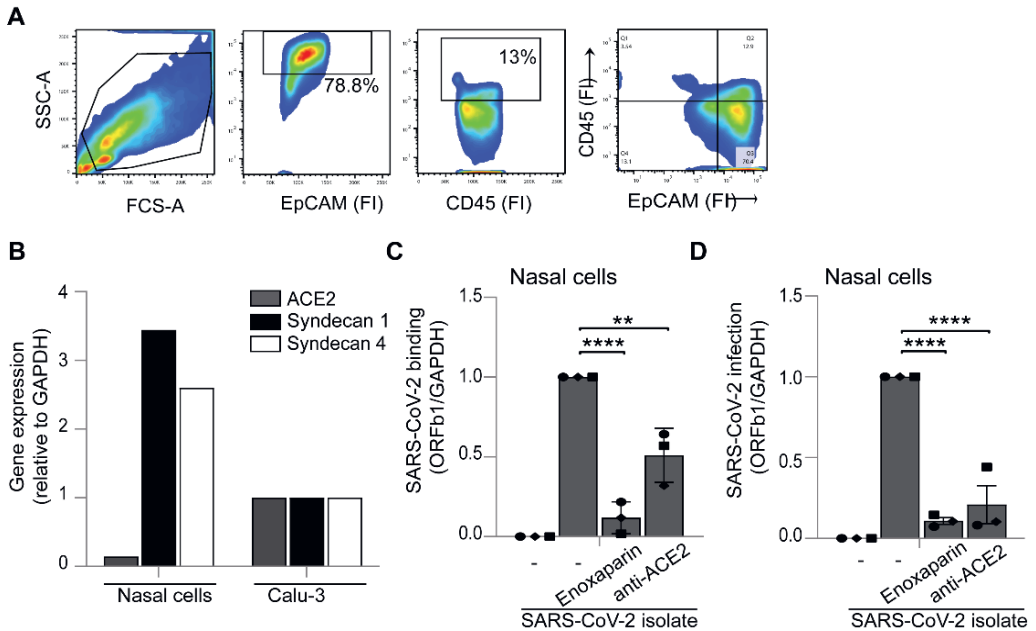


Figure 7 | SARS-CoV-2 attaches to and infects primary nasal cells via heparan sulfate proteoglycans. (A) Flow cytometry analysis of single cell suspensions from the nasal epithelium. Cells were labelled with EpCAM and CD45 antibodies and gated accordingly. (B) ACE2, Syndecan 1 and Syndecan 4 cell surface expression on nasal epithelial cells, compared to polarized epithelial Calu-3 was confirmed by quantitative real-time PCR. (C, D) Nasal epithelial cells were exposed to SARS-CoV-2 isolate (hCoV-19/Italy, 100 TCID₅₀/mL) either directly or after pre-treatment with antibodies against ACE2 cell surface receptors (1 hour at 37°C) or after pre-treatment with LMWH enoxaparin (250 IU/mL) for 30 min at 37°C. Detection of viral binding after 4 hours at 4°C (C) and persistently-infected cells lysed after 24 hours at 37°C (D) was determined by quantitative real-time PCR. Data information: Data show the mean values and error bars are the SEM. Statistical analysis was performed using (C, D) ordinary on-way ANOVA with Tukey's multiple-comparison test. *P<0.05, **P<0.01, ***P<0.001, ****P<0.0001 (C) (n=3), (D) (n=3 in duplicates).

transmission by primary mucosal DC subsets, which is independent of infection. Both UF heparin and LMWH efficiently reduced infection and transmission of SARS-CoV-2. Moreover, we show that LMWH efficiently decrease infection of primary nasal epithelial cells. Thus, heparan sulfate proteoglycans function as attachment receptors for SARS-CoV-2 on primary epithelial and dendritic cells, and targeting these receptors might prevent infection.

Our data indicate that SARS-CoV-2 binding to polarized colorectal and respiratory epithelial cells is facilitated by heparan sulfates, supporting a role for heparan sulfate proteoglycans as attachment receptors. Moreover, infection of polarized respiratory epithelial cells by SARS-CoV-2 hCoV-19/Italy strain as well as pseudovirus was inhibited by LMWH to a similar level as anti-ACE2 antibodies. Combinations of LMWH with antibodies did not further decrease infection. These data suggest that SARS-CoV-2 attaches to cells via heparan sulfate

proteoglycan, which facilitates interaction with ACE2 and subsequent infection. Indeed, treatment of SARS-CoV-2 with LMWH blocked heparan sulfate binding sites of the virus while it did not affect viral binding capacity to ACE2, suggesting that attachment of SARS-CoV-2 to heparan sulfate proteoglycans can facilitate ACE2 interaction.

Neutralizing antibodies against SARS-CoV-2 are a potential therapy for COVID-19 patients and most potent monoclonal neutralizing antibodies target the RBD site of the S protein thereby preventing interaction of S protein with ACE2²⁸. However, neutralization antibodies have also been isolated that target non-RBD sites of the S protein. Indeed, COVA1-21 targets a non-RBD site as it does not seem to interfere with ACE2²⁸, suggesting that it neutralizes either via another receptor or another mechanism. We screened different antibodies isolated from COVID-19 patients²⁸ for blocking SARS-CoV-2 binding to Syndecan 1. Two RBD antibodies COVA1-18 and COVA2-15 and one non-RBD antibody COVA1-21 were identified that blocked interaction of Syndecan 1 with SARS-CoV-2 pseudovirus as well as the SARS-CoV-2 hCoV-19/Italy strain. Notably, these three antibodies are potent neutralizing antibodies against SARS-CoV-2²⁸. Most non-neutralizing antibodies did not interfere with SARS-CoV-2 binding to Syndecan 1. These data suggest that blocking the interaction of SARS-CoV-2 with heparan sulfate proteoglycans might be a new mechanism of neutralization.

Our data strongly suggest that the S protein from SARS-CoV-2 is crucial to the interaction with heparan sulfate proteoglycans and Syndecan 1, as antibodies against the S protein blocked binding of both SARS-CoV-2 pseudovirus and a SARS-CoV-2 isolate to Syndecan-1-expressing Namalwa cells. Moreover, control pseudoviruses lacking the S protein did neither interact with Huh7.5 cells nor Syndecan-1 expressing cells, further supporting the specificity of the interaction between S protein from SARS-CoV-2 and heparan sulfate proteoglycans.

Different DC subsets are present in mucosal tissues to capture pathogens for antigen presentation. After pathogen interactions, DCs migrate into lymphoid tissues⁵². Several viruses such as HIV-1 and Dengue virus, hijack DC functions for dissemination^{47,53}. Primary LCs and DCs efficiently captured SARS-CoV-2 via heparan sulfate proteoglycans. Previously we have shown that LCs express Syndecan 4³³ and DCs express Syndecan 3 and Syndecan 4⁵⁴. Thus, our data suggest that both Syndecan 3 and 4 might be involved in SARS-CoV-2 capture. Both LCs and DCs did not express ACE2 and were not infected by SARS-CoV-2 pseudovirus. However, co-culture of SARS-CoV-2-exposed LCs and DCs with ACE2 cells led to productive infection with pseudotyped as well as a primary SARS-CoV-2 strain. Transmission was blocked by LMWH suggesting that capture by heparan sulfate proteoglycans is important for transmission. Moreover, our data indicate that SARS-CoV-2 transmission is independent of direct infection of DC subsets, suggesting that this might allow the virus from escaping neutralization by antibodies or antiviral drugs. However, the exact mechanism of this viral transfer are still not entirely clear.

The upper airways and nasal epithelium might be the primary route of infection as higher

viral load have been found in nasal swabs when compared to throat swabs⁵⁵ Moreover, nasal epithelial cells express ACE2 and the cellular serine protease TMPRSS2⁵¹. We have isolated nasal cells from healthy volunteers using a nasal brush and the majority of cells were EpCAM-positive epithelial cells and some hematopoietic cells, most likely lymphocytes and myeloid cells. Syndecan 1 and 4 transcripts were detected at high levels in nasal cell fraction, suggesting that Syndecans might be involved in virus interactions. Our data support an important role for nasal cells as the first target for SARS-CoV-2 as nasal cells efficiently captured primary SARS-CoV-2 and were also infected by SARS-CoV-2. LMWH blocked capture and infection of the nasal cells. Interestingly, the nasal cells were not cultured as done in previous studies^{56,57} suggesting that the nasal epithelial cells are a direct target for SARS-CoV-2 and that heparan sulfate proteoglycans are involved in the infection. LMWHs are already used as subcutaneous treatment of COVID-19 patients to prevent systemic clotting^{58,59}. Interestingly, here we have identified an important ability of LMWH to directly block SARS-CoV-2 binding and infection of epithelial cells as well as preventing virus transmission. Our data support the use of LMWH as prophylactic treatment for SARS-CoV-2 as well as a treatment option early in infection to block further infection and dissemination. Vaccination programs are currently running worldwide but it remains unclear whether this is sufficient for specific patients who are immunocompromised or suffer from other diseases that prevent an efficient immune response upon vaccination. LMWH prophylaxis might also be used when new SARS-CoV-2 variants arise that are not efficiently counteracted by the current vaccines.

Materials and Methods

Reagents and antibodies

The following antibodies were used (all anti-human): ACE2 (R&D), (Heparan Sulfate (clone F58-10E4) (Amsbio), digested Heparan (clone F69-3G10) (Amsbio), CD1a-APC mouse IgG1 (BD Biosciences, San Jose, CA, USA), CD207-PE (langerin) mouse IgG1 (#IM3577), PerCP-Cy™5.5-conjugated mouse IgG1 EPCAM 347199) (BD Bioscience), PE-conjugated mouse IgG1 E-Cadherin (FAB18381P) (R&D Systems), APCcy-conjugated mouse IgG1 CD45 (557833) (BD Bioscience), APC-conjugated CD14 (21620146sp) (Immunotools), PE-conjugated mouse IgG1 CD11b (101208) (Biolegend). FITC-conjugated goat-anti-mouse IgM (#31992) (Invitrogen), AF488-conjugated donkey-anti-mouse IgG2b (Invitrogen). Flow cytometric analyses were performed on a BD FACS Canto II (BD Biosciences). Data was analyzed using FlowJo vX.0.7 software (TreeStar).

The following reagents were used: Unfractionated (UF) heparin, 5.000 IE./mL (LEO). Low Molecular Weight heparins (LMWH): dalteparin, 10.000 IE anti-Xa/mL (Pfizer), tinzaparin, 10.000 IE anti-X1/0.5mL (LEO), enoxaparin, 6000 IE (60mg)/0.6 mL (Sanofi), nadroparin, 9.500 IE anti-XA/mL (Aspen). Heparinase III from *Flavobacterium heparium*, EC 4.2.2.8,

Batch 010, (Amsbio). Biotinylated SARS-CoV-2 S protein as well as neutralizing and non-neutralizing COVA antibodies were generated as described previously²⁸.

Cell lines

The Simian kidney cell line VeroE6 (ATCC® CRL-1586™) was maintained in CO₂ independent medium (Gibco Life Technologies, Gaithersburg, Md.) supplemented with 10% fetal calf serum (FCS), L-glutamine and penicillin/streptomycin (10 µg/mL). Culture was maintained at 37°C without CO₂. Huh7.5 (human hepatocellular carcinoma) cells received from Dr. Charles M. Rice⁶⁰ were maintained in Dulbecco modified Eagle medium (Gibco Life Technologies, Gaithersburg, Md.) containing 10% fetal calf serum (FCS), L-glutamine and penicillin/streptomycin (10 µg/mL). Medium was supplemented with 1mM HEPES buffer (Gibco Life Technologies, Gaithersburg, Md.). The human B cell line Namalwa (ATCC, CRL-1432) and Namalwa cells stably expressing human Syndecan 1 and Syndecan 4⁶¹ were a gift from Dr. Guido David and Dr. Philippe A Gallay. The cells were maintained in RPMI 1640 medium (Gibco Life Technologies, Gaithersburg, Md.) containing 10% fetal calf serum (FCS), penicillin/streptomycin (10 µg/mL) and 1 mM sodium pyruvate (Thermo Fisher). The expression of the different Syndecans was validated by PCR analysis using specific primers aimed against Syndecans. The human multiple myeloma cell line XG-1 was cultured in Iscove modified Dulbecco medium (Invitrogen Life Technologies) containing 10% fetal bovine serum, 100 U/mL of penicillin and 100 µg/mL of streptomycin. The medium was further supplemented with 500 pg/mL of interleukin-6 (Prospec). The CRISPR-Cas9 knockout for *Ext1* has been described previously³⁶. The human embryonic kidney 293T/17 cells (ATCC, CRL-11268) were maintained in Dulbecco modified Eagle medium (Gibco Life Technologies, Gaithersburg, Md.) containing 10% fetal calf serum (FCS), L-glutamine and penicillin/streptomycin (10 µg/mL). The human epithelial Caco-2 cells (ATCC, HTB-37™) as well as the human lung epithelial Calu-3 cells (ATCC® HTB-55™) were maintained in Dulbecco modified Eagle medium (Gibco Life Technologies, Gaithersburg, Md.) containing 10% fetal calf serum (FCS), L-glutamine and penicillin/streptomycin (10 µg/mL) and supplemented with MEM Non-Essential Amino Acids Solution (NEAA) (Gibco Life Technologies, Gaithersburg, Md.). To create a monolayer of polarized cells, Caco-2 and Calu-3 cells were maintained in 6.5 mm Transwell® with 5.0 µm Pore Polycarbonate Membrane Insert (Corning). The cells were initially seeded with a density of 25,000 cells per 6.5 mm filter insert and full polarization was reached after 2 weeks in culture. Polarization was monitored by measuring transepithelial electrical resistance (TEER).

Primary human cells

This study has been conducted in accordance with the ethical principles set out in the declaration of Helsinki and was approved by the institutional review board of the Academic

Medical Center (AMC, Amsterdam, Netherlands) and the Ethics Advisory Body of the Sanquin Blood Supply Foundation (Amsterdam, Netherlands).

CD14⁺ monocytes were isolated from the blood of healthy volunteer donors (Sanquin blood bank) and subsequently differentiated into monocyte-derived DCs as described previously⁶² (**Figure EV2E**). LCs were isolated from human epidermal sheets obtained from healthy donors after plastic surgery. Epidermal sheets were prepared as described previously^{43, 44}. Briefly, skin-grafts were obtained using a dermatome (Zimmer Biomet, Indiana USA). After incubation with Dispase II (1 U/mL, Roche Diagnostics), epidermal sheets were separated from dermis, washed and cultured in IMDM (Thermo Fischer Scientific, USA) supplemented with 10% FCS, gentamycin (20 µg/mL, Centrafarm, Netherlands), penicillin/streptomycin (10 U/mL and 10 µg/mL, respectively; Invitrogen) for 3 days after which LCs were harvested. Purity of LCs was routinely verified by flow cytometry using antibodies directed against CD207 (langerin) and CD1a (**Figure EV2F**).

Primary nasal epithelial cells were obtained from healthy volunteers. Cells were isolated from the lower nasal cavity with a brush after which they were transferred into CO₂ independent medium (Gibco Life Technologies, Gaithersburg, Md.) supplemented with 10% fetal calf serum (FCS), L-glutamine and penicillin/streptomycin (10 µg/mL). Cell surface receptor expression was determined by flow cytometry.

SARS-CoV-2 pseudovirus production

For production of single-round infection viruses, human embryonic kidney 293T/17 cells (ATCC, CRL-11268) were co-transfected with an adjusted HIV backbone plasmid (pNL4-3.Luc.R-S-) containing previously described stabilizing mutations in the capsid protein (PMID: 12547912) and a firefly luciferase gene in the *nef* open reading frame (1.35ug) and pSARS-CoV-2 expressing SARS-CoV-2 S protein (0.6ug) (GenBank; MN908947.3)²⁸. For single-round infection viruses lacking S-protein, an empty vector (pcDNA3.1(+), Thermo Fisher Scientific, #V79020.) was added instead. Transfection was performed in 293T/17 cells using genejuice (Novagen, USA) transfection kit according to manufacturer's protocol. At day 3 or day 4, pseudotyped SARS-CoV-2 virus particles were harvested and filtered over a 0.45 µm nitrocellulose membrane (SartoriusStedim, Gottingen, Germany). SARS-CoV-2 pseudovirus productions were quantified by p24 ELISA (Perkin Elmer Life Sciences).

SARS-CoV-2 production

All experiments with SARS-CoV-2 isolates were performed in a BSL-3 laboratory, following all appropriate safety and security protocols approved by the Amsterdam UMC BioSafetyGroep and performed under the environmental license obtained from the municipality Amsterdam. The following reagent was obtained from Dr. Maria R. Capobianchi through BEI Resources, NIAID, NIH: SARS-Related Coronavirus 2, Isolate Italy-

INMI1, NR-52284, originally isolated January 2020 in Rome, Italy. VeroE6 cells (ATCC® CRL-1586™) were inoculated with the SARS-CoV-2 isolate and used for reproduction of virus stocks. Cytopathic effect (CPE) formation was closely monitored and virus supernatant was harvested after 48 hours. Viral titers were determined by tissue culture infectious dose (TCID₅₀) on VeroE6 cells. In brief, VeroE6 cells were seeded in a 96 well plate at a cell density of 8.000 cells in 100 µl. After 24 hours, cells were inoculated with a 5-fold serial dilution of SARS-CoV-2 isolate in quadruplicate. Cell cytotoxicity was measured using the MTT assay 48 hours after infection. Loss of MTT staining as determined by spectrometer (OD 580 nm) is indicative of the (CPE) of SARS-CoV-2. The virus titer was determined as TCID₅₀/mL and calculated based on the Reed Muench method ⁶³.

Pseudovirus infection assays

HuH7.5 and 293T cells were exposed to 95 ng of single-round SARS-CoV-2 pseudovirus. Primary dendritic cell subsets were exposed to 190 ng and polarized Caco2 and Calu3 cells to 477.62 ng of single-round SARS-CoV-2 pseudovirus. Virus was pre-incubated with 250 IU/mL LMWH or UF heparin to addition to the cells. Viral protein production was quantified after 5 days at 37°C by measuring luciferase reporter activity. Luciferase activity (relative light units (R.L.U.)) was measured using the Luciferase assay system (Promega, USA) according to manufacturer's instructions.

Virus binding

In order to determine SARS-CoV-2 binding, target cells were seeded in a 96 well plate at a density of either 10.000 cells in 100 µl for adherent cells the day before or 100.000 cells in 100 µl for suspension cells the same day. All cells were exposed to either 95 ng/mL of SARS-CoV-2 pseudovirus or SARS-CoV-2 isolate (hCoV-19/Italy, 100 TCID₅₀/mL) for 4 hours at 4°C. After 4 hours, cells were washed extensively to remove unbound virus. Cells incubated with SARS-Cov-2 pseudovirus were lysed and binding and internalization were quantified by RETRO-TEK HIV-1 p24 ELISA according to manufacturer instructions (ZeptoMetrix Corporation). Cells incubated with SARS-Cov-2 isolate (hCoV-19/Italy) were lysed with AVL buffer and RNA was isolated with the QIAamp Viral RNA Mini Kit (Qiagen) according to the manufacturers protocol.

SARS-CoV-2 WT infection

VeroE6 cells were seeded at a density of 10.000 cells in 100 µl in a 96 well plate. After 24 hours, the cells were exposed to the SARS-CoV-2 isolate (hCoV-19/Italy, 100 TCID₅₀/mL) for 48 hours. Additionally, SARS-CoV-2 isolate was pre-incubated with 250 IU/mL of LMWH enoxaparin prior to cell inoculation. Infection was measured after 48 hours at 37°C by MTT

and determined by cell viability. Polarized Calu-3 cells that had initially been seeded with 25.000 cells/transwell (6.5 mm filter insert) prior to infection, were incubated with SARS-CoV-2 isolate (hCoV-19/Italy, 0.5 TCID₅₀/mL) for 24 hours, after which cells were washed thoroughly and new medium was added. Viral infection and secretion were determined by RT-PCR measurement of ORF-1b transcript. Primary nasal epithelial cells seeded at a density of 50.000-100.000 cells in 100 µl were incubated with SARS-CoV-2 isolate (hCoV-19/Italy, 100 TCID₅₀/mL) for 24 hours after which ORF-1b transcript was determined by RT-PCR.

Tetrazolium dye colorimetric cell viability (MTT) assay

MTT solution was added to VeroE6 cells and incubated for 2 hours at 37°C. After removing the MTT solution, MTT solvent containing 4 mM HCL and 1% Nonidet P-40 (NP40) in isopropanol was added to the cells. Homogenous solution was measured at optical density between 580 nm and 655 nm.

293T Transfection with ACE2

To generate cells expressing human ACE2, human embryonic kidney 293T/17 cells were transfected with pcDNA3.1(-)hACE2 (Addgene plasmid #1786). Transfection was performed in 293T/17 cells using the genejuice (Novagen, USA) transfection kit according to manufacturer's protocol. At 24h post-transfection, cells were washed with phosphate-buffered saline (PBS) and cultured for recovering at 37C for 24h in Dulbecco's MEM supplemented with 10% heat-inactivated fetal calf serum (FCS), L-glutamine and penicillin/streptomycin (10 U/mL) After 24h of recovery, cells were cultured in media supplemented with G418 (5mg/mL) (Thermo Fisher) and passage for 3 weeks at 37C. Surviving clones were analyzed for ACE2 expression via flow cytometry and PCR.

Transmission assays and co-culture

Per condition, 100.000 DCs or LCs/100 µl were exposed to 191.05 ng of pseudotyped SARS-CoV-2 or pseudotyped SARS-CoV-2 pre-incubated with 250 IU/mL UF heparin or LMWH enoxaparin for 30 min at 37°C. After 4 hours at 37°C, cells were harvested, extensively washed to remove unbound virus and co-cultured with Huh7.5 for 5 days at 37°C. After 5 days, DCs or LCs were washed away and Huh7.5 cells were analyzed with the Luciferase assay system (Promega, USA) according to manufacturer's instructions to determine infection based on luciferase reporter activity. Similarly, DCs or LCs were also exposed to either SARS-CoV-2 isolate (hCoV-19/Italy, 100 TCID₅₀/mL) or SARS-Cov-2 isolate pre-incubated with 250 IU/mL LMWH enoxaparin (30 min at 37°C). After 24 hours at 37°C, cells were extensively washed to remove unbound virus and co-cultured with HuH7.5 for

24 hours at 37°C. Subsequently, Huh7.5 were again washed extensively to remove DCs or LCs and Huh7.5 were lysed for isolation of viral RNA.

RNA isolation and quantitative real time PCR

Viral RNA in cells and supernatant was isolated with the QIAamp Viral RNA Mini Kit (Qiagen) according to the manufacturers protocol. cDNA was synthesized with the M-MLV reverse-transcriptase kit (Promega) and diluted 1 in 5 before further application. Cellular mRNA of cells not exposed to virus was isolated with an mRNA Capture kit (Roche) and cDNA was synthesized with a reverse-transcriptase kit (Promega). PCR amplification was performed in the presence of SYBR green in a 7500 Fast Realtime PCR System (ABI). Specific primers were designed with Primer Express 2.0 (Applied Biosystems). Primer sequences used for mRNA expression were for gene product: GAPDH, forward primer (CCATGTTTCGTCATGGGTGTG), reverse primer (GGTGCTAA GCAGTTGGTGGTG). For gene product SARS-CoV-2 ORF1b, forward primer (TGGGGTTTTACAGGTAACCT), reverse primer (AACACGCTTAACAAAGCACTC) as described previously⁶⁴. For gene product: ACE2, forward primer (GGACCCAGGAAATGTTTCAGA), reverse primer (GGCTGCAGAAAGTGACATGA). For gene product: Syndecan 1, forward primer (ATCACCTTGTCCAGCAGACCC) reverse primer (CTCCACTTCTGGCAGGACTACA). Syndecan 4, forward primer (AGGTGTCAATGTCCAGCACTGTG) reverse primer (AGCAGTAGGATCAGGAAGACGGC). The normalized amount of target mRNA was calculated from the Ct values obtained for both target and household mRNA with the equation $Nt = 2^{Ct(GAPDH) - Ct(target)}$. For relative mRNA expression, control siRNA sample was set at 1 for each donor.

Biosynthesis inhibition and enzymatic treatment

HuH7.5 cells were treated in D-PBS/0.25% BSA with 46 milliunits heparinase III (Amsbio) for 1 hour at 37°C, washed and used in subsequent experiments. Enzymatic digestion was verified by flow cytometry using antibodies directed against heparan sulfates and digested heparan sulfates.

Human ACE2 protein binding

Recombinant human ACE2 protein, kindly provided by the lab of Dr. Rogier Sanders, was coated at a concentration of 2 µg/mL on a high binding plate (Nunc MaxiSorp™ flat-bottom, Thermo Fisher) at 4°C. After overnight incubation, wells were blocked with 2 % BSA for 30 min at 37°C before being washed extensively. SARS-Cov-2 isolate (hCoV-19/Italy, 20.000 TCID₅₀/mL) was added for 4 hours at 4°C at a total of 50 µl. After 4 hours wells were lysed and SARS-CoV-2 ORF-1b transcript was determined by quantitative RT-PCR.

Statistics

All results are presented as mean \pm SEM and were analyzed by GraphPad Prism 8 software (GraphPad Software Inc.). A two-tailed, parametric Student's *t*-test for paired observations (differences within the same donor) or unpaired observation, Mann-Whitney tests (differences between different donors, that were not normally distributed) was performed. For unpaired, non-parametric observations a one-way ANOVA or two-way ANOVA test with post hoc analysis (Tukey's or Dunnet's) were performed. Statistical significance was set at * $P < 0.05$, ** $P < 0.01$ *** $P < 0.001$ **** $P < 0.0001$.

Data availability

This study includes no data deposited in external repositories.

Author contributions

M.B-J and J.E conceived and designed experiments; M.B-J, J.E, T.M.K, L.C.H, J.L.v.H performed the experiments and contributed to scientific discussion; P.J.M.B., K.E.V, M.S, G.J.d.B, B.M.N, N.A.K, M.J.v.G, and R.W.S., contributed essential research materials and scientific input. M.B-J, J.E, T.M.K and T.B.H.G analyzed and interpreted data; J.E, M.B-J and T.B.H.G. wrote the manuscript with input from all listed authors. T.B.H.G. was involved in all aspects of the study

Conflict of interest

The authors have declared that no conflict of interest exists.

Acknowledgements

We thank Jonne Snitselaar and Yoann Aldon for help with production of antibodies and Hildo Lantermans for help with the XG1/EXT1 KO cell lines. This research was funded by the Netherlands Organisation for Health Research and Development together with the Stichting Proefdiervrij (ZonMW MKMD COVID-19 grant nr. 114025008 to T.B.H.G.) and European Research Council (Advanced grant 670424 to T.B.H.G.), Amsterdam UMC PhD grant and two COVID-19 grants from the Amsterdam institute for Infection & Immunity (to T.B.H.G., R.W.S. and M.J.v.G.). This study was also supported by the Netherlands Organization for Scientific Research (NWO) through a Vici grant (to R.W.S.), and by the Bill & Melinda Gates Foundation through the Collaboration for AIDS Vaccine Discovery (CAVD), grant INV-002022 (to R.W.S.).

References

1. Zhou, P. *et al.* A pneumonia outbreak associated with a new coronavirus of probable bat origin. *Nature* **579**, 270-273 (2020).
2. Yuki, K., Fujiogi, M. & Koutsogiannaki, S. COVID-19 pathophysiology: A review. *Clin Immunol* **215**, 108427 (2020).
3. Zhu, N. *et al.* A Novel Coronavirus from Patients with Pneumonia in China, 2019. *The New England journal of medicine* **382**, 727-733 (2020).
4. Nicola, M. *et al.* The socio-economic implications of the coronavirus pandemic (COVID-19): A review. *Int J Surg* **78**, 185-193 (2020).
5. World Health Organization. Timeline of WHO's response to COVID-19; 2020.
6. Harapan, H. *et al.* Coronavirus disease 2019 (COVID-19): A literature review. *Journal of infection and public health* **13**, 667-673 (2020).
7. Ferioli, M. *et al.* Protecting healthcare workers from SARS-CoV-2 infection: practical indications. *European respiratory review : an official journal of the European Respiratory Society* **29** (2020).
8. Peiris, J.S., Yuen, K.Y., Osterhaus, A.D. & Stöhr, K. The severe acute respiratory syndrome. *The New England journal of medicine* **349**, 2431-2441 (2003).
9. Hui, K.P.Y. *et al.* Tropism, replication competence, and innate immune responses of the coronavirus SARS-CoV-2 in human respiratory tract and conjunctiva: an analysis in ex-vivo and in-vitro cultures. *Lancet Respir Med* (2020).
10. Lamers, M.M. *et al.* SARS-CoV-2 productively infects human gut enterocytes. *Science* (2020).
11. Wright, L., Steptoe, A. & Fancourt, D. Are we all in this together? Longitudinal assessment of cumulative adversities by socioeconomic position in the first 3 weeks of lockdown in the UK. *Journal of epidemiology and community health* (2020).
12. Brooks, S.K. *et al.* The psychological impact of quarantine and how to reduce it: rapid review of the evidence. *Lancet* **395**, 912-920 (2020).
13. Mathieu, E. *et al.* A global database of COVID-19 vaccinations. *Nat Hum Behav* (2021).
14. Agha, M., Blake, M., Chilleo, C., Wells, A. & Haidar, G. Suboptimal response to COVID-19 mRNA vaccines in hematologic malignancies patients. *medRxiv* (2021).
15. Boyarsky, B.J. *et al.* Antibody response to a single dose of SARS-CoV-2 mRNA vaccine in patients with rheumatic and musculoskeletal diseases. *Ann Rheum Dis* (2021).
16. Collier, D.A. *et al.* Sensitivity of SARS-CoV-2 B.1.1.7 to mRNA vaccine-elicited antibodies. *Nature* **593**, 136-141 (2021).
17. Wang, P. *et al.* Antibody resistance of SARS-CoV-2 variants B.1.351 and B.1.1.7. *Nature* **593**, 130-135 (2021).
18. Letko, M., Marzi, A. & Munster, V. Functional assessment of cell entry and receptor usage for SARS-CoV-2 and other lineage B betacoronaviruses. *Nature microbiology* **5**, 562-569 (2020).
19. Hulswit, R.J., de Haan, C.A. & Bosch, B.J. Coronavirus Spike Protein and Tropism

- Changes. *Advances in virus research* **96**, 29-57 (2016).
20. Bosch, B.J., van der Zee, R., de Haan, C.A. & Rottier, P.J. The coronavirus spike protein is a class I virus fusion protein: structural and functional characterization of the fusion core complex. *Journal of virology* **77**, 8801-8811 (2003).
 21. Li, F., Li, W., Farzan, M. & Harrison, S.C. Structure of SARS coronavirus spike receptor-binding domain complexed with receptor. *Science* **309**, 1864-1868 (2005).
 22. Wang, N. *et al.* Structure of MERS-CoV spike receptor-binding domain complexed with human receptor DPP4. *Cell research* **23**, 986-993 (2013).
 23. Burkard, C. *et al.* Coronavirus cell entry occurs through the endo-/lysosomal pathway in a proteolysis-dependent manner. *PLoS Pathog* **10**, e1004502 (2014).
 24. Xia, S. *et al.* Inhibition of SARS-CoV-2 (previously 2019-nCoV) infection by a highly potent pan-coronavirus fusion inhibitor targeting its spike protein that harbors a high capacity to mediate membrane fusion. *Cell Res* **30**, 343-355 (2020).
 25. Hoffmann, M. *et al.* SARS-CoV-2 Cell Entry Depends on ACE2 and TMPRSS2 and Is Blocked by a Clinically Proven Protease Inhibitor. *Cell* **181**, 271-280.e278 (2020).
 26. Hamming, I. *et al.* Tissue distribution of ACE2 protein, the functional receptor for SARS coronavirus. A first step in understanding SARS pathogenesis. *J Pathol* **203**, 631-637 (2004).
 27. Zou, X. *et al.* Single-cell RNA-seq data analysis on the receptor ACE2 expression reveals the potential risk of different human organs vulnerable to 2019-nCoV infection. *Frontiers of medicine* **14**, 185-192 (2020).
 28. Brouwer, P.J.M. *et al.* Potent neutralizing antibodies from COVID-19 patients define multiple targets of vulnerability. *Science* **369**, 643-650 (2020).
 29. Roderiquez, G. *et al.* Mediation of human immunodeficiency virus type 1 binding by interaction of cell surface heparan sulfate proteoglycans with the V3 region of envelope gp120-gp41. *J Virol* **69**, 2233-2239 (1995).
 30. Milewska, A. *et al.* Human coronavirus NL63 utilizes heparan sulfate proteoglycans for attachment to target cells. *J Virol* **88**, 13221-13230 (2014).
 31. Jiang, J. *et al.* Hepatitis C virus attachment mediated by apolipoprotein E binding to cell surface heparan sulfate. *J Virol* **86**, 7256-7267 (2012).
 32. Byrnes, A.P. & Griffin, D.E. Binding of Sindbis virus to cell surface heparan sulfate. *J Virol* **72**, 7349-7356 (1998).
 33. Nijmeijer, B.M. *et al.* Syndecan 4 Upregulation on Activated Langerhans Cells Counteracts Langerin Restriction to Facilitate Hepatitis C Virus Transmission. *Front Immunol* **11**, 503 (2020).
 34. Clausen, T.M. *et al.* SARS-CoV-2 Infection Depends on Cellular Heparan Sulfate and ACE2. *Cell* **183**, 1043-1057.e1015 (2020).
 35. Zhang, Q. *et al.* Heparan sulfate assists SARS-CoV-2 in cell entry and can be targeted by approved drugs in vitro. *Cell Discov* **6**, 80 (2020).
 36. Ren, Z. *et al.* Syndecan-1 promotes

- Wnt/ β -catenin signaling in multiple myeloma by presenting Wnts and R-spondins. *Blood* **131**, 982-994 (2018).
37. Kakkar, A.K. Low- and ultra-low-molecular-weight heparins. *Best practice & research. Clinical haematology* **17**, 77-87 (2004).
 38. Harcourt, J.L., Caidi, H., Anderson, L.J. & Haynes, L.M. Evaluation of the Calu-3 cell line as a model of in vitro respiratory syncytial virus infection. *J Virol Methods* **174**, 144-149 (2011).
 39. Artursson, P., Palm, K. & Luthman, K. Caco-2 monolayers in experimental and theoretical predictions of drug transport. *Adv Drug Deliv Rev* **46**, 27-43 (2001).
 40. Bacsa, S. *et al.* Syndecan-1 and syndecan-2 play key roles in herpes simplex virus type-1 infection. *The Journal of general virology* **92**, 733-743 (2011).
 41. Hayashida, K., Johnston, D.R., Goldberger, O. & Park, P.W. Syndecan-1 expression in epithelial cells is induced by transforming growth factor beta through a PKA-dependent pathway. *J Biol Chem* **281**, 24365-24374 (2006).
 42. Teng, Y.H., Aquino, R.S. & Park, P.W. Molecular functions of syndecan-1 in disease. *Matrix Biol* **31**, 3-16 (2012).
 43. de Witte, L. *et al.* Langerin is a natural barrier to HIV-1 transmission by Langerhans cells. *Nat Med* **13**, 367-371 (2007).
 44. Sarrami-Forooshani, R. *et al.* Human immature Langerhans cells restrict CXCR4-using HIV-1 transmission. *Retrovirology* **11**, 52 (2014).
 45. Merad, M., Ginhoux, F. & Collin, M. Origin, homeostasis and function of Langerhans cells and other langerin-expressing dendritic cells. *Nat Rev Immunol* **8**, 935-947 (2008).
 46. Nijmeijer, B.M. *et al.* HIV-1 exposure and immune activation enhance sexual transmission of Hepatitis C virus by primary Langerhans cells. *J Int AIDS Soc* **22**, e25268 (2019).
 47. Geijtenbeek, T.B. *et al.* DC-SIGN, a dendritic cell-specific HIV-1-binding protein that enhances trans-infection of T cells. *Cell* **100**, 587-597 (2000).
 48. Gurney, K.B. *et al.* Binding and transfer of human immunodeficiency virus by DC-SIGN+ cells in human rectal mucosa. *J Virol* **79**, 5762-5773 (2005).
 49. Tsang, N.N.Y. *et al.* Diagnostic performance of different sampling approaches for SARS-CoV-2 RT-PCR testing: a systematic review and meta-analysis. *Lancet Infect Dis* (2021).
 50. Wang, H. *et al.* Nasopharyngeal Swabs Are More Sensitive Than Oropharyngeal Swabs for COVID-19 Diagnosis and Monitoring the SARS-CoV-2 Load. *Front Med (Lausanne)* **7**, 334 (2020).
 51. Sungnak, W. *et al.* SARS-CoV-2 entry factors are highly expressed in nasal epithelial cells together with innate immune genes. *Nat Med* **26**, 681-687 (2020).
 52. Randolph, G.J., Angeli, V. & Swartz, M.A. Dendritic-cell trafficking to lymph nodes through lymphatic vessels. *Nat Rev Immunol* **5**, 617-628 (2005).
 53. Pham, A.M., Langlois, R.A. & TenOever, B.R. Replication in cells of hematopoietic origin is necessary for Dengue virus dissemination. *PLoS Pathog* **8**, e1002465 (2012).

54. de Witte, L. *et al.* Syndecan-3 is a dendritic cell-specific attachment receptor for HIV-1. *Proc Natl Acad Sci U S A* **104**, 19464-19469 (2007).
55. Zou, L. *et al.* SARS-CoV-2 Viral Load in Upper Respiratory Specimens of Infected Patients. *N Engl J Med* **382**, 1177-1179 (2020).
56. Müller, L., Brighton, L.E., Carson, J.L., Fischer, W.A., 2nd & Jaspers, I. Culturing of human nasal epithelial cells at the air liquid interface. *J Vis Exp* (2013).
57. Vanders, R.L., Hsu, A., Gibson, P.G., Murphy, V.E. & Wark, P.A.B. Nasal epithelial cells to assess in vitro immune responses to respiratory virus infection in pregnant women with asthma. *Respir Res* **20**, 259 (2019).
58. Zhai, Z. *et al.* Prevention and Treatment of Venous Thromboembolism Associated with Coronavirus Disease 2019 Infection: A Consensus Statement before Guidelines. *Thromb Haemost* **120**, 937-948 (2020).
59. World Health Organization. Clinical management of COVID-19. Interim guidance 27 May 2020: World Health Organization; 2020. Report No.: WHO/2019-nCoV/clinical/2020.5.
60. Lindenbach, B.D. *et al.* Complete replication of hepatitis C virus in cell culture. *Science* **309**, 623-626 (2005).
61. Zhang, Z., Coomans, C. & David, G. Membrane heparan sulfate proteoglycan-supported FGF2-FGFR1 signaling: evidence in support of the "cooperative end structures" model. *J Biol Chem* **276**, 41921-41929 (2001).
62. Mesman, A.W. *et al.* Measles virus suppresses RIG-I-like receptor activation in dendritic cells via DC-SIGN-mediated inhibition of PP1 phosphatases. *Cell Host Microbe* **16**, 31-42 (2014).
63. L.J. Reed, H.M. A simple method of estimating fifty per cent endpoints. *American Journal of Epidemiology* **Volume 27** (1938).
64. Chu, D.K.W. *et al.* Molecular Diagnosis of a Novel Coronavirus (2019-nCoV) Causing an Outbreak of Pneumonia. *Clin Chem* **66**, 549-555 (2020).

Supplementary material

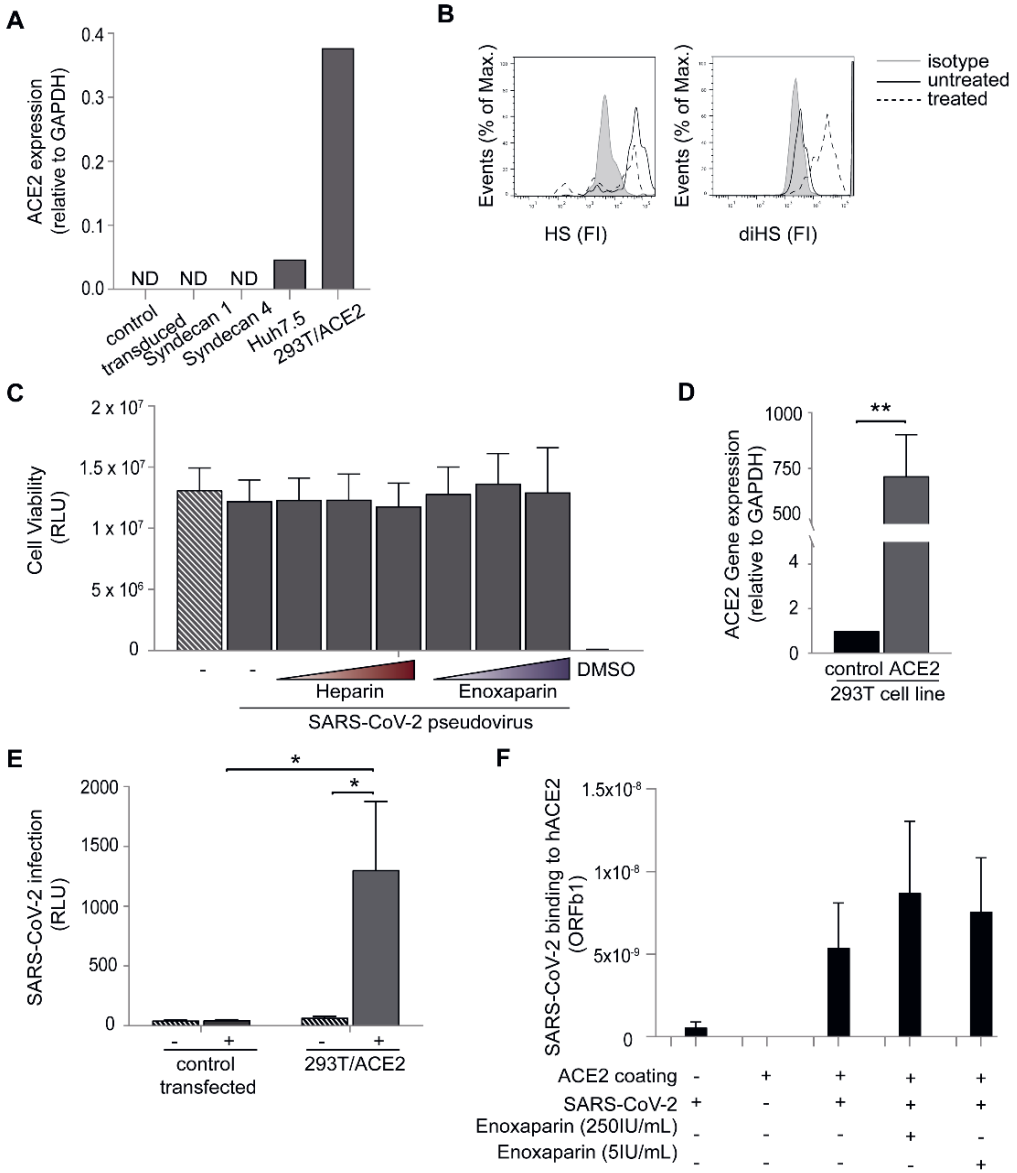


Figure EV1 | Expression of ACE2 and Heparan sulfates in their involvement in SARS-CoV-2 binding and infection.

(A) ACE2 expression was measured for different Namalwa Syndecan cell lines in comparison to Huh7.5 cells and ACE2-transfected 293T. (B) Huh7.5 cells were left untreated or treated with heparinase III for 1 hour at 37°C and heparan sulfate or digested heparan sulfate expression was determined by flow cytometry. Cells were stained for HS and diHS respectively or an isotype control mAb, directly corresponding to the specific antibody (mouse IgM and IgG2b). One representative donor out of 3 is depicted. (C) Cell Viability of infected Huh7.5 with SARS-CoV-2 pseudovirus in presence of different concentrations of UF heparin and LMWH enoxaparin (n=4 in duplicates). (D) Cell surface expression of ACE2 on 293T cells (control and ACE2 transfected) was determined by quantitative real-time PCR. (E) SARS-CoV-2 pseudovirus infection on 293T (control vs ACE2-transfected cells) was measured by

► luciferase reporter activity. (F) SARS-CoV-2 isolate binding capacity to hACE2 was measured by quantitative real-time PCR (ORFb1). SARS-CoV-2 isolate (10000 TCID₅₀/mL) was pre-incubated in presence or absence of different LMWH enoxaparin concentrations (250IU/mL and 5IU/mL) and added to a high binding ELISA plate was coated with recombinant hACE2 (2µg/mL). LMWH enoxaparin (n=3 measured in triplicates). Data information: Data show the mean values and error bars are the SEM. Statistical analysis was performed using (D) unpaired, parametric, Student t-test. *P<0.05, **P<0.01, (E) 2way-ANOVA with Dunnett's multiple-comparison test. *P<0.05, **P<0.01 (n=3 in triplicates), HS: Heparan sulfate, diHS: digested Heparan sulfate, FI: fluorescent intensity, RLU: relative light units, ND: Not determined.

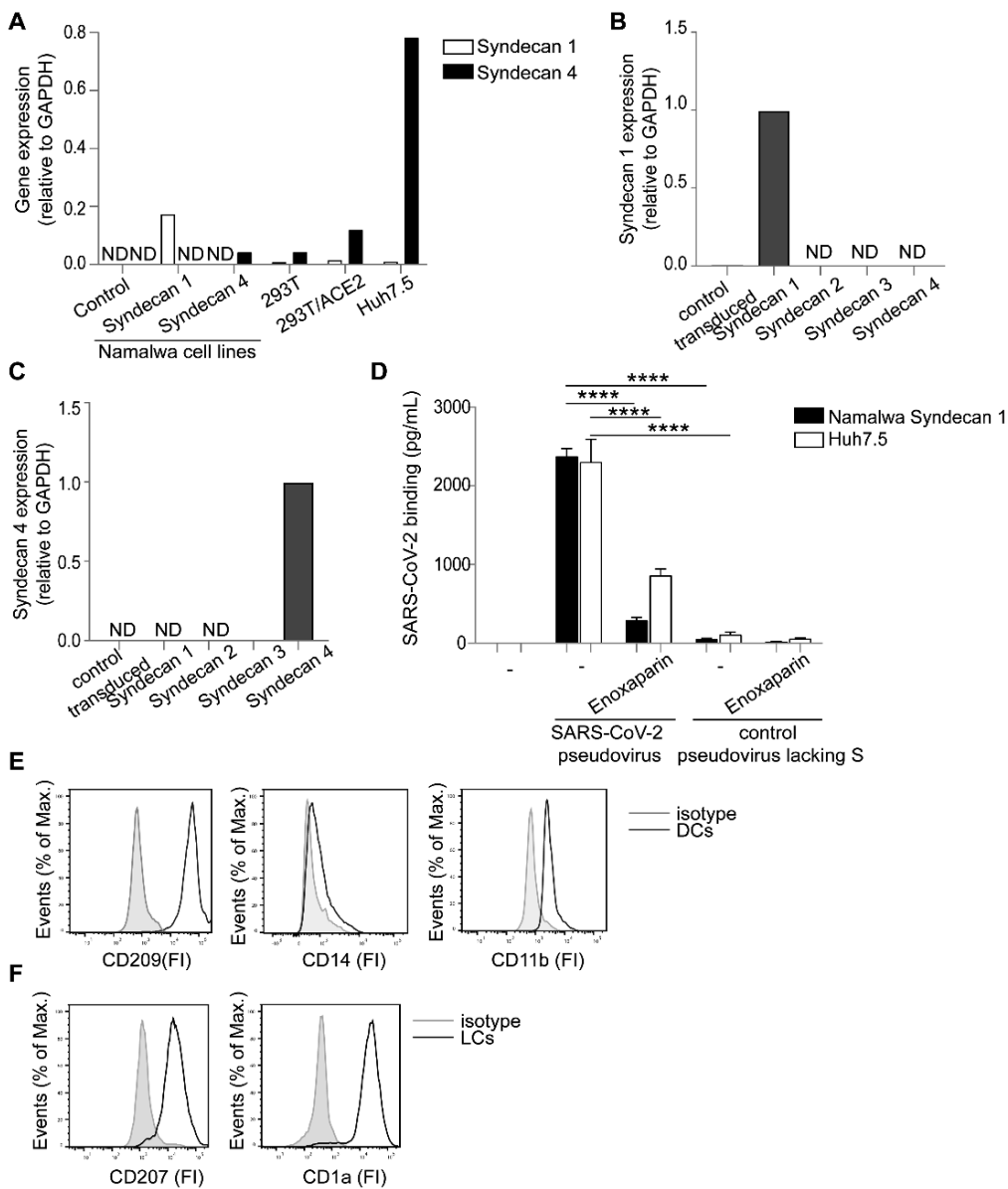


Figure EV2. Figure legend on next page

Figure EV2 | Syndecan expression, cell characterization and interaction of S protein. (A) Syndecan 1 and Syndecan 4 expression by Namalwa cell lines, 293T cell lines and Huh7.5 cells was detected by quantitative real-time PCR. Representative data for an experiment repeated more than three times with similar results. (B, C) Different Namalwa Syndecan cell lines expressing Syndecan 1 (B) or Syndecan 4 (C), determined by quantitative real-time PCR. (D) Huh7.5 and Namalwa cells ectopically expressing Syndecan 1 were exposed to SARS-CoV-2 pseudovirus or control pseudovirus lacking S protein, in presence or absence of LMWH enoxaparin (250IU/mL). Binding was measured after 4 hours at 4°C by ELISA. (E) DCs were stained with antibodies against the surface markers CD209, CD14 and CD11b and analysed by flow cytometry. (F) LCs were stained with antibodies against CD207 and CD1a and analysed by flow cytometry. The histogram shows the cell surface expression of the receptor. Data information: Data show the mean values and error bars are the SEM. Statistical analysis was performed using (D) 2way-ANOVA with Tukey's multiple-comparison test. * $P \leq 0.05$, ** $P \leq 0.01$, *** $P \leq 0.001$, **** $P \leq 0.0001$ (n=2 in triplicates). DCs: Dendritic cells, LCs: Langerhans cells, ND: Not determined, FI: fluorescent intensity.

Figure EV3 | Non-normalized SARS-CoV-2 binding and infection of cell lines. (A, B) Polarized Calu-3 were infected with SARS-CoV-2 isolate (hCoV-19/Italy, 0.5 TCID₅₀/mL) in presence or absence of antibodies against ACE2 or LMWH enoxaparin (250 IU/mL). Virus was detected after lysis by quantitative real-time PCR of viral RNA (A) and virus production was determined by detecting viral RNA in supernatant using quantitative real-time PCR (B). (C) SARS-CoV-2 isolate (hCoV-19/Italy) was pre-incubated with LMWH enoxaparin (250 IU/mL) for 30 min at 37°C. Namalwa cells expressing Syndecan 1 and 4 were exposed to 100 TCID₅₀/mL SARS-CoV-2 isolate for 4 hours at 4°C and binding was determined by quantitative real-time PCR. (D) SARS-CoV-2 isolate (hCoV-19/Italy, 100 TICD₅₀/mL) was added to Namalwa cells either directly or after pre-incubation for 30 min at 37°C with LMWH enoxaparin (250 IU/mL) or neutralizing antibodies (COVA1-18, 1-21 and 2-15), non-neutralizing antibody (COVA1-27) and a human IgG1isotype control at the concentration of 1pg/mL. Detection of viral binding to Syndecan 1 expressing Namalwa was measured after 4 hours at 4°C by quantitative real-time PCR. Data information: Data show the mean values and error bars are the SEM. Statistical analysis was performed using (B) ordinary one-way ANOVA with Tukey's multiple-comparison test. * $P \leq 0.05$, ** $P \leq 0.01$, *** $P \leq 0.001$, **** $P \leq 0.0001$ (n=3 donors measured in monoplo). (C) 2way-ANOVA with Sidak's multiple-comparison test. * $P \leq 0.05$, ** $P \leq 0.01$, *** $P \leq 0.001$, **** $P \leq 0.0001$ (n = 3 measured in triplicate). (D) ordinary one-way with Tukey's multiple-comparison test. * $P \leq 0.05$, ** $P \leq 0.01$. (n = 2 measured in duplicates).

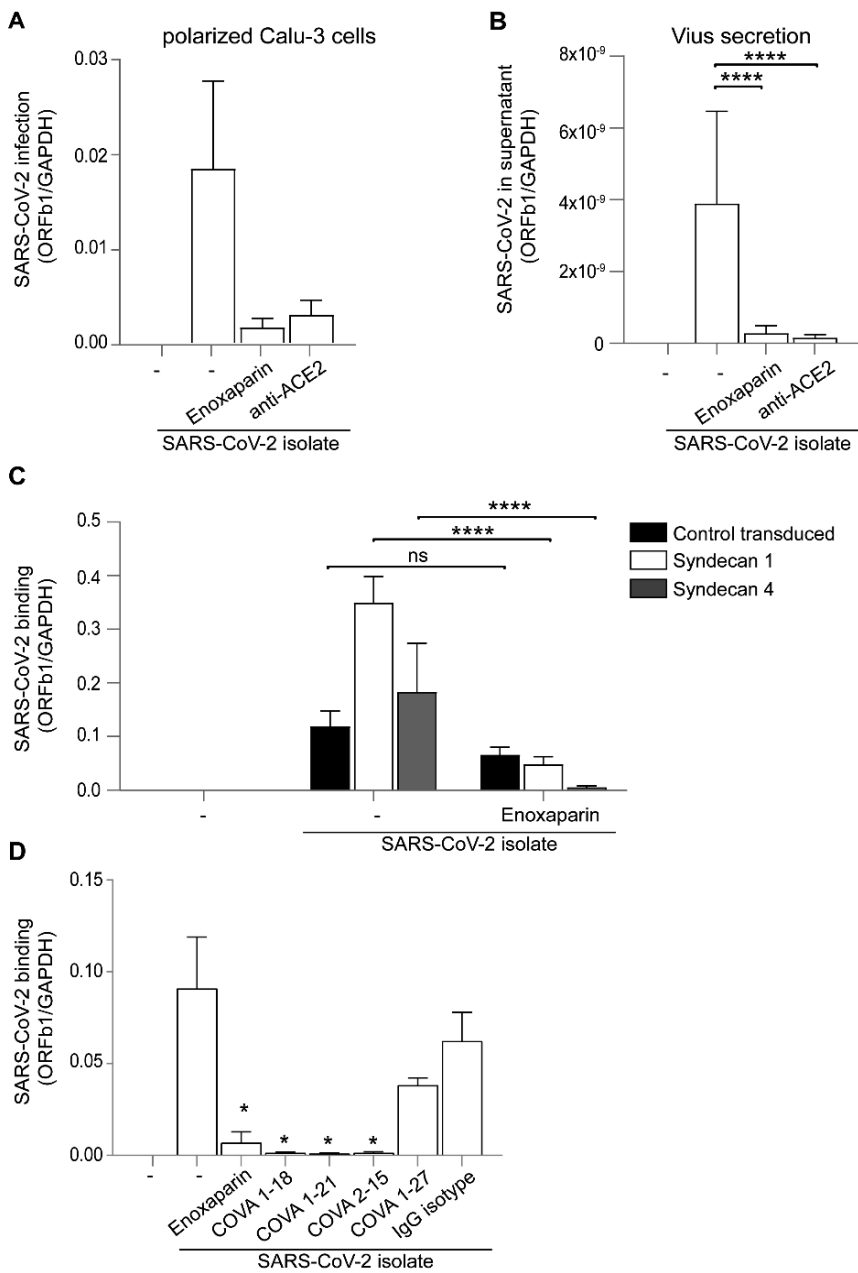


Figure EV3. Figure legend on previous page

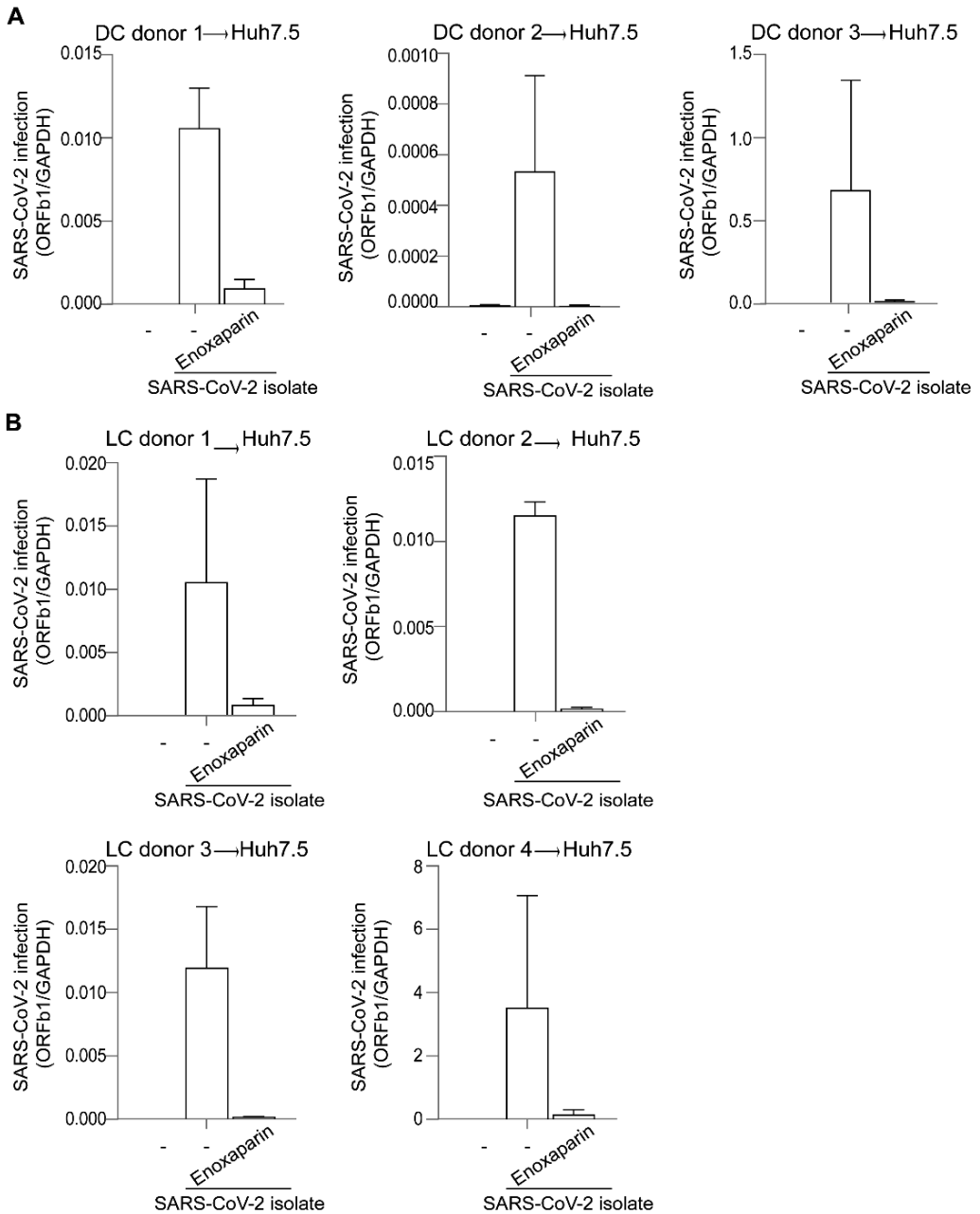


Figure EV4 | Non-normalized SARS-CoV-2 transmission by dendritic cell subsets. (A, B) SARS-CoV-2 isolate (hCoV-19/Italy, 100TCID₅₀/mL) was either pre-treated with LMWH enoxaparin (250 IU/mL) for 30 min at 37°C. DCs (n=3 independent donors) (A) and LCs (B) were exposed to untreated or pre-treated SARS-CoV-2 (isolated for 24h, washed thoroughly and subsequently co-cultured with Huh7.5 cells for another 24 hours. Quantification of viral RNA was measured by quantitative real-time PCR of Huh7.5 cells after removal of DCs or LCs.

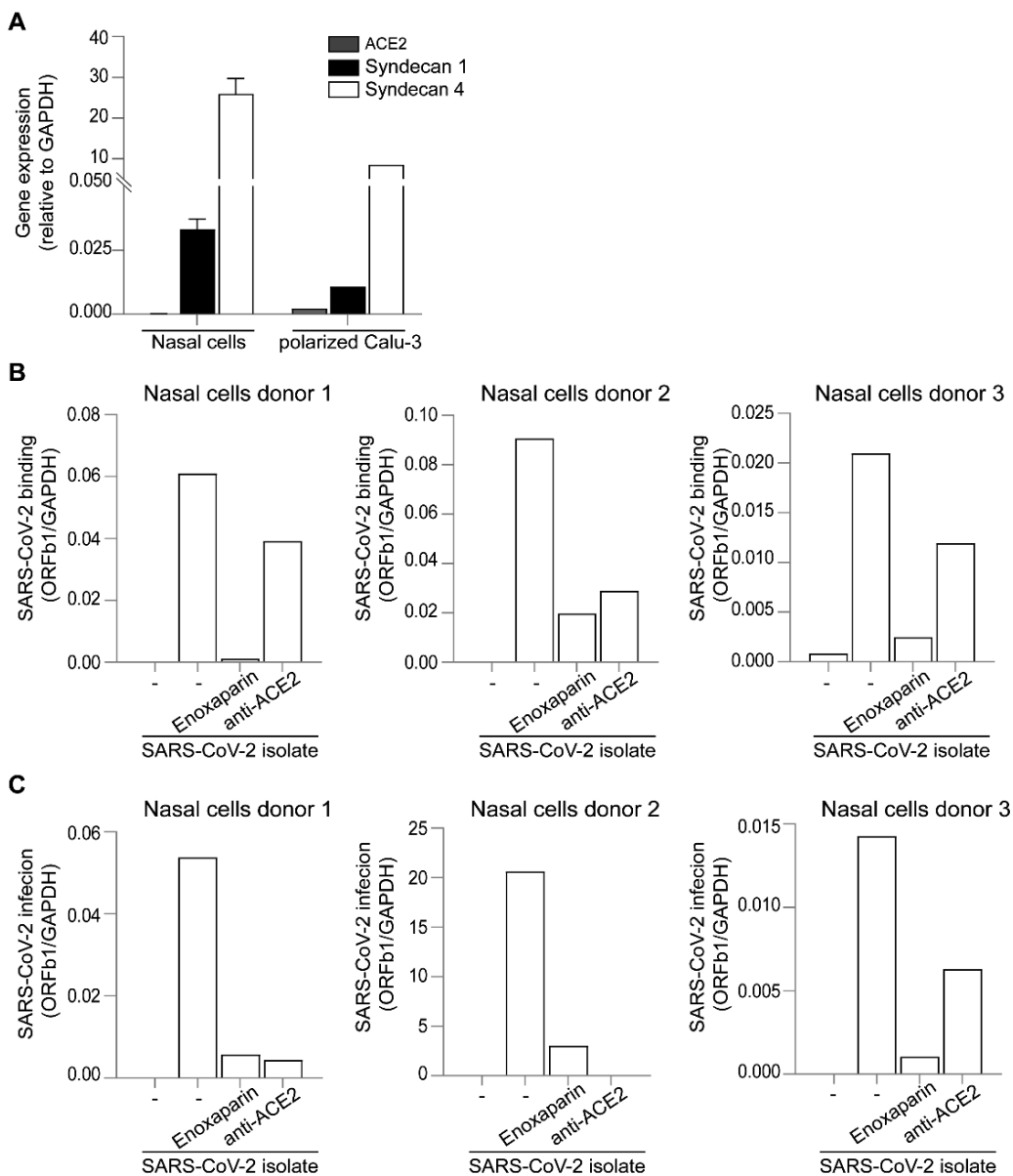


Figure EV5 | Non-normalized SARS-CoV-2 binding and infection of primary nasal cells. (A) ACE2, Syndecan 1 and Syndecan 4 cell surface expression on nasal cells compared to polarized epithelial Calu-3 was confirmed by quantitative real-time PCR. (B, C) Nasal epithelial cells were exposed to SARS-CoV-2 isolate (hCoV-19/Italy, 100TCID₅₀/mL) either directly or in presence of antibodies against ACE2 or after pre-incubation with LMWH enoxaparin (250 IU/mL). Detection of viral binding (B) and persistently-infected cells (C) was determined by quantitative real-time PCR.



CHAPTER

7

Inhalation of Low Molecular Weight Heparins as prophylaxis against SARS-CoV-2

Julia Eder^{1,2*}, Marta Bermejo-Jambrina, PhD^{1,2*}, Killian E. Vlaming, MD^{1,2*}, Tanja M. Kaptein¹, Viktoria Zaderer, PhD³, E. Marleen Kemper, PhD⁴, Doris Wilflingseder, PhD³, Sietze Reitsma, MD, PhD⁵, Godelieve J. de Bree, MD, PhD^{6,2}, Danny M. Cohn, MD, PhD^{7,8}, Teunis B. Geijtenbeek, PhD^{1,2}

¹Amsterdam UMC location University of Amsterdam, Department of Experimental Immunology, Meibergdreef 9, Amsterdam, The Netherlands

²Amsterdam institute for Infection and Immunity, Amsterdam, The Netherlands

³Institute of Hygiene and Medical Microbiology, Medical University of Innsbruck, Innsbruck, Austria.

⁴Amsterdam UMC location University of Amsterdam, Department of Pharmacy and Clinical Pharmacology, Meibergdreef 9, Amsterdam, The Netherlands

⁵Amsterdam UMC location University of Amsterdam, Department of Otorhinolaryngology, Meibergdreef 9, Amsterdam, The Netherlands.

⁶Amsterdam UMC location University of Amsterdam, Department of Internal Medicine, Meibergdreef 9, Amsterdam, The Netherlands.

⁷Amsterdam UMC location University of Amsterdam, Department of Vascular Medicine, Meibergdreef 9, Amsterdam, The Netherlands.

⁸Amsterdam institute of Cardiovascular sciences, Amsterdam, The Netherlands.

*Authors contributed equally to this paper.

Published in mBio. 2022 Dec 20;13(6):e0255822.

doi: 10.1128/mbio.02558-22. Epub 2022 Nov 3.

Abstract

New SARS-CoV-2 variants of concern and waning immunity demonstrate the need for a quick and simple prophylactic agent to prevent infection. Low molecular weight heparins (LMWH) are potent inhibitors of SARS-CoV-2 binding and infection *in vitro*. The airways are a major route for infection and therefore inhaled LMWH could be a prophylactic treatment against SARS-CoV-2. We investigated the efficacy of *in vivo* inhalation of LMWH in humans to prevent SARS-CoV-2 attachment to nasal epithelial cells in a single-center, open label intervention study. Volunteers received enoxaparin in the right and placebo (NaCl 0.9%) in the left nostril using a nebulizer. After application, nasal epithelial cells were retrieved with a brush for *ex vivo* exposure to either SARS-CoV-2 pseudovirus or an authentic SARS-CoV-2 isolate and virus attachment as determined. LMWH inhalation significantly reduced attachment of SARS-CoV-2 pseudovirus as well as authentic SARS-CoV-2 to human nasal cells. Moreover, *in vivo* inhalation was as efficient as *in vitro* LMWH application. Cell phenotyping revealed no differences between placebo and treatment groups and no adverse events were observed in the study participants. Our data strongly suggest that inhalation of LMWH is effective to prevent SARS-CoV-2 attachment and subsequent infection. LMWH are ubiquitously available, affordable and easy to apply, making them suitable candidates for prophylactic treatment against SARS-CoV-2.

Keywords: low molecular weight heparin, SARS-CoV-2, infection prevention, virus-host interactions

Importance

New SARS-CoV-2 variants of concern and waning immunity demonstrate the need for a quick and simple agent to prevent infection. Low molecular weight heparins (LMWH) have been shown to inhibit SARS-CoV-2 in experimental settings. The airways are a major route for SARS-CoV-2 infection and inhaled LMWH could be a prophylactic treatment. We investigated the efficacy of inhalation of the LMWH enoxaparin in humans to prevent SARS-CoV-2 attachment as this is a prerequisite for infection. Volunteers received enoxaparin in the right and placebo in the left nostril using a nebulizer. Subsequently, nasal epithelial cells were retrieved with a brush and exposed to SARS-CoV-2. LMWH inhalation significantly reduced binding of SARS-Cov-2 to human nasal cells. Cell phenotyping revealed no differences between placebo and treatment groups and no adverse events were observed in the participants. Our data strongly indicate that LMWH can be used to block SARS-CoV-2 attachment to nasal cells. LMWH are ubiquitously available, affordable and easily applicable, making them excellent candidates for prophylactic treatment against SARS-CoV-2.

Introduction

Severe Acute Respiratory Syndrome Coronavirus 2 (SARS-CoV-2) emerged in Wuhan (China) in 2019 and quickly spread to the rest of the world, resulting in a global health crisis^{1, 2, 3}. SARS-CoV-2 belongs to the beta coronaviruses and causes COVID-19, an influenza-like disease ranging from mild respiratory symptoms to progressive inflammatory viral pneumonia, multi-organ disease and death^{4, 5, 6}. Since 2020, large scale deployment of more than 30 approved vaccines have curbed viral spread and offered strong protection against severe disease and hospitalization^{7, 8, 9}. However, continuous emergence of Variants of Concern (VoC), which are more contagious and potentially less susceptible to current vaccines, underscore the need for additional preventive methods and novel treatments for severe COVID-19^{10, 11, 12, 13}. It is also becoming clear that vaccinations are less effective in immunocompromised people^{14, 15, 16}. Thus, there is an urgent need for prophylactic treatments that prevent SARS-CoV-2 infections to address emerging VoC or protect vulnerable patient groups.

One of the routes of viral transmission is person-to-person via aerosolized droplets from the upper, conducting and lower airways of infected people^{17, 18, 19}. Upon inhalation, droplets depending on the size can reach the upper or lower airways where infection can occur in airway epithelial cells²⁰. Therefore, a potential strategy for a prophylactic agent is to interfere with viral entry into airway epithelial cells, blocking infection at the earliest stage.

Angiotensin-converting enzyme 2 (ACE-2) is the main receptor used by SARS-CoV-2; the viral Spike (S) protein interacts with ACE-2 leading to viral entry into human cells^{21, 22, 23}. ACE-2 is expressed by different epithelial cells of the respiratory tract as well as alveolar macrophages^{24, 25}. Recent studies have shown that SARS-CoV-2 interacts strongly with heparan sulfate proteoglycans (HSPG) to attach to the cells, a prerequisite for infection via ACE-2^{26, 27, 28}. HSPG are highly sulfated, negatively charged transmembrane receptors that are broadly expressed by different cells including respiratory epithelial cells^{29, 30, 31}. In the nose, the olfactory neuroepithelium is rich in HSPG expression³². HSPG are also ubiquitously present in the lungs, where they are involved in maintaining the endothelial surface layer, pulmonary development, cellular signaling and early immune activation^{33, 34}. A range of viruses including HIV-1, HCV and Human coronavirus NL63 exploit HSPG for cellular attachment^{35, 36, 37}. On epithelial cells, the HSPG family members Syndecan 1 and 4 have been shown to mediate SARS-CoV-2 attachment and infection²⁸. Heparin and low molecular weight heparins (LMWH) competitively block SARS-CoV-2 binding to epithelial cells^{27, 38} and thereby prevent infection. LMWH have long been used in the clinic as anticoagulant therapeutics^{39, 40} and LMWH might be used as prophylactic treatments to prevent infection of SARS-CoV-2.

Here we investigated whether *in vivo* nasal inhalation of LMWH enoxaparin protects against SARS-CoV-2.

Materials and Methods

Study design

We designed a single center, non-randomized controlled trial conducted at the Amsterdam UMC in Amsterdam. The study was registered at the European drug regulatory affairs for Clinical Trials (EudraCT) under code 2020-003992-16, at the Dutch clinical trial registry under code NL9430, and was conducted in accordance with the principles of Good Clinical Practice and the Declaration of Helsinki, in compliance with all relevant national and international regulations. The study was approved by the local ethics committee (METC) and granted under code METC 2020_223 in accordance with national guidelines. The local ethics committee reviewed and approved the study and it is registered at the national body responsible for supervising clinical trials under code NL75272.018.20

Medication was aseptically prepared at the pharmacy department. All analyses were performed within the Laboratory of Experimental Immunology within the Amsterdam UMC. All work with SARS-CoV-2 was performed in a biosafety laboratory level 3 facility at our institution. Volunteers were recruited from the University of Amsterdam. All participants provided written informed consent before any study procedures were performed.

Participants

Based on previous *in vitro* data we expected to observe a reduction of 50% SARS-CoV-2 virus binding between treatment and placebo samples, to achieve a power of >80% at 0,05 statistical significance 12 volunteers would be needed per SARS-CoV-2 variant. The recruitment period lasted from 07/01/2021 till 14/12/2021, during this period a total of 36 volunteers were assessed for eligibility. Volunteer inclusion was done longitudinally to investigate whether all conditions could be performed for each volunteer, an extra volunteer would be included if this was not the case. Both genders were eligible to participate. Other inclusion criteria were age between 18 and 65 years, the ability to provide written informed consent, good physical health, which was defined as not suffering from any illness or disease obstructing general daily functioning, and to sufficiently understand Dutch in the opinion of the research physician taking informed consent. Exclusion criteria were positivity for SARS-CoV-2, as was tested during the study visit with a commercial SARS-CoV-2 antigen test (SARS-CoV-2 Antigen Rapid Test Kit, JOYSBIO (Tianjin) Biotechnology Co. Ltd), the presence of nasal-septum defects, usage of intranasal medication, frequent nosebleeds (defined as >1/month), a tympanic temperature exceeding 38,5 degrees Celsius during the clinical visit, anamnestic or physical evidence of a respiratory infection in the four weeks prior to the clinical visits, a known allergy or intolerance to LMWH or heparin-related products, a medical history of heparin induced thrombocytopenia (HIT), the presence of mental disorders that would interfere with

adherence to study procedures or behavior making a volunteer unlikely to comply with study procedures in the opinion of the research physician present during the clinical visit. Vaccination status was self-reported with all volunteers receiving the enoxaparin treatment were fully vaccinated according to national guidelines (1x COVID-19 vaccine Janssen, Janssen. 2x Comirnaty, BioNTech/Pfizer or 2x Spikevax, Moderna mRNA vaccine). Additionally, 6 unvaccinated volunteers and 1 partially vaccinated volunteer were included for analysis of SARS-CoV-2 binding. However, these 7 volunteers were excluded from enoxaparin block analysis due to insufficient treatment application. Inclusion of volunteers and processing of volunteer material is displayed in detail in **Figure. 1**.

Enoxaparin administration

Enoxaparin at a dose of 4500IU and placebo (saline NaCl 0,9%) were administered in the nasal cavity using a nebulizer (MAD Nasal™ Intranasal Mucosal Atomization Device). We selected LMWH enoxaparin (Clexane Forte, 150mg/ml) as we previously have shown that it effectively blocks SARS-CoV-2 infection *in vitro*²⁸. Nebulization efficiency was investigated with a green tracer dye. Enoxaparin concentrations were not measured as this was technical challenging but the same enoxaparin concentration was applied to every volunteer. Volunteers first received 370 µL of saline solution (NaCl 0,9%) in the left nasal cavity using a nebulizer (MAD Nasal™ Intranasal Mucosal Atomization Device). A total of 300 µL of fluid was administered, as 70 µL remained within the dead space of the nebulizer. 100 µL was nebulized per 10-minute intervals to facilitate absorption by the nasal mucosa and epithelial cells were removed using a nasal brush (CytoSoft brush). Subsequently, 370 µL of LMWH enoxaparin (Clexane Forte, 150mg/ml) was administered in the right nasal cavity in an identical fashion as for the left nostril described above. After 30 min, cells were removed using a similar procedure. Participants were observed for the occurrence of adverse events during the study procedures. At 24 hours after treatment follow-up was performed via a telephone call. Brushes containing nasal epithelium were stored in an 1.5mL sterile microcentrifuge tube containing 0,5 ml of Iscove's Modified Dulbecco's Medium (IMDM), enriched with 10% Fetal Calf Serum (FCS), 1% Penicillin/Streptomycin, 1% L-Glutamin and 20 µg/ml Gentamycin (Thermo Fischer Scientific, USA) to maintain vitality of obtained cells.

Nasal cell characterization

Cell population characterization from the nasal tissue was performed by flow cytometric analyses of intracellular and cell surface expression markers. The gating strategy for FACS analysis is shown in **Figure. 3**. Single cells were further gated from the living population. Isolated cells were washed once with PBS and stained for Pan-Cytokeratin (panC) as well as CD45 to distinguish between epithelial or lymphoid origin. Additionally, cells were analyzed for the expression of ACE-2 and heparan sulfates (extracellular only) and other epithelial

markers (EpCAM and Mucin 5b (Muc-5b)) as well as lymphoid markers CD3, CD11b and CD11c. Some samples for flow cytometry, but not virus attachment analysis, were contaminated with erythrocytes and were excluded. Flow Cytometry analysis were performed on a BD FACS Canto II (BD Biosciences) and data was analyzed using FlowJo v10.8.1 (Software by Treestar).

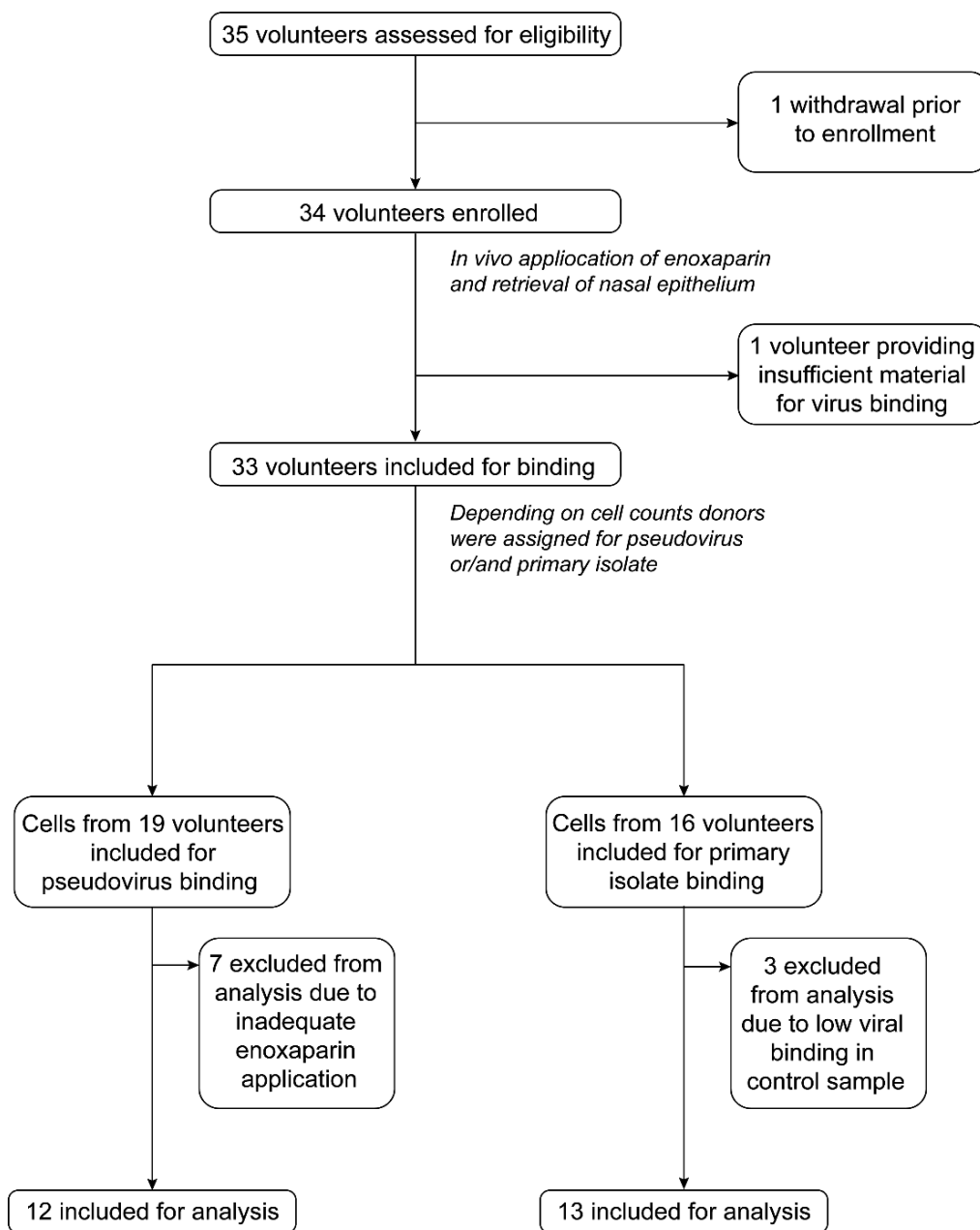


Figure 1. Figure legend on next page.

Figure 1 | Flowchart of the volunteer inclusion. Volunteers were recruited within the AMC between 07/01/2021 and 14/12/2021. Both genders were eligible to participate. Inclusion criteria were an age between 18 and 65, good physical health (defined as not suffering from any illness or disease obstructing general daily functioning), sufficient understanding of the Dutch language to comply to study procedures. Exclusion criteria were a positive SARS-CoV-2 antigen test (SARS-CoV-2 Antigen Rapid Test Kit, JOYSBIO (Tianjin) Biotechnology Co. Ltd), nasal-septum defects, usage of intranasal medication, frequent nosebleeds (>1/month), fever during the study visit (tympanic temperature >38,5°C during clinical visit), anamnestic or physical evidence of a respiratory infection in the four weeks prior to the clinical visit, a known allergy or intolerance to LMWH or heparin-related products, a medical history of heparin induced thrombocytopenia (HIT), the presence of mental disorders that would interfere with adherence to study procedures. Description of the inclusion process and parameters analysis: 35 volunteers were assessed for eligibility, 1 volunteer withdrew prior to enrolment. 34 volunteers were enrolled and received placebo and 4500IE enoxaparin via nasal spray. Subsequently nasal epithelium was withdrawn and counted. 1 volunteer provided insufficient cellular material for all experiments and binding was subsequently not performed. Cells were plated and distributed into three categories for exposure to different viruses. 19 donors provided material for pseudovirus binding. After the first 7 donors we have adapted the protocol due to inefficient application of enoxaparin as measured by a tracer dye and these donors were excluded from the analysis. 12 donors were included for analysis. 16 donors provided material for authentic SARS-CoV-2 virus binding. 3 donors were excluded for analysis as the virus failed to bind in the placebo samples. 13 donors were included for analysis. There was overlap between donors, with 2 donors providing material for both SARS-CoV-2 pseudovirus and authentic virus binding.

VeroE6 culture

VeroE6 cells (ATCC® CRL-1586™) were cultured in CO₂ independent medium (Gibco Life Technologies, Gaithersburg, Md.) supplemented with 10% fetal calf serum (FCS), L-glutamine, and penicillin/streptomycin (10 µg/mL). Culture was maintained at 37°C without CO₂. The VeroE6-ACE2-TMPRSS2 cell line (NISBC, 101003) expresses high levels of ACE2 and TMPRSS2⁴¹. These cells were maintained in Dulbecco's modified Eagle's high glucose medium supplemented with 10% FCS, 1% L-Glutamine, 1% Penicillin/Streptomycin; all reagents were obtained from Sigma Aldrich, Missouri, USA) at 37C with a saturation of 5% CO₂.

Viruses

SARS-CoV-2 pseudovirus consists of a single round virus with an HIV-1 backbone (pNL4-3.Luc.R-S-) containing mutations in the capsid protein (as described in⁴²) and a firefly luciferase gene in the nef open reading frame as well as pSARS-CoV-2 expressing SARS-CoV-2 S protein (GenBank; MN908947.3)⁴³. The wild-type (WT) authentic SARS-CoV-2 virus hCoV-19/WT, was obtained from Dr. Maria R. Capobianchi through BEI Resources, NIAID, NIH: SARS-Related Coronavirus 2, Isolate Italy-INMI1, NR-52284, originally isolated January 2020 in Rome, Italy. SARS-CoV-2 authentic virus stocks from primary isolates were produced in VeroE6 cells. Cytopathic effect (CPE) formation was closely monitored and after 48 hours the virus supernatant was harvested. Viral titers were

determined by tissue culture infectious dose (TCID₅₀) on VeroE6 cells. In short, VeroE6 cells were seeded in a 96 well plate at a cell density of 10.000 cells. The following day the cells were inoculated with a 5-fold serial dilution of SARS-CoV-2 isolate in quadruplicate. Cell cytotoxicity was measured using an MTT assay 48 hours after infection. Loss of MTT staining as determined by spectrometer (OD 580 nm) is indicative of SARS-CoV-2 induced CPE. Viral titer was determined as TCID₅₀/mL and calculated based on the method first proposed by Reed & Muench⁴⁴. SARS-CoV-2 WT virus (BEI Resources, Manassas, VA, USA; CFAR/NIBSC; Nr-52281) was used for the 3D epithelial cell model of I human bronchial epithelial (NHBE) cultures and propagated according to the manufacturer's instructions. Clinical specimens for SARS-CoV-2 VoC Delta (B.1.617.2) and Omicron (BA.5) were isolated from COVID-19 positive swabs (Ethics statement, ECS1166/2020) and cultured as previously described⁴⁵.

***Ex vivo* SARS-CoV-2 binding to nasal epithelial cells**

After isolation from the nasal cavity, epithelial cells were subjected to SARS-CoV-2 pseudovirus and authentic SARS-CoV-2 virus. SARS-CoV-2 pseudovirus binding was performed with 100.000 cells per condition, while binding with the authentic virus was performed with 50.000 cells per condition. Cells were seeded in a 96 well round bottom plate within 4 hours of retrieval from the nasal cavity and incubated with either 95 ng/mL SARS-CoV-2 pseudovirus or 100 TCID₅₀/mL of authentic virus (hCoV-19, WT) for 4 hours at 4°C. In order to determine whether *in vivo* inhalation provided the most optimal block, a condition was included where viruses were incubated with 250 IU/mL of LMWH enoxaparin for 30 min at 37°C before being added to cells from volunteers. The cells were subsequently washed to remove any unbound virus. Cells incubated with SARS-CoV-2 pseudovirus were lysed after 4 hours and binding and internalization were quantified by RETRO-TEK HIV-1 p24 ELISA according to manufacturer instructions (ZeptoMetrix Corporation). Cells incubated with SARS-CoV-2 isolate (hCoV-19/WT) were lysed with AVL buffer and RNA was isolated with the QIAamp Viral RNA Mini Kit (Qiagen) according to the manufacturers' protocol. cDNA was synthesized with the M-MLV reverse-transcriptase kit (Promega) and diluted 1 in 5 before further application. Virus quantification was performed using RT-PCR in the presence of SYBR green in a 7500 Fast Realtime PCR System (ABI). Primer sequences used for mRNA expression were for gene product: GAPDH, forward primer (CCATGTTTCGTCATGGGTGTG), reverse primer (GGTGCTAA GCAGTTGGTGGTG). For gene product SARS-CoV-2 ORf1b, forward primer (TGGGGTTTTACAGGTAACCT), reverse primer (AACACGCTTAACAAAGCACTC) as described previously⁴⁶. The normalized amount of target mRNA was calculated from the Ct values obtained for both target and household mRNA with the equation $Nt = 2Ct(GAPDH) - Ct(target)$.

Enoxaparin application *in vitro*

VeroE6 cells were seeded with 10.000 cells/well in a 96-well plate with CO₂ independent medium. The following day, authentic SARS-CoV-2 virus (10.500 TCID₅₀/ml) was incubated with different concentrations of enoxaparin for 30 min at 37°C. Subsequently, the virus/enoxaparin mix was added to the VeroE6 cells. Binding of SARS-CoV-2 was determined after 4 hours of incubation at 4°C whereas SARS-CoV-2 infection was measured after 24 hours of incubation at 37°C. Alternatively, enoxaparin was applied directly to the cells for 30 min before exposure to authentic SARS-CoV-2. Binding and infection were performed as described above. SARS-CoV-2 levels were determined by RT-PCR as described above.

3D epithelial cell model of Caco-2

The human epithelial Caco-2 cell line (ATCC, HTB-37™) was used for SARS-CoV-2 binding in addition to patient material. The cells were cultured on a 5.0 µm microporous filters with an air-liquid interface to achieve a polarized monolayer in a static *in vitro* 3D epithelial model. The model was maintained in Dulbecco modified Eagle medium (Gibco Life Technologies, Gaithersburg, Md.) containing 10% fetal calf serum (FCS), L-glutamine and penicillin/streptomycin (10 µg/mL) and supplemented with MEM Non-Essential Amino Acids Solution (NEAA) (Gibco Life Technologies, Gaithersburg, Md.). Polarization was monitored by trans epithelial electrical resistance (TEER) and full polarization was reached after 3 weeks in culture, as described previously²⁸. Caco-2 cells express ACE-2 as well as heparan sulfates. Upon full polarization, the cells were exposed to SARS-CoV-2 pseudovirus for 4 hours at 4°C or authentic virus (hCoV-19/WT) for 24 hours at 37°C before lysis.

3D epithelial cell model of normal human bronchial epithelial cells

Normal human bronchial epithelial (NHBE, Lonza, catalog no. C-2540S) cells were cultured in air-liquid interphase (ALI) as described previously^{47,48}. cells were seeded onto GrowDexT (UPM)-coated 0.33-cm² porous (0.4-µm) polyester membrane inserts with a seeding density of 1 × 10⁵ cells per Transwell (Costar, Corning, NY, USA). The cells were grown to near-confluence in submerged culture for 2 to 3 days in specific epithelial cell growth medium according to the manufacturer's instructions. Cultures were maintained in a humidified atmosphere with 5% CO₂ at 37°C and then transferred to ALI culture. The epithelium was differentiated using airway medium from Stemcell. Under these conditions the cells develop stable tight junctions and are highly mucus producing⁴⁸. The number of days in tissue development was designated relative to initiation of ALI culture, corresponding to day 0 and monitored by TEER. Enoxaparin spray was applied to the apical side of the fully polarized epithelia prior SARS-CoV-2 infection. The spray application corresponded to approximately 50 µL of liquid well dispersed over the tissue culture. The

apical application was carefully performed to not mechanically disrupt the epithelial surface. TEER values were measured using an EVOM voltohmmeter with STX-2 chopstick electrodes (World Precision Instruments, Stevenage, United Kingdom). Measurements on cells in ALI culture were taken immediately before the medium was exchanged. For measurements, 0.1 ml and 0.7 ml of medium were added to the apical and basolateral chambers, respectively.

SARS-CoV-2 was added at a concentration of MOI0.1 for each authentic SARS-CoV-2 strain (WT, and VoC Delta (B.1.617.2) and Omicron (BA.5)). Infection was measured after 24 hours incubation at 37°C. SARS-CoV-2 RNA (140 µL) was extracted using FavorPrep Viral RNA Mini Kit (FAVORGEN, Ping-Tung, Taiwan), according to manufacturer's instructions. Sequences specific to region N1 of Nucleocapsid gene published on the CDC website (<https://www.cdc.gov/coronavirus/2019-ncov/lab/rt-pcr-panel-primer-probes.html>) were used. Luna Universal Probe One-Step RT-PCR Kit (New England BioLabs, Ipswich, Mass) was used for target amplification, and runs were performed on the CFX96 real-time detection system (Bio-Rad). For absolute quantification using the standard curve method, SARS-CoV-2 RNA was obtained as a PCR standard control from the National Institute for Biological Standards and Control UK (Ridge, UK).

Statistical analysis

The power calculation of our sample size was based on our requirements for the primary endpoint. Based on this it was determined we would require sufficient cells of 12 volunteers to achieve >80% powering with a certainty of 95%. Statistical analysis of obtained data was performed using Graphpad Prism 9 (Graphpad Software Inc.). Normal distribution of baseline data (Age, sex, cell-count per brush) was not assumed due to the distribution of samples and the small sample size. It was calculated for both cohorts using the Shapiro-Wilk test and found not to be normally distributed. A two-tailed student's t-test was used for paired observations, Mann-Whitney tests were performed for unpaired observations (Differences between donors or cohorts was seen as paired, differences between individual donors as unpaired.). One-way ANOVA, Two-way ANOVA and Mann-Whitney tests were performed for unpaired non-parametric observations. IC50 was calculated using a sigmoidal nonlinear regression. Statistical significance for our results was set *P< 0.05, **P<0.01, ***P<0.001, ****P<0.0001.

Role of the funding source

The funders of the study had no role in study design, data collection, data analysis, data interpretation, or writing of the manuscript.

Results

Baseline characteristics

35 Volunteers were assessed for eligibility to participate in the clinical study. One volunteer withdrew prior to enrollment. 34 volunteers were enrolled. Vaccination status was assessed by way of self-reporting. Of the first seven volunteers, six were included prior to the start of the Dutch national SARS-CoV-2 vaccination campaign and were not vaccinated at inclusion. One volunteer was employed within healthcare and had received one dose of BioNTech/Pfizer mRNA vaccine as part of the early Dutch vaccination roll-out in January 2021. All other 27 volunteers were fully vaccinated according to national guidelines (1x COVID-19 vaccine Janssen, Janssen. 2x Comirnaty, BioNTech/Pfizer or 2x Spikevax, Moderna mRNA vaccine). After the initial 7 volunteers we changed the procedure for application of enoxaparin to provide a more homogenous coverage of enoxaparin. Therefore the first 7 volunteers were excluded from the analyses of the enoxaparin efficacy study.

In total, 25 samples were included for virus binding, material for this was provided by 23 volunteers, with two volunteers providing samples for both viruses. Of these 13 were male and 10 female. Ages ranged between 18 and 65 years with the majority of volunteers being between 20 and 32 years of age with a median age of 33. Only two volunteers were above the age of 60. Details are displayed within **Table 1**.

Table 1: Baseline characteristics

| Characteristic | All (n = 23) | SARS-CoV-2 Pseudovirus (n = 12) |
|---|-------------------------------------|---------------------------------|
| Age* | 33 (21-60) | 33.2 (21-60) |
| Female | 43.4% | 33.3% |
| Vaccination status | 100% fully vaccinated | 100% fully vaccinated |
| SARS-CoV-2 infection in medical history | 0% | 0% |
| SARS-CoV-2 antigen test | 100% negative | 100% negative |
| Tympanic temperature upon study visit* | 36.7°C (36.0°C - 37.4°C) | 36.7°C (36.0°C - 37.3°C) |
| Characteristic | Authentic SARS-CoV-2 Virus (n = 13) | Controls (n = 7) (only placebo) |
| Age* | 31.4 (21-55) | 31.9 (21-59) |
| Female | 46.2% | 42.9% |
| Vaccination status | 100% fully vaccinated | 14% partially vaccinated |
| SARS-CoV-2 infection in medical history | 0% | 0% |
| SARS-CoV-2 antigen test | 100% negative | 100% negative |
| Tympanic temperature upon study visit* | 36.7°C (36.1°C - 37.4°C) | 36.3°C (36.0°C - 37.1°C) |

*Age & Tympanic temperature: mean (range)

Enoxaparin prevents SARS-CoV-2 binding and infection of human epithelial cells *in vitro*

SARS-CoV-2 pseudovirus strongly bound to polarized Caco-2 cells in a 3D epithelial model and binding was significantly inhibited by enoxaparin ($p < 0,001$) (**Figure. 2A**). The authentic SARS-CoV-2 isolate (WT) efficiently infected the polarized Caco-2 cells and infection was significantly inhibited by enoxaparin ($p < 0,001$) to a similar extent as observed with the blocking anti-ACE-2 antibody (**Figure. 2B**). These results strongly suggest that SARS-CoV-2 pseudovirus and authentic SARS-CoV-2 bind to epithelial cells and enoxaparin effectively blocks SARS-CoV-2 binding as well as infection, supporting the use of enoxaparin as a prophylactic treatment against SARS-CoV-2^{28, 38}. To investigate how long enoxaparin remains effective after application, we performed a time course using a 3D epithelial cell model with primary normal human bronchial epithelial (NHBE) cells⁴⁷. NHBE cells were cultured for a period of multiple weeks in transwells containing an air-liquid interphase (ALI), leading to the formation of intact ciliated pseudostratified epithelia with high mucus production, making this 3D respiratory model a suitable model for investigating effect of drugs on epithelial tissues. Enoxaparin was sprayed from about 2.5 cm distance onto the apical side of fully differentiated epithelia to mimic enoxaparin distribution within the nasal cavity. To monitor how long the protective effect of enoxaparin against SARS-CoV-2 remains intact, NHBE cells were infected with authentic SARS-CoV-2 (WT) after enoxaparin exposure at different time points (0.5 h, 4 h, 16 h, 24 h). Interestingly, enoxaparin protected the epithelial cells against infection for up to 16 hours and at 24 hours the protective effect was mostly lost (**Figure. 2C**). In order to investigate the effect of enoxaparin on not only the WT strain of SARS-CoV-2 but also two of the most recent and contagious VoC, NHBE cells were pre-treated with enoxaparin for 30 min prior the addition of different authentic SARS-CoV-2 viral strains (WT, and VoC Delta (B.1.617.2) and Omicron (BA.5)) and kept in culture for 3 days. At day 3 post-infection, polarized NHBE cells were analyzed for transepithelial electrical resistance (TEER) (**Sup. Figure. 1A**), as an indicator for the integrity status of the tissue. TEER values significantly dropped upon SARS-CoV-2 infection with all strains compared to the uninfected condition, whereas enoxaparin pre-incubation restored TEER to same level as uninfected cells (**Sup. Figure. 1A**). These data suggest that enoxaparin protects tissue integrity upon SARS-CoV-2 exposure by limiting infection. At day 3 post infection, SARS-CoV-2 infection of the different variants was analyzed by RT-PCR (**Sup. Figure. 1B**). SARS-CoV-2 WT and the two VoC Delta (B.1.617.2) and Omicron (BA.5) efficiently infected polarized epithelial cells in the 3D model albeit at different efficiencies (**Sup. Figure. 1B**). Notably, enoxaparin blocked the infection of the three different strains as efficiently, suggesting that enoxaparin inhibition is independent of the SARS-CoV-2 variant. We next investigated the efficacy of enoxaparin to block infection of VeroE6 cells, which are highly susceptible to SARS-CoV-2. We determined the IC₅₀ value for enoxaparin of SARS-CoV-2 binding to Vero cells at 156 IU/ml (**Sup. Figure. 2A**) and selected 250 IU/ml for

subsequent *in vitro* experiments. We investigated whether there is a difference in inhibition when enoxaparin is applied to the cells or the virus. Either VeroE6 cells or authentic SARS-CoV-2 were exposed to enoxaparin and infection was measured. Pre-incubation of either SARS-CoV-2 or VeroE6 cells with enoxaparin inhibited SARS-CoV-2 binding (**Sup. Figure. 2B**), suggesting that enoxaparin interferes with SARS-CoV-2 infection at both cellular and viral level. We further compared the efficiency of enoxaparin to block binding as well as infection of SARS-CoV-2. Our data show that there is higher background when blocking binding compared to infection, which is almost completely blocked by enoxaparin (**Sup. Figure. 2C**). At lower concentrations enoxaparin is less efficient at blocking infection than binding. As we use high enoxaparin concentration, our data suggest that the inhibition of binding corresponds to block in infection.

Characterization of nasal epithelial cells

Volunteers inhaled both placebo and LMWH enoxaparin into separate nostrils and we investigated the cellular fitness and composition of the isolated cells from each nostril. Nasal cells were stained epithelial and lymphocyte surface markers and analyzed by flow cytometry (**Figure. 3A**). The majority of cells expressed the epithelial marker pan-cytokeratin⁴⁹ whereas a small percentage of cells expressed CD45 (**Figure. 3A, B**), suggesting that the isolated cells are epithelial cells. Moreover, EpCAM and Mucin-5b were expressed by epithelial subsets. Importantly, cells isolated from the nasal cavity expressed ACE-2 and heparan sulfates (**Figure. 3A, C**), indicating their vulnerability to SARS-CoV-2 infection. Besides epithelial cells, a low percentage of lymphoid and myeloid cells, as indicated by expression of CD3, CD11b and CD11c, were detected in the isolated cell fraction (**Figure. 3C**). Notably, no significant differences for the cell markers were detected between the placebo and enoxaparin treated cell samples (**Figure. 3D**), strongly suggesting no interference of enoxaparin on cell receptor expression or cell activation upon treatment. These data strongly suggest that nasal epithelial cells are a potential target for SARS-CoV-2 and that *in vivo* enoxaparin inhalation did neither affect expression levels of SARS-CoV-2 receptors nor cellular composition.

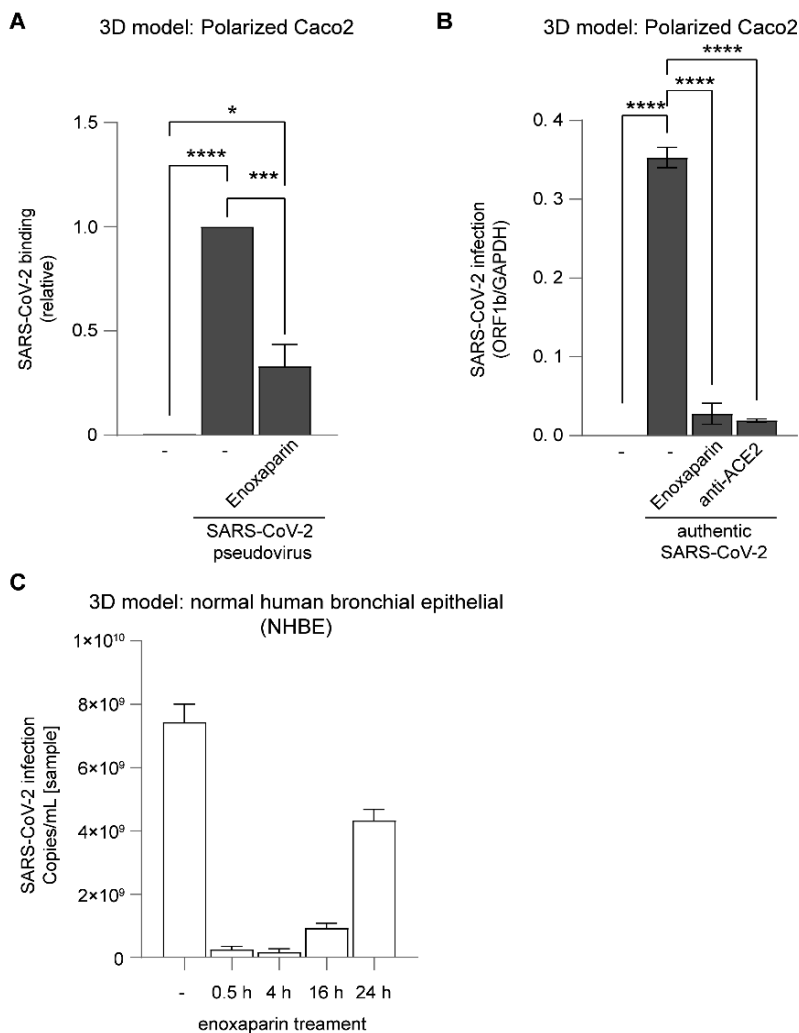


Figure 2 | SARS-CoV-2 binding and infection of polarized epithelial cells is blocked by LMWH enoxaparin. (A) SARS-CoV-2 pseudovirus binding was measured in polarized Caco-2 cells that were cultured in a static 3D model. The virus was either directly added or upon prior incubation with an *in vitro* enoxaparin (250IU) control for 30 minutes. Binding with SARS-CoV-2 pseudovirus was measured using a p24 ELISA. (B) Polarized Caco-2 were infected with authentic SARS-CoV-2 (Italy TCID50 104) either without or in presence of antibodies against ACE2 or after prior *in vitro* incubation with LMWH enoxaparin (250IU) for 30 minutes. Authentic SARS-CoV-2 was detected after lysis by quantitative RT-PCR of viral RNA. (C) A 3D epithelial cell model of polarized normal human bronchial epithelial cells was treated with enoxaparin (nebulization) and SARS-CoV-2 was added at different time points (0.5h, 4h, 16h and 24h). SARS-CoV-2 infection was measured by quantitative RT-PCR of viral RNA after 24 hours. Data show the mean values and error bars are the SEM. Statistical analysis was performed using (A) ordinary one-way ANOVA with Tukey’s multiple-comparison test. *p= 0.0203, ***p= 0.0005, ****p < 0.0001 (n = 2), (B) ordinary one-way ANOVA with Tukey’s multiple-comparison test. ****p < 0.0001 (n = 2), (C) (n=2).

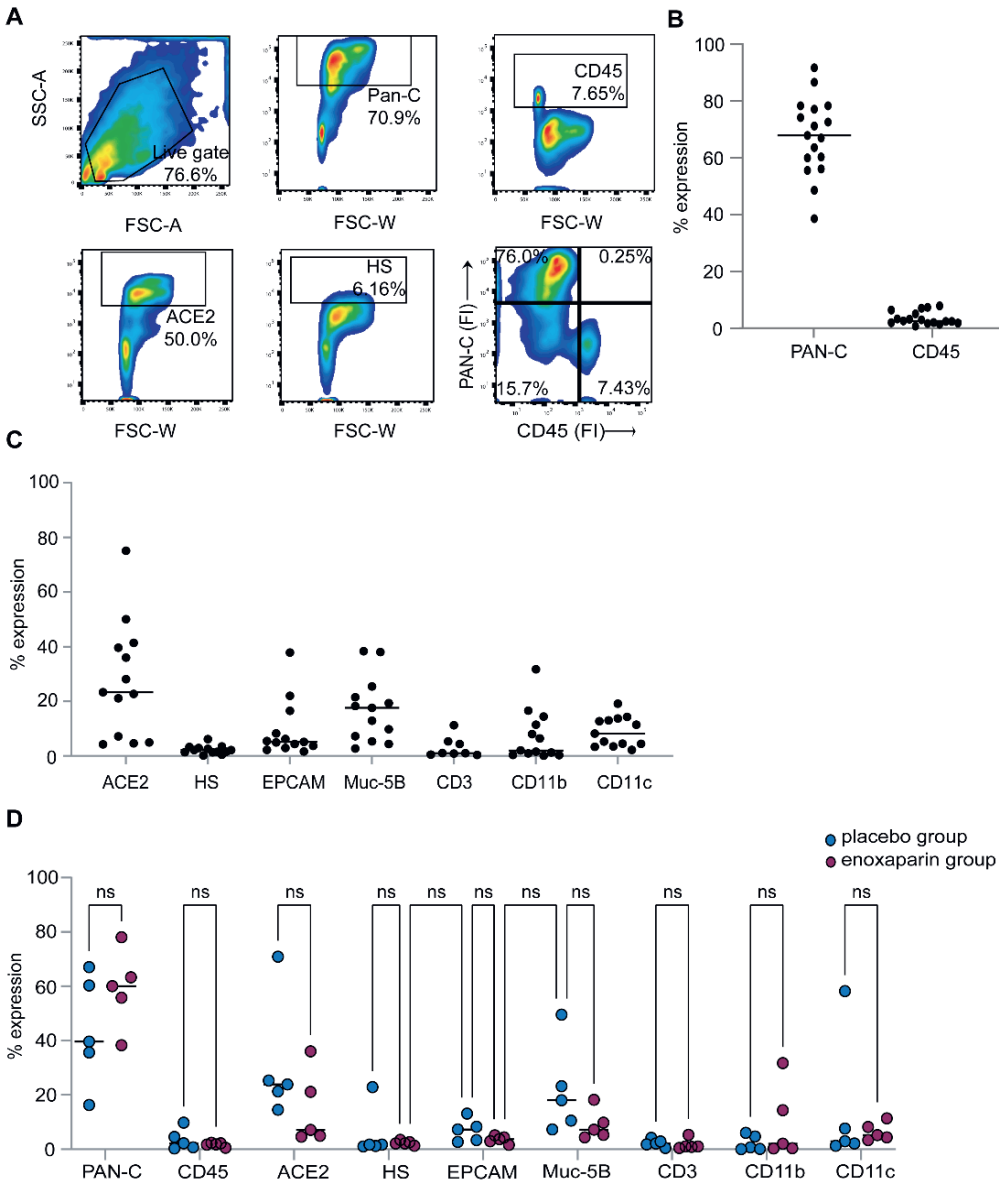


Figure 3 | Characterization of primary human nasal epithelial cells. (A) Flow cytometry analysis of single cell suspensions from the nasal epithelium. (A-B) Primary human nasal epithelial cells isolated from the nasal mucosa of healthy volunteers after treatment with either placebo (saline solution) or LMWH enoxaparin were directly labelled with pan cytokeratin (Pan-C) and CD45. Additionally, cells were labelled with antibodies against ACE2 and heparan sulfate (HS) (n=17). (C) Cells from the LMWH enoxaparin treated nostril were additionally stained with antibodies against the surface markers EPCAM, Muc-5B, CD3, CD11b and CD11c (n=17, 4 donors excluded; CD3 n=8). (D) Cells from both the placebo and LMWH enoxaparin treated nose were stained for Pan-C, CD45, ACE2, HS, EPCAM, Muc-5B, CD3, CD11b and CD11c (n=9, 4 donors excluded). The cellular phenotype was monitored using flow cytometry analysis. ns= Not significant.

In vivo enoxaparin inhalation prevents SARS-CoV-2 pseudovirus binding to nasal epithelial cells

We isolated cells from the placebo treated nasal cavity of volunteers that were either unvaccinated, partially vaccinated, or fully vaccinated at time of treatment. The cells were subjected to SARS-CoV-2 pseudovirus for 4 hours and binding was determined. Notably, no significant difference was observed between virus attachment to cells from unvaccinated and vaccinated individuals (**Figure. 4A**), suggesting that vaccination does not directly interfere with SARS-CoV-2 binding to nasal epithelial cells.

Next we investigated the effect of *in vivo* enoxaparin treatment on *ex vivo* virus attachment. Cells isolated from placebo- and enoxaparin-treated volunteers were exposed to SARS-CoV-2 pseudovirus and binding of SARS-CoV-2 was compared between both groups. SARS-CoV-2 pseudovirus bound efficiently to cells isolated from the placebo group (**Figure. 4B**). Strikingly, SARS-CoV-2 pseudovirus binding was significantly lower in the enoxaparin treated group than the placebo group (**Figure. 4B**). Direct comparison of cells treated with LMWH enoxaparin or NaCl 0,9% from all donors supported the inhibitory effect of *in vivo* inhalation of enoxaparin on SARS-CoV-2 pseudovirus binding as nasal inhalation of enoxaparin significantly reduced of SARS-CoV-2 pseudovirus binding compared to the placebo group ($p=0,0003$) (**Figure. 4C**). Moreover, we investigated whether the inhalation of enoxaparin was as efficient as *in vitro* pre-incubation with enoxaparin prior to virus exposure. We therefore compared SARS-CoV-2 pseudovirus binding of placebo and enoxaparin group with binding when enoxaparin was added *in vitro* prior to virus exposure (**Figure. 4D**). The inhibitory effect of *in vivo* inhalation of enoxaparin was comparable to the *in vitro* addition of enoxaparin, suggesting that *in vivo* inhalation of enoxaparin is as efficient in inhibiting virus binding as can be achieved *in vitro*. These data strongly suggest that *in vivo* inhalation of enoxaparin strongly inhibits SARS-CoV-2 pseudovirus binding to nasal epithelial cells.

Enoxaparin inhalation prevents SARS-CoV-2 authentic virus isolate binding to nasal epithelial cells

We next compared binding of an authentic SARS-CoV-2 isolate (hCoV-19/WT) to cells from placebo- and enoxaparin-treated volunteers. Freshly isolated cells were exposed to the authentic SARS-CoV-2 and binding was measured by quantitative RT-PCR. The authentic virus strongly bound to cells from the placebo group while the cells exposed to enoxaparin showed a decrease in virus binding (**Figure. 5A, B**). We observed donor differences between binding of SARS-CoV-2 to nasal cells but binding of authentic SARS-CoV-2 isolate was significantly reduced ($p=0,049$) when comparing the placebo and *in vivo* LMWH enoxaparin inhalation groups (**Figure. 5A, B**). Moreover, *in vivo* inhalation of enoxaparin was as efficient as *in vitro* pre-incubation of SARS-CoV-2 with enoxaparin as the observed inhibition of

SARS-CoV-2 binding in the *in vivo* inhalation group was not further inhibited with *in vitro* pre-incubation of SARS-CoV-2 (Figure. 5C). Moreover, *in vitro* enoxaparin blocked SARS-CoV-2 in the placebo group as efficient as *in vivo* inhalation, strongly suggesting that *in vivo* inhalation of enoxaparin is as efficient in inhibiting SARS-CoV-2 binding to nasal cells

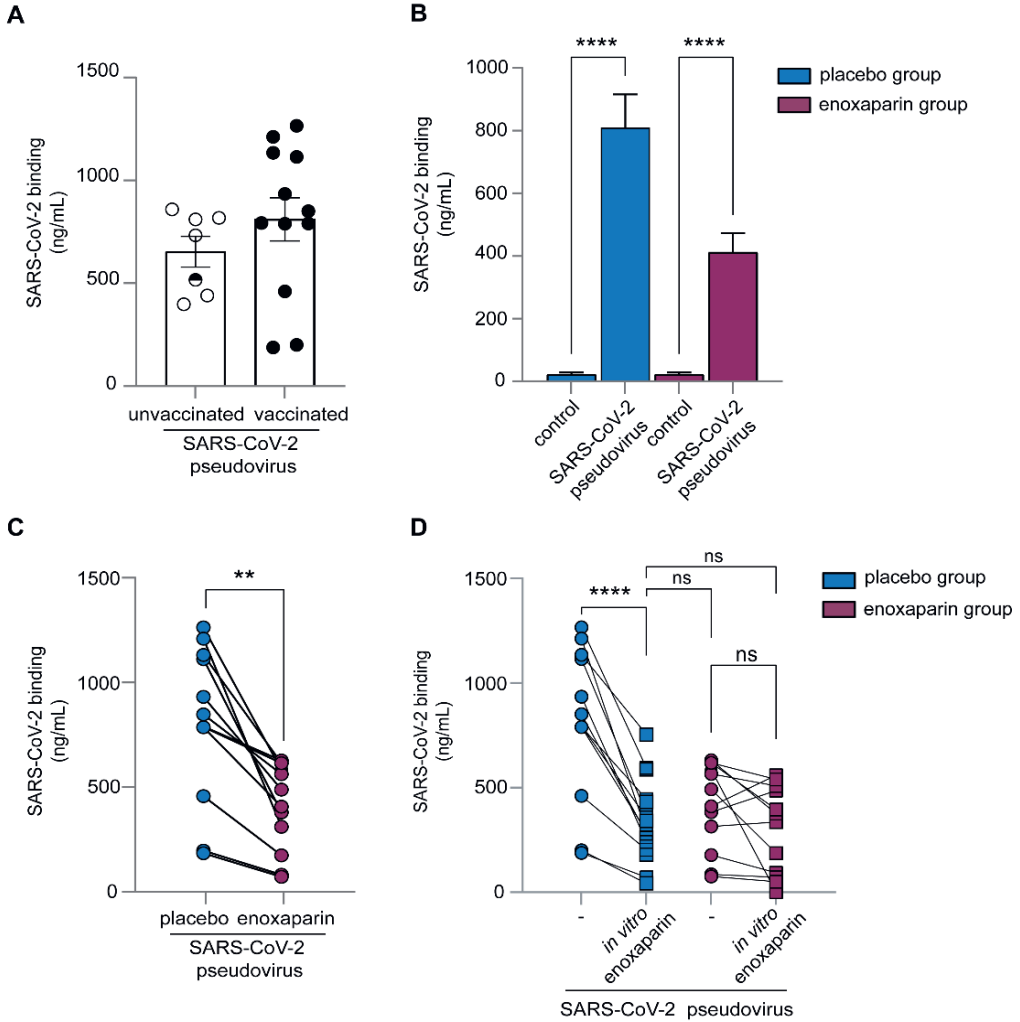


Figure 4 | *In vivo* enoxaparin inhalation prevents SARS-CoV-2 pseudovirus binding to nasal epithelial cells (A) Nasal epithelial cells isolated from the placebo treated volunteers (either unvaccinated (white circle, n=6), partially vaccinated (white/black circle, n=1) or fully vaccinated (black circle, n=12)) were exposed to SARS-CoV-2 pseudovirus. Binding was measured after 4h by ELISA. (B-C) Nasal epithelial cells isolated from the nostrils of volunteers were treated with either a placebo or LMWH enoxaparin were exposed to SARS-CoV-2 pseudovirus (D) in presence or absence of an additional *in vitro* enoxaparin condition (250IU) and binding was measured after 4h by ELISA. Data show the mean values and error bars are the SEM. Statistical analysis was performed using (B) 2way ANOVA with Tukey's multiple-comparison test. ****p < 0.0001 (n = 12), (C) two-tailed, unpaired, non-parametric, Mann-Whitney test. **p= 0.0043 (n=12). (D) 2way ANOVA with Tukey's multiple-comparison test. ****p < 0.0001, ns= Not significant (n=12).

as can be achieved *in vitro*. These data strongly suggest that the protocol is suitable to investigate the effect of *in vivo* inhalation of enoxaparin or other reagents on SARS-CoV-2 binding.

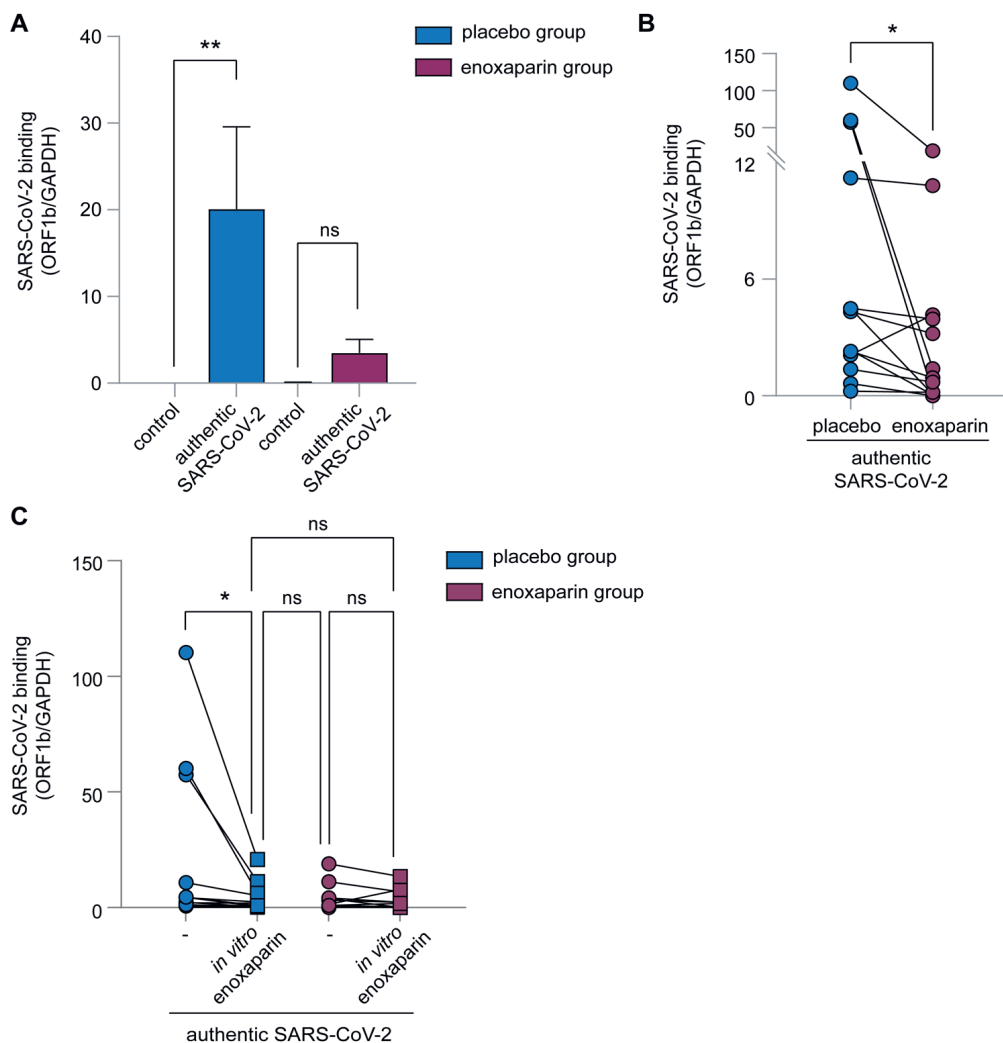


Figure 5 | *In vivo* enoxaparin inhalation prevents authentic SARS-CoV-2 binding to nasal epithelial cells.

(A-B) Nasal epithelial cells retrieved from the nasal cavity of healthy volunteers after exposure to placebo (saline solution, left nostril) and LMWH enoxaparin (right nostril) were exposed to authentic SARS-CoV-2 (hCoV-19 Italy) for 4h at 4C compared to an uninfected control sample (A). (C) Additionally, authentic SARS-Cov-2 was incubated in presence or absence of *in vitro* LMWH enoxaparin (250IU) for 30 min before inoculation of epithelial cells. (A-C) Virus binding was measured after 4h by real-time RT-PCR. Data show the mean values and error bars are the SEM. Statistical analysis was performed using (A) 2way ANOVA with Tukey's multiple-comparison test. **p = 0.0036, *p=0.0315 (n = 12), (B) two-tailed, unpaired, non-parametric, Mann-Whitney test. **p= 0.0387. ns= Not significant.

Adverse events and follow up

No adverse events (AE) or severe adverse events (SAE) occurred during of the trial. A follow-up period of 24 hours was maintained for all volunteers. This follow-up time corresponded with 5 times the $T_{1/2}$ of enoxaparin. After 24 hours follow-up no adverse events were reported by volunteers.

Discussion

LMWH is commonly used as an anti-coagulant and considered safe especially external usage. Here we performed a single center, non-randomized controlled trial where we investigate the potency of inhaled LMWH to prevent SARS-CoV-2 binding, which is a prerequisite to infection. Notably, *in vivo* inhalation blocked SARS-CoV-2 attachment to nasal epithelial cells from the human study participants. *In vivo* inhalation was as efficient as *in vitro* application, strongly suggesting that not only the developed protocol is suitable for investigating protective effects of compounds against SARS-CoV-2 in an *in vivo* setting but also that inhalation is effective in blocking SARS-CoV-2 infection.

Although ACE-2 is the main receptor for SARS-CoV-2, several studies have shown that HSPG act as attachment receptors for SARS-CoV-2 and binding of SARS-CoV-2 to HSPG is required for infection^{26, 28, 37}. Unfractionated heparin or different LMWH interfere with SARS-CoV-2 binding to HSPG and therefore prevent infection *in vitro*^{27, 38}. As *in vitro* infection depends on prior binding to HSPG, it is tempting to speculate that *in vivo* infection is even more dependent on first attachment to HSPG due to air flow and low virus concentrations. Interestingly, our data showed that pre-incubation of either SARS-CoV-2 or epithelial cells with LMWH blocked SARS-CoV-2 binding and infection, further supporting the use of heparins and LMWH to prevent SARS-CoV-2 infection and transmission^{27, 28, 38}.

In current clinical practice, heparins, and their LMWH counterparts, are given as an antithrombotic agents in pulmonary, cardiac and vascular medicine^{39, 50, 51}. The use of these anticoagulants is widespread and considered safe⁵². Studies involving inhaled heparins have shown that bronchially and pulmunal applied heparins do not increase plasma anti-Xa activity even in high doses^{52, 53, 54}. We analyzed the nasal cells isolated from the volunteers by flow cytometry and observed that the majority of cells express epithelial markers. Only low percentages of lymphoid and myeloid cells were detected. Interestingly, enoxaparin inhalation did not affect the cellular composition and we did not observe an increased influx of lymphocytes. These data suggest that enoxaparin inhalation does not lead to inflammation. Neither did we observe any adverse effects of the enoxaparin inhalation in the healthy volunteers. These data therefore strongly suggest that nasal enoxaparin inhalation is safe and does not significantly change the mucosal integrity.

Elimination of enoxaparin from the body happens through direct filtration in the kidneys (10% of the total dose) or metabolic degradation via desulphurization and depolymerization

in the liver to smaller fragments⁵⁵. While the half-life is well understood in humans, being approximately 5 hours after single subcutaneous dose⁵⁵, the longevity of LMWH in mucosal tissues however is poorly understood. Interestingly, enoxaparin application to the 3D epithelial cell model of normal human bronchial epithelial cells protected against infection with authentic SARS-CoV-2 for up to 16 hours, suggesting that enoxaparin remains longer effective in mucosal tissues compared to subcutaneous injection.

We observed variation in virus attachment between different volunteers, which could be caused by variation in susceptibility to SARS-CoV-2. We observed differences between ACE-2 expression but there was no correlation between the observed binding variations. Moreover, anatomical and physiological differences exist between volunteers, which may affect either the effect or the final dose applied to the mucosal surface. Interestingly, we did not observe any differences between SARS-CoV-2 pseudovirus binding to epithelial cells from vaccinated and unvaccinated volunteers, indicating that vaccination status does not cause the observed variations in virus attachment.

Our data confirm that a vast majority of cells covering the nasal mucosa are of epithelial origin and the presence of both ACE-2 and HSPG on the nasal epithelium in our study suggests these cells are at risk of infection by SARS-CoV-2^{24, 56}. In the current study we observed a strong binding of SARS-CoV-2 pseudovirus to the cells isolated from the nose, suggesting that indeed SARS-CoV-2 efficiently interacts with nasal epithelial cells and this might lead to infection of the host. Inhalation of enoxaparin effectively blocked binding of SARS-CoV-2 pseudovirus as well as authentic SARS-CoV-2 to the nasal cell fraction.

These data demonstrate that enoxaparin inhalation prevents interaction of SARS-CoV-2 to nasal cells and this might be used as prophylaxis. Moreover, it suggests that HSPGs are relevant in human susceptibility to SARS-CoV-2. Our study further shows that application of enoxaparin *in vivo* is as efficient in blocking SARS-CoV-2 binding as *in vitro* addition of enoxaparin prior to virus binding^{28, 38}. These findings not only underscore the relevance of LMWH as inhalation prophylaxis to SARS-CoV-2 but also show that our current protocol is suitable to study interventions to prevent SARS-CoV-2 binding.

Inhibition of binding was taken as a measure of protection as several studies show that blocking binding of SARS-CoV-2 prevents infection as binding²⁴ is a pre-requisite for ACE-2 dependent infection^{28, 57, 58, 59}. Indeed, enoxaparin blocked both binding and infection of SARS-CoV-2 in the 3D primary human epithelial model, with the protection offered not only for the SARS-CoV-2 WT isolate, but also in the Delta (B.1.617.2) and Omicron (BA.5) variants, suggesting that enoxaparin inhibition is insensitive to changes observed in current VoC and might therefore be a broad inhibitor of SARS-CoV-2 and VoC.

In the volunteer study we focused on SARS-CoV-2 binding as a measure of infection as it is a short procedure allowing assessment of inhalation treatment. Infection of SARS-CoV-2 requires culturing of the primary isolated nasal cells at 37°C for 24 hours, which would affect cell viability and more importantly differentiation state of the cells. By comparing SARS-CoV-2 binding to nasal cells isolated from the placebo and *in vivo* enoxaparin

inhalation groups we were able to assess enoxaparin efficacy as a prophylaxis without major confounding factors.

As infection of humans with SARS-CoV-2 in a study setting poses several ethical challenges, especially as we cannot predict severity of COVID-19 in healthy individuals, we designed a non-randomized controlled trial involving *in vivo* medication and *ex vivo* virus exposure. While the first human SARS-CoV-2 challenge study was recently completed ⁶⁰, safety concerns remain ⁶¹.

The risk of using heparin or LMWH in a preventive setting would be loss of hemostasis. We did not observe any bleeding or other adverse effects in the study participants. Previous research has investigated the bronchial application of heparins in the context of asthma and have shown LMWH do not lead to an increase in bleeding. Studies conducted revealed that various heparins could be inhaled at doses higher than current therapeutic levels without an increase in bleedings or alteration of both prothrombin time and activated partial thromboplastin time when comparing study groups receiving nebulized heparins compared to best clinical practice ^{62,63}. Current clinical practice uses enoxaparin at a dose of 100IU/kg. Ahmed *et al.* nebulized either 200IU/kg enoxaparin or 80.000IU unfractionated heparin and found no adverse events in the trial population. We have demonstrated efficient inhibition of SARS-CoV-2 binding using a total of 4500IU enoxaparin. *In vitro* addition of enoxaparin did not further decrease binding supporting the efficiency of *in vivo* block by inhalation. This indicates inhalation of enoxaparin is a suitable way to protect the epithelium and the concentration used in this study results in maximum block.

Interestingly, critically ill COVID-19 patients that were treated with LMWH, resulted in lower mortality ⁶⁴. An explanation is that this reduction in mortality is due to the anticoagulative properties of LMWH and their associated reduction in pulmonary thrombotic events ^{65,66}. Yet there is persistent evidence that LMWH have advantage above other anticoagulants as they also curtailed the duration of the SARS-CoV-2 infection ⁶⁷. Additionally, administering LMWH to COVID-19 patients is associated with shorter time to SARS-CoV-2 swab negativity in the case of infection ⁶⁸. Similarly it has been observed that competition of LMWH with HSGP to bind SARS-CoV-2 mitigates the chance of a cytokine storm ⁶⁹. This might indicate a powerful method to prevent or curb outbreaks of SARS VoC or novel future CoV epidemics. With the rise of new VoC that contain mutations allowing them to evade immunity gained by vaccines or prior SARS-CoV-2 infection ⁷⁰, it has become paramount to find alternative strategies to prevent SARS-CoV-2 infection and transmission. It is even possible that VoC have a higher affinity for HSPG as recently suggested ⁷¹, which supports prophylactic use of enoxaparin. Mutations in the surface of the omicron VoC render the virus highly positively charged, suggesting a higher affinity to HS ⁷². Preliminary data with left over nasal epithelial cells showed that the VoC Delta bound to nasal cells from placebo group and was blocked by *in vivo* enoxaparin inhalation similar to the SARS-Cov-2 primary isolate (hCoV/WT), indicating that *in vivo* inhalation of enoxaparin is a prophylactic to prevent VoC infections. However, due to insufficient material we were unable to power this accordingly.

Nevertheless, a reduction in infection of both delta and omicron variants was observed in our 3D epithelial model, indicating a similar mechanism as with the authentic isolate.

To date, we and others have proposed the use of heparin or LMWH to prevent SARS-CoV-2 infection and transmission^{27, 38}. Our data strongly suggest that direct *in vivo* application of LMWH enoxaparin to the nasal epithelium prevents SARS-CoV-2 attachment, a pre-requisite for infection and transmission of different SARS-CoV-2 variants.

Conclusion

In this study we have demonstrated that LMWH inhalation is an efficient and safe prophylactic treatment preventing SARS-CoV-2 attachment to nasal epithelial cells. Our *in vivo* exposure/*ex vivo* analysis model allows us to mitigate the risk to human volunteers while preserving the ability to work with an as-close-to-real setting as possible. Furthermore, we severely limit the risks inflicted on our volunteers using *ex vivo* virus exposure. The use of brushes to retrieve nasal epithelial cells also reduces the burden on our volunteers. LMWH are relatively cheap, widely available and previous experience with nasal/bronchial application of these medications reveal it to be safe. This could make LMWH an excellent tool to limit the spread of SARS-CoV-2, and possible new VoC.

Author contributions

JE and MB-J conceived and designed experiments. KV designed the clinical study, recruited the study participants and collected material. JE, MB-J and TMK, performed the experiments, acquired data and analyzed data. JE, MB-J, KV, DMC and TBHG interpreted data and contributed to scientific discussion. VZ helped with experiments and data analysis. EMK and SR contributed to study design and treatment application. EMK, SR, DMC, GJdB, helped with study design and contributed to scientific input. DW contributed materials and added to scientific discussion. DMC, JE, KV, MB-J, and TBHG wrote the manuscript with input from all listed authors. TBHG perceived of the original study idea and was involved in all aspects of the study. All authors had access to all of the data in this study and approved the final version of the manuscript. The corresponding author vouches for the completeness and accuracy of the data.

Funding

This research was further funded through a ZonMW-NWO grant (Dutch Research Council/Nederlandse organisatie voor Wetenschappelijk Onderzoek) together with the Stichting Proefdiervrij (ZonMW MKMD COVID-19 grant with project number 114025008) as well as the European Research Council (Advanced grant 670424).

Conflict of interest

The authors have no conflicts of interest to disclose.

Acknowledgments

We thank Neeltje Koostra and Ad van Nuenen for their help with the authentic SARS-CoV-2 culture and production. We also thank Maurice Kroon for help with the LMWH enoxaparin preparation. This research was supported by a Work Visit Grant of the Amsterdam institute for Infection and Immunity.

References

1. Zhou, P. *et al.* A pneumonia outbreak associated with a new coronavirus of probable bat origin. *Nature* **579**, 270-273 (2020).
2. Shivalkar, S. *et al.* Outbreak of COVID-19: A Detailed Overview and Its Consequences. In: Asea, A.A.A. & Kaur, P. (eds). *Coronavirus Therapeutics – Volume II: Clinical Management and Public Health*. Springer International Publishing: Cham, 2021, pp 23-45.
3. Wu, F. *et al.* A new coronavirus associated with human respiratory disease in China. *Nature* **579**, 265-269 (2020).
4. Lu, R. *et al.* Genomic characterisation and epidemiology of 2019 novel coronavirus: implications for virus origins and receptor binding. *Lancet (London, England)* **395**, 565-574 (2020).
5. Guan, W.J. *et al.* Clinical Characteristics of Coronavirus Disease 2019 in China. *The New England journal of medicine* **382**, 1708-1720 (2020).
6. Cummings, M.J. *et al.* Epidemiology, clinical course, and outcomes of critically ill adults with COVID-19 in New York City: a prospective cohort study. *Lancet (London, England)* **395**, 1763-1770 (2020).
7. Unicef. COVID-19 Vaccine Market Dashboard. [cited 2022 11-02] Available from: <https://www.unicef.org/supply/covid-19-vaccine-market-dashboard>
8. Cohn, B.A., Cirillo, P.M., Murphy, C.C., Krigbaum, N.Y. & Wallace, A.W. SARS-CoV-2 vaccine protection and deaths among US veterans during 2021. *Science* **375**, 331-336 (2022).
9. Chen, X., Huang, H., Ju, J., Sun, R. & Zhang, J. Impact of vaccination on the COVID-19 pandemic in U.S. states. *Sci Rep* **12**, 1554 (2022).
10. Emary, K.R.W. *et al.* Efficacy of ChAdOx1 nCoV-19 (AZD1222) vaccine against SARS-CoV-2 variant of concern 202012/01 (B.1.1.7): an exploratory analysis of a randomised controlled trial. *Lancet (London, England)* **397**, 1351-1362 (2021).
11. Sanders, R.W. & de Jong, M.D. Pandemic moves and countermoves: vaccines and viral variants. *Lancet (London, England)* **397**, 1326-1327 (2021).
12. Moore, J.P. & Offit, P.A. SARS-CoV-2 Vaccines and the Growing Threat of Viral Variants. *Jama* **325**, 821-822 (2021).
13. Collie, S., Champion, J., Moultrie, H., Bekker, L.G. & Gray, G. Effectiveness of BNT162b2 Vaccine against Omicron Variant in South Africa. *The New England journal of medicine* **386**, 494-496 (2022).
14. Sun, J. *et al.* Association Between Immune Dysfunction and COVID-19 Breakthrough Infection After SARS-CoV-2 Vaccination in the US. *JAMA Internal Medicine* **182**, 153 (2022).
15. Ehmsen, S. *et al.* Antibody and T cell immune responses following mRNA COVID-19 vaccination in patients with cancer. *Cancer Cell* **39**, 1034-1036 (2021).
16. Geisen, U.M. *et al.* Immunogenicity and safety of anti-SARS-CoV-2 mRNA vaccines in patients with chronic

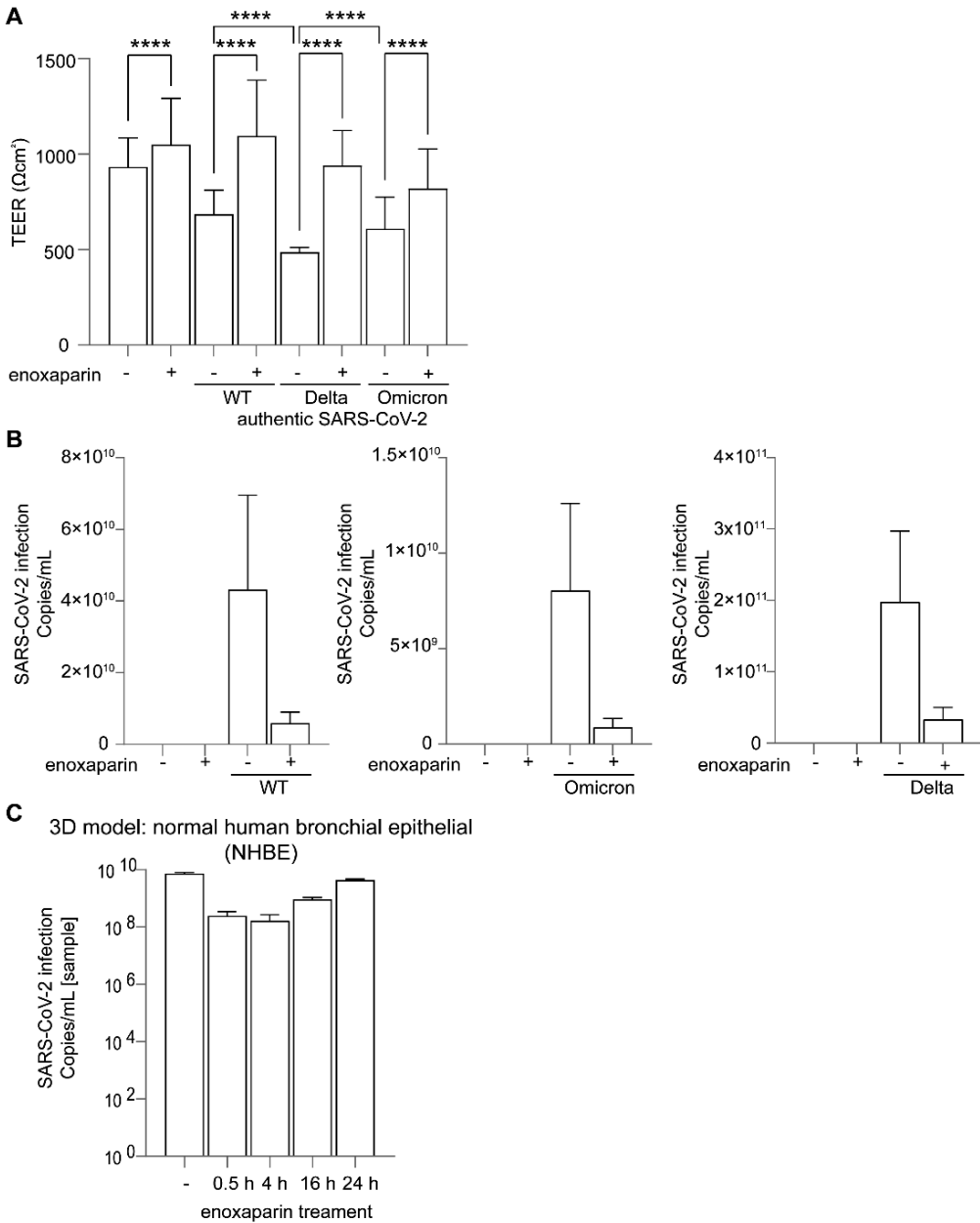
- inflammatory conditions and immunosuppressive therapy in a monocentric cohort. *Annals of the Rheumatic Diseases* **80**, 1306-1311 (2021).
17. Jarvis, M.C. Aerosol Transmission of SARS-CoV-2: Physical Principles and Implications. *Front Public Health* **8**, 590041 (2020).
 18. Rutter, H. *et al.* Visualising SARS-CoV-2 transmission routes and mitigations. *Bmj* **375**, e065312 (2021).
 19. Johnson, T.J. *et al.* Viral load of SARS-CoV-2 in droplets and bioaerosols directly captured during breathing, speaking and coughing. *Sci Rep* **12**, 3484 (2022).
 20. Madas, B.G. *et al.* Deposition distribution of the new coronavirus (SARS-CoV-2) in the human airways upon exposure to cough-generated droplets and aerosol particles. *Sci Rep* **10**, 22430 (2020).
 21. Hoffmann, M. *et al.* SARS-CoV-2 Cell Entry Depends on ACE2 and TMPRSS2 and Is Blocked by a Clinically Proven Protease Inhibitor. *Cell* **181**, 271-280.e278 (2020).
 22. Yang, J. *et al.* Molecular interaction and inhibition of SARS-CoV-2 binding to the ACE2 receptor. *Nat Commun* **11**, 4541 (2020).
 23. Lan, J. *et al.* Structure of the SARS-CoV-2 spike receptor-binding domain bound to the ACE2 receptor. *Nature* **581**, 215-220 (2020).
 24. Lee, I.T. *et al.* ACE2 localizes to the respiratory cilia and is not increased by ACE inhibitors or ARBs. *Nat Commun* **11**, 5453 (2020).
 25. Song, X. *et al.* Little to no expression of angiotensin-converting enzyme-2 on most human peripheral blood immune cells but highly expressed on tissue macrophages. *Cytometry A* (2020).
 26. Clausen, T.M. *et al.* SARS-CoV-2 Infection Depends on Cellular Heparan Sulfate and ACE2. *Cell* **183**, 1043-1057.e1015 (2020).
 27. Zhang, Q. *et al.* Heparan sulfate assists SARS-CoV-2 in cell entry and can be targeted by approved drugs in vitro. *Cell Discov* **6**, 80 (2020).
 28. Bermejo-Jambrina, M. *et al.* Infection and transmission of SARS-CoV-2 depend on heparan sulfate proteoglycans. *Embo j* **40**, e106765 (2021).
 29. Sarrazin, S., Lamanna, W.C. & Esko, J.D. Heparan sulfate proteoglycans. *Cold Spring Harb Perspect Biol* **3** (2011).
 30. Hayashida, K., Johnston, D.R., Goldberger, O. & Park, P.W. Syndecan-1 expression in epithelial cells is induced by transforming growth factor beta through a PKA-dependent pathway. *J Biol Chem* **281**, 24365-24374 (2006).
 31. Haeger, S.M. *et al.* Epithelial Heparan Sulfate Contributes to Alveolar Barrier Function and Is Shed during Lung Injury. *Am J Respir Cell Mol Biol* **59**, 363-374 (2018).
 32. Milho, R., Frederico, B., Efstathiou, S. & Stevenson, P.G. A heparan-dependent herpesvirus targets the olfactory neuroepithelium for host entry. *PLoS Pathog* **8**, e1002986 (2012).
 33. Tanino, Y. *et al.* Syndecan-4 Regulates Early Neutrophil Migration and Pulmonary Inflammation in Response to Lipopolysaccharide. *American Journal of Respiratory Cell and Molecular Biology*

- 47, 196-202 (2012).
34. Haeger, S.M., Yang, Y. & Schmidt, E.P. Heparan Sulfate in the Developing, Healthy, and Injured Lung. *American Journal of Respiratory Cell and Molecular Biology* **55**, 5-11 (2016).
 35. Nijmeijer, B.M. *et al.* Syndecan 4 Upregulation on Activated Langerhans Cells Counteracts Langerin Restriction to Facilitate Hepatitis C Virus Transmission. *Front Immunol* **11**, 503 (2020).
 36. de Witte, L. *et al.* Syndecan-3 is a dendritic cell-specific attachment receptor for HIV-1. *Proc Natl Acad Sci U S A* **104**, 19464-19469 (2007).
 37. Milewska, A. *et al.* Human coronavirus NL63 utilizes heparan sulfate proteoglycans for attachment to target cells. *J Virol* **88**, 13221-13230 (2014).
 38. Tandon, R. *et al.* Effective Inhibition of SARS-CoV-2 Entry by Heparin and Enoxaparin Derivatives. *J Virol* **95:10.1128/jvi.01987-20** (2021).
 39. Holbrook, A. *et al.* Evidence-based management of anticoagulant therapy: Antithrombotic Therapy and Prevention of Thrombosis, 9th ed: American College of Chest Physicians Evidence-Based Clinical Practice Guidelines. *Chest* **141**, e152S-e184S (2012).
 40. Cundiff, D.K., Manyemba, J. & Pezzullo, J.C. Anticoagulants versus non-steroidal anti-inflammatories or placebo for treatment of venous thromboembolism. *Cochrane Database Syst Rev*, CD003746 (2006).
 41. Matsuyama, S. *et al.* Enhanced isolation of SARS-CoV-2 by TMPRSS2-expressing cells. *Proc Natl Acad Sci U S A* **117**, 7001-7003 (2020).
 42. Kootstra, N.A., Munk, C., Tonnu, N., Landau, N.R. & Verma, I.M. Abrogation of postentry restriction of HIV-1-based lentiviral vector transduction in simian cells. *Proc Natl Acad Sci U S A* **100**, 1298-1303 (2003).
 43. Brouwer, P.J.M. *et al.* Potent neutralizing antibodies from COVID-19 patients define multiple targets of vulnerability. *Science* **369**, 643-650 (2020).
 44. REED, L.J. & MUENCH, H. A SIMPLE METHOD OF ESTIMATING FIFTY PER CENT ENDPOINTS¹². *American Journal of Epidemiology* **27**, 493-497 (1938).
 45. Tseng, H.F. *et al.* Effectiveness of mRNA-1273 against SARS-CoV-2 Omicron and Delta variants. *Nat Med* **28**, 1063-1071 (2022).
 46. Chu, D.K.W. *et al.* Molecular Diagnosis of a Novel Coronavirus (2019-nCoV) Causing an Outbreak of Pneumonia. *Clin Chem* **66**, 549-555 (2020).
 47. Zaderer, V., Hermann, M., Lass-Flörl, C., Posch, W. & Wilflingseder, D. Turning the World Upside-Down in Cellulose for Improved Culturing and Imaging of Respiratory Challenges within a Human 3D Model. *Cells* **8** (2019).
 48. Chandorkar, P. *et al.* Fast-track development of an in vitro 3D lung/immune cell model to study Aspergillus infections. *Sci Rep* **7**, 11644 (2017).
 49. Karantza, V. Keratins in health and cancer: more than mere epithelial cell markers. *Oncogene* **30**, 127-138 (2011).
 50. Anderson, F.A., Jr., Zayaruzny, M., Heit, J.A., Fidan, D. & Cohen, A.T. Estimated annual numbers of US acute-care hospital patients at risk for venous

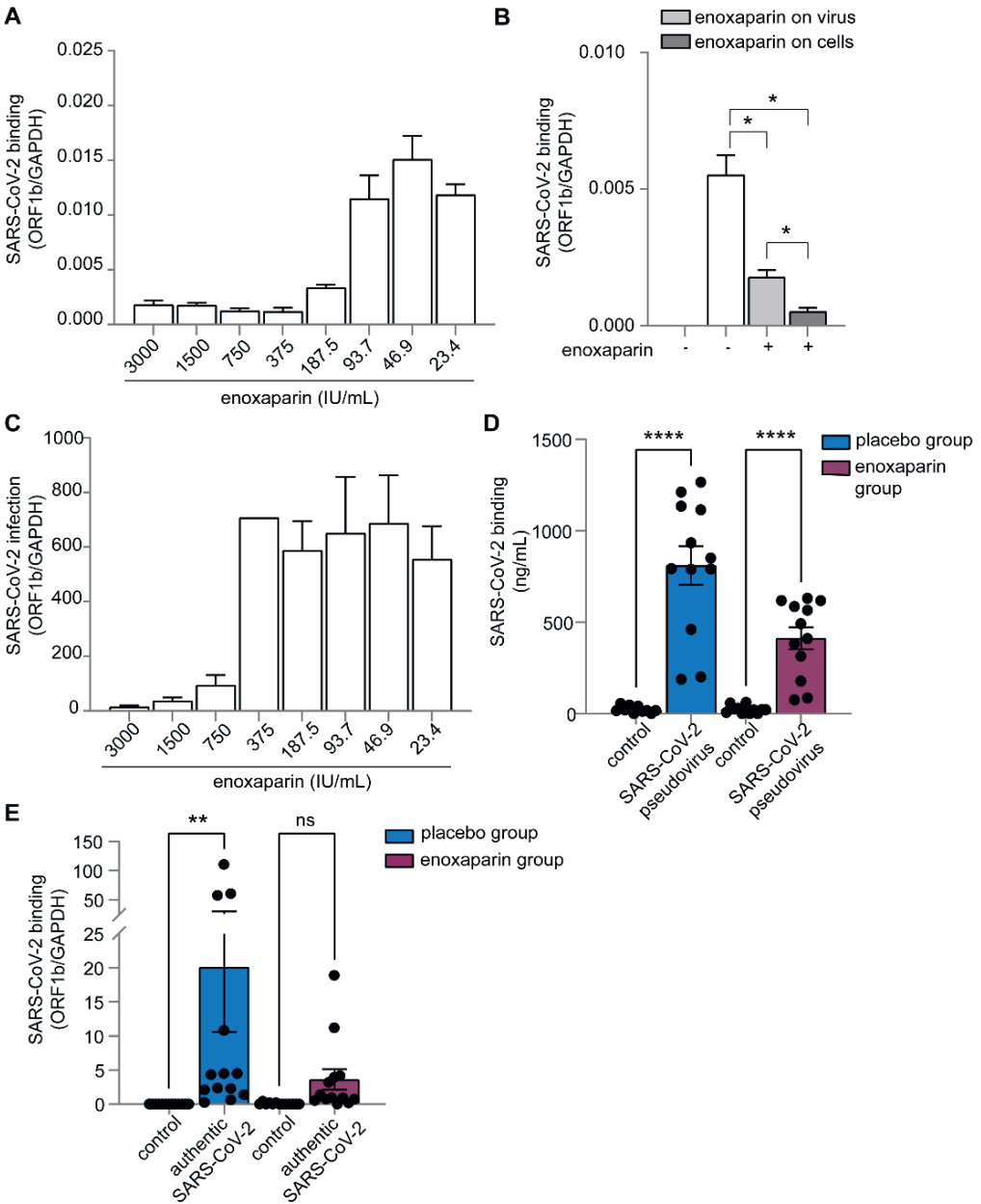
- thromboembolism. *Am J Hematol* **82**, 777-782 (2007).
51. Horlander, K.T., Mannino, D.M. & Leeper, K.V. Pulmonary embolism mortality in the United States, 1979-1998: an analysis using multiple-cause mortality data. *Arch Intern Med* **163**, 1711-1717 (2003).
 52. Gouin-Thibault, I., Pautas, E. & Siguret, V. Safety Profile of Different Low-Molecular Weight Heparins Used at Therapeutic Dose. *Drug Safety* **28**, 333-349 (2005).
 53. Philipp Markart, M.D., 1 Robert Nass, 1 Clemens Ruppert, Ph.D., 1 Lukas Hundack, M.D., 1 & Malgorzata Wygrecka, P.D., 2 Martina Korfei, Ph.D., 1 Rolf H Boedeker, Ph.D., 3 Gerd Staehler, M.D., 4 Hartmut Kroll, M.D., 5 Gerhard Scheuch, Ph.D., 6 Werner Seeger, M.D., 1 and Andreas Guenther, M.D. 1. Safety and Tolerability of Inhaled Heparin in Idiopathic Pulmonary Fibrosis. *JOURNAL OF AEROSOL MEDICINE AND PULMONARY DRUG DELIVERY* **Volume 23, number 3** (2010).
 54. Shute, J.K., Puxeddu, E. & Calzetta, L. Therapeutic use of heparin and derivatives beyond anticoagulation in patients with bronchial asthma or COPD. *Curr Opin Pharmacol* **40**, 39-45 (2018).
 55. EMA. Inhixa : EPAR - Product information: European Medicines Agency; 2016 26/10/2016 last updated 2022. Report No.: EMEA/H/C/004264 - IB/0084.
 56. Hamming, I. *et al.* Tissue distribution of ACE2 protein, the functional receptor for SARS coronavirus. A first step in understanding SARS pathogenesis. *J Pathol* **203**, 631-637 (2004).
 57. Wang, C. *et al.* Membrane Nanoparticles Derived from ACE2-Rich Cells Block SARS-CoV-2 Infection. *ACS Nano* **15**, 6340-6351 (2021).
 58. El-Shennawy, L. *et al.* Circulating ACE2-expressing extracellular vesicles block broad strains of SARS-CoV-2. *Nature Communications* **13** (2022).
 59. Rajpoot, S. *et al.* A Novel Therapeutic Peptide Blocks SARS-CoV-2 Spike Protein Binding with Host Cell ACE2 Receptor. *Drugs in R&D* **21**, 273-283 (2021).
 60. Killingley, B. *et al.* Safety, tolerability and viral kinetics during SARS-CoV-2 human challenge in young adults. *Nat Med* (2022).
 61. Rapeport, G. *et al.* SARS-CoV-2 Human Challenge Studies - Establishing the Model during an Evolving Pandemic. *The New England journal of medicine* **385**, 961-964 (2021).
 62. Ahmed, T., Gonzalez, B.J. & Danta, I. Prevention of exercise-induced bronchoconstriction by inhaled low-molecular-weight heparin. *Am J Respir Crit Care Med* **160**, 576-581 (1999).
 63. Dixon, B. *et al.* Nebulised heparin for patients with or at risk of acute respiratory distress syndrome: a multicentre, randomised, double-blind, placebo-controlled phase 3 trial. *The Lancet Respiratory Medicine* **9**, 360-372 (2021).
 64. Tang, N. *et al.* Anticoagulant treatment is associated with decreased mortality in severe coronavirus disease 2019 patients with coagulopathy. *J Thromb Haemost* **18**, 1094-1099 (2020).
 65. Spyropoulos, A.C. *et al.* Efficacy and

- Safety of Therapeutic-Dose Heparin vs Standard Prophylactic or Intermediate-Dose Heparins for Thromboprophylaxis in High-risk Hospitalized Patients With COVID-19. *JAMA Internal Medicine* **181**, 1612 (2021).
66. Paolisso, P. *et al.* Preliminary Experience With Low Molecular Weight Heparin Strategy in COVID-19 Patients. *Front Pharmacol* **11**, 1124 (2020).
67. Pereyra, D. *et al.* Low-molecular-weight heparin use in coronavirus disease 2019 is associated with curtailed viral persistence: a retrospective multicentre observational study. *Cardiovascular Research* (2021).
68. Trunfio, M. *et al.* Early low-molecular-weight heparin administration is associated with shorter time to SARS-CoV-2 swab negativity. *Antiviral Therapy* **25**, 327-333 (2021).
69. Shi, C. *et al.* The Potential of Low Molecular Weight Heparin to Mitigate Cytokine Storm in Severe COVID-19 Patients: A Retrospective Cohort Study. *Clinical and Translational Science* **13**, 1087-1095 (2020).
70. Cao, Y. *et al.* Omicron escapes the majority of existing SARS-CoV-2 neutralizing antibodies. *Nature* (2021).
71. Hudák, A., Veres, G., Letoha, A., Szilák, L. & Letoha, T. Syndecan-4 Is a Key Facilitator of the SARS-CoV-2 Delta Variant's Superior Transmission. *Int J Mol Sci* **23** (2022).
72. Nie, C. *et al.* Charge Matters: Mutations in Omicron Variant Favor Binding to Cells. *Chembiochem*, e202100681 (2022).

Supplementary material



Supplemental Figure 1 | (A-B) Polarized normal human bronchial epithelial cells in the 3D epithelial cell model were exposed to enoxaparin (250 IU/ml) via nebulization and subsequently infected with authentic SARS-CoV-2 variants (MOI 0.1), WT, Delta (B.1.617.2) and Omicron (BA.5). Tissue integrity was monitored by TEER (Ω/cm^2) measurements (A) using EVOM voltohmmeter and SARS-CoV-2-RNA copy numbers/mL were determined (B). Data show the mean values and error bars are the SEM. Statistical analysis was performed using (A) 2way ANOVA with Tukey's multiple-comparison test. **** $p < 0.0001$ ($n = 3$), (B) 2way ANOVA with Tukey's multiple-comparison test. WT ** $p = 0.0017$, Delta * $p = 0.0189$, Omicron * $p = 0.0461$ ($n = 3$).



Supplemental Figure 2 | (A) VERO E6 cells were exposed to authentic SARS-CoV-2 pretreated with different concentrations of enoxaparin (23.4IU/mL-3000IU/mL) for 4 hours before binding was determined by RT-PCR. (B) Enoxaparin treatment effect was determined by virus binding to VeroE6 cells after 4 hours. Enoxaparin was added either to authentic SARS-CoV-2 or to the VERO E6 cells for 30 min prior to virus inoculation. (C) Infection of VeroE6 cells with authentic SARS-CoV-2 pretreated with different concentrations of enoxaparin (23.4IU/mL-3000IU/mL) was determined after 24 hours was determined by RT-PCR. Data show the mean values and error bars are the SEM. (B) One-way ANOVA with Tukey's multiple-comparison test. (Virus vs treated virus)*p=0.0366, (Virus vs treated cells)*p=0.0140, (treated virus vs treated cells) *p=0.0102, (A+C) (n=3 in duplicates; C at 375IU/ml n=1 due to technical issues), (B) (n=3 in monoplo).



CHAPTER

General Discussion

8

Epidemics outbreaks of pathogens have dominated the past centuries and are likely to occur with increasing frequency and severity in the future ¹. SARS-CoV-2, Zika virus, HIV-1 and HCV are only some of viral pathogens that have affected the life and health of hundreds of millions of people worldwide. While strategies to prevent outbreaks of emerging viruses and anti-viral therapies targeting existing infections are improving each year, so is the risk of outbreaks with pandemic potential. Increased globalization, population growth and climate change, amongst other factors, are contributing to the introduction of new viruses into the human population and further global spread.

This thesis covers different viruses with varying degrees of pandemic potential. Once a virus enters the body, it encounters various host cells at mucosal sites that are meant to protect against infection. However, ‘successful’ viruses are known to hijack host cells and overcome intrinsic and extrinsic defense mechanisms in order to establish infection and initiate dissemination. These viral mechanisms are similar amongst viruses, despite different modes of transmission. The studies presented in the previous chapters outline how viruses interact with host cells, how they either infect cells or are being degraded, and at what point viral therapies are needed to boost protection. In order to perform this research, and study viruses in contact with their natural human target cells, we developed *in vitro* and *ex vivo* models using isolated cells as well as *ex vivo* tissue. We further established a randomized trial of healthy volunteers from whom we extracted epithelial cells post treatment. Here we discuss these findings in a broader context in order to elucidate how this knowledge can be used to design novel antiviral strategies for combating viral infections now, and to prepare for future pandemics.

Heparan sulfates during viral infection and dissemination

Heparan sulfate proteoglycans (HSPGs) constitute a major part of the glycocalyx surrounding mammalian cells ². Covalently attached heparan sulfate (HS) chains on HSPGs are heavily sulfated glycosaminoglycans that exude negative charge ³. Under healthy circumstances, HSPGs act as receptors and co-receptors for various ligands and influence key processes in cell adhesion, signaling and motility ^{4, 5, 6}. Given these central roles and ubiquitous expression, it is unsurprising that HSPGs are subverted by viral, bacterial and parasitic pathogens ⁷. HSPGs influence initial steps in virus infection, such as adhesion to and invasion of host cells ^{8, 9, 10} and dissemination into systemic circulation ¹¹. Importantly, HSPGs are highly conserved amongst vertebrates and invertebrates ^{6, 12}, which also makes them attractive targets for emerging zoonotic viruses after species “spill over” ¹³ and highlight their importance as therapeutic targets.

Viruses attach to HSPGs

In **chapter 6** we show that the HSPGs Syndecan 1 and 4 are targeted by SARS-CoV-2 on epithelial cells and our data suggest that this interaction is followed by ACE-2 mediated infection¹⁴. Importantly, inhibiting SARS-CoV-2 binding to HSPGs abrogated epithelial cell infection and production of new virions, supporting the role of HSPGs as SARS-CoV-2 co-receptors. These data are in line with other studies that demonstrate SARS-CoV-2 binds HSPGs prior to ACE-2 engagement^{15, 16, 17, 18} and SARS-CoV-2 simultaneously stays bound to HSPG and ACE-2 without the need to disassociate¹⁶. Conformational changes have been proposed to be responsible for SARS-CoV-2 dependence on HSPGs as co-receptors for infection. In order to bind ACE2, SARS-CoV-2 requires the RBD of its S protein to be in the “up” or “open” formation^{19, 20, 21, 22}. The negatively charged HS binding sites on HSPGs are found in close proximity to ACE-2 and the SARS-CoV-2 S protein trimers bind HS through their receptor binding domain (RBD), which contains a subdomain consisting of positively charged amino acid residues¹⁵. Binding of the RBD to HS increases the “open” conformation of the S protein and leads to stabilizing in order to better bind ACE-2¹⁵. Interestingly, the binding affinity of SARS-CoV-2 to HS is similar in both the closed and open conformation¹⁵, yet lacks specificity²³, indicating HSPG are less biased receptors that allow SARS-CoV-2 to come into close proximity to more specialized infection receptors. Computational models have identified putative HS binding sites in the SARS-CoV-2 RBD^{15, 24, 25}, which are maintained during viral evolution²⁶. Interestingly variants of concern (VoC) have mutations in the putative HS binding sites that result in higher positive charge and have led to the hypothesis that VoC Delta (B.1.617.2) and Omicron (B.1.1.529) might have higher affinity to HS than the ancestral SARS-CoV-2^{26, 27, 28}, which could explain their improved transmission and infection rates. Mutations that resulted in increased positive charge and improved binding to HS were also observed *in vitro* following serial passaging²⁹.

Attachment to HS is further conserved amongst other coronaviruses including SARS-CoV, MERS-CoV and HCoV-NL63 that show similar binding to HSPGs^{17, 30, 31, 32, 33} and highlights the broad therapeutic potential of preventing HSPG attachment of coronaviruses.

Even though viruses preferentially use HSPGs as attachment receptors, data on Herpes Simplex virus (HSV) suggest that HSPGs can also be exploited for direct cell entry^{34, 35}. However, we did not observe SARS-CoV-2 infection of ACE-2 negative cells that expressed HSPGs (**chapter 4** and **6**), indicating that SARS-CoV-2 still requires ACE-2 for productive infection^{14, 36}.

Thus, HS alone or bound to HSPGs are tremendously important for viruses like SARS-CoV-2 by facilitating attachment and allowing for subsequent engagement of obligate entry receptors. Their highly conserved expression may promote zoonosis yet simultaneously provides the opportunity to develop therapeutics to prevent infection with SARS-CoV-2 but also other viruses.

Viruses exploit HSPGs for dissemination

Dendritic cell (DC) subsets present at barrier tissues are equipped with receptors that allow for viral capture and antigen presentation, but that can also be exploited for infection and dissemination^{37,38,39,40}. One set of receptors expressed on DCs subsets are HSPGs. Previous work from our group described Syndecan 3 expression on monocyte derived DCs (moDCs)⁸ whereas we showed that LCs express mainly Syndecan 4 (**chapter 5**⁴¹). Interestingly, Syndecan 4 expression increased upon LC maturation⁴¹. These data are in line with a previous report in which Syndecan 4 was upregulated on activated LCs and moDCs whereas Syndecan 1 expression was decreased⁴². Upregulation of Syndecan 4 was further associated with DC/LC motility and suggests a role for HSPGs in DC migration⁴². Upregulation of Syndecan 4 also occurs in presence of inflammatory stimuli^{43,44}, while HSV-1 infection has been shown to increase the expression of Syndecan 1 and 2⁹.

In **chapter 5** we explore the involvement of Syndecan 4 in HCV dissemination from mucosal barrier sites targeted during sexual transmission⁴¹. Under healthy conditions, LCs are in an immature state and express high levels of langerin. Yet upon migration or stimulation, langerin expression on LCs decreases^{45,46,47,48,49}. In parallel to the decrease in langerin, we observed upregulation of Syndecan 4 that bound HCV⁴¹. Activated LCs successfully transferred HCV to hepatic target cells in contrast to immature LCs that did not transmit HCV. Langerin was restrictive towards HCV transmission as evidenced by increased HCV transmission upon langerin block. These data indicate opposing roles for Syndecan 4 and langerin in HCV dissemination. While others have shown that HCV attaches to Syndecans expressed on hepatocytes⁵⁰ or cell lines^{51,52}, their role in HCV dissemination still remains largely elusive and should be investigated further in more detail. Particularly in light of sexual transmission upon which HCV still needs to reach target cells located in the liver.

As mentioned above, SARS-CoV-2 also attaches to HSPGs, and in particular, Syndecan 1 and 4^{14,53,54}. In line with our observations on HCV, Syndecans expressed on moDCs and LCs facilitated transfer of SARS-CoV-2 to ACE-2 expressing target cells (**chapter 6**¹⁴), indicating a role for Syndecans in SARS-CoV-2 dissemination. As neither of the DC subsets in our studies were productively infected, this suggests that SARS-CoV-2 is transmitted via a *trans*-infection pathway. Furthermore, transmission of SARS-CoV-2 was also abrogated when blocking HSPGs and hence suggests that HSPGs are involved in both SARS-CoV-2 infection and dissemination.

For HIV-1, interactions with HSPGs have been established in the past and involve roles in both infection and viral transfer to target cells^{8,11,55,56}. However, the role for HSPGs in Zika virus infection remains largely unclear. Multiple studies suggest that Zika virus is not engaging HSPGs for cell attachment^{57,58,59}. In line with these data, we did not observe Zika virus binding to HSPGs and also did not obtain any evidence that HPGs are involved in Zika virus transfer by LCs (data not shown).

Hence, it is becoming increasingly clear that HSPGs are not only crucial for many viruses to attach to cells but are also involved in capture and viral transfer from the site of initial infection to favored target tissues.

CLRs and TLRs in viral sensing and capture

Apart from HSPGs, viruses interact with many other host surface receptors expressed on DCs lining barrier tissues. Amongst those are the pathogen recognition receptors (PRRs) C-type lectins (CLRs) and Toll-like receptors (TLRs).

The CLR DC-SIGN is well-known to be subverted by viruses like HIV-1, Cytomegalovirus, Ebola virus and dengue virus for *cis*- as well as *trans*-infection^{60, 61, 62, 63, 64, 65, 66}. In contrast, binding to langerin can result in viral degradation in Birbeck granules, a process that has been extensively studied for HIV-1^{38, 45, 67}. However, langerin can also be used for viral entry and infection as has been observed for Influenza A virus⁶⁸, suggesting a viral-specific mechanism that determines whether langerin acts as an infection or degradation receptor. Usutu virus, another member of the Flavivirus family, infects LCs in the skin with the help of langerin and retains the ability to replicate efficiently instead of being degraded⁶⁹. In **chapter 2** we showed that Zika virus targets DC-SIGN on moDCs upon which the cells become infected, induce type I IFN responses and transfer Zika virus to target cells⁷⁰. However, while DC-SIGN proved crucial for Zika virus infection of moDCs, the closely related langerin receptor did not engage Zika virus on LCs⁷⁰ and block of langerin neither increased nor abrogated infection, IFN production or viral transfer. These data indicate that CLRs have specific roles in Zika virus infection and dissemination.

TLRs are transmembrane PRRs expressed by DCs. TLRs 1, 2, 4, 5 and 6 are located on the cell membrane whereas TLRs 3, 7, 8 and 9 are expressed intracellularly on endosomes^{71, 72}. TLR4 is primarily activated by components of Gram-negative bacteria, primarily LPS^{73, 74}. To a lesser extent, TLR4 can also be stimulated by toxins from Gram positive bacteria⁷⁵ and viral glycoproteins^{76, 77}. Recently, it was suggested that the SARS-CoV-2 S protein is a ligand for TLR4 and triggers pro-inflammatory responses^{78, 79, 80}. However, our results in **chapter 4** did not corroborate these claims and instead we observed neither binding of the SARS-CoV-2 S protein to TLR4 nor subsequent cell activation or cytokine induction in moDCs. These results were confirmed with a SARS-CoV-2 pseudovirus as well as a replicative SARS-CoV-2 isolate³⁶. The lack of TLR triggering on moDCs points to an evasion strategy employed by SARS-CoV-2 to avoid activation of the immune system. Interestingly, moDCs that were genetically modified to ectopically express ACE-2 were readily infected with and activated by SARS-CoV-2, indicating that instead of cell surface TLRs, intracellular receptors do sense SARS-CoV-2. These findings are supported by data that show that the cytosolic RNA sensors Rig-I and MDA5 recognize SARS-CoV-2 and induce type I IFN responses *in vitro*^{81, 82}. Interestingly, while SARS-CoV-2 did not directly activate DCs, we observed indirect DC

activation and upregulation of costimulatory molecules during co-culture with other SARS-CoV-2 infected cells. A similar mechanism was proposed for pro-inflammatory macrophage activation through infected epithelial cells⁸² and might explain inflammatory responses in COVID19 patients. CLRs and TLRs are thus important DC receptors that sense viruses at barrier tissues which can lead to either transmission, restriction or immune activation.

In **chapter 3** we observed that stimulation of immature vaginal LCs with TLR4 ligand LPS not only leads to cell activation and maturation but also renders them more susceptible to HIV-1 infection with increased potential for HIV-1 transfer to target cells⁴⁶. These data suggest that TLR4 stimulation increases HIV-1 infection of immature vaginal LCs, and thus imply a role for genital inflammation in the acquisition and dissemination risk of HIV-1.

Transcriptional analyses of vaginal antigen presenting cells suggest that they are activated through sensing of bacterial components via TLR4, resulting in pro-inflammatory cytokine secretion. These high pro-inflammatory cytokine levels and subsequent lymphocyte recruitment is further associated with a high diversity of different bacteria and a lack of *Lactobacillus spp.* in the vaginal microbiota⁸³. Decreased dominance of *Lactobacillus spp.* and overgrowth of diverse anaerobic bacteria in the vagina alters the balance of the microbiota and is called bacterial vaginosis (BV)⁸⁴. Women with BV are at increased risk of acquiring HIV-1 and are more likely to transmit HIV-1 to a sexual partner^{85,86}. A recent study from our group demonstrated that exposure of immature LCs to the anaerobic, gram negative bacterium *Prevotella timonensis* enhances HIV-1 uptake, yet does not increase productive infection⁴⁷. Exposed LCs further protected HIV-1 from degradation, turning them into viral reservoirs with the ability to transfer HIV-1 to other target cells⁴⁷ further underlining a role for BV in HIV-1 infection. The sensitivity of vaginal LCs to LPS might also be involved in increased susceptibility to HIV-1, as LPS enhanced transmission by LCs and support the hypothesis that bacterial co-infections and BV increase the risk of sexual HIV-1 acquisition.

Taken together, these data indicate that interactions between viruses and receptors are highly specific. The data further underscore the importance of studying different viral target cells isolated from physically relevant tissues to gain a better understanding about infection at various virus target sites.

The right model for the right virus

Identification and investigation of viral infections can be challenging without the right models. Most viruses are species specific and adaptation of human viruses to their host restricts studies in non-human tissues or animal models. Ideally, human pathogens are studied on human tissues and/or cells to mimic human physiological conditions and provide insights into critical stages of viral infection and disease progression.

Vaginal mucosa: a primary tissue encountered during sexual transmission

Vaginal mucosa constitutes an important viral entry site for sexually transmitted viruses (partially discussed in ⁸⁷) with vaginal LCs being one of the first target cells encountered by HIV-1 ^{88, 89}.

When phenotyping vaginal LCs in **chapter 3**, vaginal LCs expressed the major TLRs including TLR2 and TLR4 ⁴⁶ whereas skin-derived LCs that do not express TLR4 ⁹⁰. However, immature LCs isolated from the epidermis as well as the epithelium of vaginal mucosa expressed high levels of CD1a and langerin, which indicates that they are both “classic LCs” ^{45, 91, 92, 93}.

Recent studies have suggested that other, DC-like subsets are present in mucosal barrier tissues of the vaginal tract that show LC-like characteristics. Unlike “classic LCs”, the CD1a⁺ vaginal epithelial cells (VEDCs) described by Pena-Cruz *et al.* in vaginal mucosa do not harbor Birbeck granules while expressing langerin. The authors argue this makes them more susceptible to HIV-1 infection than skin-derived LCs ⁹⁴. Another CD1a⁺ cell was described in the epidermis and anogenital mucosa that expressed CD11c but low levels of langerin ⁹⁵. Again, the authors did not detect Birbeck granules. Similar to VEDCs, these cells were susceptible to HIV-1 infection and transmission and are particularly enriched in anogenital mucosa ⁹⁵. However, little more is known about the phenotype and functionality of these LC-like cells. As we have observed in **chapter 3** ⁴⁶ and others before us ^{45, 48, 49}, activated LCs express little langerin and are more susceptible to HIV-1 infection than immature LCs. This phenotype is highly similar to that of the VEDC and CD1a⁺ dermal DCs described and might allude to the fact that the latter are actually LCs in an activated or differentiated state. Langerin expression is highly associated with the formation of Birbeck granules ^{96, 97} and activated LCs contain fewer and smaller Birbeck granules compared to immature LCs ⁹⁷. These discrepancies might explain why the groups of Pena-Cruz and Bertram ^{94, 95} did not detect Birbeck granules in their cultures. However, as we did not visualize Birbeck granules, we cannot exclude the possibility that our cell cultures also contain some cells that are not classic LCs even though we did not observe HIV-1 infection on immature vaginal LCs. Moreover, as we observed differences between vaginal and skin derived LCs pertaining to their TLR expression, it is possible that there are other, phenotypic differences, that allow for tissue-specific roles of LCs and support the use of vaginal mucosa over epidermis when studying sexually transmitted viruses.

Cohort studies to monitor progress of chronic virus-host interactions

For chronic viral infections like HIV-1, it is important to not only study the effects of initial contact between virus and human host, but also to follow the virus over time. Even though there are antiretroviral therapies (ART) available that prevent viral replication, HIV-1

infected individuals still cannot be cured of the virus through standard practice, and instead rely on lifelong treatment^{98, 99}.

Since the early stages of the HIV-1/AIDS pandemic, longitudinal cohort studies of people living with HIV-1 and people at risk for HIV-1 infection are implemented to identify risk factors, infection incidence and disease progression^{100, 101, 102}. Importantly, the sample collections available from cohort studies are used to monitor HIV-1 infection over time with regards to the virus^{103, 104, 105}, the host cells involved during infection¹⁰⁶ and the status of the immune response¹⁰⁷. These human tissue samples are further crucial to determine the effects of HIV-1 as well as treatment on the immune system^{108, 109}. More recently, cohort study samples have been crucial in order to study the latent HIV-1 reservoir^{110, 111}. Additionally, treatment interruption studies have identified characteristics of people that are superior post treatment controllers^{112, 113, 114}, taking further steps towards understanding the interplay between virus and host. The use of *ex vivo* tissues from cohort studies remains an attractive alternative and allows the study of cells that are either newly infected or already well adapted to the challenges of an HIV-1 infection. Moreover, a randomized controlled trial where therapeutics are administered to HIV-1 negative volunteers combined with an *ex vivo* viral inoculation (as described in **chapter 7**) remains a possibility to study effectivity and safety of novel therapeutics.

Challenging humans to move from bench to bedside

Even though a human virus challenge is not an option for chronic viruses like HIV-1, controlled human infection models have been employed to study diseases for decades and have led to significant advancement in clinical studies^{115, 116, 117}. The risks and benefits of challenging humans with viruses always need to be carefully assessed and ethically acceptable^{118, 119, 120} and in May 2020 the WHO specified eight key criteria specifically for a challenge with the newly emerged SARS-CoV-2¹²¹.

To this date, there has only been one SARS-CoV-2 challenge study, that was finalized in 2022¹²². Killingley and colleagues investigated the effects of nasally introduced SARS-CoV-2 inoculum and the viral kinetics of a primary infection. Importantly, all participants were young adults between the ages of 18 and 29 and the inoculum was a low 10 TCID₅₀, increasing patient safety but narrowing the study scope especially since elderly are at higher risk of severe COVID19¹²². For other respiratory diseases like influenza and rhinovirus infections, human challenge studies are much more common^{123, 124, 125}. Yet human challenge studies have not only been conducted for respiratory viruses but also vector-borne diseases like malaria where challenge studies are now an integral part of the vaccine and drug development cycle^{117, 126, 127, 128}. The causative agent for malaria is transmitted via mosquito vectors and human infection is either introduced by direct sporozoites injection^{129, 130} or through bites of infected mosquitoes^{126, 131, 132}. A similar approach could be taken for Zika virus. Indeed, in 2016 a human challenge study was proposed for Zika virus but was

ultimately denied by the ethics committee due to concerns about bystander risks that were not involved in the study and the justified benefits amidst many other studies conducted simultaneously¹³³. However, since the 2016 epidemic, many of the initial parameters have since changed and there is more information available to mitigate risks¹³⁴, and the idea might be revisited. Our data on Zika virus target cells in the skin further support a human challenge model with mosquito/skin contact, similar to what is already standard procedure for malaria research. More focus is shifting towards the use of human challenge studies as recently evidenced by a call made to consider a human infection models in HCV research¹³⁵. However, even though therapeutics against HCV are excellent¹³⁶, to this date no human challenge studies have been approved, indicating that challenging humans with viruses is not without its hurdles yet.

On the nose: SARS-CoV-2 and nasal epithelia

In **chapter 6**, we investigated the potential of low molecular weight heparins (LMWHs) as therapeutics against SARS-CoV-2 infection and observed a decrease in binding as well as infection when cells were inoculated with LMWHs prior to SARS-CoV-2 exposure. From the array of LMWHs tested for their inhibitory potential against SARS-CoV-2, enoxaparin displayed the most efficient block against SARS-CoV-2 binding¹⁴ and was subsequently used for follow-up studies. In order to ascertain the preventative effect of LMWHs on human nasal cells stationed at one of the first sites of interaction with SARS-CoV-2, we retrieved epithelial cells from the human noses. The cells removed from these tissues were inoculated with LMWHs as well as SARS-CoV-2 shortly after collection in order to maintain their phenotypic integrity. As we observed a decrease of SARS-CoV-2 binding and infection upon LMWH inoculation *in vitro*¹⁴, we were interested to investigate whether LMWHs retain their antiviral properties *in vivo*.

Therefore, we designed a non-randomized controlled trial (**chapter 7**). Importantly, this approach is not a human challenge model as it did not involve infection of human study participants and instead relied on *ex vivo* infection of human tissues post treatment¹³⁷ (**Figure 1**). The epithelial cells retrieved from human nasal mucosa were inoculated with SARS-CoV-2 *ex vivo* in both **chapter 6** and **7**^{14, 137}. However, in **chapter 7**, the LMWH enoxaparin was applied with the aid of a nose spray directly into the nostril of healthy participant *in vivo* before epithelial cell retrieval¹³⁷. This approach allowed for the combination of controlled application of a therapeutic directly to humans with *ex vivo* virus inoculation and analysis. Another advantage of this specific set-up is the opportunity to administer both a placebo as well as the medication (enoxaparin) to the same individual, decreasing the chance of differences between donors. Moreover, the small sample size and single center approach allowed for swift prove of concept that demonstrated the safety of LMWHs as intervention. But most importantly, this approach allowed for testing of the efficacy of LMWHs as prevention against SARS-CoV-2 infection without the need of a human

virus challenge, an approach that was not a possibility with such a high-risk, pandemic virus at the time.

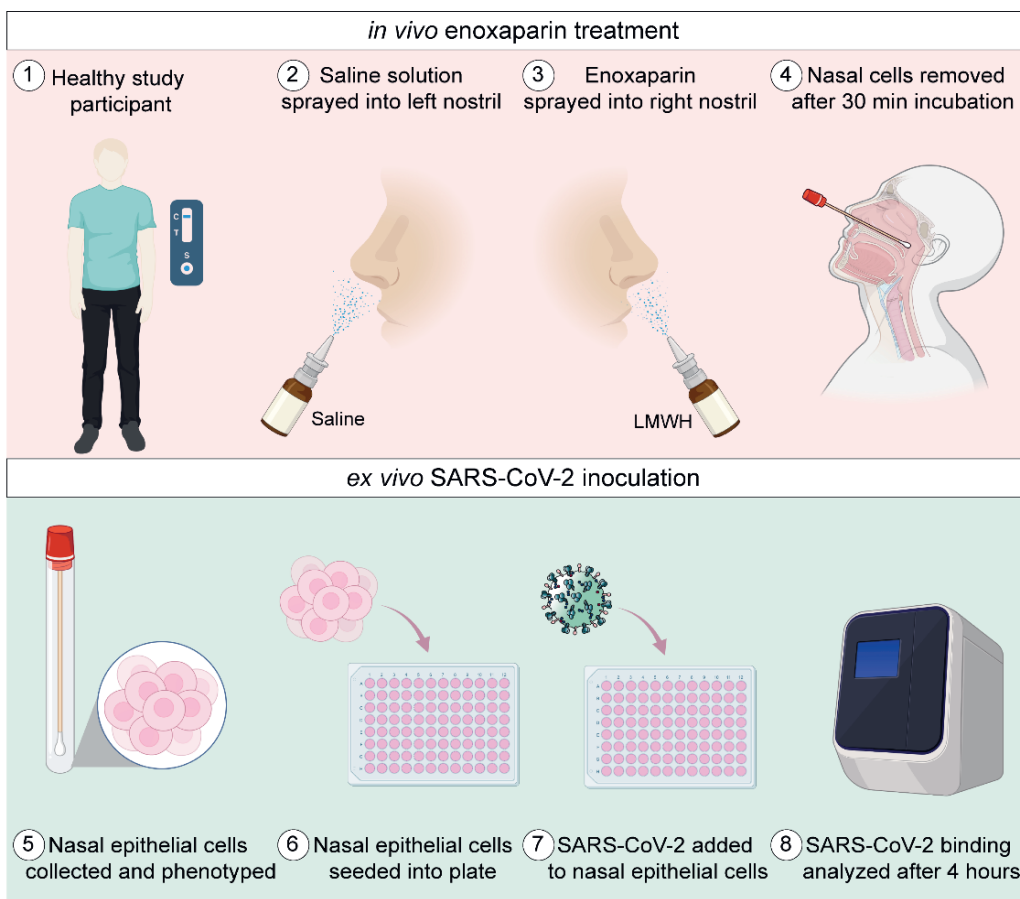


Figure 1 | Schematic overview non-randomized controlled trial. Firstly, healthy volunteers are recruited and a general health check as well as a lateral flow test to exclude SARS-Cov-2 infection are performed. A spray containing saline solution is then sprayed into the left nostril of the participant. After 30 minutes, nasal epithelial tissue is removed with a brush. Subsequently, enoxaparin is sprayed into the right nostril of the same participant with the same device. After 30 minutes of incubation, nasal epithelial tissue is again removed with a brush. The brushes containing the nasal cells are deposited in collection tubes filled with cell medium and transported into a laboratory. The epithelial cells are removed from the brushes through centrifugation and counted. A part of the cells is then phenotyped via flow cytometry while the other part is seeded in a culture plate. The seeded cells are exposed to SARS-CoV-2 for four hours. Additionally, some cells are exposed to SARS-CoV-2 and enoxaparin. After four hours, the cells are lysed and SARS-Cov-2 binding is analyzed via RT-PCR. Created with Biorender.com

We further employed a 3D epithelial cell model of polarized normal human bronchial epithelial cells. Due to the prolonged culture time of more than 50 days these polarized epithelial cells closely resemble human nasal epithelial cells as they produce mucus and have beating cilia¹³⁸. The epithelial cells are cultured at an air-liquid interface to further

mimic human airway epithelium^{138, 139}. These 3D cultures contain epithelial cells in a monolayer that can be inoculated with SARS-CoV-2 to investigate infection over multiple time points. Unlike with the primary nasal epithelial cells, we were able to investigate SARS-CoV-2 infection in the 3D cultures as well as long-term effects of enoxaparin *in vitro*¹³⁷. Moreover, 3D cultures could be sprayed with enoxaparin prior to virus inoculation, similar to applications in humans. The cells used in the 3D culture model described in **chapter 7** are normal bronchial epithelial cells of primary human origin, that in 3D cultures closely resemble human tissues^{138, 140, 141}. Alternatively, primary human epithelial cells removed during bronchoscopy can also be directly used and cultured¹⁴².

To summarize, human cells/tissues located at virus entry sites enabled the study of early infection events without the need of animal models. The freshly isolated cells retained phenotypic characteristics comparable to cells characterized in *ex vivo* models whereas 3D culture models can mimic physiological conditions for long-term cultures. The possibility to treat and stimulate these tissues prior to virus inoculation further provide an intriguing target to study viral therapies and preventative methods as well as their toxicity, helping the advancement of research from bench to bedside. Challenging humans directly with viruses takes this approach one step further but it does not fit all viruses or tissues and the risks and benefits need to be carefully considered.

Low molecular weight heparins as protection against infection

In **chapters 5**⁴¹, **6**¹⁴ and **7**¹³⁷ we investigated whether heparin and LMWHs inhibit infection and transmission of HCV and SARS-CoV-2. Heparin is a linear glycosaminoglycan that is commonly used as an anticoagulant and antithrombotic drug¹⁴³. Even though heparin is still administered more than 80 years after its initial discovery¹⁴⁴, it has been widely replaced by LMWHs like enoxaparin, dalteparin and tinzaparin, due to their smaller size, higher pharmacokinetic predictability and lower risk of side effects^{145, 146}. LMWHs are fractured from heparin through depolymerization and consist of short polysaccharide chains^{147, 148}. Since the start of the SARS-CoV-2 pandemic, the potential of heparin and LMWHs during viral infections has shifted into focus again. Subcutaneous administration of heparin and LMWHs to COVID-19 patients was associated with decreased mortality and better clinical outcome^{149, 150, 151}, potentially due to anti-inflammatory properties of the drugs^{152, 153}. Moreover, heparin and LMWHs have been shown to prevent virus binding by us (**chapters 5, 6 and 7**^{14, 41, 137}) and others^{15, 154, 155}. SARS-CoV-2 binds heparin with similar affinity as it does HSPGs^{15, 27} and it has been hypothesized that heparin occupies binding sites on SARS-CoV-2 that subsequently cannot engage with host HSPGs^{27, 154}. Therefore, these anticoagulants have been proposed to be repurposed as antivirals^{14, 15, 27, 154}.

Intranasal injection or nebulization of heparin has been explored in a phase 3 trial for people at risk of respiratory distress syndrome¹⁵⁶ and in a pre-clinical study of asthmatic children reducing bronchial hyper reactivity to medication¹⁵⁷. In this thesis we could demonstrate the intranasal injection with LMHW is safe, easy to use and resulted in protection of human epithelial cells against SARS-CoV-2 infection (**Chapter 7**¹³⁷) marking it as a viable prophylactic treatment against SARS-CoV-2. Importantly, the protection against SARS-CoV-2 was similar between the original Wuhan strain and two of the latest VoC, Delta (B.1.617.2) and Omicron (BA.5)¹³⁷, underscoring the broad-spectrum activity of LMWHs.

Heparin and LMWHs are safe, available in abundance, cheap and easily applicable. By blocking the binding to HSPGs, they target a wide range of different viruses. This feature makes them particularly attractive as antivirals in the early stages of a pandemic with airborne viruses when no specific preventative and therapeutic antiviral strategies are available yet.

Concluding remarks and future prospective

Despite differences in their mode of transmission, (pandemic) viruses often encounter similar cellular and molecular host factors at human barrier tissues. The cells located at these barrier sites can in turn either perturb or aid invading viruses in establishing disease. While it can be advantageous for the virus to employ multiple transmission routes, it also presents an opportunity for generalized therapeutic approaches.

In this thesis we have studied four distinct viruses (Zika virus, SARS-CoV-2, HIV-1 and HCV) with unique and overlapping transmission routes. Human *in vitro* and *ex vivo* models allowed the study of host-virus interactions in a physiologically relevant environment and provided us with important insights into early infection events. Cellular compositions and phenotypes can vary between tissues and influence infection while cell activation state and changes in the microbiota influence susceptibility and increase the potential of a virus to disseminate away from the barrier and into other tissues.

Once a virus encounters the human host, it first has to attach to host cells. We unraveled an important role for the ubiquitously expressed HPGS not only as attachment receptors supporting infection but also as facilitators of viral dissemination on cells that are not permissive for infection. The expression of the HSPG Syndecan 4 as well as the CLR langerin on LCs changes depending on activation state and indicate that receptor expressing influences the role cells play in viral protection or exacerbation.

Based on clinical and fundamental studies, including those presenting in this thesis, HSPG binding of viruses can be prevented by applying heparin or its LMWH derivatives. LMWHs, are already on the market and commonly used as anticoagulants. The potential of LMWHs as preventive antiviral therapy has the further advantage to both abrogate infection and dissemination. During the emergence of a new pandemic virus, a swift abrogation of

transmission is crucial to slow down the spread. However, protection against a new virus is difficult to achieve without any knowledge on the pathogen to develop virus specific antivirals or vaccination. LMWHs present a class of medication that is safe to use, easy to apply to mucosal surfaces like the nose, and most importantly, protect against a broad spectrum of viral pathogens.

The rise of mutated SARS-CoV-2 VoC underscored the need for fast acting antivirals with broad tropism to curb further spread even in demographics with high immunity obtained through vaccination or previous infection with an older strain. Our data demonstrated that LMWHs block viral attachment to the same extent for different SARS-CoV-2 VoC and it can be speculated that they also protect against future variants that effectively evade vaccine induced immunity. Even though the WHO declared an end to the COVID-19 global health emergency in May 2023 ¹⁵⁸, the threat of SARS-CoV-2 to public health remains, even if the virus is considered endemic. Moreover, as seen in the past few years, the world is on high alert for newly emerging viruses as well as variants of concern and therefore the use of LMWHs as therapeutic to protect against new viral pandemics might be a valuable tool in the future and should be explored further.

References

1. Marani, M., Katul, G.G., Pan, W.K. & Parolari, A.J. Intensity and frequency of extreme novel epidemics. *Proceedings of the National Academy of Sciences* **118**, e2105482118 (2021).
2. Karamanos, N.K., *et al.* Proteoglycan Chemical Diversity Drives Multifunctional Cell Regulation and Therapeutics. *Chem Rev* **118**, 9152-9232 (2018).
3. Esko, J.D., Kimata, K. & Lindahl, U. Proteoglycans and Sulfated Glycosaminoglycans. in *Essentials of Glycobiology* (eds. Varki, A., *et al.*) (Cold Spring Harbor Laboratory Press Copyright © 2009, The Consortium of Glycobiology Editors, La Jolla, California., Cold Spring Harbor (NY), 2009).
4. Sarrazin, S., Lamanna, W.C. & Esko, J.D. Heparan sulfate proteoglycans. *Cold Spring Harb Perspect Biol* **3**(2011).
5. Vlodaysky, I., Barash, U., Nguyen, H.M., Yang, S.M. & Ilan, N. Biology of the Heparanase-Heparan Sulfate Axis and Its Role in Disease Pathogenesis. *Semin Thromb Hemost* **47**, 240-253 (2021).
6. Bishop, J.R., Schuksz, M. & Esko, J.D. Heparan sulphate proteoglycans fine-tune mammalian physiology. *Nature* **446**, 1030-1037 (2007).
7. Bartlett, A.H. & Park, P.W. Heparan Sulfate Proteoglycans in Infection. in *Glycans in Diseases and Therapeutics* (ed. Pavão, M.S.G.) 31-62 (Springer Berlin Heidelberg, Berlin, Heidelberg, 2011).
8. de Witte, L., *et al.* Syndecan-3 is a dendritic cell-specific attachment receptor for HIV-1. *Proc Natl Acad Sci U S A* **104**, 19464-19469 (2007).
9. Bacsa, S., *et al.* Syndecan-1 and syndecan-2 play key roles in herpes simplex virus type-1 infection. *J Gen Virol* **92**, 733-743 (2011).
10. Dalrymple, N. & Mackow, E.R. Productive dengue virus infection of human endothelial cells is directed by heparan sulfate-containing proteoglycan receptors. *J Virol* **85**, 9478-9485 (2011).
11. Bobardt, M.D., *et al.* Contribution of proteoglycans to human immunodeficiency virus type 1 brain invasion. *J Virol* **78**, 6567-6584 (2004).
12. Merton Bernfield, *et al.* Functions of Cell Surface Heparan Sulfate Proteoglycans. *Annual Review of Biochemistry* **68**, 729-777 (1999).
13. Parrish, C.R., *et al.* Cross-species virus transmission and the emergence of new epidemic diseases. *Microbiol Mol Biol Rev* **72**, 457-470 (2008).
14. Bermejo-Jambrina, M., *et al.* Infection and transmission of SARS-CoV-2 depend on heparan sulfate proteoglycans. *Embo j* **40**, e106765 (2021).
15. Clausen, T.M., *et al.* SARS-CoV-2 Infection Depends on Cellular Heparan Sulfate and ACE2. *Cell* **183**, 1043-1057.e1015 (2020).
16. Liu, L., *et al.* Heparan Sulfate Proteoglycans as Attachment Factor for SARS-CoV-2. *ACS Cent Sci* **7**, 1009-1018 (2021).
17. Chu, H., *et al.* Host and viral determinants for efficient SARS-CoV-2 infection of the human lung. *Nature*

- Communications* **12**, 134 (2021).
18. Zhang, Q., *et al.* Heparan sulfate assists SARS-CoV-2 in cell entry and can be targeted by approved drugs in vitro. *Cell Discov* **6**, 80 (2020).
 19. Costello, S.M., *et al.* The SARS-CoV-2 spike reversibly samples an open-trimer conformation exposing novel epitopes. *Nature Structural & Molecular Biology* **29**, 229-238 (2022).
 20. Henderson, R., *et al.* Controlling the SARS-CoV-2 spike glycoprotein conformation. *Nature Structural & Molecular Biology* **27**, 925-933 (2020).
 21. Walls, A.C., *et al.* Structure, Function, and Antigenicity of the SARS-CoV-2 Spike Glycoprotein. *Cell* **181**, 281-292.e286 (2020).
 22. Wrapp, D., *et al.* Cryo-EM structure of the 2019-nCoV spike in the prefusion conformation. *Science* **367**, 1260-1263 (2020).
 23. Parafioriti, M., *et al.* Evidence for Multiple Binding Modes in the Initial Contact Between SARS-CoV-2 Spike S1 Protein and Cell Surface Glycans. *Chemistry* **29**, e202202599 (2023).
 24. Schuurs, Z.P., *et al.* Evidence of a putative glycosaminoglycan binding site on the glycosylated SARS-CoV-2 spike protein N-terminal domain. *Comput Struct Biotechnol J* **19**, 2806-2818 (2021).
 25. Kim, S.Y., *et al.* Characterization of heparin and severe acute respiratory syndrome-related coronavirus 2 (SARS-CoV-2) spike glycoprotein binding interactions. *Antiviral Res* **181**, 104873 (2020).
 26. Kim, S.H., *et al.* GlycoGrip: Cell Surface-Inspired Universal Sensor for Betacoronaviruses. *ACS Central Science* **8**, 22-42 (2022).
 27. Paiardi, G., *et al.* The binding of heparin to spike glycoprotein inhibits SARS-CoV-2 infection by three mechanisms. *Journal of Biological Chemistry* **298**, 101507 (2022).
 28. Kearns, F.L., *et al.* Spike-heparan sulfate interactions in SARS-CoV-2 infection. *Curr Opin Struct Biol* **76**, 102439 (2022).
 29. Shiliaev, N., *et al.* Natural and Recombinant SARS-CoV-2 Isolates Rapidly Evolve In Vitro to Higher Infectivity through More Efficient Binding to Heparan Sulfate and Reduced S1/S2 Cleavage. *J Virol* **95**, e0135721 (2021).
 30. Milewska, A., *et al.* Human coronavirus NL63 utilizes heparan sulfate proteoglycans for attachment to target cells. *J Virol* **88**, 13221-13230 (2014).
 31. Lang, J., *et al.* Inhibition of SARS Pseudovirus Cell Entry by Lactoferrin Binding to Heparan Sulfate Proteoglycans. *PLOS ONE* **6**, e23710 (2011).
 32. Milewska, A., *et al.* Entry of Human Coronavirus NL63 into the Cell. *J Virol* **92**(2018).
 33. Hao, W., *et al.* Binding of the SARS-CoV-2 spike protein to glycans. *Science Bulletin* **66**, 1205-1214 (2021).
 34. Shukla, D., *et al.* A Novel Role for 3-O-Sulfated Heparan Sulfate in Herpes Simplex Virus 1 Entry. *Cell* **99**, 13-22 (1999).
 35. Tiwari, V., *et al.* Role for 3-O-Sulfated Heparan Sulfate as the Receptor for Herpes Simplex Virus Type 1 Entry into Primary Human Corneal

- Fibroblasts. *Journal of Virology* **80**, 8970-8980 (2006).
36. van der Donk, L.E.H., *et al.* SARS-CoV-2 infection activates dendritic cells via cytosolic receptors rather than extracellular TLRs. *Eur J Immunol* **52**, 646-655 (2022).
 37. Bermejo-Jambrina, M., *et al.* C-Type Lectin Receptors in Antiviral Immunity and Viral Escape. *Frontiers in Immunology* **9**(2018).
 38. Ribeiro, C.M., *et al.* Receptor usage dictates HIV-1 restriction by human TRIM5 α in dendritic cell subsets. *Nature* **540**, 448-452 (2016).
 39. Geijtenbeek, T.B., *et al.* Identification of DC-SIGN, a novel dendritic cell-specific ICAM-3 receptor that supports primary immune responses. *Cell* **100**, 575-585 (2000).
 40. Wilson, N.S. & Villadangos, J.A. Regulation of Antigen Presentation and Cross-Presentation in the Dendritic Cell Network: Facts, Hypothesis, and Immunological Implications. in *Advances in Immunology*, Vol. 86 (ed. Alt, F.W.) 241-305 (Academic Press, 2005).
 41. Nijmeijer, B.M., *et al.* Syndecan 4 Upregulation on Activated Langerhans Cells Counteracts Langerin Restriction to Facilitate Hepatitis C Virus Transmission. *Front Immunol* **11**, 503 (2020).
 42. Averbeck, M., *et al.* Switch in syndecan-1 and syndecan-4 expression controls maturation associated dendritic cell motility. *Exp Dermatol* **16**, 580-589 (2007).
 43. Okuyama, E., *et al.* Molecular mechanisms of syndecan-4 upregulation by TNF- α in the endothelium-like EAhy926 cells. *J Biochem* **154**, 41-50 (2013).
 44. Zhang, Y., Pasparakis, M., Kollias, G. & Simons, M. Myocyte-dependent regulation of endothelial cell syndecan-4 expression. Role of TNF- α . *J Biol Chem* **274**, 14786-14790 (1999).
 45. de Witte, L., *et al.* Langerin is a natural barrier to HIV-1 transmission by Langerhans cells. *Nature Medicine* **13**, 367-371 (2007).
 46. van Teijlingen, N.H., *et al.* Immune activation of vaginal human Langerhans cells increases susceptibility to HIV-1 infection. *Sci Rep* **13**, 3283 (2023).
 47. van Teijlingen, N.H., *et al.* Vaginal bacterium *Prevotella timonensis* turns protective Langerhans cells into HIV-1 reservoirs for virus dissemination. *Embo j* **41**, e110629 (2022).
 48. Fahrback, K.M., *et al.* Activated CD34-Derived Langerhans Cells Mediate Transinfection with Human Immunodeficiency Virus. *Journal of Virology* **81**, 6858-6868 (2007).
 49. Valladeau, J., *et al.* The monoclonal antibody DCGM4 recognizes Langerin, a protein specific of Langerhans cells, and is rapidly internalized from the cell surface. *Eur J Immunol* **29**, 2695-2704 (1999).
 50. Lefèvre, M., Felmlee, D.J., Parnot, M., Baumert, T.F. & Schuster, C. Syndecan 4 is involved in mediating HCV entry through interaction with lipoviral particle-associated apolipoprotein E. *PLoS One* **9**, e95550 (2014).
 51. Shi, Q., Jiang, J. & Luo, G. Syndecan-1 serves as the major receptor for attachment of hepatitis C virus to the

- surfaces of hepatocytes. *J Virol* **87**, 6866-6875 (2013).
52. Grigorov, B., *et al.* Hepatitis C virus infection propagates through interactions between Syndecan-1 and CD81 and impacts the hepatocyte glycocalyx. *Cell Microbiol* **19**(2017).
 53. Hudák, A., Veres, G., Letoha, A., Szilák, L. & Letoha, T. Syndecan-4 Is a Key Facilitator of the SARS-CoV-2 Delta Variant's Superior Transmission. *Int J Mol Sci* **23**(2022).
 54. Prieto-Fernández, E., *et al.* Hypoxia reduces cell attachment of SARS-CoV-2 spike protein by modulating the expression of ACE2, neuropilin-1, syndecan-1 and cellular heparan sulfate. *Emerg Microbes Infect* **10**, 1065-1076 (2021).
 55. de Parseval, A., *et al.* A highly conserved arginine in gp120 governs HIV-1 binding to both syndecans and CCR5 via sulfated motifs. *J Biol Chem* **280**, 39493-39504 (2005).
 56. Saphire, A.C., Bobardt, M.D., Zhang, Z., David, G. & Gallay, P.A. Syndecans serve as attachment receptors for human immunodeficiency virus type 1 on macrophages. *J Virol* **75**, 9187-9200 (2001).
 57. Gao, H., *et al.* Role of heparan sulfate in the Zika virus entry, replication, and cell death. *Virology* **529**, 91-100 (2019).
 58. Ghezzi, S., *et al.* Heparin prevents Zika virus induced-cytopathic effects in human neural progenitor cells. *Antiviral Res* **140**, 13-17 (2017).
 59. Tan, C.W., Sam, I.C., Chong, W.L., Lee, V.S. & Chan, Y.F. Polysulfonate suramin inhibits Zika virus infection. *Antiviral Res* **143**, 186-194 (2017).
 60. Trumpfheller, C., Park, C.G., Finke, J., Steinman, R.M. & Granelli-Piperno, A. Cell type-dependent retention and transmission of HIV-1 by DC-SIGN. *International Immunology* **15**, 289-298 (2003).
 61. Halary, F., *et al.* Human cytomegalovirus binding to DC-SIGN is required for dendritic cell infection and target cell trans-infection. *Immunity* **17**, 653-664 (2002).
 62. Alvarez, C.P., *et al.* C-type lectins DC-SIGN and L-SIGN mediate cellular entry by Ebola virus in cis and in trans. *J Virol* **76**, 6841-6844 (2002).
 63. Geijtenbeek, T.B., *et al.* DC-SIGN, a dendritic cell-specific HIV-1-binding protein that enhances trans-infection of T cells. *Cell* **100**, 587-597 (2000).
 64. Arrighi, J.F., *et al.* DC-SIGN-mediated infectious synapse formation enhances X4 HIV-1 transmission from dendritic cells to T cells. *J Exp Med* **200**, 1279-1288 (2004).
 65. Lee, B., *et al.* cis Expression of DC-SIGN allows for more efficient entry of human and simian immunodeficiency viruses via CD4 and a coreceptor. *J Virol* **75**, 12028-12038 (2001).
 66. Tassaneeritthep, B., *et al.* DC-SIGN (CD209) mediates dengue virus infection of human dendritic cells. *J Exp Med* **197**, 823-829 (2003).
 67. van den Berg, L.M., *et al.* Caveolin-1 mediated uptake via langerin restricts HIV-1 infection in human Langerhans cells. *Retrovirology* **11**, 123 (2014).
 68. Ng, W.C., *et al.* The C-type Lectin Langerin Functions as a Receptor for

- Attachment and Infectious Entry of Influenza A Virus. *J Virol* **90**, 206-221 (2016).
69. Martin, M.F., *et al.* Usutu Virus escapes langerin-induced restriction to productively infect human Langerhans cells, unlike West Nile virus. *Emerg Microbes Infect* **11**, 761-774 (2022).
70. Eder, J., *et al.* Transmission of Zika virus by dendritic cell subsets in skin and vaginal mucosa. *Frontiers in Immunology* **14**(2023).
71. Kumar, H., Kawai, T. & Akira, S. Toll-like receptors and innate immunity. *Biochem Biophys Res Commun* **388**, 621-625 (2009).
72. Blasius, A.L. & Beutler, B. Intracellular toll-like receptors. *Immunity* **32**, 305-315 (2010).
73. Beutler, B. & Rietschel, E.T. Innate immune sensing and its roots: the story of endotoxin. *Nat Rev Immunol* **3**, 169-176 (2003).
74. Chow, J.C., Young, D.W., Golenbock, D.T., Christ, W.J. & Gusovsky, F. Toll-like receptor-4 mediates lipopolysaccharide-induced signal transduction. *J Biol Chem* **274**, 10689-10692 (1999).
75. Malley, R., *et al.* Recognition of pneumolysin by Toll-like receptor 4 confers resistance to pneumococcal infection. *Proc Natl Acad Sci U S A* **100**, 1966-1971 (2003).
76. Kurt-Jones, E.A., *et al.* Pattern recognition receptors TLR4 and CD14 mediate response to respiratory syncytial virus. *Nat Immunol* **1**, 398-401 (2000).
77. Scherm, M.J., Gangloff, M. & Gay, N.J. Activation of Toll-like receptor 4 by Ebola virus-shed glycoprotein is direct and requires the internal fusion loop but not glycosylation. *Cell Rep* **41**, 111562 (2022).
78. Shirato, K. & Kizaki, T. SARS-CoV-2 spike protein S1 subunit induces pro-inflammatory responses via toll-like receptor 4 signaling in murine and human macrophages. *Heliyon* **7**, e06187 (2021).
79. Zhao, Y., *et al.* SARS-CoV-2 spike protein interacts with and activates TLR4. *Cell Research* **31**, 818-820 (2021).
80. Bhattacharya, M., *et al.* Immunoinformatics approach to understand molecular interaction between multi-epitopic regions of SARS-CoV-2 spike-protein with TLR4/MD-2 complex. *Infect Genet Evol* **85**, 104587 (2020).
81. Sampaio, N.G., *et al.* The RNA sensor MDA5 detects SARS-CoV-2 infection. *Scientific Reports* **11**, 13638 (2021).
82. Thorne, L.G., *et al.* SARS-CoV-2 sensing by RIG-I and MDA5 links epithelial infection to macrophage inflammation. *Embo j* **40**, e107826 (2021).
83. Anahtar, Melis N., *et al.* Cervicovaginal Bacteria Are a Major Modulator of Host Inflammatory Responses in the Female Genital Tract. *Immunity* **42**, 965-976 (2015).
84. Coudray, M.S. & Madhivanan, P. Bacterial vaginosis-A brief synopsis of the literature. *Eur J Obstet Gynecol Reprod Biol* **245**, 143-148 (2020).
85. Atashili, J., Poole, C., Ndumbe, P.M., Adimora, A.A. & Smith, J.S. Bacterial vaginosis and HIV acquisition: a meta-analysis of published studies. *Aids* **22**,

- 1493-1501 (2008).
86. Hoang, T., *et al.* The cervicovaginal mucus barrier to HIV-1 is diminished in bacterial vaginosis. *PLoS Pathog* **16**, e1008236 (2020).
 87. Julia Eder, N.H.v.T., Teunis B.H. Geijtenbeek. The right model for the right virus. Vol. 2023 (Nature Portfolio, Nature Portfolioa Microbiology Community, 2023).
 88. Ballweber, L., *et al.* Vaginal langerhans cells nonproductively transporting HIV-1 mediate infection of T cells. *J Virol* **85**, 13443-13447 (2011).
 89. Hladik, F., *et al.* Initial events in establishing vaginal entry and infection by human immunodeficiency virus type-1. *Immunity* **26**, 257-270 (2007).
 90. Flacher, V., *et al.* Human Langerhans Cells Express a Specific TLR Profile and Differentially Respond to Viruses and Gram-Positive Bacteria¹. *The Journal of Immunology* **177**, 7959-7967 (2006).
 91. Mizumoto, N. & Takashima, A. CD1a and langerin: acting as more than Langerhans cell markers. *J Clin Invest* **113**, 658-660 (2004).
 92. Collin, M., McGovern, N. & Haniffa, M. Human dendritic cell subsets. *Immunology* **140**, 22-30 (2013).
 93. Romani, N., Clausen, B.E. & Stoitzner, P. Langerhans cells and more: langerin-expressing dendritic cell subsets in the skin. *Immunol Rev* **234**, 120-141 (2010).
 94. Pena-Cruz, V., *et al.* HIV-1 replicates and persists in vaginal epithelial dendritic cells. *J Clin Invest* **128**, 3439-3444 (2018).
 95. Bertram, K.M., *et al.* Identification of HIV transmitting CD11c+ human epidermal dendritic cells. *Nature Communications* **10**, 2759 (2019).
 96. Valladeau, J., *et al.* Langerin, a novel C-type lectin specific to Langerhans cells, is an endocytic receptor that induces the formation of Birbeck granules. *Immunity* **12**, 71-81 (2000).
 97. McDermott, R., *et al.* Reproduction of Langerin/CD207 traffic and Birbeck granule formation in a human cell line model. *J Invest Dermatol* **123**, 72-77 (2004).
 98. Deeks, S.G., *et al.* International AIDS Society global scientific strategy: towards an HIV cure 2016. *Nat Med* **22**, 839-850 (2016).
 99. Grijzen, M.L., *et al.* No Treatment versus 24 or 60 Weeks of Antiretroviral Treatment during Primary HIV Infection: The Randomized Primo-SHM Trial. *PLOS Medicine* **9**, e1001196 (2012).
 100. Jansen, I.A., *et al.* Ongoing HIV-1 transmission among men who have sex with men in Amsterdam: a 25-year prospective cohort study. *AIDS* **25**, 493-501 (2011).
 101. Mustanski, B., Ryan, D.T., Newcomb, M.E., D'Aquila, R.T. & Matson, M. Very High HIV Incidence and Associated Risk Factors in a Longitudinal Cohort Study of Diverse Adolescent and Young Adult Men Who Have Sex with Men and Transgender Women. *AIDS Behav* **24**, 1966-1975 (2020).
 102. van den Hoek, J.A., Coutinho, R.A., van Haastrecht, H.J., van Zadelhoff, A.W. & Goudsmit, J. Prevalence and risk factors of HIV infections among drug users and drug-using prostitutes in Amsterdam. *Aids* **2**, 55-60 (1988).
 103. Foster, T.L., *et al.* Resistance of




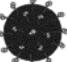

- Transmitted Founder HIV-1 to IFITM-Mediated Restriction. *Cell Host Microbe* **20**, 429-442 (2016).
104. Rachinger, A., *et al.* HIV-1 envelope diversity 1 year after seroconversion predicts subsequent disease progression. *Aids* **26**, 1517-1522 (2012).
 105. Wymant, C., *et al.* A highly virulent variant of HIV-1 circulating in the Netherlands. *Science* **375**, 540-545 (2022).
 106. Clark, I.C., *et al.* HIV silencing and cell survival signatures in infected T cell reservoirs. *Nature* **614**, 318-325 (2023).
 107. Dijkstra, M., *et al.* Cohort profile: the Netherlands Cohort Study on Acute HIV infection (NOVA), a prospective cohort study of people with acute or early HIV infection who immediately initiate HIV treatment. *BMJ Open* **11**, e048582 (2021).
 108. Kroeze, S., *et al.* Plasma Inflammatory Biomarkers Predict CD4+ T-cell Recovery and Viral Rebound in HIV-1 Infected Africans on Suppressive Antiretroviral Therapy. *J Infect Dis* **224**, 673-678 (2021).
 109. Streeck, H., *et al.* Dissecting drivers of immune activation in chronic HIV-1 infection. *EBioMedicine* **83**, 104182 (2022).
 110. Bruner, K.M., *et al.* A quantitative approach for measuring the reservoir of latent HIV-1 proviruses. *Nature* **566**, 120-125 (2019).
 111. Jiang, C., *et al.* Distinct viral reservoirs in individuals with spontaneous control of HIV-1. *Nature* **585**, 261-267 (2020).
 112. Sáez-Cirión, A., *et al.* Post-treatment HIV-1 controllers with a long-term virological remission after the interruption of early initiated antiretroviral therapy ANRS VISCONTI Study. *PLoS Pathog* **9**, e1003211 (2013).
 113. Blazkova, J., *et al.* Distinct mechanisms of long-term virologic control in two HIV-infected individuals after treatment interruption of anti-retroviral therapy. *Nat Med* **27**, 1893-1898 (2021).
 114. Climent, N., *et al.* Immunological and virological findings in a patient with exceptional post-treatment control: a case report. *Lancet HIV* **10**, e42-e51 (2023).
 115. Darton, T.C., *et al.* Design, recruitment, and microbiological considerations in human challenge studies. *Lancet Infect Dis* **15**, 840-851 (2015).
 116. Roestenberg, M., Hoogerwerf, M.A., Ferreira, D.M., Mordmüller, B. & Yazdanbakhsh, M. Experimental infection of human volunteers. *Lancet Infect Dis* **18**, e312-e322 (2018).
 117. Choy, R.K.M., *et al.* Controlled Human Infection Models To Accelerate Vaccine Development. *Clin Microbiol Rev* **35**, e0000821 (2022).
 118. Shah, S.K., *et al.* Ethics of controlled human infection to address COVID-19. *Science* **368**, 832-834 (2020).
 119. Bamberly, B., Selgelid, M., Weijer, C., Savulescu, J. & Pollard, A.J. Ethical Criteria for Human Challenge Studies in Infectious Diseases. *Public Health Ethics* **9**, 92-103 (2016).
 120. WHO. WHO guidance on the ethical conduct of controlled human infection studies. (World Health Organization, Geneva, 2021).
 121. WHO. Key criteria for the ethical

- acceptability of COVID-19 human challenge studies. . in *Working Group for Guidance on Human Challenge Studies in COVID-19* (WHO, WHO, 2020).
122. Killingley, B., *et al.* Safety, tolerability and viral kinetics during SARS-CoV-2 human challenge in young adults. *Nat Med* **28**, 1031-1041 (2022).
 123. Lambkin-Williams, R., Noulin, N., Mann, A., Catchpole, A. & Gilbert, A.S. The human viral challenge model: accelerating the evaluation of respiratory antivirals, vaccines and novel diagnostics. *Respiratory Research* **19**, 123 (2018).
 124. Lambkin-Williams, R. & DeVincenzo, J.P. A COVID-19 human viral challenge model. Learning from experience. *Influenza Other Respir Viruses* **14**, 747-756 (2020).
 125. Sinha, A., *et al.* Loss of adaptive capacity in asthmatic patients revealed by biomarker fluctuation dynamics after rhinovirus challenge. *Elife* **8**(2019).
 126. Spring, M., Polhemus, M. & Ockenhouse, C. Controlled human malaria infection. *J Infect Dis* **209 Suppl 2**, S40-45 (2014).
 127. Stanisic, D.I., McCarthy, J.S. & Good, M.F. Controlled Human Malaria Infection: Applications, Advances, and Challenges. *Infection and Immunity* **86**, 10.1128/iai.00479-00417 (2018).
 128. Cooper, M.M., Loiseau, C., McCarthy, J.S. & Doolan, D.L. Human challenge models: tools to accelerate the development of malaria vaccines. *Expert Rev Vaccines* **18**, 241-251 (2019).
 129. Sulyok, M., *et al.* DSM265 for Plasmodium falciparum chemoprophylaxis: a randomised, double blinded, phase 1 trial with controlled human malaria infection. *Lancet Infect Dis* **17**, 636-644 (2017).
 130. Roestenberg, M., *et al.* Controlled human malaria infections by intradermal injection of cryopreserved Plasmodium falciparum sporozoites. *Am J Trop Med Hyg* **88**, 5-13 (2013).
 131. Rampling, T., *et al.* Safety and High Level Efficacy of the Combination Malaria Vaccine Regimen of RTS,S/AS01B With Chimpanzee Adenovirus 63 and Modified Vaccinia Ankara Vectored Vaccines Expressing ME-TRAP. *J Infect Dis* **214**, 772-781 (2016).
 132. Hall, C.E., *et al.* Mosquito Bite-Induced Controlled Human Malaria Infection with Plasmodium vivax or P. falciparum Generates Immune Responses to Homologous and Heterologous Preerythrocytic and Erythrocytic Antigens. *Infect Immun* **87**(2019).
 133. Palacios, R. & Shah, S.K. When could human challenge trials be deployed to combat emerging infectious diseases? Lessons from the case of a Zika virus human challenge trial. *Trials* **20**, 702 (2019).
 134. Vannice, K.S., *et al.* Demonstrating vaccine effectiveness during a waning epidemic: A WHO/NIH meeting report on approaches to development and licensure of Zika vaccine candidates. *Vaccine* **37**, 863-868 (2019).
 135. Liang, T.J., Feld, J.J., Cox, A.L. & Rice, C.M. Controlled Human Infection Model — Fast Track to HCV Vaccine? *New England Journal of Medicine* **385**, 1235-

- 1240 (2021).
136. Lombardi, A. & Mondelli, M.U. Hepatitis C: Is eradication possible? *Liver Int* **39**, 416-426 (2019).
 137. Eder, J., *et al.* Inhalation of Low Molecular Weight Heparins as Prophylaxis against SARS-CoV-2. *mBio* **13**, e0255822 (2022).
 138. Zaderer, V., Hermann, M., Lass-Flörl, C., Posch, W. & Wilflingseder, D. Turning the World Upside-Down in Cellulose for Improved Culturing and Imaging of Respiratory Challenges within a Human 3D Model. *Cells* **8**(2019).
 139. Posch, W., *et al.* C5aR inhibition of nonimmune cells suppresses inflammation and maintains epithelial integrity in SARS-CoV-2-infected primary human airway epithelia. *J Allergy Clin Immunol* **147**, 2083-2097.e2086 (2021).
 140. Zaderer, V., *et al.* GlyPerA™ effectively shields airway epithelia from SARS-CoV-2 infection and inflammatory events. *Respiratory Research* **24**, 88 (2023).
 141. Zaderer, V., *et al.* ColdZyme® protects airway epithelia from infection with BA.4/5. *Respiratory Research* **23**, 300 (2022).
 142. Ravi, A., *et al.* Imprinting of bronchial epithelial cells upon in vivo rhinovirus infection in people with asthma. *ERJ Open Res* **8**(2022).
 143. Wang, P., *et al.* Heparin: An old drug for new clinical applications. *Carbohydrate Polymers* **295**, 119818 (2022).
 144. Lim, G.B. Discovery and purification of heparin. *Nature Reviews Cardiology* (2017).
 145. Hirsh, J., *et al.* Parenteral anticoagulants: American College of Chest Physicians Evidence-Based Clinical Practice Guidelines (8th Edition). *Chest* **133**, 141s-159s (2008).
 146. Merli, G.J. & Groce, J.B. Pharmacological and clinical differences between low-molecular-weight heparins: implications for prescribing practice and therapeutic interchange. *P t* **35**, 95-105 (2010).
 147. Shriver, Z., *et al.* Cleavage of the antithrombin III binding site in heparin by heparinases and its implication in the generation of low molecular weight heparin. *Proc Natl Acad Sci U S A* **97**, 10365-10370 (2000).
 148. Weitz, J.I. Low-molecular-weight heparins. *The New England journal of medicine* **337**, 688-698 (1997).
 149. Tang, N., *et al.* Anticoagulant treatment is associated with decreased mortality in severe coronavirus disease 2019 patients with coagulopathy. *J Thromb Haemost* **18**, 1094-1099 (2020).
 150. Parisi, R., *et al.* Different Anticoagulant Regimens, Mortality, and Bleeding in Hospitalized Patients with COVID-19: A Systematic Review and an Updated Meta-Analysis. *Semin Thromb Hemost* **47**, 372-391 (2021).
 151. Rentsch, C.T., *et al.* Early initiation of prophylactic anticoagulation for prevention of coronavirus disease 2019 mortality in patients admitted to hospital in the United States: cohort study. *Bmj* **372**, n311 (2021).
 152. Young, E. The anti-inflammatory effects of heparin and related compounds. *Thromb Res* **122**, 743-752 (2008).
 153. Shi, C., *et al.* The Potential of Low Molecular Weight Heparin to Mitigate

- Cytokine Storm in Severe COVID-19 Patients: A Retrospective Cohort Study. *Clin Transl Sci* **13**, 1087-1095 (2020).
154. Mycroft-West, C.J., *et al.* Heparin Inhibits Cellular Invasion by SARS-CoV-2: Structural Dependence of the Interaction of the Spike S1 Receptor-Binding Domain with Heparin. *Thromb Haemost* **120**, 1700-1715 (2020).
155. Tandon, R., *et al.* Effective Inhibition of SARS-CoV-2 Entry by Heparin and Enoxaparin Derivatives. *J Virol* **95**(2021).
156. Dixon, B., *et al.* Nebulised heparin for patients with or at risk of acute respiratory distress syndrome: a multicentre, randomised, double-blind, placebo-controlled phase 3 trial. *Lancet Respir Med* **9**, 360-372 (2021).
157. Stelmach, I., *et al.* The effect of inhaled heparin on airway responsiveness to histamine and leukotriene D4. *Allergy Asthma Proc* **24**, 59-65 (2003).
158. UN^News. WHO chief declares end to COVID-19 as a global health emergency. (2023).

ADDENDUM

-  **Summary**
-  **Samenvatting**
-  **PhD Portfolio**
-  **List of Publications**
-  **Curriculum Vitae**
-  **Acknowledgements**

Summary

Unravelling early pathogenesis of pandemic and epidemic viruses: Infection and viral dissemination at barrier tissues

In this thesis, we describe the interactions of four different viruses: Zika virus, SARS-CoV-2, HIV-1 and HCV with cells and molecules at human epithelial barrier tissues. We aimed to better understand what happens at the earliest stages of infection once a viral pathogen has breached the skin or mucosal surfaces. Immune cells like DCs at barrier tissues are crucial for host defense and prevention of disease exacerbation but can be corrupted by viruses to invade the host and disseminate the virus to other organs.

In **chapter 2**, we investigated how dendritic cell (DC) subsets located in the skin and vaginal mucosa, contribute to Zika virus infection and dissemination of the virus to other target cells. Strikingly, monocyte derived DCs (moDC) were readily infected by Zika virus whereas neither skin nor vaginal Langerhans cells (LCs) were susceptible to infection. We further observed that moDC infection was facilitated by DC-SIGN, a c-type lectin (CLR) expressed on some DC subsets but not LCs. Interestingly, both moDCs and LCs successfully captured and transmitted Zika virus to target cells, regardless of infection. These data indicate an important role for DC subsets in the skin and vaginal mucosa as Zika virus targets for infection and/or dissemination.

In **chapter 3** we investigated the role of vaginal LCs, either immature or activated, during HIV-1 infection. Interestingly, while immature vaginal LCs were refractory to HIV-1 infection, LC activation rendered them susceptible. We determined that in contrast to skin-derived LCs, immature vaginal LCs expressed a range of TLRs, including TLR4. Subsequently, immature vaginal LCs stimulated with bacterial TLR4 agonists could be infected with HIV-1, similar to vaginal LCs activated through migration. Moreover, TLR4 stimulated LCs transmitted HIV-1 to target cells whereas immature LCs did not, indicating that these cells are no longer protective. These data suggest that TLR stimulation, as happens during bacterial co-infection, increases susceptibility of vaginal LCs to HIV-1 infection and indicates a role for the vaginal microbiome during sexual transmission of HIV-1.

The interactions of TLRs expressed on moDCs with SARS-CoV-2 were studied in **chapter 4**. Neither SARS-Cov-2 spike protein alone nor the wild type SARS-CoV-2 isolate were able to activate TLR4. Moreover, SARS-CoV-2 did not activate, infect or incite cytokine production in exposed moDCs, indicating that SARS-CoV-2 evades recognition by TLRs to prevent activation of the immune response. Strikingly, moDCs rendered susceptible to SARS-CoV-2 infection by ectopic expression of ACE-2 produced high levels of type I IFNs and other cytokines, indicating that intracellular receptors rather than extracellular TLRs, are responsible for immune activation during SARS-CoV-2 infection.

In **chapter 5** we studied Heparan sulfate proteoglycans (HSPGs) as crucial attachment

receptors for HCV. We observed that the HSPG Syndecan 4 is upregulated on activated LCs, and is crucial for HCV transmission, whereas langerin abrogated both HCV infection and transmission. These data indicate that the two receptors have adversary effects either increasing or decreasing HCV transmission. Hence, we identified Syndecan 4 expressed on activated LCs as an important receptor for HCV capture and transmission that might explain HCV dissemination from mucosal barrier sites following sexual transmission. Importantly, heparin and low molecular weight heparins (LMWHs) blocked the engagement of Syndecan 4 with HCV and decreased HCV transmission, indicating a potential role for LMWHs as preventative therapy against HCV dissemination.

In **chapter 6**, we studied which (co-)receptors are involved in SARS-CoV-2 attachment, infection and transmission. We identified Syndecan 1 and 4 as crucial attachment receptors for SARS-CoV-2 that aided ACE-2 mediated infection of epithelial cells. Both the SARS-CoV-2 pseudovirus as well as the replicating SARS-CoV-2 patient isolate strongly bound to Syndecans expressed on epithelial cells and this interaction could be blocked by adding heparin or LMWHs. We showed that antibodies isolated from COVID-19 patients deterred interactions of SARS-CoV-2 with Syndecan 1, indicating a protective mechanism of neutralizing antibodies not involving ACE-2 block. Moreover, Syndecans expressed on DCs and LCs are crucial for SARS-CoV-2 transmission, irrespective of ACE-2 mediated infection. These data indicate that Syndecans are not only important attachment receptors required for SARS-CoV-2 infection of epithelial cells but are also involved in viral dissemination from entry sites to organs throughout the body. Importantly, LMWHs efficiently inhibited SARS-CoV-2 engagement with Syndecans on primary epithelial cells, suggesting a use for them to prevent SARS-CoV-2 infection.

The use of LMWHs as therapeutics against SARS-CoV-2 in a non-randomized controlled trial is described in **chapter 7**. We evaluate safety parameters of LMWH when applied to nasal mucosa in healthy volunteers and analyzed the efficacy of LMWHs to prevent SARS-CoV-2 infection *ex-vivo*. We selected the LMWH enoxaparin as a candidate therapeutic against SARS-CoV-2 and administered enoxaparin to healthy volunteers with the help of a nasal spray in one nostril while all study participants received a placebo in the other nostril as a control. No adverse effects of enoxaparin treatment were observed for any of the study participants. Nasal epithelial cells retrieved with a brush, were phenotyped and inoculated with SARS-CoV-2 *ex vivo*. Importantly, cells treated with enoxaparin bound SARS-CoV-2 significantly less than the placebo treated cells, while not displaying any changes in phenotype. This accounted not only for the ancestral SARS-CoV-2 strain but also the Delta and Omicron VoC. Additional *in vitro* enoxaparin administration did not further abrogate SARS-CoV-2 binding, suggesting that the *in vivo* administered dose of enoxaparin is sufficient. These data let us to conclude that enoxaparin might be used as an easy and safe preventative therapeutic against SARS-CoV-2 infection with broad protection also against VoC.

In **Chapter 8** we discuss the findings from this thesis in a broader context. We studied four wild type viruses that all strongly influenced global health in the last decades. And through the *ex vivo* access of human tissues, we gained insight into early virus-host-interactions at different barrier tissues.

Samenvatting

Het ontrafelen van vroege pathogenese van pandemische en epidemische virussen: infectie en virale verspreiding bij barrièreweefsels

In dit proefschrift beschrijven we de interacties tussen vier verschillende virussen: het Zika-virus, SARS-CoV-2, hiv en HCV met cellen en moleculen in menselijke epitheelbarriëretissues. We probeerden beter te begrijpen wat er gebeurt in de eerste stadia van infectie nadat een virus de huid of slijmvliezen heeft doorbroken. Immuncellen zoals DC's in barrièreweefsels zijn cruciaal voor het reguleren van de afweer van de gastheer en het voorkomen van verergering van de ziekte, echter kunnen ze gecorrumpereerd worden door virussen om de gastheer binnen te dringen en het virus naar andere organen te verspreiden.

In **hoofdstuk 2** onderzochten we hoe dendritische cel (DC) subsets die zich bevinden in de huid en vaginale slijmvliezen bijdragen aan de Zika-virusinfectie en de verspreiding van het virus naar andere cellen. Opvallend genoeg werden van monocyt-afgeleide DC's (moDC's) efficiënt geïnfecteerd door het Zika-virus, terwijl zowel de huid- als de vaginale Langerhanscellen (LC's) niet vatbaar waren voor infectie. We hebben verder waargenomen dat de infectie van moDC's werd vergemakkelijkt door DC-SIGN, een c-type lectine (CLR) dat wordt uitgedrukt op sommige DC-subsets maar niet op LC's. Interessant genoeg wordt Zika-virus efficiënt gebonden door zowel moDC's als LC's en deze cellen dragen het virus over aan andere cellen. Deze resultaten geven aan dat DC-subsets in de huid en vaginale slijmvliezen een belangrijke rol spelen als Zika-virus doelwitten voor infectie en/of verspreiding.

In **hoofdstuk 3** onderzochten we de rol van vaginale LC's, zowel niet-geactiveerd als geactiveerd, tijdens een hiv-infectie. Interessant genoeg waren niet-geactiveerde vaginale LC's ongevoelig voor hiv-infectie, terwijl geactiveerde LC's juist vatbaar waren voor hiv. We ontdekten dat in tegenstelling tot uit huid verkregen LC's, vaginale LC's een reeks van TLR's tot expressie brachten waaronder TLR4. Vervolgens konden niet-geactiveerde vaginale LC's, gestimuleerd met bacteriële TLR4-agonisten, worden geïnfecteerd met hiv, vergelijkbaar met vaginale LC's die geactiveerd waren door migratie. Gestimuleerde TLR4-LC's dragen hiv-1 over aan andere cellen, terwijl niet-geactiveerde LC's dat niet deden, wat aangeeft dat deze TLR4-geactiveerde LC's niet langer beschermend zijn. Deze gegevens suggereren dat TLR-stimulatie, zoals bij bacteriële co-infectie, de vatbaarheid van vaginale LC's voor hiv-infectie verhoogt en wijzen op een rol van het vaginale microbioom tijdens seksuele overdracht van hiv.

De interacties van TLR's op moDC's met SARS-CoV-2 werden bestudeerd in **hoofdstuk 4**. Noch het spike-eiwit van SARS-CoV-2 alleen, noch het wildtype SARS-CoV-2-isolaat konden TLR4 activeren. Bovendien leidde SARS-CoV-2 niet tot infectie van moDC's en ook niet to

cytokine productie in moDC's, wat aangeeft dat SARS-CoV-2 herkenning door TLR's ontwijkt om activering van het immuunrespons te voorkomen. Opvallend genoeg produceerden moDC's, die vatbaar waren gemaakt voor SARS-CoV-2-infectie door ectopische expressie van ACE-2, hoge niveaus type I-interferon en andere cytokines. Dit geeft aan dat intracellulaire receptoren, maar niet extracellulaire TLR's, verantwoordelijk zijn voor immuun activatie tijdens SARS-CoV-2-infectie.

In **hoofdstuk 5** hebben we Heparansulfaat proteoglycanen (HSPG's) bestudeerd als cruciale receptoren voor het Hepatitis C virus (HCV). We hebben waargenomen dat het HSPG Syndecan 4 werd opgereguleerd op geactiveerde LC's en cruciaal was voor HCV-overdracht, terwijl langerin zowel HCV-infectie als -overdracht onderdrukte. Deze gegevens geven aan dat de twee receptoren tegenstrijdige effecten hebben, waarbij HCV-overdracht wordt verhoogd of verminderd. Daarom hebben we Syndecan 4, dat tot expressie wordt gebracht op geactiveerde LC's, geïdentificeerd als een belangrijke receptor voor HCV-opname en -overdracht, wat de verspreiding van HCV vanuit barrièreweefsels na seksuele overdracht zou kunnen verklaren. Belangrijk is dat heparine en laagmoleculairegewichtheparines (LMWH's) de binding van Syndecan 4 aan HCV blokkeerden en HCV-overdracht verminderden, wat wijst op een mogelijke rol voor LMWH's als preventieve therapie tegen HCV-verspreiding.

In **hoofdstuk 6** hebben we onderzocht welke (co-)receptoren betrokken zijn bij SARS-CoV-2-binding, -infectie en -overdracht. We hebben Syndecan 1 en 4 geïdentificeerd als cruciale bindingsreceptoren voor SARS-CoV-2 die ACE-2-gemedieerde infectie van epitheelcellen ondersteunen. Zowel het SARS-CoV-2-pseudovirus als het replicerende SARS-CoV-2-isolaat bond sterk aan Syndecans op epitheelcellen, en deze interactie kon worden geblokkeerd door heparine of LMWH's toe te voegen. We hebben aangetoond dat antilichamen geïsoleerd uit COVID-19-patiënten interacties van SARS-CoV-2 met Syndecan 1 verhinderden, wat wijst op een beschermend mechanisme van neutraliserende antilichamen dat niet afhankelijk is van ACE-2-blokkade. Bovendien zijn Syndecans die tot expressie worden gebracht op DC's en LC's cruciaal voor SARS-CoV-2-overdracht, ongeacht de ACE-2-gemedieerde infectie. Deze gegevens geven aan dat Syndecans niet alleen belangrijke receptoren zijn die nodig zijn voor SARS-CoV-2-infectie van epitheelcellen, maar ook betrokken zijn bij de virale verspreiding naar organen in het hele lichaam. Belangrijk is dat LMWH's SARS-CoV-2-interactie met Syndecans op primaire epitheelcellen efficiënt remmen, wat wijst op een gebruik ervan om SARS-CoV-2-infectie te voorkomen.

Het gebruik van LMWH's als therapeutica tegen SARS-CoV-2 in een niet-gerandomiseerde gecontroleerde studie wordt beschreven in **hoofdstuk 7**. We hebben veiligheidsparameters van LMWH geëvalueerd wanneer deze werd aangebracht op het neusslijmvlies bij gezonde vrijwilligers en de werkzaamheid van LMWH's geanalyseerd om SARS-CoV-2-infectie *ex vivo* te voorkomen. We hebben LMWH Enoxaparine geselecteerd als een kandidaat-therapeutisch middel tegen SARS-CoV-2 en toegediend aan gezonde vrijwilligers met behulp van een neusspray. Enoxaparine werd toegediend in één neusgat, terwijl de studie-

deelnemers een placebo kregen in het andere neusgat ter controle. Er werden geen nadelige effecten van Enoxaparine-behandeling waargenomen bij de studie-deelnemers. Neusepitheelcellen verkregen met een borsteltje werden gefenotypeerd en *ex vivo* geïnoculeerd met SARS-CoV-2. Cellen behandeld met Enoxaparine bonden minder SARS-CoV-2 dan cellen behandeld met een placebo, terwijl er geen veranderingen in fenotype werden waargenomen. Dit gold niet alleen voor de voorouderlijke SARS-CoV-2-stam, maar ook voor de Delta- en Omicron-varianten. Extra *in vitro* toediening van Enoxaparine had geen verdere invloed op de binding van SARS-CoV-2, wat erop wijst dat de *in vivo* toegediende dosis Enoxaparine voldoende is. Deze gegevens leiden tot de conclusie dat Enoxaparine mogelijk kan worden gebruikt als een eenvoudige en veilige preventieve therapie tegen SARS-CoV-2-infectie met brede bescherming, ook tegen varianten of concern.

In **hoofdstuk 8** bespreken we de bevindingen van dit proefschrift in een bredere context. We hebben vier virussen bestudeerd die allemaal een sterke invloed hebben gehad op de mondiale gezondheid in de afgelopen decennia. Door de *ex vivo* toegang tot menselijk weefsel hebben we inzicht gekregen in vroege virus-host-interacties bij verschillende barrièretissues. Onze bevindingen hebben implicaties voor de ontwikkeling van nieuwe strategieën om infectie en verspreiding van deze virussen te voorkomen.

PhD Portfolio

Summary of PhD Training and Teaching

PhD student: Julia Eder

Period: October 2017 – June 2023

PhD Supervisors: Prof. Dr. T.B.H. Geijtenbeek and Dr. N.A. Kootstra

| Courses | Year | ECTS |
|---|-------------|-------------|
| AMC World of Science | 2017 | 0.7 |
| Advanced Immunology | 2018 | 2.9 |
| Project management | 2018 | 0.6 |
| Infectious Diseases | 2018 | 1.3 |
| Entrepreneurship in Health and Life Sciences | 2021 | 1.5 |
| Research Integrity | 2022 | 2.0 |
| Oral Presentations | | |
| Dutch Society of Immunology Congress (NVVI) Winterschool | 2017 | 0.5 |
| EXIM seminar 6x | 2018-2023 | 3.0 |
| European Congress of Immunology (ECI) | 2018 | 0.5 |
| Dutch Annual Virology Symposium (DAVS) | 2019 | 0.5 |
| European Congress of Virology (ECV) | 2019 | 0.5 |
| Netherlands Conference on HIV Pathogenesis, Epidemiology, Prevention and Treatment (NCHIV) | 2019 | 0.5 |
| Dutch Society of Immunology Congress (NVVI) Winterschool | 2019 | 0.5 |
| Dutch Society of Immunology Congress (NVVI) Winterschool | 2020 | 0.5 |
| UvA Open Days lecture | 2021 | 0.5 |
| European Congress of Immunology (ECI) | 2021 | 0.5 |
| Dutch Young Virologists Seminar (DYVS) | 2021 | 0.5 |
| AI&II PhD retreat | 2021 | 0.5 |
| AI&II Annual meeting | 2022 | 0.5 |
| 16 th International Symposium on Dendritic Cells 2022 (DC 2022) | 2022 | 0.5 |

Poster Presentations

| | | |
|--|------|-----|
| 15 th International Symposium on Dendritic Cells 2022 (DC 2018) | 2018 | 0.5 |
| European Congress of Virology (ECV) | 2019 | 0.5 |
| Dutch Society of Immunology Congress (NVVI), Winterschool | 2022 | 0.5 |

(Inter)national Conferences

| | | |
|---|---|-----|
| Dutch Society of Immunology Congress (NVVI) Winterschool, Noordwijkerhout, NL | 2017, 2019, 2020, 2022 (May), 2022 (December) | 2.5 |
| 15 th International Symposium on Dendritic Cells 2022, Aachen, DE | 2018 | 0.5 |
| European Congress of Immunology (ECI), Amsterdam, NL | 2018 | 0.5 |
| Dutch Annual Virology Symposium (DAVS), Amsterdam, NL | 2019 | 0.5 |
| European Congress of Virology (ECV), Rotterdam, NL | 2019 | 0.5 |
| Netherlands Conference on HIV Pathogenesis, Epidemiology, Prevention and Treatment (NCHIV), Amsterdam, NL | 2019 | 0.5 |
| European Congress of Immunology (ECI), Online | 2021 | 0.5 |
| Netherlands Conference on HIV Pathogenesis, Epidemiology, Prevention and Treatment (NCHIV), Online | 2021 | 0.5 |
| AI&II Annual meeting, Amsterdam, NL | 2022 | 0.5 |
| 16 th International Symposium on Dendritic Cells 2022, Cairns, Australia | 2022 | 0.5 |

Seminars, Workshops and Masterclasses

| | | |
|--|------------------|-----|
| Weekly EXIM Seminars | 2017-2022 | 5.0 |
| Yearly EXIM retreat | 2018, 2022 | 1.0 |
| Yearly AI&II meeting | 2018, 2019, 2022 | 1.5 |
| AI&II PhD retreat | 2018, 2021 | 1.0 |
| Dutch Arbovirus Research Network meeting | 2018 | 0.5 |
| Cellular Imaging – From Pixel to publication | 2018 | 0.2 |
| Masterclass Prof. Dr. Fauci | 2019 | 0.5 |
| Career Thursdays | 2019 | 0.5 |
| SARS-CoV-2 work meetings | 2020-2021 | 1.0 |
| Dutch Young Virologists Seminar (DYVS) | 2021-2022 | 1.0 |

Lecturing and Student supervision

| | | |
|--|------------------|-----|
| Supervision of medical students during Immunology course | 2018 | 0.5 |
| Supervision of Master student internship | 2018, 2021 | 4.0 |
| Assessment of High school students (Viruskenner) | 2019, 2020, 2022 | 0.6 |
| Supervision of Master student literature thesis | 2020 | 1.0 |
| Lecture as part of UvA Master Biomedical Sciences | 2021, 2022 | 1.0 |

Grants

| | |
|-------------------------|------|
| AI&II work visit grant | 2019 |
| Keystone scholarship | 2020 |
| ECI Participation grant | 2021 |
| AI&II Travel grant | 2022 |
| NVVI Travel grant | 2022 |

Other Activities

| | | |
|--|-----------|-----|
| Member of the AI&II PhD committee | 2018-2020 | 1.5 |
| Blogpost Proefdiervrij | 2022 | |
| Blogpost "Behind the paper" Nature Portfolio | 2023 | |

Total **47.8**

List of publications

Eder, J.*, Bermejo-Jambrina, M.*, Helgers, L. C.*, Hertoghs, N.*, Nijmeijer, B. M.*, Stunnenberg, M.*, & Geijtenbeek, T. B. H. (2018). C-Type Lectin Receptors in Antiviral Immunity and Viral Escape. *Frontiers in immunology*, 9, 590. <https://doi.org/10.3389/fimmu.2018.00590>

*equal contribution

Nijmeijer, B. M., Eder, J., Langedijk, C. J. M., Kaptein, T. M., Meeussen, S., Zimmermann, P., Ribeiro, C. M. S., & Geijtenbeek, T. B. H. (2020). Syndecan 4 Upregulation on Activated Langerhans Cells Counteracts Langerin Restriction to Facilitate Hepatitis C Virus Transmission. *Frontiers in immunology*, 11, 503. <https://doi.org/10.3389/fimmu.2020.00503>

Eder, J.*, Bermejo-Jambrina, M.*, Kaptein, T. M., van Hamme, J. L., Helgers, L. C., Vlaming, K. E., Brouwer, P., van Nuenen, A. C., Spaargaren, M., de Bree, G. J., Nijmeijer, B. M., Kootstra, N. A., van Gils, M. J., Sanders, R. W., & Geijtenbeek, T. B. H. (2021). Infection and transmission of SARS-CoV-2 depend on heparan sulfate proteoglycans. *The EMBO journal*, 40(20), e106765. <https://doi.org/10.15252/embj.2020106765>

*equal contribution

van der Donk, L. E. H., Eder, J., van Hamme, J. L., Brouwer, P. J. M., Brinkkemper, M., van Nuenen, A. C., van Gils, M. J., Sanders, R. W., Kootstra, N. A., Bermejo-Jambrina, M., & Geijtenbeek, T. B. H. (2022). SARS-CoV-2 infection activates dendritic cells via cytosolic receptors rather than extracellular TLRs. *European journal of immunology*, 52(4), 646–655. <https://doi.org/10.1002/eji.202149656>

Eder, J.*, Bermejo-Jambrina, M.*, Vlaming, K. E.*, Kaptein, T. M., Zaderer, V., Kemper, E. M., Wilflingseder, D., Reitsma, S., de Bree, G. J., Cohn, D. M., & Geijtenbeek, T. (2022). Inhalation of Low Molecular Weight Heparins as Prophylaxis against SARS-CoV-2. *mBio*, e0255822. <https://doi.org/10.1128/mbio.02558-22>

*equal contribution

van Teijlingen, N. H., Eder, J., Sarrami-Forooshani, R., Zijlstra-Willems, E. M., Roovers, J. W. R., van Leeuwen, E., Ribeiro, C. M. S., & Geijtenbeek, T. B. H. (2023). Immune activation of vaginal human Langerhans cells increases susceptibility to HIV-1 infection. *Scientific reports*, 13(1), 3283. <https://doi.org/10.1038/s41598-023-30097-x>

Eder, J., Zijlstra-Willems, E., Koen, G., Kootstra, N. A., Wolthers, K. C., & Geijtenbeek, T. B. (2023). Transmission of Zika virus by dendritic cell subsets in skin and vaginal mucosa. *Frontiers in immunology*, 14, 1125565. <https://doi.org/10.3389/fimmu.2023.1125565>

Curriculum Vitae

Julia Eder was born in Schwarzach im Pongau, Austria on April 29th, 1992. After graduating from a higher-level secondary commercial college in 2011 she started her study of Biomedicine and Biotechnology at the University for Veterinary Medicine in Vienna. From there she graduated with a Bachelor in Science (BSc.) with honors in 2015. After completing her bachelor's degree, Julia moved to the Netherlands where she was accepted into the Research Master Biomedical Sciences at the Vrije Universiteit (VU) in Amsterdam. As part of this study she completed two research internships at the Department of Experimental Immunology at the Amsterdam UMC – location Amsterdam Medical Centers (AMC). During her first internship she studied the distribution and functionality of lymphoid cell subsets in fetal lung under the supervision of Dr. Bianca Blom. Her second internship was completed in the group of Prof. Dr. Teunis Geijtenbeek, where she researched the role of Heparan sulfate proteoglycans during Hepatitis C transmission of human primary Langerhans cells. This sparked a keen interest in the interplay between viruses and host receptors involved in binding, infection and transmission. After graduation from the VU *cum laude* with a Master's degree in 2017, she therefore returned to the group of Prof. Dr. Geijtenbeek to pursue a PhD in immunology. For the past 4 years she has been studying the interaction of different viruses with cell surface attachment receptors. Since March 2020, Julia has strongly focused on the newly emerged SARS-CoV-2 virus and together with Marta Bermejo-Jambrina and Killian Vlaming has set up a study that looks at the importance of Heparan sulfate proteoglycans in viral attachment and subsequent infection and virus transmission. Since the start of this project, a whole new line of research on SARS-CoV-2 has been set up in the Host Defense group that now involves a whole team of people as well as healthy volunteers donating their epithelial cells for research into infection prevention. Outside of her work, Julia likes to read fiction, collect plants and go hiking in her native country. The work she has performed for the past years is summarized in this thesis.



Acknowledgements

This last part of my thesis is arguably the most important and the part that many people will likely read first (if they even make it to the rest). It is where I thank everyone who has helped me get through these past few years and supported me in finishing all my projects.

Theo, you are the person I am most thankful for, as you believed in me during my internship and offered me a chance to stay. Back then I had only the faintest idea of what I wanted to do for my PhD but since I had already gotten very attached to the Host Defense group and the work I could do there. I was not ready yet to say goodbye and frankly it is still hard now. I am also thankful for your relentless efforts in trying to instill some positivity and confidence in me, even though I know I tested your patience with my negativity. I am still not the most self-assured researcher but I am a lot more confident in what I do compared to where I started. It helped that I could always come by to complain or celebrate and that you would try your best to help. I never took that as granted. Thank you for not being a micromanager and letting me come up with my own ideas, experiments and failures.

Neeltje, thank you for all the advice, help and input I received from you over the years. I could come with any virus-related question and your patience in answering them knew no bounds. Your door was always open and no question stupid enough to ask or at least that is the impression you gave me. Your quick replies despite your busy schedule were always a relieve to me as it ensured that I could continue on as quick as possible and your encouraging words made me feel as if I had indeed achieved something amazing. You were instrumental in getting us permission for the SARS-CoV-2 work. Your passion for virology and science in general are an inspiration.

Maartje, I would not have even made it this far without you. You gave me a chance to be your intern and introduced me to the world of viruses and Syndecans. You also taught me a lot about safely working in different labs which gave me a head start for my PhD. I could always come to you with questions - during my internship and as a colleague. Your matter-of-fact attitude and no-nonsense outlook have always appealed to me and I could not have wished for a better supervisor. You re-started the Syndecan work in the group and I am lucky to not only be one of your co-authors in *chapter 4* but to also have learned about low molecular weight heparins and to use that knowledge for the SARS-CoV-2 projects.

I also want to thank all my **committee members** for taking the time to read through my thesis and to question me about it during my defense.

A lot of the data generated in this thesis was made possible through tissue donations from **Boerhaave Medical Center** and **Bergman Clinics**. I want to thank everyone involved in material collection, organization and transport. As well as the people whose tissue we were able to use. A special thank you to **Nienke** for establishing the collaboration with Bergman Clinics and set up the protocols so I could successfully work with vaginal tissue and also be a co-author on her project described in *chapter 3*. Thank you for putting all this work in and pave the way for me to develop the assays further. I also want to thank all the **study**

participants of our non-randomized controlled study in *chapter 7*.

Stefanie and **Killian**, my trusted paranymphs, colleagues and friends. Thank you for helping me getting this book finished and making my defense day run as smooth as possible. Stefanie, I could fill books with stories about you but I will leave most of them between us. You are a creature of beauty and light and thrive in sunshine. Unfortunately for you, the Netherlands does not always provide that. Your positive outlook on life and focus on the pretty things within - and outside - the PhD, helped remind me that work is not everything. Our daily bike rides to the AMC were always a great opportunity for deep conversations, laughter and venting about life. You tried to get me starting pole dancing but instead I only made it to twerk class with you. I wish you all the best with finishing your PhD and that you find something afterwards that makes you really happy. Dear Killian, without you, the randomized controlled trial would not have happened. You might not be fully at home in the lab but you are amazing at writing METCs and starting collaborations with all kinds of people. I am still trying to learn that skill from you, the same as I hope my teachings in the ML-II rubbed off on you. You are fiercely loyal and even though I did not always appreciate it at the time your positive attitude and cheerful demeanor helped cheer me up during the lower points not mentioned in *chapter 7* and beyond.

Marta, when I met you I could tell straight away that you are a hard worker and enthusiastic researcher. An impression that was confirmed with time. Working together with you on two papers has been such a pleasure. Your relentless work ethic and motivation to go further are inspiring to the point of intimidating. Our collaboration always felt like an equal partnership even though I didn't always think I could keep up. I am glad we could go through the lockdowns together and spend so much time together at the AMC. Besides work I am fondly remembering our daily bike rides, wine evenings and shared holidays. You are one of my biggest inspiration for working in academia and I hope to be as zealous and motivated as you after this.

Esther, I so appreciate all the help you provided for my projects over the past few years, as evidenced in *chapter 2 & 3*. I am not the most organized person and often come up with new ideas and complicated set-ups rather last-minute. And I am sure that was not always easy but you never complained and instead just fixed it. Your mastery of immature LC isolation is unmatched and guaranteed high yields to work with. Our work discussions were best held over a cappuccino where we could not only talk about the experiments at hand but also everything else. You often had valuable input on the protocols or spotted mistakes that I had made. Sorry also for all the times you were stuck passing cells in the ML-II.

I also had the privilege to work together with our other two great analysts **Tanja** and **John**. Tanja you were with us on the SARS-Cov-2 projects from the beginning and I really enjoyed getting to know you better during the lockdowns when we had the AMC almost to ourselves. You are a hard worker and dedicated scientist and helped immensely to get this whole new branch of work started. I could always trust you to do a great job with any experiment and was sad when left us for other projects. John, this is where you took over

and I must say I am just as grateful to your help. You are a virus master and made sure we always had good SARS-CoV-2 virus to work with – even if it meant multiple tries to get these titers up. Your deadpan-humor and fondness of pranks still rattles me and even after all these years you manage to fool me more often I would like to admit.

Lieve, I am thankful to have worked together with you and get to know you as a committed and steadfast researcher who made her mark in not two but widely different areas. Your work on SARS-CoV-2 and TLR4 led to the work displayed in *chapter 5* where I had the privilege to help out and become one of your co-authors. You are super precise in the lab, well-organized and a clear writer. You taught me how to CRISPR and while I did not continue with it, that had nothing to do with your methods. I have also seen you supervising students and think you would make an excellent teacher should you ever feel like a career switch. You joined our group as an adoptee and even though you did not have it easy at first, you are soon finishing with an amazing book yourself. Congratulations!

Leanne, you and I pretty much started together and now also finish only weeks apart, making you an integral part of my PhD journey as well as a coveted office mate. We could discuss everything from fashion over music to Harry Potter as well as our Flaviviruses. You also contributed to the work in *chapter 6* and spent the first months of the pandemic together in our little group at the AMC. I will miss dancing together in the labs to the early 2000 jams at the end of the day and will fondly remember your moves in the booty shake pants at all the conferences we have been at together. I hope you will bring them to your own defense party in September! Also thank you for organizing the skin.

Marleen, my almost neighbor. I am thankful to have had you as a colleague and short-time Australia travel partner. You are a reliable and thoughtful scientist who does not shy away from big experiments and even though you did not have an easy start you found your place and I can only imagine it getting even better. **Sonja**, thank you for answering any questions I threw your way, no matter how difficult they were. And for always being sharp in our weekly meetings and asking the questions that nobody else will think about. **Floor**, I wish you all the best with the rest of your PhD and hope that you can make all the different nanobodies that your heart desires. **Tracy**, it has been far too long since I heard your infectious laughter and smelled your coconutty hair. You light up any room and it is physically impossible to be in a bad mood with you around.

Dear **Carla, Renée, Alex, Anusca** and **Kharishma**, thank you for all the work related - and unrelated - conversations we had over the past years. Carla, thank you for providing answers to my most outlandish questions and coming up with meaningful feedback. Your passion for science and innovative ideas are inspiring to me. I also enjoyed our non-work related discussions around the lunch table. Renée, thank you for the help you provided to any of my FACS related problems. You always seemed to be interested in anything I did and talked about. You are someone who lifts others up. Good luck with your new industry chapter! Alex, I first met you when you started your internship and your enthusiasm for science as well as science communication was clearly evident. You are very thoughtful and

passionate about so many things in life and I am glad I got to share some of that with you. You also always seemed to have multiple lives being a science blogger, Yoga teacher and cyclist besides spending hours together in the lab or at the office at the end of the day.

Stefanie, Jade and Shirley, thanks for all the fun we had down at M01. Stefanie, I am glad to have had you as my office companion for the past two years and enjoyed all the conversations we had and all the help you provided. You are very curious and genuinely interested in everyone's research and seem to always have a thoughtful question ready.

Ad, thanks to you I could work in a well-organized and functional ML-III lab. You were vital in getting the SARS-CoV-2 work started and set up work protocols to ensure a safe work environment throughout the pandemic and beyond. It was always a pleasure working with you and you were there whenever I needed any help. But besides your work I also fondly remember your jokes good-natured laugh.

Karel, Marga, Irma, Brigitte, Agnes, Olga, Arginell, Lisa, Pien, Vladimir and Robin, thank you for always being there for me when I needed any help in or outside the lab. Marga, thank you for all the times you closed my flow at the end of the day.

Noémi, I am thankful to know you as a colleague, friend, travel buddy and unsuspecting super-spreader-event host. You are an incredibly smart and fun person and I will fondly remember both the nights out and work discussions we had. You know how to enjoy - and document - the good things in life and I hope you can continue to do so after finishing your PhD. (Even) better things are coming your way, for sure!

Melissa and Zita, thank you for the warm welcome and you gave me when I first started my internship and later PhD journey. That and the hysterical laughter we shared often enough. Melissa, you only started shortly before I first came to the group and we went through a lot of the same PhD stages together and I believe we both grew up a lot in that time. Zita, I always admired your perseverance through hours of commuting followed by hours in the lab without ever losing your humor or ability to perform well in the lab.

Thank you also to my students, **Judith and Kimberley** for teaching me how to be a supervisor and improve my teaching and project management skills.

Liebe **Mama, Papa, David und Jonas**, danke für jegliche Unterstützung die ihr mir mein ganzes Leben lang gegeben habt. Ihr wart vielleicht nicht unbedingt begeistert über meine Studienwahl und Präferenz weit weg von zu Hause zu wohnen aber ihr habt mich trotzdem immer zu 100% unterstützt und nie versucht mir meine Träume auszureden. Dafür bin ich euch wirklich sehr dankbar. Ihr hab mir auch die finanzielle Freiheit gegeben um mein Studium stressfrei abzurunden, etwas das ich nie für selbstverständlich genommen habe.

Dear **Ard**, I will forever be thankful for everything you did for me these past years. You listened to me when I had to vent and complain and made sure there was dinner when I was coming home. You never complained about the long hours I spent at work and never did anything but encourage me in everything I did. I could not wish for a more supportive partner and I hope we can still continue to make our life together in this next chapter.

